The Vendian-Cambrian System of Siberia: Correlation, Tectonics and Petroleum Geology

by

SHANE MITCHELL PELECHATY

M.Sc. Geology
Queen's University, Canada 1990

B.Sc. Geology
Brandon University, Canada 1987

Submitted To The Department Of Earth, Atmospheric And Planetary Sciences In Partial Fulfillment Of The Requirements For Degree Of

DOCTOR OF PHILOSOPHY
At The
Massachusetts Institute Of Technology

February 1997

Signature of Author .....
Department of Earth, Atmospheric and Planetary Sciences
November 8, 1996

Certified by .....
John Grotzinger
Professor of Geology
Thesis Advisor

Certified by .....
Tom H. Jordan
Department Head

The Vendian-Cambrian System of Siberia: Correlation, Tectonics and Petroleum Geology

by

SHANE MITCHELL PELECHATY

Submitted to the Department of Earth, Atmospheric and Planetary Sciences on December 22, 1996 in partial Fulfillment of the Requirements for the Degree of Doctor of Philosophy in Geology

ABSTRACT

Integrated carbon isotope chemostratigraphic and sequence stratigraphic data from late Vendian and Early Cambrian strata throughout the Siberian platform are used to constrain correlations, basin development, plate tectonic interpretations, and the distribution of Vendian petroleum. The Vendian System of northern Siberia (ca. 555 to 543 Ma) includes 300 to 500 m of ramp carbonates that formed in an east-facing passive margin basin. These strata are partitioned into high-resolution (1 to 3 Ma) time slices, which allows recognition of inter-sequence stratigraphic patterns, and variations in subsidence and uplift across the basin. The post-Vendian record is marked by a major paleokarst at the Vendian-Cambrian boundary, which reflects an elevated rift-shoulder that developed across the northern margin of the Siberian craton. A sequence of Early Cambrian (Nemakit-Daldyn stage; <100 m thick) shelf deposits overlies the karst and further records rifting from 543 to 530 Ma with influx of siliciclastic sediments from the north, bimodal volcanism, local block faulting, and continued uplift. Cambrian-age limestones onlap the Nemakit-Daldyn shelf sequence and provide evidence for the development of a northerly depositional gradient, which is interpreted to mark the onset of differential subsidence. A Siberia-Laurentia connection is proposed on the basis of regional tectonostratigraphic correlation of rocks in Siberia and Laurentia (i.e. Franklinian basin), correlation of basement geology, paleomagnetic data and facies patterns in Siberia. The conjugate basins demonstrate separation of the two cratons by Early Cambrian time and the final disintegration of Rodinia.

Correlation of Vendian carbonates across the Siberian platform reveals the development of three cratonic sequences that record high-frequency (<5 m.y.) fluctuations in sea level. In Siberia, they build a larger-scale depositional sequence that forms the youngest of two such sequences that occur in many Neoproterozoic basins world-wide. Their association with glacial deposits suggests a glacioeustatic origin, however, sea floor spreading associated with the breakup of Rodinia also is a likely mechanism for the inferred Vendian eustatic record.

Vendian-age bitumen occurs in Vendian and Cambrian reservoirs across northern Siberia. The regional distribution of reservoirs reflects the aerial extent of the rift-shoulder, while locally, the quality and continuity of individual reservoir units reflect the interplay between karst erosion and subkarst facies development. Collectively, this petroleum province and others elsewhere in Siberia, the Middle East and China underscore the importance of the Vendian period as a viable petroleum system.

Thesis Advisor: John Grotzinger
Title: Professor of Geology

Acknowledgements

My Ph.D. dissertation represents the culmination of a number of vastly different experiences that included the help of many individuals. I extend my sincerest "Спасибо" to all of them.

Firstly, I thank John Grotzinger, my thesis advisor for offering me a superb research project and for the opportunity to study at M.I.T. I am also grateful for his inspirational introduction to sedimentary geology many years ago when he first hired me to join him as part of a Geological Survey of Canada field party in northern Canada. My committee members also included Sam Bowring, Paul Hoffman and Andy Knoll. For Sam, I can not say enough for the support and encouragement he has given me at M.I.T. I thank Paul for leading me to the Canadian Archipelago literature and for his support and editorial comments on the Siberia-Laurentia paper - it has been a great privilage to work with a great Canadian. I thank Andy Knoll not only for providing a solid foundation for my thesis but for graciously giving his time to reading and editing my work.

I thank Maxus Energy Corporation of Dallas Texas for their financial support of this research and the help of Les Niemi, Sam Milner and Martin Schuepback. I thank Yakutsk Geophysica for their superb logistical support and, in particular, Sergei Boresov for his invaluable expediting talents. The Student Research Fund Committee of EAPS also contributed funds for my trips to Namibia and Siberia.

I spent a complete year in Siberia during the course of my Ph.D. My experiences there were arduous and challenging but were mixed with pleasant memories because of the kindness and hospitality of many individuals. I thank my translator, Aleksei Bailikh, from my first season in Siberia. I worked with many capable and knowledgable geologists that I would like to acknowledge. First and foremost, I thank Vladimir Zhernovsky who assisted me during many of my Siberian expeditions - to him I owe a

debt of gratitude for his hard work and friendship; I also thank Stefan Bengtson, Vladimir Kashirtsev, Petr Kolosov, Artem Kushinsky, Valdimir Missarzshevsky, Ivan Moskvitin, Petr Petrov, Vladimir Sovestanov, Misha Semikhatov, Vladimir Sergeev and Tolia Valkov.

The geochemical results for this dissertation were generated at Harvard University, for which I am grateful to Jay Kaufman; and at the University of Michigan, for which I am grateful to Kacey Lohmann, in addition to opening his beer taps and for many engaging discussions. I also thank many people that I have met through the years during my Ph.D. for providing insight into key geological problems: Julie Bartley, Clark Burchfiel, Nick Christie-Blick, Linda Kay, Tony Prave, Gerry Ross, Bruce Runnegar, John Southard and many others.

In the graduate trenches at M.I.T., I thank Jen Carlson, Meg Coleman, Dave Hawkins, C.J. Northrop, Mike Pope, Beverly Saylor, Dawn Sumner and Cathy Summa, and my squash partners who have provided a solid training for my upcoming European social life: Kip Hodges, Gerard Roe, Bonnie Souter, Jim Van Orman and Francoise Robe, who first introduced me to the sport and much more . . . I can't forget about the tea hour and beer hour gang and, of course, Ida Green for the foresight in providing the most important break of the day. I thank Garrett Eastman in the Lindgren Library for his tours through the stacks; and Kirsten Barges, Dan Burns, Nancy Delaire, Stacey Frangos, Beverly Kozol-Tattlebaum and Pat Walsh for helping me through the administrative web. Marcia McNutt is thanked for being an inspirational teacher and for advising my second general's project.

To my parents, Bruce and Judy Pelechaty, to my brothers, Michael and Darcy, to my sister, Lisa, and to her wonderful family, Brian, Dustin, Mitchell and Jordan, I thank you all for providing *the* rock for my life at M.I.T.

I have not words for Francoise, first a stranger on the 16th floor and then my wife at 60 Otis - but with some discussions of FFT's in between. I leave with M.I.T. my thesis but I take with me the most wonderful prize of all: thank you Francoise for all of your support and love and for a future together - I'll see you at home for supper!

Table of Contents

Chapter 1

Introduction

This Ph.D. dissertation is a compendium of papers on the Vendian-Cambrian sedimentary geology of the Siberian platform in eastern Russia. We study the application of integrated carbon isotope chemostratigraphy and sequence stratigraphy for high-resolution correlation of non-fossiliferous, carbonate-dominated deposits across Siberia and between individual basins world-wide. These results are used to investigate basin dynamics, tectonics, eustasy and petroleum geology.

Chapter 2 develops the carbon isotope chemostratigraphy for Vendian carbonates of the northeast Siberian platform. We investigate the role of diagenesis, depositional facies, basin subsidence and stratigraphic completeness on the preservation of the carbon isotope profiles. Large-scale secular variation in isotopic carbon is recognized across the basin as well as small-scale signals related to local diagenetic effects. Key secular isotopic excursions are used to construct chemochrons (time-lines) for intrabasinal chemostratigraphy.

Chapter 3 incorporates the chemostratigraphy into a regional sequence stratigraphic synthesis and depositional facies analysis of Vendian and Early Cambrian sedimentary deposits of northern Siberia. This integrated correlation partitions the rock units into 1 to 3 m.y. time slices, which are used to constrain the history of regional basin development.

In chapter 4, we extend the tectonic investigation of the northern Siberian basin to constrain the plate tectonic history of the Siberian craton. Comparative geology of northern Laurentia (i.e. North American craton) and Siberia is used to link these cratons during terminal Neoproterozoic time and to constrain timing of their separation during the final stages in the breakup of the Neoproterozoic supercontinent Rodinia.

Chapter 5 outlines a similarly detailed and integrated chronostratigraphy for Vendian-age deep water deposits on the southern margin of the Siberian platform. Platform-wide correlation of Vendian-age stratigraphic sections is used to develop a high-resolution chronostratigraphic model for the Vendian System of Siberia. This chronostratigraphy is compared with key stratigraphic sections in a number of basins outside of Siberia in order to investigate the history and related mechanisms of global sea level change.

Finally, chapter 6 highlights the petroleum geology of the Olenek uplift in a regional stratigraphic and tectonic framework established in the preceding chapters. The northern margin of the Siberian platform is recognized as an important Vendian-age petroleum province. In the context of a global stratigraphy and comparative petroleum geology, we argue that the Vendian period represents a major petroleum system marked by wide-spread deposition of organic-rich marine sediments akin to the petroleum systems of the Phanerozoic record.

Chapter 2

Evaluation of $\delta^{13}C$ isotope stratigraphy for intrabasinal correlation: Vendian strata of northeast Siberia[1]

[1]Pelechaty, S.M., Kaufman, A.J., and Grotzinger, J.P., 1996, Evaluation of $\delta^{13}C$ isotope stratigraphy for intrabasinal correlation: Vendian strata of northeast Siberia: Geological Society of America Bulletin, v. 108, p. 992-1003.

ABSTRACT

Integrated sedimentologic, stratigraphic, and geochemical ($\delta^{13}C$, $\delta^{18}O$, Fe, Mn and Sr) data from Vendian-to-Cambrian-age carbonate-ramp deposits of the northeast Siberian platform (Olenek uplift and Kharaulakh Mountains region) are used to constrain primary, time-dependent oscillations in the carbon isotope record, and to evaluate $\delta^{13}C$ chemostratigraphy for high-resolution intrabasinal correlation. The Vendian $\delta^{13}C$ record of northeast Siberia reflects global variations seen elsewhere by displaying in ascending order, a strong positive isotopic shift to values near +6 ‰ (herein named the P-interval), an intermediate interval of relatively little isotopic change (I-interval), which shows, in some sections, a monotonic decrease in $\delta^{13}C$ from +2 ‰ at the base to near 0 ‰ at the top, and a negative excursion to ~ -4 ‰ (N-interval) just beneath the Vendian-Cambrian boundary. In addition to secular isotopic shifts, these strata exhibit local small-scale signals related to intrabasinal variations in subsidence, erosion, and diagenetic alteration (e.g., degradation of organic matter, dolomitization, hydrothermal and burial effects). These local, intrabasinal processes, in some cases, have modified both the magnitude and form of the primary isotopic excursions, which are used as the basis for correlation in all studies. Carbon isotope profiles provide an important method to evaluate intrabasinal variations in subsidence, erosion and stratigraphic completeness. These profiles reflect increasing subsidence along the platform-to-basin transition, while progressive truncation of isotopic profiles along this trend illustrate pronounced uplift and erosion of ramp strata along unconformity surfaces.

INTRODUCTION

An emerging $\delta^{13}C$ record of secular variation for Vendian strata is providing an important tool for temporal correlation of rocks that contain only a limited assemblage of flora and fauna necessary for high resolution chronostratigraphy (Knoll and Walter, 1992). Many workers have identified comparable $\delta^{13}C$ profiles (i.e. $\delta^{13}C$ variations displayed with respect to stratigraphic thickness) from Vendian (ca. 610 to 543 Ma; Harland and others, 1989; Bowring and others, 1993; Grotzinger and others, 1995) sections around the world (summarized in Ripperdan, 1994; Kaufman and Knoll, 1995), including northwestern Canada (Narbonne and others, 1994), southern China and Morocco (Lambert and others, 1987; Kirschvink and others, 1991; Magaritz and others, 1991), Namibia (Kaufman and others, 1991), Australia (Walter and others, 1995), and Siberia (Magaritz and others, 1986; Pokrovsky and Venagradov, 1991; Kirschvink and others, 1991; Magaritz and others, 1991; Brasier and others, 1993, 1994; Pokrovsky and Missarzhevsky, 1993; Knoll and others, 1995a; 1995b; Pelechaty and Grotzinger, 1993; Pelechaty and others, 1995). This work has formed the basis for the recognition of large-scale secular variations in paleo-oceanic $\delta^{13}C$ preserved in Vendian carbonates and organic carbon. An oscillating carbon isotope record characterizes Vendian strata overlying diamictites deposited during the latest Proterozoic glaciation (Knoll and Walter, 1992). A prominent negative excursion is noted in carbonate rocks immediately above the diamictites that leads into a positive excursion with $\delta^{13}C$ values as high as +6 ‰, and then into an interval of relatively invariant $\delta^{13}C$ values near 0 ‰ culminating in a distinctive shift to negative values before returning again to 0 ‰ near the Precambrian-Cambrian boundary (Knoll and Walter, 1992; Brasier and others, 1993; Kaufman and Knoll, 1995). The stratigraphic sections used to develop the Vendian chemostratigraphic framework are from isolated sedimentary basins that record a variety of tectonic, depositional, and

diagenetic processes. Importantly, similar large-scale $\delta^{13}C$ variations have emerged despite this geologic diversity.

High-resolution, intrabasinal correlation of Vendian strata using $\delta^{13}C$ chemostratigraphy to assess the influence of depositional and diagenetic processes on the $\delta^{13}C$ isotopic record has not yet been attempted. These processes are known to have diverse effects on primary $\delta^{13}C$ compositions of carbonate (Allen and Matthews, 1982; Arthur and others, 1983; Schidlowski and others, 1984). Diagenetic and stratigraphic studies are necessary to resolve the origin of small-scale variations in carbon isotope values in order to utilize this chronostratigraphic tool for intrabasinal correlations.

The profiles used for correlation are isotopic records that appear continuous in rock thickness, but they are not continuous in time because of depositional hiatuses resulting from unsteady sediment accumulation inherent to stratigraphic sections (Sadler, 1981). The relative completeness of isotopic profiles, however, can be assessed by comparing many profiles from different depositional settings across a single sedimentary basin (Anders and others, 1987; Sadler, 1987). Such a study provides a method to examine relative variations in sediment accumulation rate, which may serve as a proxy for basin subsidence.

This paper presents a detailed geochemical study of several carbonate-dominated stratigraphic sections from the same sedimentary basin. The basin is exposed in the Olenek uplift and Kharaulakh Mountains area of the northeastern corner of the Siberian platform, Russia (Fig. 2.1). Geochemical data (i.e., $\delta^{13}C$, $\delta^{18}O$, Fe, Mn, and Sr) are presented within a sedimentologic and stratigraphic context in order to assess secular and local signals in the $\delta^{13}C$ composition of the carbonate sediments. In addition to globally-recognized, first-order $\delta^{13}C$ shifts, smaller-scale variations are also recognized; these are evaluated in conjunction with stratigraphic and sedimentologic data for use in high-resolution, intrabasinal correlations.

The $\delta^{13}C$ profiles are constructed using stratigraphically closely-spaced carbonate samples of minimally-altered depositional components. The role of diagenesis in altering the $\delta^{13}C$ composition is assessed by carrying out both component and whole-rock sampling to determine intra-sample $\delta^{13}C$ heterogeneity. Standard petrographic, cathodoluminescent, and geochemical proxies are used to determine alteration of carbonate. This work forms the foundation for an integrated basin analysis study using carbon isotope chemostratigraphy and sequence stratigraphy (Pelechaty and others, 1995; 1996).

GEOLOGICAL SETTING: STRATIGRAPHY AND DEPOSITIONAL FACIES

Stratigraphy

Vendian carbonate rocks are exposed along several river valleys in the Olenek uplift, and along the Lena River 100 km to the east in the Kharaulakh Mountains in the northeastern part of the Siberian platform (Fig. 2.1). The carbonates consist of both limestone and dolostone. From the Olenek uplift, these strata dip gently outward in all directions, and are offset by small-scale (10's m of displacement), steeply-dipping normal faults (Krasilshchikov and Biterman, 1970). In the Kharaulakh Mountains, strata form west-verging folds of the post-Cretaceous Verkoyansk fold-thrust belt (Rodgers, 1991).

Vendian strata are less than 500 m in thickness and are bounded by regional unconformities. The Riphean-Vendian boundary is an angular unconformity that cuts down deepest into Riphean strata of the southern Olenek uplift. The Vendian-Cambrian boundary is a paleokarst erosion surface overlain by Early Cambrian (Nemakit-Daldyn Stage) siliciclastic and minor limestone strata, and rare volcanic deposits (Repina and others, 1974; Valkov, 1987; Khomentovsky and Karlova, 1993; Bowring and others,

1993; Knoll and others, 1995a). These strata thin eastward towards the Kharaulakh Mountains and are everywhere overlain by distinctively red, hyolithid-bearing Tommotian limestone.

Throughout the Olenek uplift, Vendian strata of the Khorbosuonka Group are less than 320 m thick, and comprise three formations (Sokolov and Fedonkin, 1984; Khomentovsky, 1990; Shenfel, 1991; Pelechaty and Grotzinger, 1993; Knoll and others, 1995a; Fig. 2.2): the Mastakh Formation, less than 50 m of conglomerate and dolostone; the Khatyspyt Formation, up to 180 m of black, bituminous limestone; and the Turkut Formation, 80 to 300 m of buff dolostone. The Mastakh Formation is truncated toward the southern Olenek uplift (sections 2 and 3) where the entire Khorbosuonka Group is represented by the Turkut Formation (Khomentovsky, 1990). In the Kharaulakh Mountains, rocks stratigraphically equivalent to the Khorbosuonka Group are known as the Kharayutekh Formation. They are completely exposed at section 5, and only the upper part of the formation is exposed at section 6. The lower, middle and upper members of the Kharayutekh Formation contain mixed dolostone, bituminous limestone and minor siliciclastic rocks, and have been interpreted to correlate with the Mastakh, Khatyspyt and Turkut formations, respectively (Shapovalova and Shpunt, 1982; Khomentovsky, 1990).

The age of these Vendian strata is tightly constrained. The Khorbosuonka Group contains Ediacaran soft-bodied metazoan fossils in the Khatyspyt Formation (Sokolov and Fedonkin 1984; Karlova 1987; Vodanjuk 1989; Missarzhevsky 1989; Knoll and others, 1995a), and exhibits $\delta^{13}C$ profiles similar to other latest Vendian intervals (Kaufman and others, 1991; Narbonne and others, 1994; Knoll and others, 1995a; reviewed in Kaufman and Knoll, 1995). The isotopic profile at the Khorbosuonka River contains a lower positive excursion, an interval of isotopic values near 0 ‰, and an upper negative shift at the top of the Turkut Formation (see section 4 and inset; Fig. 2.2). Knoll and others (1995a) correlated the positive isotopic shift through the

Mastakh and lower Khatyspyt formations with a similar positive isotopic excursion in the Zaris Formation of the Nama Group, Namibia. Following this correlation, U-Pb radiometric dates from volcanic ash beds interlayered with sedimentary rocks of the Nama Group allow calibration of the isotopic profiles (Grotzinger and others, 1995), and provide an age of 549 Ma for the top of the positive shift, 544 Ma for the base of the negative shift, and 543 Ma for the top of the negative shift and the Precambrian-Cambrian boundary (see inset; Fig. 2.2). This age for the boundary is also consistent with an upper intercept U-Pb age of 543.8+5.1/-1.3 Ma from a volcanic breccia at the base of the Kessyusa Formation overlying the Khorbosuonka Group (Bowring and others, 1993). The part of the Khorbosuonka Group that exhibits the positive shift is comprised of the Mastakh Formation, which forms a single depositional sequence (Knoll and others, 1995a), and the lower Khatyspyt Formation. A maximum age of 555 Ma is estimated for the base of the Khorbosuonka Group on the basis of a conservative over-estimate for the time required to form a depositional sequence (Vail and others, 1984; Christie-Blick and others, 1995). Thus, the Khorbosuonka and correlative units in northeast Siberia are considered to span a maximum of 10 m.y. during latest Vendian time.

Depositional facies

Knoll and others (1995a) described four main carbonate ramp facies, including, tidal flat, lagoon, shoal and distal, along the Khorbosuonka River (Figs. 2.1 and 2.2). Karstic features developed at the top of the Vendian interval truncate most of these facies. Minor siliciclastic deposits of marine and terrestrial origin are present at the base of these sections. These facies are briefly summarized below along with additional sedimentologic and stratigraphic observations from across the Olenek uplift and Kharaulakh Mountains (Pelechaty and Grotzinger, 1993). More detailed facies descriptions are given by Pelechaty and others (1996).

Tidal flat facies

The tidal flat facies (entirely dolostone) is composed mainly of thin-bedded, desiccation-cracked microbial laminites, minor rippled and planar laminated oolite, and edge-wise conglomerate. Early diagenetic chert nodules and white cauliflower chert, which signify the former presence of calcium sulfate evaporites, are only locally developed in the Mastakh Formation (Knoll and others, 1995a).

Lagoon facies

The lagoon facies (entirely dolostone) is characterized by intercalated thin- to medium-bedded stromatolitic biostromes, rare rudstone, grainstone and mudstone, and green shale layers between dolostone beds. These deposits have been interpreted to record sedimentation within a low-energy, shallow-water lagoonal setting (Knoll and others, 1995a).

Shoal facies

The shoal facies comprises mainly trough cross-stratified rudstone, grainstone and packstone as amalgamated units with sharp, erosive bases. Deposits are intraclastic to oncolitic. Minor stromatolitic biostromes and mudstones form interbeds, signifying incursions of lagoonal conditions in the shoal environment.

Distal ramp facies

The distal ramp facies consists of black, bituminous limestone and buff dolostone (mudstone and wackestone). These recessive deposits form nodular beds, massive debris flow units, and finely-laminated distal turbidites (Knoll and others, 1995a). Small-scale flutes and guttercasts, and soft-sediment slumps associated with the deposits are indicative of distal ramp settings. Some of the limestones contain up to 5% total organic carbon. They produce a strong fetid odor when fractured and are considered mature

petroleum source units (Chersky, 1986; Bolshakov, 1987). The preservation of ubiquitous organic matter in the limestones indicates that the environment was likely anoxic or had high sedimentation (e.g., North, 1990).

Karst

Karst facies at the top of the Turkut Formation along the Khorbosuonka River (Knoll and others, 1995a) also extend throughout the Olenek uplift and Kharaulakh Mountains. The paleokarst is represented by an extensive erosion surface with up to 20 m of local relief associated with potholes, shallow sinkholes, karren, and decimeter-scale caves filled with Cambrian sandstone. In the Olenek uplift, typically buff dolostones of the Turkut Formation are stained red in color owing to the development of terra rossa along this ancient subaerial exposure surface (e.g., Estaban and Klappa, 1983; James and Choquette, 1984; Pelechaty and others, 1991).

Siliciclastic facies

Minor siliciclastic deposits consist of conglomerate, sandstone and shale. Trough and hummocky cross-stratified marine sandstone and minor shale of the lower Khatyspyt Formation (section 4; Fig. 2.2) are also present in the lower Turkut Formation in the southern Olenek uplift, and in the lower Kharayutekh Formation (section 5), where sandstone is intercalated with mudcracked shale and stromatolitic dolostone of shallow-marine origin (Fig. 2.2). The lower Mastakh Formation contains up to 10 m of intercalated quartz-pebble conglomerate and sandstone, both showing planar stratification and unidirectional cross-bedding. Beds show abundant truncation and channelization features. Collectively, these attributes are interpreted to signify deposition of channel-floor dunes in braided rivers (e.g., Walker and Cant, 1984).

Stratigraphically, the shallowest-water tidal flat and lagoonal facies are found primarily in the southern Olenek uplift, whereas deeper-water shoal and distal ramp

facies dominate sections of the northern Olenek uplift and Kharaulakh Mountains (Fig. 2.2). The stratigraphic variation of facies is interpreted to record a general northeast platform-to-basin transition (Read, 1983; Grotzinger, 1989).

GEOCHEMISTRY: SAMPLING, ANALYSES, AND RESULTS

Over 320 carbonate samples were evaluated using standard petrographic, cathodoluminescent, and geochemical proxies (e.g., $\delta^{13}C$, $\delta^{18}O$, Fe, Sr, and Mn) to assess diagenetic history, and to recognize least-altered samples (Table 2.1). The following sections outline procedures that were employed for sample collection, laboratory preparation, and analysis.

Sampling and analytical procedures

Component (e.g. individual allochems) and whole-rock samples were collected using a motorized drill equipped with variably sized (2 to 0.5 mm diameter) drill bits. Whole-rock samples were collected where components were too fine-grained for individual sampling. A suite of mainly whole-rock samples were also collected from the lower Kytyngeder River section (section 2 in Fig. 2.2) in order to test the geochemical variation between whole-rock and component sampling. Whole-rock samples were drilled from areas on thick sections devoid of macroscopic diagenetic fabrics.

Duplicate standard-size thin sections and 1 mm thick sections were made for each component sample. The types of carbonate components that were selected for sampling were determined from plain-light microscopic and cathodoluminescent analyses of thin sections. Sample locations were then spotted on complementary thick sections and drilled. The carbonate composition (e.g. calcite versus dolomite) of samples

was determined using hydrochloric acid in the field, and by staining thin sections with Alizarin red-S.

Both depositional and diagenetic components were collected. In some cases two separate powdered samples were taken from a single thick section (e.g., a depositional and a diagenetic sample, or two separate depositional samples) in order to assess intra-sample geochemical variation. For organic-rich carbonate rocks (i.e. black, bituminous limestone), samples of dark, organic-rich layers and light, organic-poor layers were obtained to evaluate isotopic effects related to the alteration of sedimentary organic matter. Depositional components that were sampled included micritic carbonate from massive and laminated detrital sediment (e.g., mudstone and wackestone), intraclasts, oncolitic cortices, and oolitic cortices of packstone, grainstone and rudstone, and from domal to stratiform stromatolites (Table 2.1). Diagenetic components include neomorphic pseudospar and spar, and late-stage, void-filling blocky spar and baroque dolomite (e.g., Bathurst, 1975; James and Klappa, 1983; Choquette and James, 1987; Zempolich and others, 1988). These features typically are characterized by high Fe and Mn contents, and are dull to non-luminescent.

Procedures for sample preparation, and stable isotopic (carbon and oxygen) and major element analyses (Fe, Mn, and Sr) follow those described in detail by Derry and others (1992) and Narbonne and others (1994).

Results

The geochemical ($\delta^{13}C$ and $\delta^{18}O$ values, and Fe, Mn, and Sr abundance) and petrographic data are summarized in Table 2.1. Both $\delta^{13}C$ and $\delta^{18}O$ are reported as ‰ PDB. Graphically, $\delta^{13}C$ data are plotted as profiles with corresponding stratigraphic sections (Fig. 2.2), and additional plots are presented to illustrate observed geochemical trends.

Major element data

Major element abundance data (Fe, Mn, and Sr) are plotted versus $\delta^{18}O$ in order to evaluate post-depositional alteration (e.g., Brand and Veizer, 1980; Bathurst and Land, 1986; Brasier and others, 1994; Fig. 2.3). Much of the $\delta^{18}O$ data ranges from -2 to -10 ‰, and shows little variation in either Fe (< 5000 ppm) or Mn (< 400 ppm) concentration. As expected, the diagenetic components (e.g. burial cement and neomorphic carbonate) are enriched in Fe and Mn (e.g., Grover and Read, 1983; Figs. 2.3a and 2.3b). Also, dolomudstones of the lower member of the Kharayutekh Formation at section 5 (Fig. 2.4) are enriched in Fe (up to 19,000 ppm) and Mn (up to 9, 000 ppm), exhibit high Mn/Sr ratios, and dull to very-dull to non-luminescence. These particular depositional components are interpreted to be altered despite minimal recrystallization and lack of evidence for additional $\delta^{18}O$ depletion. This alteration is stratigraphically restricted to the lower part of the Vendian succession and is interpreted to be related to migration of burial fluids along the Riphean-Vendian unconformity. Apart from these diagenetically altered carbonates and other late-burial cements, the lack of correlation of Fe and Mn abundance with $\delta^{18}O$ suggests that throughout this region the depositional components are minimally altered.

Sr abundance is also uncorrelated with $\delta^{18}O$ but varies with depositional facies (Fig. 2.3c). The distal ramp limestones (between 200 and 2500 ppm Sr) are enriched in Sr relative to their dolostone counterparts and dolostones of other facies (< 200 ppm). Even the distal ramp limestones (i.e., black, bituminous limestone) are enriched compared to the shoal facies limestones (i.e., oncolitic grainstone and rudstone), which plot together with dolostones. The high Sr concentrations of the distal ramp limestones suggest that these sediments were originally aragonitic in composition (Davis, 1977; James and Choquette, 1984; Aissaoui, 1985; Tucker, 1986). The dolomitic distal ramp facies probably lost Sr after deposition through dolomitization. Additional field and petrographic observations further suggest an aragonitic mineralogy for these

limestones. Fabric-selective porosity is typical of carbonates directly beneath the paleokarst at the top of the Turkut and Kharayutekh formations. Within grainstones and rudstones, porosity formed by selective dissolution of mudstone intraclasts, which form the nuclei of oncoids, while oncoidal rims remain intact. Although now completely dolomitized, selective dissolution strongly suggests that these rocks were bimineralic, and that the mudstone intraclasts were composed of a relatively more soluble calcium carbonate form (i.e., aragonite).

$\delta^{13}C$ Profiles

Five $\delta^{13}C$ profiles were constructed from analyses of organic-poor, depositional carbonate components for the Olenek uplift (sections 1, 2, and 3) and Kharaulakh Mountains (sections 5 and 6; Fig. 2.2). An additional, previously published $\delta^{13}C$ profile by Knoll and others (1995a) from the Olenek uplift is included (section 4).

Khorbosuonka River (section 4): The Khorbosuonka River $\delta^{13}C$ profile reveals prominent excursions interpreted as secular variations (Knoll and others, 1995a). The base of the profile is marked by a distinct positive excursion, defined by $\delta^{13}C$ values that rise up section from near +2 to +6 ‰ through the Mastakh Formation and then decline to values near 0 ‰ in the lower Khatyspyt Formation. Values through the remainder of the Khatyspyt Formation are variable, ranging between -4 and +4 ‰, with some of the variation likely associated with early organic diagenesis in these bituminous limestones (Knoll and others, 1995a). An upper interval of little change with $\delta^{13}C$ values near 0 ‰ characterizes the lower Turkut Formation at this section. This is followed by a negative excursion to values near - 3 ‰ beginning approximately 20 m below the top of the Turkut Formation.

Olenek River (section 1): The Olenek River profile has a $\delta^{13}C$ pattern similar, in some respects, to the profile at section 4. The base of the profile here shows moderately positive $\delta^{13}C$ values (up to +3 ‰) in the Khatyspyt Formation that decrease

at the boundary of the overlying Turkut Formation to 0 ‰, which then extend further upwards through the lower 80 m of the formation. A well-defined negative excursion to -3.5 ‰ begins 50 m beneath the upper Turkut Formation boundary (Fig. 2.2).

Oolahan Ooekhtekh River (section 3): This profile exhibits a $\delta^{13}C$ profile that is slightly different from the profiles 1 and 4. Positive $\delta^{13}C$ values up to +4 ‰ mark the base of the section, and these decrease to 0 ‰ over 50 m of stratigraphic section. Above this, most of the Turkut Formation is characterized by little change in $\delta^{13}C$ with values ranging between - 1 and -2 ‰. Unlike $\delta^{13}C$ profiles at sections 1 and 4, this segment contains carbonates which are relatively invariant and consistently depleted in ^{13}C. The top of the section, approximately 60 m beneath the upper Turkut Formation boundary, exhibits positive values near +1 ‰.

Kytyngeder River (section 2): The Turkut Formation in the Kytyngeder River profile, consisting of primarily whole-rock data, shows greater isotopic variability (ranging between -4 and +3 ‰) than that recognized in the Turkut Formation at section 3 located only 15 km to the north. The upper Kytyngeder River profile includes strata (~ 60 m) not exposed along the Oolahan Ooekhtekh River (section 3); isotopic compositions of carbonates here are from component samples and are similar to those in the upper part of section 3 with $\delta^{13}C$ values near +1 ‰.

Chekurov anticline (section 5): The Chekurov anticline profile has a few data points in the lower part of the middle member of the Kharayutekh Formation with values up to +4 ‰. These are followed up section by slightly variable $\delta^{13}C$ values that are less than 0 ‰ near an 80 m thick diabase sill. Above this, at the lower contact of the upper member, $\delta^{13}C$ values are near +2 ‰ and decrease to -1 ‰ at the top of the section.

Bokursky anticline (section 6): $\delta^{13}C$ values in the Bokursky anticline profile are variably enriched in ^{13}C, ranging between 0 and +3.5 ‰.

The $\delta^{13}C$ profiles are composed of isotopic carbon values from a variety of depositional facies. However, facies appear not to influence the isotopic composition of

carbonate. Within the invariant isotopic interval (I-interval; see below), all facies have overlapping $\delta^{13}C$ values that range between -2 and +2 ‰ (Fig. 2.5a).

DISCUSSION OF GEOCHEMICAL RESULTS: DIAGENETIC MODIFICATION OF $\delta^{13}C$ VALUES

The possibility of diagenetic alteration of $\delta^{13}C$ values of carbonate samples was investigated on various scales, from mm-scale variations within samples to km-scale variations across the basin. The following section discusses the possible effects of various diagenetic processes, including, organic diagenesis, dolomitization, meteoric diagenesis, contact metamorphic effects, and burial diagenesis.

Organic-matter diagenesis

Bituminous limestones and uncommon dolostones of distal ramp facies contain abundant organic carbon as dark interstitial material. In several cases, both organic-rich and organic-poor subsamples were collected from the same hand specimen (Table 2.2). In most cases, organic-rich portions of samples are depleted in ^{13}C relative to their organic-poor counterparts. This depletion is generally interpreted to record the incorporation of carbonate formed during the *in situ* oxidation of organic matter producing isotopically light CO_2 (Irwin and others, 1977). Some variation in $\delta^{13}C$ values through the Khatyspyt Formation at section 4 (Knoll and others, 1995a), and the Kharayutekh Formation at sections 5 and 6 may also be related to this process.

Dolomitization

In some cases $\delta^{13}C$ variations appear to be related to the distribution of limestone and dolostone in these sections, rather than to temporal changes in the isotopic

composition of seawater. For example, the $\delta^{13}C$ variation shown in the middle and upper members of the Kharayutekh Formation in the profile at section 5 is correlated with the distribution of carbonate mineralogy (Figs. 2.2, 2.4 and 2.5b). In general, the limestones in this section are depleted in ^{13}C relative to dolostones. At least four interpretations can be used to explain these variations.

(1) The distribution of limestones stratigraphically above and below the dolostones in this section is coincident with small-scale secular variations in seawater $\delta^{13}C$.

(2) The observed isotopic trend could be a signal of depth-dependent variations in ancient seawater ^{13}C. Modern oceans do show a negative gradient in $\delta^{13}C$ with depth, which is recorded in carbonates precipitated along this gradient. Surface waters are enriched in ^{13}C owing to up-take and removal of ^{12}C during photosynthetic production of biomass (Berger and Vincent, 1986); oxidation of isotopically light organic matter at depth additionally enhances the seawater carbon-isotopic gradient. In the upper member of the Kharayutekh Formation at section 5, the occurrence of shallow-water dolostones and deep-water limestones suggest depth-dependent variations. However, at the top of the formation, both shallow- and deep-water limestones occur, and both have similar $\delta^{13}C$ values. The lack of absolute constraints on water depths and samples of coeval deposits representative of varying water depths makes it difficult to determine whether an isotopic gradient existed in seawater at this time. Nonetheless, given the existing data, it seems unlikely that depth-dependent variations are controlling the isotopic differences between limestones and dolostones.

(3) The isotopic difference could be related to the authigenic formation of dolomite directly from Vendian seawater. Sheppard and Schwarcz (1970) inferred on the basis of results of high temperature experiments, that at temperatures at sedimentary conditions dolomite is enriched in ^{13}C by as much as 2 to 3 ‰ relative to calcite, if both phases are in isotopic equilibrium. For an equilibrium isotope effect to

have resulted in the present distribution of $\delta^{13}C$ values would require that both calcite and dolomite precipitated from seawater with a constant carbon-isotopic composition. Ooids within tidal flat facies dolostones exhibit well preserved, concentrically-laminated, cortical fabrics suggestive of an original calcitic mineralogy (e.g., Tucker, 1983). This observation suggests that the dolomite in these sections is not primary in origin, and argues against the suggestion that limestone and dolostone may have formed contemporaneously.

(4) Lastly, it is possible that differences in $\delta^{13}C$ values in this section and elsewhere in the basin may be related to secondary dolomitization, such that these samples now more closely reflect the isotopic composition of the dolomitizing fluids. In particular, this may occur in section 5 where dolostones have high Mn/Sr ratios and are enriched in $\delta^{13}C$ relative to the limestones in the same section (Figs. 2.2 and 2.4). A few studies have demonstrated that dolomitization can lead to enrichment of isotopic-carbon. For example, reflux-style dolomitization of limestone in the presence of brines enriched in ^{13}C through anaerobic fermentation (i.e., methanogenesis) has been interpreted to result in a positive offset of primary $\delta^{13}C$ values of dolomitic samples from Paleozoic reefs (Sears and Lucia, 1980; Cercone and Lohmann, 1987). The offset is caused by the addition of newly-formed dolomite with significantly enriched ^{13}C compositions. While incorporation of even small amounts of CO_2 formed as a byproduct of bacterial methanogenesis can alter $\delta^{13}C$ values of sediments, it seems unlikely that this processs would effect every sample in a succession to the same degree.

Meteoric diagenesis

In carbonate-dominated successions, meteoric diagenesis is common, and has been found elsewhere to modify the isotopic and elemental composition of carbonate. Following earlier studies (e.g., Knoll and others, 1995a), samples with Mn/Sr > 10 and

$\delta^{18}O < -10$ ‰ are chosen to be altered. Permeable limestones, particularly those interbedded with siliciclastic rocks, can be altered by such meteoric diagenesis, such as from the basal part of the Kharayutekh Formation (Figs. 2.2 and 2.4). The stratigraphic significance of these isotopic compositions is interpreted with caution. On the other hand, thick limestone units from this basin are considered unaltered on the basis of low Mn/Sr values, high Sr abundances, and little altered $\delta^{18}O$ values. The $\delta^{13}C$ values from these facies are interpreted to record primary secular variations.

Karst-related diagenesis has been found elsewhere to alter the isotopic composition of carbonate. In this case, fluids are enriched in ^{18}O through evaporation and depleted in ^{13}C by the addition of soil CO_2 (Allen and Matthews, 1982; Beeunas and Knauth, 1985). However, while negative trends in $\delta^{13}C$ values are seen in sections 1 and 4 (Fig. 2.2), no trend is noted in the other sections immediately beneath the paleokarst. Also, there is no discernible variation in $\delta^{18}O$ of samples approaching this basin-wide exposure surface (Fig. 6). The negative $\delta^{13}C$ excursion seen in a few of these northern Siberian profiles also have been noted in Precambrian-Cambrian boundary sections from southern Siberia, Morocco, northwest Canada, China and Iran (summarized in Kaufman and Knoll, 1995) where no exposure surfaces have been recognized. These are all interpreted as records of secular variation rather than diagenetic alteration.

Contact-metamorphic effects

High-temperature effects associated with igneous bodies appears to deplete carbonate with respect to ^{13}C and ^{18}O. The isotopic effects of diabase intrusion may be evident in section 5 (Fig. 2.2) in the lower part of the Kharayutekh Formation. The carbonates near the sills are depleted in ^{13}C but have $\delta^{18}O$ values similar to carbonates throughout the section (Figs. 2.2, 2.4 and 2.6).

At section 6, dolostones are highly altered in outcrop showing evidence of internal brecciation and development of crackle breccia, with fractures and intra-block zones filled with very coarse crystalline spar. This style of alteration is often attributed to hydrothermal activity, which may result in significant isotopic alteration (see covariance of ^{13}C and ^{18}O; Fig. 2.5c). An unaltered version of this profile may have consisted of all values near +2 ‰, which may represent the invarient isotopic interval (i.e., the I-interval; see below) between the lower positive and upper negative shifts. High-temperature alteration of these carbonates may have occurred in earliest Cambrian time during extrusion of basaltic lavas now present in the lower Tyuser Formation overlying the Vendian carbonates (Vidal and others, 1995). Lacking elemental data for these samples, it is difficult to evaluate further diagenetic alteration, but we view these $\delta^{13}C$ values with caution.

Burial diagenesis

Subsamples within individual hand specimens show burial precipitates are systematically depleted in $\delta^{18}O$ relative to marine depositional components (Fig. 2.5b; Table 2.3), which is typical of diagenetically-altered carbonate (Lohmann, 1982; Arthur and others, 1983; Grover and Read, 1983; Choquette and James, 1987). However, there seems to be no preferential change in ^{13}C of depositional components relative to burial cements (Table 2.3).

INTEGRATION OF GEOLOGICAL AND GEOCHEMICAL DATA

Correlation of the $\delta^{13}C$ profiles

For the purpose of intrabasinal correlation, the terminal Vendian $\delta^{13}C$ chemostratigraphic record in northeast Siberia is divided into three isotopically-defined

intervals, and include with decreasing age (see inset in Fig. 2.2): a positive shift (P-interval), an interval of relatively invariant isotopic composition (I-interval), and a negative shift (N-interval).

Correlation of the $\delta^{13}C$ profiles of the Olenek uplift and Kharaulakh Mountains is based on integration of both the isotopic data and regional stratigraphic and sedimentologic trends. The proposed chemostratigraphic correlation is also supported by sequence stratigraphic correlation of these same sections, which is described elsewhere (Pelechaty and others, 1995; 1996). The most complete $\delta^{13}C$ record in this region, as shown by the profile at section 4 (Knoll and others, 1995a), exhibits distinct, large-magnitude oscillations ideal for chemostratigraphic correlation. This isotopic record includes all three isotopic intervals. The P-interval is well-developed through the Mastakh and lower Khatyspyt formations and is interpreted to correlate with the basal positive excursions at sections 1, 2, and 3 in the Olenek uplift area. It is less confidently correlated with the basal part of the middle member of the Kharayutekh Formation at section 5 where the excursion is defined by only a few data points. Correlation of these positive shifts is supported stratigraphically by the recognition of a significant marine flooding surface (A in Fig. 2.2) at this level, defined by a sharp transition from shallow-water dolostones to black, bituminous limestones of the distal ramp facies that can be correlated throughout this region.

The I-interval is developed across the basin but varies greatly in its stratigraphic thickness. The I-interval at section 4 is correlated with similar intervals at sections 1, 2, and 3 in the Olenek uplift, and, in the Kharaulakh Mountains, with almost the entire isotopic profile at section 5, and with the profile at section 6, which is interpreted to reflect an altered primary signal (Figs. 2.2 and 2.5c). This correlation reveals pronounced thickening of the I-interval from section 1 to section 5: from 75 m at section 1, to 200 m at section 4, and to at least 420 m at section 5; the N-interval is not preserved in section 5, where the total stratigraphic thickness of the I-interval is

unknown. The I-interval at section 6 probably correlates with part of the I-interval in the upper member of the Kharayutekh Formation at section 5 on the basis of correlation of additional prominent flooding surfaces seen at both sections (B in Fig. 2.2). Because of variations in facies, mineralogy, igneous activity, and diagenesis across the basin, it is unclear whether the small-scale variations in the I-interval reflect secular variation and/or diagenetic alterations.

Overlying the I-interval, the N-interval is well developed only at sections 1 and 4. In general, the isotopic intervals appear to be progressively truncated beneath the paleokarst capping the Turkut and Kharayutekh formations from section 1 towards section 6.

Depositional effects on $\delta^{13}C$ excursions

The geometry of the $\delta^{13}C$ profiles is considered to record variations in the long-term sediment accumulation rate (≈ subsidence rate), and the distribution and magnitude of hiatuses within the sedimentary basin. These effects have not received much prior attention because of a primary focus on intercontinental rather than intrabasinal correlations.

Sediment accumulation rate

The obvious effect of accumulation rate on the ^{13}C isotopic record is to modify the general form of isotopic excursions. Areas of low sediment accumulation show a condensed record in some cases with abrupt isotopic changes. In contrast, sites of high sediment accumulation are marked by isotopic profiles with generally smoother isotopic variations. For the shallow-water carbonates discussed here, where variations in depositional water depth (< tens of meters) are small relative to the thickness of the deposits (hundreds of meters), sediment accumulation rate is considered to be related to

variations in the rate of tectonic subsidence (Schlager, 1981; Sadler, 1981). In particular, in this basin strata of the I-interval accumulated either entirely near sea level (sections 2 and 3), or shoaled to sea level at the close of I-interval time (sections 1, 4, and 5).

Relative to the P-interval and N-interval at the base and top of these sections, respectively, the I-interval has been considered a significant isotopic interval that occupies a thick portion of the Vendian stratigraphic record (e.g. Knoll and Walter, 1992; Narbonne and others, 1994; Knoll and others, 1995a). The significance of the I-interval, in terms of rock thickness, varies across the Olenek uplift and Kharaulakh Mountains and is interpreted to reflect variations in sediment accumulation rate. Subsidence increased towards the Kharaulakh Mountains during P-interval and I-interval times. Section 1 is located farthest to the west, and indicates that this part of the basin was associated with, on average, lower subsidence rates. The basin underwent eastward-increasing subsidence from the eastern Olenek uplift to the Kharaulakh Mountains at section 5. This is consistent with the regional platform-to-basin transition: mainly tidal flat facies in the southern Olenek area to mixed shoal and distal ramp facies further eastwards.

The observed subsidence pattern during I-interval time shows that rates were relatively lower at section 1 but greater to the south (sections 2 and 3) and east (section 4) over a distance of 45 km. The regions of greater subsidence show contrasting depositional responses. To the south, at sections 2 and 3, tidal flat sediments appear to have accumulated at rates equal to that of local subsidence, whereas to the east at section 4, subsidence outpaced sediment accumulation, causing drowning of the platform and deposition of deeper-water, outer ramp sediments, followed by shoaling.

The intervening region at section 1 may represent a foreland bulge. However, the spatial dimensions of the postulated tectonic bulge approaches the lower size limits of other peripheral bulges (Karner and Watts, 1983; Waschbusch and Royden, 1992;

McCormick and Grotzinger, 1992). Section 1 is located furthest to the west, and may partially reflect onlap onto the craton in a region of lower subsidence during I-interval time. This interpretation is further supported by unpublished seismic profiles that show westward thinning of Vendian strata. Local syn-sedimentary block faulting may also have lead to complex subsidence patterns observed in the Olenek uplift (e.g. Bechstädt and Boni, 1989) during the close of the Vendian during N-interval time and during development of the unconformity that caps the Turkut and Kharayutekh formations.

Hiatuses

The distribution and magnitude of depositional hiatuses within the stratigraphic record are complex and represent much geologic time (Sadler, 1981; Anders and others, 1987). This attribute of the stratigraphic record adds a distinct randomness to preservation of isotopic events, which affects both form and magnitude of carbon isotope excursions. In northeast Siberia, the paleokarst unconformity which caps the Turkut and Kharayutekh formations is a prominent hiatal surface that shows systematic variations in the amount of erosion throughout the Olenek uplift and Kharaulakh Mountains area. This erosion has had the effect of partially erasing the carbon isotope record. The $\delta^{13}C$ profiles show progressive down-cutting of the Turkut and equivalent strata from section 1 towards the southern Olenek uplift, and towards the Kharaulakh Mountains where erosion has removed strata well beneath N-interval-age deposits (section 6).

The unconformity defining the top of the Turkut and Kharayutekh formations also variably truncates Vendian strata across the Siberian platform based on comparison of carbon isotope profiles. This unconformity is expressed throughout the eastern Siberian platform as either a well-developed paleokarst or as a subtle stratigraphic surface (Khomentovsky, 1990). Erosion along this surface appears to have been more

pronounced in northern Siberia than in the south. The N-interval is variably truncated across the north, from the western Anabar region (Pokrovsky and Venagradov, 1991; Pokrovsky and Missarzhevsky, 1993; Knoll and others, 1995b), to the Kharaulakh Mountains, while to the south, a complete N-interval with values that return to 0 ‰ at the top of Vendian strata, is developed at sections along the Lena and Aldan rivers (Magaritz and others, 1986, 1991; Kirschvink and others, 1991; Brasier and others, 1994).

CONCLUSIONS

Latest Vendian-age carbonate-dominated strata of the Olenek uplift and Kharaulakh Mountains in northeast Siberia provide a unique opportunity to examine variations between many $\delta^{13}C$ profiles within a single sedimentary basin. These carbon isotope profiles record secular oscillations in $\delta^{13}C$, as well as secondary signals. The Vendian system in this region exhibits three prominent secular isotopic events, which are observed in several other basins world-wide: an older positive shift (P-interval) with values up to +6 ‰, an invariant interval (I-interval) with values between +1 and -2 ‰, and a younger negative shift (N-interval) characterized by values to -4 ‰.

Both the magnitude and form of these secular oscillations vary from profile to profile and are considered to reflect the effects of diagenetic and depositional processes. A variety of early- to late-stage diagenetic processes (i.e., organic-matter diagenesis, dolomitization, burial diagenesis and contact metamorphic effects) may alter the magnitude of the secular shifts, which is well displayed between limestone and dolostone at some sections. The small-scale isotopic variation observed in the I-interval in this basin probably reflects both secular and diagenetic signals. However, further investigation of stratigraphic sections through the I-interval is needed to distinguish between secular and local signals.

Depositional processes modify the pattern of primary isotopic shifts. For instance, variations in subsidence rate affects the stratigraphic thickness of isotopic events, while variations in erosion associated with unconformities truncate isotopic signals. This implies that the carbon isotope profiles from other parts of the Siberian platform, and from other sedimentary basins may be missing key isotopic events, or partial events that are spliced together forming complex, incomplete records.

Because of the variability of carbon isotope records within a sedimentary basin, additional geochemical, sedimentologic, and stratigraphic data are required to unravel complexities of diagenesis and basin dynamics, and their effects on the preservation of primary isotopic-carbon preserved in carbonate. However, despite small-scale complications provided by non-secular isotopic signals preserved within carbon isotope profiles, chemostratigraphy provides a useful method for high-resolution intrabasinal correlation, and resolving basin dynamics (see Pelechaty et al., 1996; Pelechaty, 1996).

REFERENCES

Aissaoui, D.M., 1985, Botryoidal aragonite and its diagenesis: Sedimentology, v. 32, p. 345-362.

Allen, J.R., and Matthews, R.K., 1982, Isotope signatures associated with early meteoric diagenesis: Sedimentology, v. 29, p. 797-817.

Anders, M.H., Krueger, S.W., and Sadler, P.M., 1987, A new look at sedimentation rates and the completeness of the stratigraphic record: Journal of Geology, v. 95, p. 1-14.

Arthur, M.A., Anderson, T.F., Kaplan, I.R., Veizer, J., and Land, L.S., 1983, Stable isotopes in sedimentary geology: SEPM Short Course No. 10, 435 p.

Bathurst, R.G.C., 1975, Carbonate sediments and their diagenesis: Developments in Sedimentology 12: Amsterdam, Elsevier Scientific Publication Co., 658 p.

Bathurst, R.G.C. and Land, L.S., 1986, Part 5: Diagenesis 1, *in* Warme, J. E., and Stanley, K. W., eds., Carbonate Depositional Environments: Modern and Ancient: Golden, Colorado, Colorado School of Mines Quarterly, 81, p. 1-41.

Bechstädt, T., and Boni, M., 1989, Tectonic control on the formation of a carbonate platform: The Cambrian of southwestern Sardinia: *in* Crevello, P.D., Wilson, J.L., Sarg, J.F., and Read, J.F., eds., Controls on Carbonate Platform and Basin Development: SEPM Special Publication No. 44, p. 107-122.

Beeunas, M.A., and Knauth, L.P., 1985, Preserved stable isotope signatures of subaerial diagenesis in the 1.2 Ga Mescal Limestone, central Arizona: Implications for the timing and development of a terrestrial plant cover: Geological Society of America Bulletin, v. 96, p. 737-745.

Berger, W.H., and Vincent, E., 1986, Deep-sea carbonates: reading the carbon isotope signal: Geologishes Rundshau, v. 75, p. 249-269.

Bolshakov, Y.A., 1987, Geology and geochemistry of oil and gas, and coal, Yakutia: Russian Academy of Sciences, Yakutia, 143 p. (in Russian)

Bowring, S.A., Grotzinger, J.P., Isachsen, C.E., Knoll, A.H., Pelechaty, S.M., and Kolosov, P., 1993, Calibrating rates of early Cambrian evolution: Science, v. 261, p. 1293-1298.

Brasier, M.D., Khomentovsky, V.V., and Corfield, R.M., 1993, Stable isotopic calibration of the earliest skeletal fossil assemblages in eastern Siberia (Precambrian-Cambrian boundary): Terra Nova, v. 5, p. 225-232.

Brasier, M.D., Corfield, R.M., Derry, L.A., Rozanov, A.Y., and Zhuravlev, A.Y., 1994, Multiple $\delta^{13}C$ excursions spanning the Cambrian explosion to the Botomian crisis in Siberia: Geology, v. 22, p. 455-458.

Brand, U., and Veizer, J., 1980, Chemical diagenesis of a multicomponent system-1. Trace elements: Journal of Sedimentary Petrology, v. 50, p. 1219-1236.

Cercone, K.R., and Lohmann, K.C., 1987, Early diagenesis of middle Silurian pinnacle reefs, northern Michigan,*in* Cercone, K.R., and Budai, J.M., eds.: Ordovician and Silurian Rocks of the Michigan Basin and its Margins: Michigan Basin Geological Society Special Publication No. 4, p. 109-130.

Chersky, H.V., 1986, Upper Precambrian-Phanerozoic oil and gas deposits, eastern part of the Siberian platform: Russian Academy of Sciences, Yakutia, 123 p. (in Russian).

Choquette, P.W., and James, N.P., 1987, Diagenesis no. 12. Diagenesis in Limestones - 3. The deep burial environment: Geoscience Canada, v. 14, p. 3-35.

Christie-Blick, N., Dyson, I.A., and von der Borch, C.C., 1995, Sequence stratigraphy and the interpretation of Neoproterozoic earth history: Precambrian Research, v. 73, p. 3-26.

Davis, G.R., 1977, Former magnesium calcite and aragonitic submarine cements in Upper Paleozoic reefs of the Canadian Arctic: Geology, v. 5, p. 11-15.

Derry, L.A., Kaufman, A.J., and Jacobsen, S.B., 1992, Sedimentary cycling and environmental change in the Late Proterozoic: Evidence from stable and radiogenic isotopes: Geochemica et Cosmochimica Acta, v. 56, p. 1317-1329.

Estaban, M., and Klappa, C.F., 1983, Subaerial Exposure, *in* Scholle, P. A., Bebout, D. G., and Moore, C. H., eds., Carbonate Depositional Environments: Tulsa, American Association of Petroleum Geologists, Memoir 33, p. 1-93.

Grotzinger, J.P., 1989, Facies and evolution of Precambrian carbonate depositional systems: Emergence of the modern platform archetype, *in* Crevello, P.D., Wilson, J.L., Sarg, J.F., and Read, J.F., eds., Controls on Carbonate Platform and Basin Development: SEPM Special Publication No. 44, p. 79-106.

Grotzinger, J.P., Bowring, S.A., Saylor, B.Z., and Kaufman, A.J., 1995, Biostratigraphic and geochronologic constraints on early animal evolution: Science, v. 270, p. 598-604.

Grover, G.J., and Read, J.F., 1983, Paleoaquifer and deep-burial related cements defined by regional cathodoluminescence patterns, Middle Ordovician carbonates, Virginia: American Association of Petroleum Geologists Bulletin, v. 67, p. 1275-1303.

Harland, B.W., Armstrong, R.L., Cox, A.V., Smith, A.G., and Smith, D.G., 1989, A Geologic Time Scale: Cambridge, Cambridge University Press, 263 p.

Irwin, H., Curtis, C., and Coleman, M., 1977, Isotopic evidence for source of diagenetic carbonates formed during burial of organic-rich sediments: Nature, v. 269, p. 209-213.

James, N.P., and Choquette, P.W., 1983, Limestones: Introduction: Geoscience Canada, v. 10, p. 159-161.

James, N.P., and Choquette, P.W., 1984, Diagenesis 9. Limestones - the meteoric diagenetic environment: Geoscience Canada, v. 11, p. 161-194.

James, N.P., and Klappa, C.F., 1983, Petrogenesis of Early Cambrian reef limestones, Labrador: Canada: Journal of Sedimentary Petrology, v. 53, p. 1051-1096.

Karlova, G.A., 1987, First findings of skeletal fauna in the Turkut Formation of the Olenek uplift: Doklady Academica Science USSR, v. 292, p. 204-205 (in Russian).

Karner, G.D., and Watts, A.B., 1983, Gravity anomalies and flexure of the lithosphere at mountain ranges: Journal of Geophysical Research, v. 88, p. 10449-10477.

Kaufman, A.J., Hayes, J.M., Knoll, A.H., and Germs, G.J.B., 1991, Isotopic compositions of carbonates and organic carbon from upper Proterozoic successions in Namibia: stratigraphic variation and the effects of diagenesis and metamorphism: Precambrian Research, v. 49, p. 301-327.

Kaufman, A.J. and Knoll, A.H., 1995, Neoproterozoic variations in the C-isotopic composition of seawater: Stratigraphic and biogeochemical implications: Precambrian Research, v. 73, p. 27-49.

Khomentovsky, V.V., 1990, Chapter 5: Vendian of the Siberian Platform, Sokolov, B. S., and Fedonkin, M. A., eds.: Berlin, Springer-Verlag, 2, 103-183 p.

Khomentovsky, V.V., and Karlova, G.A., 1993, Biostratigraphy of the Vendian-Cambrian beds and the lower Cambrian boundary in Siberia: Geological Magazine, v. 130, p. 29-45.

Kirschvink, J.L., Magaritz, M., Ripperdan, R.L., Zhuravlev, A.Y., and Rozanov, A.Y., 1991, The Precambrian-Cambrian boundary: Magnetostratigraphy and carbon isotopes resolve correlation problems between Siberia, Morocco, and south China: GSA Today, v. 1, p. 69-91.

Knoll, A.H., Grotzinger, J.P., Kaufman, A.J., and Kolosov, P., 1995a, Integrated approaches to terminal Proterozoic stratigraphy: An example from the Olenek Uplift, northeastern Siberia: Precambrian Research, v. 73, p. 251-270.

Knoll, A.H., Kaufman, A.J., Semikatov, M.A., Grotzinger, J.P., and Adams, W.E., 1995b, Sizing up the sub-Tommotian unconformity in Siberia: Geology, v. 23, p. 1139-1143..

Knoll, A.H. and Walter, M.R., 1992, Latest Proterozoic stratigraphy and Earth History: Nature, v. 356, p. 673-678.

Krasilshchikov, A.A., and Biterman, I.M., 1970, Proterozoic group of the Olenek uplift, *in* Markov, F.G., ed., Geology of the USSR Western Part of the Yakutian ASSR, Nedra, p. 91-100 (in Russian).

Lambert, I.B., Walter, M.R., Wenlong, Z., Songnian, Lu., and Guogan, Ma., 1987, Paleoenvironmental and carbon isotope stratigraphy of Upper Proterozoic carbonates of the Yangtze Platform: Nature, v. 325, p. 140-142.

Lohmann, K.C., 1982, Inverted J carbon and oxygen isotopic trends - criteria for shallow meteoric phreatic diagenesis: Geological Society of America Abstract with Program, p. 548.

Magaritz, M., Hoser, W.T., and Kirschvink, J.L., 1986, Carbon-isotope events across the Precambrian-Cambrian boundary on the Siberian platform: Nature, v. 320, p. 258-259.

Magaritz, M., Kirschvink, J.L., Latham, A., Zhuravlev, A.Y., and Rozanov, A.Y., 1991, Precambrian-Cambrian boundary problem: Carbon isotope correlations for Vendian and Tommotian time between Siberia and Morocco: Geology, v. 19, p. 847-850.

McCormick, D.S., and Grotzinger, J.P., 1992, Evolution and significance of an overfilled alluvial foreland basin: Burnside Formation (1.9 Ga), Kilohigok Basin, N.W.T., Canada: Basin Research, v. 4, p. 253-278.

Missarzhevsky, V.V., 1989, Oldest skeletal fossils and stratigraphy of Precambrian and Cambrian boundary beds: Nauka, v. 221, p. (in Russian).

Narbonne, G.M., Kaufman, A.J., and Knoll, A.H., 1994, Integrated chemostratigraphy and biostratigraphy of the upper Windermere Supergroup (Neoproterozoic), Mackenzie Mountains, northwestern Canada: Geological Society of America Bulletin, v. 106, p. 1281-1292.

North, F.K., 1990, Petroleum Geology: Boston, Unwin Hyman, 631 p.

Pelechaty, S.M., 1996, Stratigraphic evidence for the Siberia-Laurentia connection and Early Cambrian rifting: Geology, v. 24, p. 719-722.

Pelechaty, S.M., James, N.P., Kerans, C., and Grotzinger, J.P., 1991, A middle Proterozoic paleokarst unconformity and associated sedimentary rocks, Elu Basin, northwest Canada: Sedimentology, v. 38, p. 775-797.

Pelechaty, S.M., and Grotzinger, J.P., 1993, Correlation of Vendian carbonate rocks between the Olenek uplift and Kharaulakh Mountains, northern Siberia: Geological Association of America Abstract, Progr. 25, p. A337.

Pelechaty, S.M., Grotzinger, J.P., and Kaufman, A.J., 1995, Application of combined isotopic-carbon chemostratigraphy and sequence stratigraphy for basin analysis: An example from the Vendian-Cambrian interval of northeast Siberia: Geological Society of America Abstracts and Program, v. 27, p. A330.

Pelechaty, S.M., Grotzinger, J.P., Kashirtsev, V.A., and Zhernovsky, V. P., 1996, Chemostratigraphic and sequence stratigraphic constraints on Vendian-Cambrian basin dynamics, Northwest Siberian craton: Journal of Geology, v. 104, p, 543-564.

Pokrovsky, B.G., and Missarzhevsky, V.V., 1993, Isotope correlation of Precambrian and Cambrian of the Siberian platform: Akademiya Nauk SSSR, Doklady, V. 329, p. 768-771. (in Russian)

Pokrovsky, B.G., and Venagradov, V.E., 1991, Isotopic composition of strontium, oxygen and carbon in upper Precambrian carbonates of the western area of the Anabar uplift (Kotyikan River): Akademiya Nauk SSSR, Doklady, v. 320, p. 1245-1250 (in Russian).

Read, J.F., 1983, Carbonate platform facies models: AAPG Bulletin, v. 69, p. 1-21.

Repina, L.N., Lazarenko, N.P. and Meshkova, N.P., 1974, Lower Cambrian. biostratigraphy and Facies of Kharaulakh: Nauka, Moscow, 300 p. (in Russian).

Ripperdan, R.L., 1994, Global variations in carbon isotope composition during the latest Neoproterozoic and earliest Cambrian: Annual Reviews in Earth Planetary Sciences, v. 22, p. 385-417.

Rodgers, J., 1991, Fold-and-thrust belts in sedimentary rocks. Part 2: Other examples, especially variants: American Journal of Science, v. 291, p. 825-886.

Sadler, P.M., 1981, Sediment accumulation rates and the completeness of stratigraphic sections: Journal of Geology, v. 89, p. 569-584.

Sadler, P.M., 1987, Sedimentation rates: Are thicker sections more complete?: Geological Society of America Abstracts and Programs, p. 827.

Schidlowski, M., Matzigkeit, U. and Krumbein, W.E., 1984, Superheavy organic carbon from hypersaline microbial mats: Naturwissenschaften, v. 71, p. 303-308.

Schlager, W., 1981, The paradox of drowned reefs and carbonate platforms: Geological Society of America Bulletin, v. 92, p. 197-211.

Sears, S.O., and Lucia, F.J., 1980, Dolomitization of northern Michigan Niagara reefs by brine refluxion and freshwater/seawater mixing, *in* Zenger, D.H., Dunham, J.B., and Ethington, R.L., eds., Concepts and Models of Dolomitization: SEPM Special Publication No. 28, p. 215-235.

Shapovalova, E.G., and Shpunt, B.R., 1982, Chapter 2: Stratigraphy, *in* Shpunt, B. R., Shapovalova, E. G., and Shamshena, E. A., eds.: Late Precambrian of the northern Siberian platform: Hovosibersk, Russian Academy of Science, 224 p. (in Russian).

Shenfel, V.Y., 1991, Late Precambrian of the Siberian Platform, Novasibersk, Science Academy of USSR, 185 p. (in Russian).

Sheppard, S.M.F., and Schwarcz, H.P., 1970, Fractionation of carbon and oxygen isotopes and magnesium between coexisting metamorphic calcite and dolomite: Contributions to Mineralogy and Petrology, v. 26, p. 161-198.

Sokolov, B., and Fedonkin, M.A., 1984, The Vendian as the terminal system of the Precambrian: Episodes, 7, p. 12-19.

Tucker, M.E., 1983, Calcitic, aragonitic and mixed calcitic-aragonitic ooids from the mid-Proterozoic Belt Supergroup, Montana: Sedimentology, v. 31, p. 627-644.

Tucker, M.E., 1986, Formerly aragonitic limestones associated with tillites in the Late Proterozoic of Death Valley, California: Journal of Sedimentary Petrology, v. 56, p. 818-830.

Vail, P.R., Hardenbol, J., and Todd, R.G., 1984, Jurassic unconformities, chronostratigraphy, and sea-level changes from seismic stratigraphy and biostratigraphy, *in* J. S. Schlee, ed., Interregional unconformities and hydrocarbon accumulations: AAPG Memoir 36, p. 129-144.

Valkov, A.K., 1987, Biostratigraphy of the lower Cambrian of the East Siberian Platform, Moscow, Moscow Science, 136 p. (in Russian).

Vidal, G., Moczydlowsky, M., and Rudavskaya, V.R., 1995, Constraints on the early Cambrian radiation and correlation of the Tommotian and Nemakit-Daldynian regional stages of eastern Siberia: Journal of the Geological Society of London, v. 152, p. 499-510.

Vodanjuk, S.A., 1989, Soft-bodied metazoan remains of the Khatyspyt Formation, Olenek uplift, *in* Khomentovsky, V. V., Sovetov, Y. K., Shenfel, V. Y., Yakshen, M. C., and Moryaken, V. B., eds., Late Precambrian and early Paleozoic of Siberia: Questions of Stratigraphy: Hovosibersk, Russian Academy of Sciences, 61-74 p. (in Russian).

Walker, R.G., and Cant, D.J., 1984, Sandy fluvial systems, *in* Walker, R. G., ed., Facies Models: Geoscience Canada, p. 71-90.

Walter, M.R., Veevers, J.J., Calver, C.R., and Grey, 1995, Neoproterozoic stratigraphy of the Centralian Superbasin, Australia: Precambrian Research, v. 73, p. 173-195.

Waschbusch, P.J., and Royden, L.H., 1992, Spatial and temporal evolution of foredeep basins: lateral strength variations and inelastic yielding in continental lithosphere: Basin Research, v. 4, p. 179-196.

Zempolich, W.G., Wilkinson B.H., and Lohmann, K.C., 1988, Diagenesis of Late Proterozoic carbonates: the Beck Spring Dolomite of Eastern California: Journal of Sedimentary Petrology, v. 58, p. 656-672.

LIST OF TABLES

LIST OF FIGURES

TABLE 2.1. RESULTS OF GEOCHEMICAL AND PETROGRAPHIC ANALYSES

Number	Height (m)	δ13C (‰ PDB)	δ18O (‰ PDB)	Mn (ppm)	Sr (ppm)	Fe (ppm)	Comments
Chekurov anticline data							
KHA-2	17.2	0.8	-9.3	1391	53	11059	D silt; M*
KHA 3	20.2	2.4	-4.7	1597	56	18568	D silt; M
KHA 4	23.2	1.1	-6.6	2406	47	18792	D silt; M
KHA 5	61.6	-0.7	-3.5	8876	111	40059	D mud; S
KHA 6aa	79.8	3.5	-12.3	3823	56	33311	D mud; M
KHA 6ab	79.8	1.5	-4.6	2296	58	16933	D mud; M
KHA 6b	79.8	1.1	-5.7	1938	43	15192	D mud; M
KHA 7	81.3	-0.9	-4.1	1297	67	91750	D mud; M
KHA 8	81.7	0.4	-6.0	1725	67	15630	D mud; M
KHA 9	93	-0.3	-9.0	136	562	1790	L bmud; M
KHA 10	95.3	-0.7	-7.1	57	595	1847	L bmud; M
KHA 11	96.9	0.0	-8.1	83	619	2217	L bmud; M
KHA 12a	102.9	0.2	-6.9	73	221	1811	L bmud; M
KHA 12b	102.9	-2.0	-6.5	198	143	3661	L bmud; OM
KHA 14	112.9	-1.0	-8.6	166	1006	2849	L bmud; M
KHA 15	114.9	-0.7	-8.6	27	1801	1704	L bmud; M
KHA 16	116.9	-0.5	-7.2	72	1374	1951	L bmud; M
KHA 17	118.2	0.0	-6.0	293	634	1859	L bmud; M
KHA 18	120	-2.6	-5.5	98	328	1492	L mud; M
KHA 19	122.8	-0.7	-4.2	171	651	1630	L mud; M
KHA 20	125.4	-0.8	-7.5	85	618	1464	L mud; M
KHA 21	128.5	-0.7	-6.8	47	515	1503	L mud; M
KHA 22	131.6	-0.8	-8.7	65	577	1809	L mud; M
KHA 23	134.3	-1.5	-6.2	36	790	1624	L mud; M
KHA 24	137.5	-0.1	-8.2	34	507	1521	L mud; M
KHA 24b	137.5	-0.5	-7.7	213	51	N.D.	L mud; S
KHA 25	140.5	1.5	-8.4	11	329	1398	L mud; M
KHA 26	143.5	0.9	-6.1	15	1093	1679	L mud; M
KHA 27	209.5	-3.6	-7.0	11	807	1724	L mud; M
KHA 28a	214.7	0.6	-7.7	200	107	2056	D mud; M
KHA 28b	216	0.4	-7.2	163	92	1524	D mud; NS
KHA 28bb	216	1.4	-9.8	120	459	N.D.	D mud; S
KHA 29	217.9	1.2	-3.6	45	59	1667	D mud; M
KHA 30	220.9	1.1	-7.1	53	62	1597	D mud; M
KHA 30b	220.9	-0.3	-11.7	726	59	9270	D mud; S
KHA 31	221.9	-3.6	-3.8	31	62	1420	D grst; M
KHA 32	223.9	0.5	-6.0	N.D.†	N.D.	N.D.	D grst; Mc
KHA 33	226.9	0.4	-5.8	N.D.	N.D.	N.D.	D grst; Mc
KHA 34	229.9	0.9	-5.8	810	49	12744	D grst; Mc
KHA 35	232.9	1.2	-7.2	1177	70	19238	D grst; Mc
KHA 36a	238.9	0.5	-6.3	535	62	7315	D grst; M
KHA 36b	238.9	1.4	-6.9	789	40	12080	D grst; NS
KHA 37	239.9	0.7	-4.1	N.D.	N.D.	N.D.	D grst; NS
KHA 38	242.9	1.2	-5.3	N.D.	N.D.	N.D.	D grst; Mc
KHA 39	244.5	1.1	-5.4	636	44	9219	D grst; NS
KHA 40	248.6	0.8	-3.7	N.D.	N.D.	N.D.	D grst; NS
KHA 41a	250	0.5	-4.4	1125	62	28133	D grst; Mc
KHA 41b	250	0.2	-5.6	945	55	25767	D grst; NS
KHA 42	251.6	-0.5		N.D.	N.D.	N.D.	D grst; NS
KHA 43	255.6	1.3	-3.0	N.D.	N.D.	N.D.	D grst; WRx
KHA 44	258.6	0.4	-4.9	928	58	26462	D grst; Mc
KHA 45	260.6	0.9	-3.7	1076	80	32450	D grst; Mc
KHA 46	263.6	-0.1	-2.7	1088	47	11266	D grst; Mc
KHA 47	266.6	0.6	-5.9	897	45	10010	D strom; M
KHA 48	269.6	0.2	-7.6	N.D.	N.D.	N.D.	D grst; Mc
KHA 49a	275.6	1.1	-6.0	N.D.	N.D.	N.D.	D grst; M

Number	Height (m)	δ13C (‰ PDB)	δ18O (‰ PDB)	Mn (ppm)	Sr (ppm)	Fe (ppm)	Comments
KHA 49b	275.6	0.6	-8.5	N.D.	N.D.	N.D.	D grst; S
KHA 50	278.6	-0.5	-10.1	751	34	9177	D grst; M
KHA 51	281.6	1.3	-3.6	236	25	3320	D grst; M
KHA 52	284	0.4	-3.6	703	81	10123	D grst; M
KHA 53	287	0.9	-5.7	418	70	6453	Dgrst; WX
KHA 54	290	-0.9	-4.7	N.D.	N.D.	N.D.	D grst; M
KHA 55	293	0.6	-6.0	465	37	7460	D grst; M
KHA 56	296	0.2	-4.8	652	49	10153	D grst; Mc
KHA 57	299	1.1	-6.3	604	50	10205	D grst; M
KHA 58a	304	-1.9	-5.2	680	39	11446	D grst; M
KHA 58b	304	0.0	-9.5	544	36	9559	D grst; NS
KHA 59	305	1.2	-5.2	638	51	11800	D grst; M
KHA 60	306	-0.4	N.D.	N.D.	N.D.	N.D.	D grst; WX
KHA 61	311	0.2	N.D.	N.D.	N.D.	N.D.	D grst; M
KHA 62	314	-0.6	N.D.	N.D.	N.D.	N.D.	D bio; M
KHA 63	317	-0.3	-2.4	387	52	8073	D grst; M
KHA 64	320	0.4	N.D.	N.D.	N.D.	N.D.	D grst; M
KHA 65	323	0.1	N.D.	N.D.	N.D.	N.D.	D strom; M
KHA 66	326	-0.7	N.D.	N.D.	N.D.	N.D.	D strom; M
KHA 67a	329	-0.4	N.D.	N.D.	N.D.	N.D.	D silt; M
KHA 67b	329	-1.0	-2.2	N.D.	N.D.	N.D.	D silt; M
KHA 68	332	-0.2	-4.1	845	73	15394	D bio; M
KHA 69	337	-0.1	-7.5	202	102	3592	D bsilt; M
KHA 70	339	-0.2	-5.0	102	116	N.D.	L bmud; M
KHA 71	341	0.1	-6.3	7	1053	1524	L bmud; M
KHA 72	344	-0.4	-3.4	23	1313	2047	L bmud; M
KHA 73	347	0.4	-7.4	6	1047	1697	L bmud; M
KHA 74	350	-0.7	-8.5	266	83	1847	L bmud; M
KHA 75	353	-0.0	-8.0	75	338	1926	L bmud; M
KHA 76	356	-0.3	-7.4	33	580	1706	L bmud; M
KHA 77	359	-0.1	-6.6	34	474	1633	L bmud; M
KHA 78	362	-0.1	-6.6	67	366	1744	L bmud; M
KHA 79	365	-0.2	-5.4	43	568	1642	L bmud; M
KHA 80	368	-0.4	-6.8	66	292	1862	L mud; M
KHA 81	371	-0.1	-5.4	40	220	1936	L mud; M
KHA 82	374	-1.1	-7.3	112	817	1969	L mud; M
KHA 83	377	-0.3	-8.8	53	235	1447	L mud; M
KHA 84	380	-0.2	-6.2	113	440	2156	L mud; M
KHA 84b	380	-0.3	-7.5	99	151	N.D.	L mud; S
KHA 85	383	-0.3	-3.1	205	1836	1746	L mud; M
KHA 86	386	-0.5	-6.7	56	313	1818	L mud; M
KHA 87	389	-0.4	-7.9	37	118	1516	L mud; M
KHA 88	392	-0.0	-2.9	14	1991	2454	L mud; M
KHA 89a	395	-0.4	-2.8	9	1943	1533	L mud; M
KHA 89b	395	-0.2	-6.0	86	324	4199	L mud; M
KHA 90	398	-0.2	-7.3	97	131	2101	L mud; M
KHA 91a	401	-0.2	-5.1	45	563	2858	L mud; M
KHA 92	404	-0.6	-7.9	74	115	1816	L mud; M
KHA 93a	407	-0.2	-3.9	330	676	28596	L mud; M
KHA 93b	407	-0.4	-7.0	79	239	2694	L mud; M
KHA 94a	410	-0.4	-6.8	56	265	1891	L mud; M
KHA 94b	410	0.0	-3.1	180	1377	1862	L mud; M
KHA 95	413	0.0	-3.5	212	1685	1693	L mud; M
KHA 96	416	0.1	-6.8	54	278	1876	L mud; M
KHA 97	427	-0.5	-6.6	165	1634	2338	L mud; M
KHA 98	422	-0.4	-3.2	40	1443	1954	L mud; M
KHA 99	425	-0.6	-3.4	54	1923	2057	L mud; M
KHA 100	457	-0.6	-7.2	96	266	1932	L mud; M
KHA 100b	457	-0.3	-14.3	N.D.	N.D.	N.D.	L mud; S

Number	Height (m)	δ13C (‰ PDB)	δ18O	Mn	Sr (ppm)	Fe	Comments
KHA 101a	459	0.8	-7.5	418	54	11246	D grst; BS
KHA 101b	459	-0.2	-9.0	150	122	1860	L grst; NS
KHA 102	460.5	-0.2	-7.7	130	166	1899	L grst; S
KHA 103a	462	-1.1	-9.7	623	45	5549	D grst; BS
KHA 103b	462	-0.2	-8.2	117	125	2181	L grst; MC
KHA 104	463.5	-0.6	-8.0	107	169	1925	L grst; WX
KHA 105a	466	-0.2	-7.9	1701	2279	36515	L grst; MC
KHA 105b	466	1.4		315	57	4815	D grst; BS
KHA 106a	466.5	-0.6	-12.6	314	85	5033	D grst; BS
KHA 107a	468	-0.4	-7.7	104	173	2145	L grst; MC
KHA 107b	468	-0.2	-7.0	105	515	2228	L grst; S
KHA 108	469.5	-0.4	-8.0	82	106	1550	L grst; MC
KHA 109a	471	0.0	-7.9	126	68	N.D.	L grst; MC
KHA 109b	471	-0.0	-7.8	78	400	N.D.	L grst; S
KHA 110	472.5	-0.0	-8.9	12	1408	N.D.	L grst; MC
KHA 111a	474	0.1	-7.2	128	178	N.D.	L grst; MC
KHA 111b	474	-0.2	-6.9	129	281	N.D.	L grst; S
KHA 112	475.5	-0.5	-9.1	134	225	N.D.	L grst; MC
KHA 113a	477	-0.5	-8.4	53	112	N.D.	L grst; MC
KHA 113b	477	-0.0	-3.1	94	778	N.D.	L grst; S
KHA 114	478.5	-0.6	-8.4	80	66	N.D.	L grst; MC
KHA 115	480	-0.7	-8.1	83	204	N.D.	L grst; MC
Bokursky	**Anticline**	**data**					
KFC 1	3	0.1	-8.5	N.D.	N.D.	N.D.	D mud; NS
KFC 2	6	-0.5	-6.6	N.D.	N.D.	N.D.	D mud; NS
KFC 3	9	0.9	-6.6	N.D.	N.D.	N.D.	D mud; M
KFC 4	12	1.9	-5.8	N.D.	N.D.	N.D.	D mud; M
KFC 5	15	1.8	-6.1	N.D.	N.D.	N.D.	D grst; MC
KFC 6a	18	1.1	-6.7	N.D.	N.D.	N.D.	D mud; M
KFC 6b	18	0.9	-7.9	N.D.	N.D.	N.D.	D mud; S
KFC 7	21	1.5	-5.9	N.D.	N.D.	N.D.	D mud; M
KFC 9	27	0.2	-8.5	N.D.	N.D.	N.D.	D mud; M
KFC10	30	0.8	-6.4	N.D.	N.D.	N.D.	D mud; M
KFC 11	33	0.2	-7.0	N.D.	N.D.	N.D.	D mud; M
KFC 12	36	0.9	-5.3	N D.	N.D.	N.D.	D grst; MC
KFC 14	42	0.7	-6.5	N.D.	N.D.	N.D.	D mud; M
KFC 15a	45	1.5	-5.9	N.D.	N.D.	N.D.	D mud; OM
KFC 15b	45	2.3	-5.3	N.D.	N.D.	N.D.	D mud; M
KFC 16a	48	2.0	-4.7	N.D.	N.D.	N.D.	D mud; OM
KFC 16b	48	2.3	-1.6	N.D.	N.D.	N.D.	D mud; M
KFC17	51	1.9	-1.4	N.D.	N.D.	N.D.	D mud; M
KFC 18	54	2.2	-3.7	N.D.	N.D.	N.D.	D mud; M
KFC 19a	57	2.1	-4.0	N.D.	N.D.	N.D.	D mud; OM
KFC 19b	57	3.3	-3.7	N.D.	N.D.	N.D.	D mud; S
KFC 20	60	1.6	-6.0	N.D.	N.D.	N.D.	D mud; M
KFC 21a	63	1.9	-8.0	N.D.	N.D.	N.D.	D mud; OM
KFC 21b	63	2.3	-8.6	N.D.	N.D.	N.D.	D mud; M
Oolahan	**Ooekhtekh**	**River**	**data**				
KR 721	0	3.3	-3.5	99	63	1530	D mud; M
KR 722	1.5	3.0	-4.2	164	62	2143	D mud; M
KR 701	5.5	3.0	-5.4	100	78	1715	D mud; M
KR 702	7	2.6	-4.5	96	71	1974	D grst; MC
KR 703	8.5	1.9	-5.1	125	65	2662	D grst; MC
KR 704	11.7	2.6	-5.1	140	49	2402	D grst; MC
KR 706	17.7	1.0	-4.3	52	53	1069	D grst; WX
KR 708	26.7	1.0	-5.5	104	50	1506	D grst; WX
KR 709	29.7	0.7	-5.3	103	42	1703	D grst; WX
KR 710	32.7	0.2	-8.9	118	44	1551	D grst; MC
KR 711	35.7	0.2	-3.6	123	66	2078	D grst; MC

Number	Height (m)	δ13C (‰ PDB)	δ18O (‰ PDB)	Mn (ppm)	Sr (ppm)	Fe (ppm)	Comments
KR 712	38.7	0.9	-3.8	114	55	2110	D strom; M
KR 713	41.7	0.4	-8.8	149	53	1931	D strom; M
KR 715	47.7	-0.6	-7.8	312	48	3220	D strom; M
KR 717	53.7	-0.2	-7.5	261	47	2649	D strom; M
KR 719	59.7	-0.7	-5.8	139	43	2071	D strom; M
KR 720	62.7	-0.6	-4.6	118	43	1686	D mud; M
KR 601	63	-0.7	-3.8	58	52	825	D mud; M
KR 603	69	-0.7	-7.9	139	32	1913	D grst; MC
KR 605	75	-0.8	-4.0	69	39	1071	D grst; WX
KR 610	90	-1.9	-6.4	84	55	1974	D grst; WX
KR 612	96	-1.0	-2.8	62	56	1426	D grst; WX
KR 614	102	-0.7	-7.8	69	40	1823	D grst; MC
KR 617	111	-1.2	-3.8	53	44	1756	D silt; M
KR 503	118	-0.9	-6.9	N.D.	N.D.	N.D.	D grst; WX
KR 505	124	-0.7	-2.7	N.D.	N.D.	N.D.	D bio; M
KR 507	130	-1.0	-3.3	N.D.	N.D.	N.D.	D grst; WX
KR 509	139	-1.0	-6.5	N.D.	N.D.	N.D.	D grst; WX
KR 511	145	-0.9	-7.8	N.D.	N.D.	N.D.	D grst; MC
KR 301	150	0.0	-11.9	N.D.	N.D.	N.D.	D mud; M
KR 303	154	-1.3	-2.9	N.D.	N.D.	N.D.	D grst; MC
KR 305	158	-1.1	-5.3	N.D.	N.D.	N.D.	D bio; M
KR 308	161.5	-0.8	-7.6	N.D.	N.D.	N.D.	D bio; M
KR 310	165	-1.3	-7.5	N.D.	N.D.	N.D.	D grst; MC
KR 311	168	-0.4	-8.0	N.D.	N.D.	N.D.	D grst; WX
KR 312	171	-1.0	-4.8	N.D.	N.D.	N.D.	D bio; M
KR 313	174	-2.6	-1.4	N.D.	N.D.	N.D.	D bio; M
KR 314	177	-0.8	-6.0	N.D.	N.D.	N.D.	D bio; M
KR 315	180	-0.6	-9.0	N.D.	N.D.	N.D.	D bio; M
KR 316	183	-1.2	-6.3	N.D.	N.D.	N.D.	D bio; M
KR 04	234	0.7	-6.6	N.D.	N.D.	N.D.	D grst; WX
KR 05	237	0.8	-7.8	N.D.	N.D.	N.D.	D grst; WX
KR 07	239.5	1.1	-5.3	N.D.	N.D.	N.D.	D grst; WX
KR 09	242.5	0.8	-7.6	N.D.	N.D.	N.D.	D grst; WX
Olenek River data							
O 668	0	2.5	-11.1	144.8	49	1813	D mud; M
O 670	4	2.2	-11.0	125	54	1797	D mud; M
O 672	8	2.8	-11.0	106	31	1543	D mud; M
O 674	12	1.4	-9.9	142	87	2571	D mud; M
O 676	16	0.6	-9.6	172.6	110	2738	D mud; M
O 678	20	0.3	-12.1	141	137	1701	D mud; M
O 613	22	0.8	-5.8	71.5	63	1876	D mud;M
O 615	26	1.3	-14.0	73.7	38	1177	D grst; MC
O 617	30	0.2	-10.3	121	47	1498	D mud; M
O 619	34	0.6	-8.7	112.8	54	1661	D mud; M
O 621	38	0.5	-9.4	85.5	30	1319	D mud; M
O 632	38.5	0.8	-9.8	95.7	53	1522	D grst; WX
O 634	42.5	0.5	-10.4	103.9	37	1397	D grst; WX
O 636a	46.8	0.5	-7.9	78	33	1573	D grst; MX
O 636b	46.8	0.3	-8.9	86	30	1443	D grst; MX
O 638	50.9	0.4	-8.9	86	35	1417	D mud; M
O 640	54.9	0.3	-7.7	91	40	1280	D strom; M
O 642	58.9	0.5	-8.7	128.9	28	1736	D strom; M
O 644	62.1	0.4	-9.3	104	31	1704	D grst; WX
O 646	67.1	0.3	-9.3	131	32	1970	D grst; MC
O 650	74.6	-0.1	-7.0	61.6	17	865	D grst; WX
O 652	79	-0.4	-5.5	94.5	43	1496	D mud; M
O 654	83	0.0	-5.5	80	29	1280	D pkst; M
O 658	91	-0.2	-8.2	113	32	1560	D grst; MC
O 660	95	-0.2	-7.9	156	50	1971	D grst; MC

Number	Height (m)	δ13C (‰ PDB)	δ18O	Mn	Sr (ppm)	Fe	Comments
O 662	99	0.0	-9.0	146	34	2634	D grst; MC
O 664	103	-1.4	-3.8	211	50	2087	D strom; M
O 666	107	-2.1	-6.9	377	59	6502	D grst; MC
O 721	107.8	-1.3	-6.6	130	51	2151	D strom; M
O 724	113.7	-1.9	-4.6	192	61	2929	D mud; M
O 725	115.7	-1.7	-13.3	235	55	4191	D mud; M
O 726	117.7	-2.2	-3.4	271	54	3028	D strom; M
O 727	119.6	-2.3	-4.9	240.9	48	3787	D mud; M
O 728	121.6	-2.0	-4.2	353	58	392	D strom; M
O 730	126.6	-2.5	-8.9	395.7	57	3248	D grst; MC
O 731	128.6	-2.5	-5.6	393.5	47	3197	D strom; M
O 732	130.6	-2.6	-4.2	539	53	4987	D strom; M
O 733	131.6	-2.5	-4.2	635.9	54	5789	D grst; WX
O 734	133.6	-2.6	-9.5	583	50	4605	D strom; M
O 735	138	-3.4	-2.9	647.7	57	4217	D strom; M
O 736	141	-2.5	-8.9	901	75	3830	D strom; M
O 737	143	-2.6	-4.2	1188	73	11765	D strom; M
Kytyngeder	**River**	**data**					
KR 1403	0	1.7	-4.5	N.D.	N.D.	N.D.	D pkst; WX
KR 1405	4	1.5	-6.7	N.D.	N.D.	N.D.	D mud; WX
KR 1409	9	2.9	-2.9	N.D.	N.D.	N.D.	Dmud; M
KR 1501	15	-1.6	-4.2	N.D.	N.D.	N.D.	D grst; WX
KR 1503	20	-0.8	-4.0	N.D.	N.D.	N.D.	D pkst; WX
KR 1506	25.7	-3.1	-3.8	N.D.	N.D.	N.D.	Dmud; M
KR 1508	29.8	-0.0	-5.7	N.D.	N.D.	N.D.	D mud; WX
KR 1511	35.5	-1.9	-5.3	N.D.	N.D.	N.D.	D mud; WX
KR 1514	40.2	-1.8	-3.1	N.D.	N.D.	N.D.	D mud; WX
KR 1520	45.2	1.3	-4.1	N.D.	N.D.	N.D.	D pkst; WX
KR 1524	449.5	-0.1	-2.9	N.D.	N.D.	N.D.	D grst; WX
KR 1526	54.3	1.0	-7.6	N.D.	N.D.	N.D.	D grst; WX
KR 1529	60.3	0.5	-4.6	N.D.	N.D.	N.D.	D grst; WX
KR 1534	71.2	0.0	-3.0	N.D.	N.D.	N.D.	D bio; M
KR 1536	77	0.8	-3.9	N.D.	N.D.	N.D.	D mud; M
KR 1539	82	0.1	-4.5	N.D.	N.D.	N.D.	D grst; WX
KR 1542	87	-0.6	-3.3	N.D.	N.D.	N.D.	D grst; WX
KR 1901	88	0.4	-5.9	N.D.	N.D.	N.D.	D grst; WX
KR 1904	94	-0.3	-4.0	N.D.	N.D.	N.D.	D strom; WX
KR 1907	100	-0.0	-5.9	N.D.	N.D.	N.D.	D strom; M
KR 1910	106	-0.9	-4.5	N.D.	N.D.	N.D.	D strom; WX
KR 1911	110	-0.8	-2.0	N.D.	N.D.	N.D.	D strom; M
KR 1913	114	-2.1	-2.4	N.D.	N.D.	N.D.	D strom; M
KR 2303	124	1.1	0.1	N.D.	N.D.	N.D.	D strom; M
KR 2404	133	1.0	-6.0	N.D.	N.D.	N.D.	D mud; M
KR 2408	137	1.0	-8.7	N.D.	N.D.	N.D.	D mud; M
KR 2411	141.5	-1.4	-1.9	N.D.	N.D.	N.D.	D mud; M
KR 2416	146	-1.1	-0.8	N.D.	N.D.	N.D.	D bio; WX
KR 2420	149	-1.0	-2.3	N.D.	N.D.	N.D.	D mud; M
KR 2425	153	-1.5	-2.0	N.D.	N.D.	N.D.	D mud; M
KR 2505	156	0.6	-3.3	N.D.	N.D.	N.D.	D pkst; WX
KR 2510	161.1	-0.3	-3.0	N.D.	N.D.	N.D.	D mud; M
KR 2513	165.8	-0.9	-1.6	N.D.	N.D.	N.D.	D strom; WX
KR 2515	170.3	-1.2	-3.9	N.D.	N.D.	N.D.	D mud; M
KR 2611	244	1.0	-4.8	N.D.	N.D.	N.D.	D bio; WX
KR 2617	253	1.1	-7.3	N.D.	N.D.	N.D.	D grst; WX
KR 2619	256	0.9	-13.7	N.D.	N.D.	N.D.	D bio; M
KR 2620	258	0.6	-6.2	N.D.	N.D.	N.D.	D bio; M
KR 2622	263	0.6	-10.8	N.D.	N.D.	N.D.	D bio; M
KR 2624	270	1.0	-5.3	N.D.	N.D.	N.D.	D bio, M
KR 2626	282	-0.5	-4.0	N.D.	N.D.	N.D.	D grst; M

KR 2629	286	0.1	-5.3	N.D.	N.D.	N.D.	D bio; M
KR 2631	287	-0.4	-1.9	N.D.	N.D.	N.D.	D pkst; WX

*Symbols used for petrographic descriptions: (lithology) D, dolostone; L, limestone; (sediment type) grst, grainstone; pkst, packstone; silt, siltstone; mud, mudstone; bmud, bituminous mudstone; strom, stromatolite; bio, biolaminite; (microscopic component) M, micrite; OM, micrite with abundant sedimentary organic matter; NS, neomorphic spar; MC micritic clast; S, void-filling spar; BS, baroque spar; WX, whole rock sample.

†Not determined

TABLE 2.2. ISOTOPIC COMPARISON OF ORGANIC-RICH AND ORGANIC POOR CARBONATE

Number	A Organic-rich sample δ13C	A Organic-rich sample δ18O	B Organic-poor sample δ13C	B Organic-poor sample δ18O	A-B
KHA 12b,a	-2.0	-6.4	0.2	-6.9	-2.2
KHA 36a,b	0.5	-6.3	1.4	-6.9	-0.9
KHA 41b,a	0.2	-5.6	0.5	-4.4	-0.3
KHA 67a,b	-0.4	N.D.*	-1.0	-2.2	0.6
KHA 89a,b	-0.4	-2.8	-0.2	-6.1	-0.2
KHA 93a,b	-0.2	-3.9	-0.4	-7.0	0.2
KHA 94b,a	0.0	-3.1	-0.4	-6.8	0.4
KFC 15a,b	1.5	-5.9	2.3	-5.3	-0.8
KFC 16a,b	2.0	-4.7	2.3	-1.6	-0.3
KFC 19a,b	2.1	-4.0	3.3	-3.7	-1.2
KFC 21a,b	1.9	-8.0	2.3	-8.6	-0.4

* Not Determined

TABLE 2.3. ISOTOPIC COMPARISON OF DEPOSITIONAL AND DIAGENETIC COMPONENTS WITHIN SAMPLES

Number	A Diagenetic Comp*		B Depositional Comp		A - B
	δ13C	δ18O	δ13C	δ18O	
KHA 6ab,aa	3.5	-12.3	1.5	-4.6	2.0
KHA 24,b	-0.5	-7.7	-0.1	-8.2	-0.4
KHA 28a,bb	1.4	-9.8	0.6	-7.7	0.8
KHA 30,b	-0.3	-11.7	1.0	-7.1	-1.3
KHA 49a,b	0.6	-8.5	1.1	-10.1	-0.5
KHA 58a,b	0.0	-9.5	-1.9	-5.2	1.9
KHA 84a,b	-0.3	-7.5	-0.2	-6.2	-0.1
KHA 100,b	-0.2	-14.3	-0.6	-7.2	0.4
KHA 103b,a	-1.1	-9.7	-0.2	-8.2	-0.9
KHA 105a,b	1.4	N.D.†	-0.2	-7.9	1.6
KHA 107a,b	-0.2	-7.0	-0.4	-7.7	0.2
KHA 109a,b	0.0	-7.8	0.0	-7.9	0.0
KHA 111a,b	-0.2	-6.9	0.1	-3.1	-0.3
KFC 6a,b	0.9	-7.9	1.1	-6.7	-0.2

* Diagenetic components include pseudospar, spar, and baroque dolomite
† Not Determined

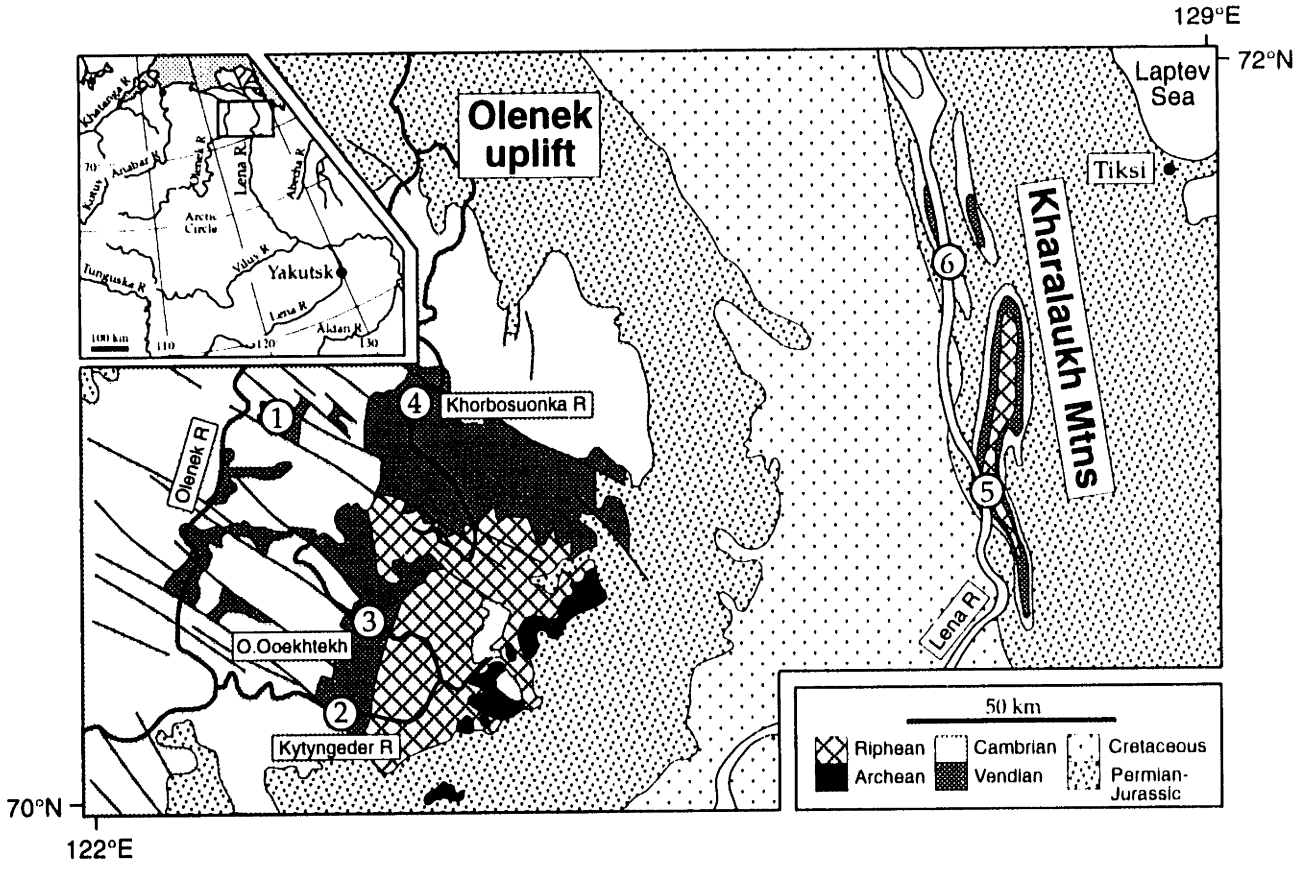
129°E
72°N
Laptev Sea
Olenek uplift
Tiksi
Kharalaukh Mtns
Yakutsk
Khorbosuonka R
Olenek R
O.Ooekhtekh
Kytyngeder R
Lena R
50 km
Riphean
Archean
Cambrian
Vendian
Cretaceous
Permian-Jurassic
70°N
122°E

Figure 2.1

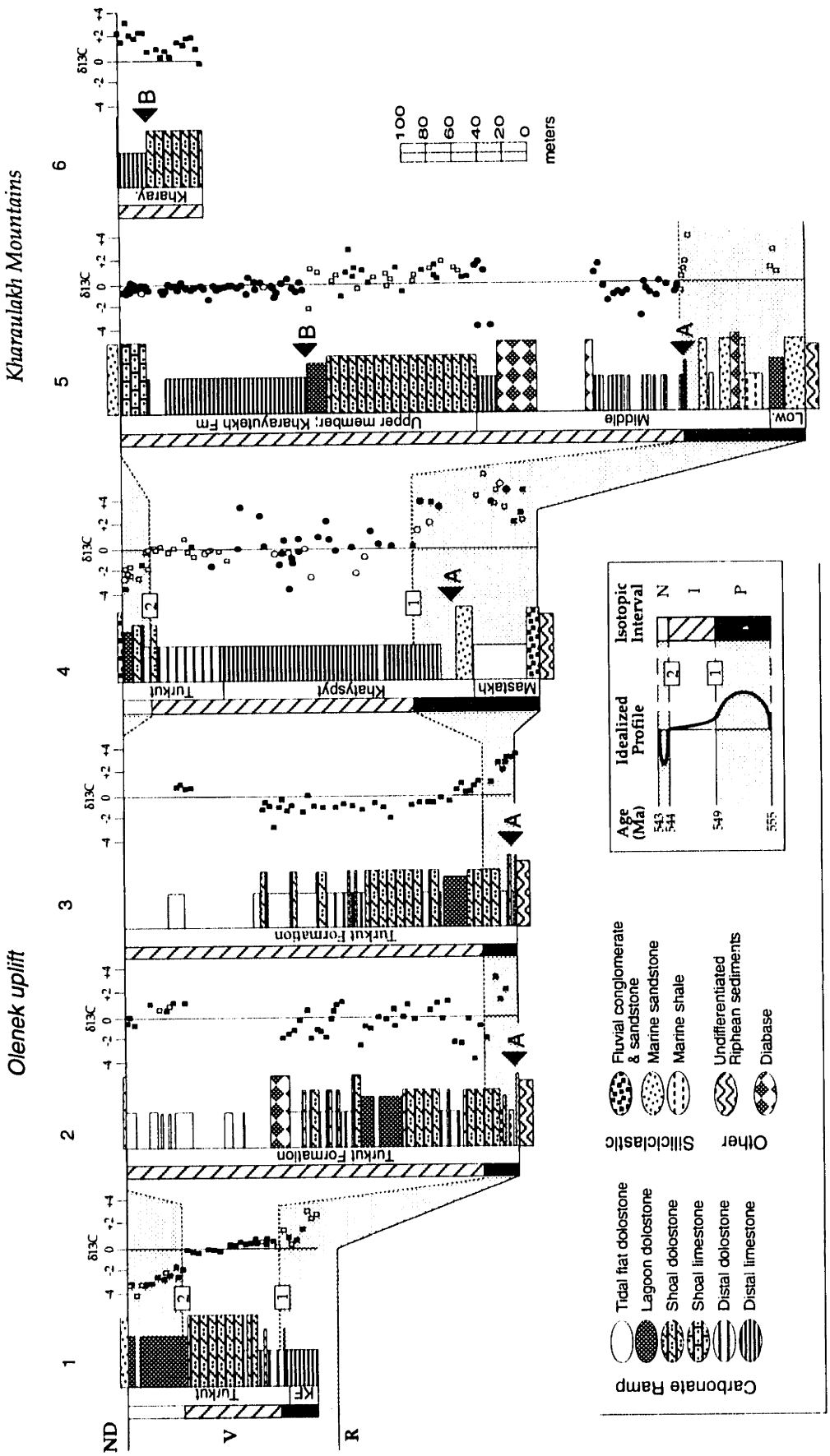
Olenek uplift
Kharaulakh Mountains
ND
V
R
KF
Turkut
Turkut Formation
Khatyspyt
Mastakh
Upper member: Kharaylakh Fm
Middle
Low
Khatay
meters
100
80
60
40
20
0
δ13C
Age (Ma)
Idealized Profile
Isotopic Interval
N
I
P
543
544
549
555
Carbonate Ramp
Tidal flat dolostone
Lagoon dolostone
Shoal dolostone
Shoal limestone
Distal dolostone
Distal limestone
Siliciclastic
Fluvial conglomerate & sandstone
Marine sandstone
Marine shale
Other
Undifferentiated Riphean sediments
Diabase

Figure 2.2

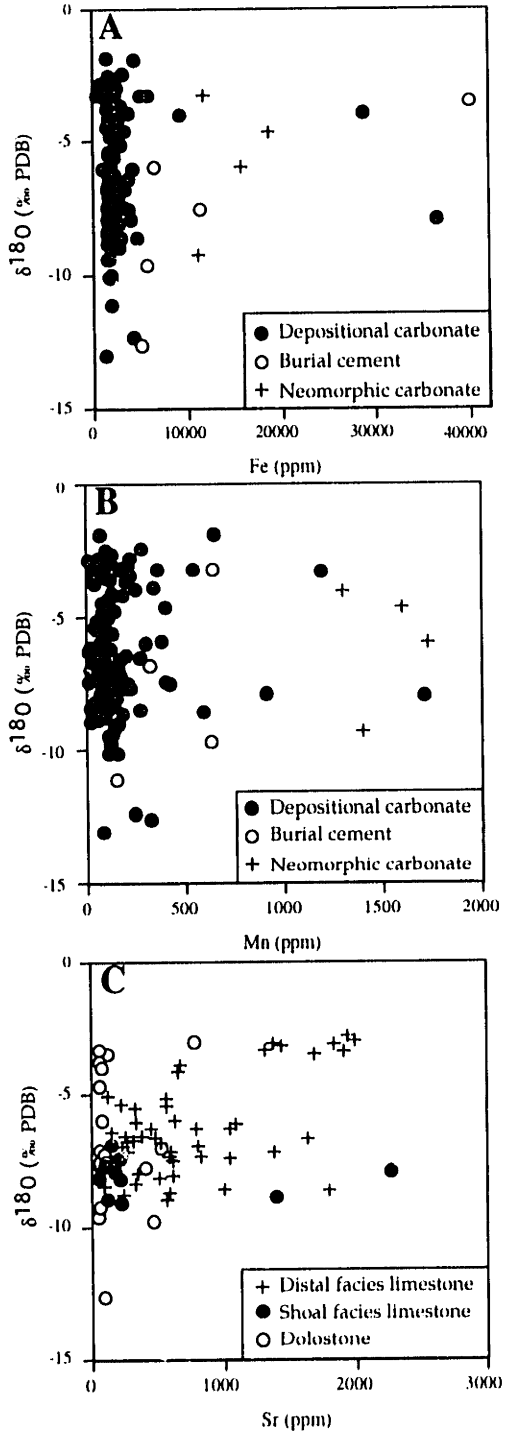
A
δ18O (‰ PDB)
0
-5
-10
-15
0
10000
20000
30000
40000
Fe (ppm)
Depositional carbonate
Burial cement
Neomorphic carbonate
B
δ18O (‰ PDB)
0
-5
-10
-15
0
500
1000
1500
2000
Mn (ppm)
Depositional carbonate
Burial cement
Neomorphic carbonate
C
δ18O (‰ PDB)
0
-5
-10
-15
0
1000
2000
3000
Sr (ppm)
Distal facies limestone
Shoal facies limestone
Dolostone

Figure 2.3

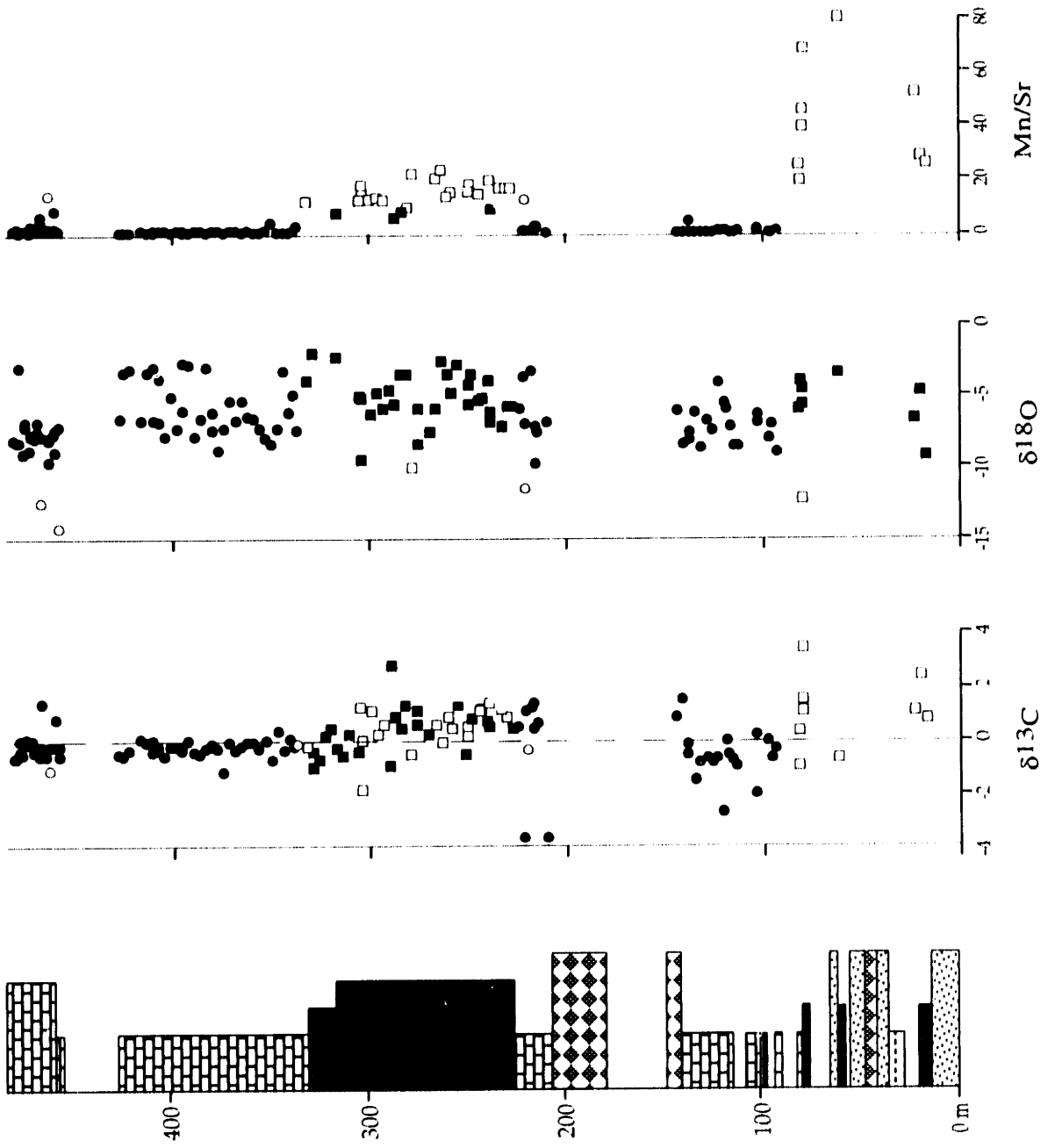

Figure 2.4

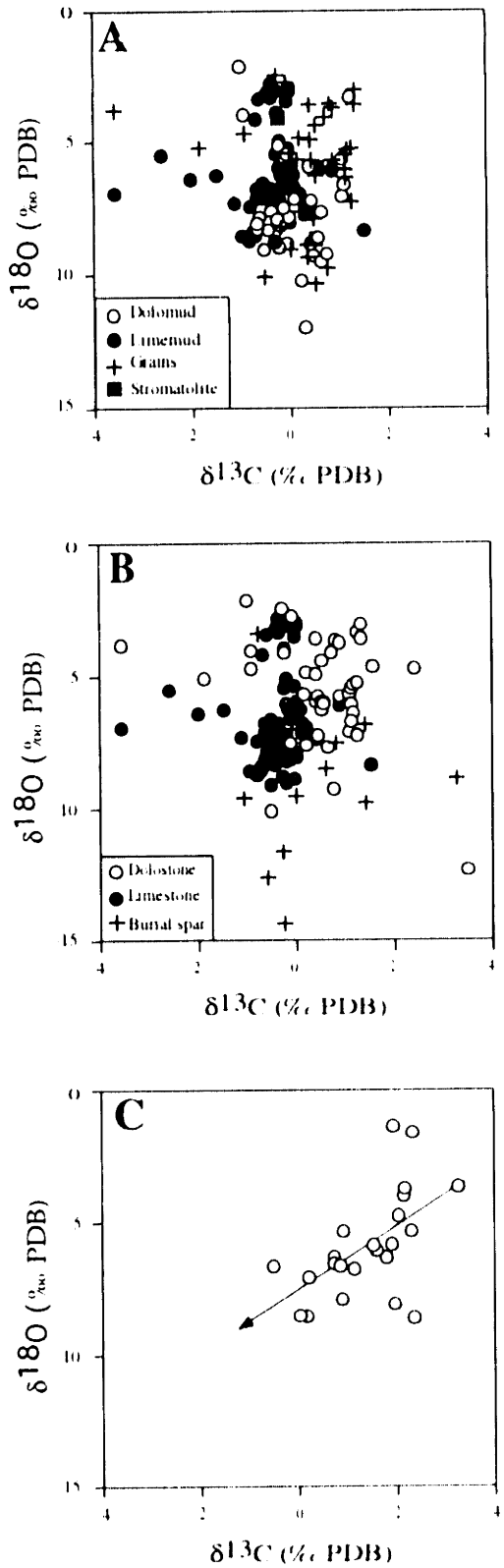
A
δ18O (‰ PDB)
δ13C (‰ PDB)
Dolomud
Limemud
Grains
Stromatolite
B
δ18O (‰ PDB)
δ13C (‰ PDB)
Dolostone
Limestone
Burial spar
C
δ18O (‰ PDB)
δ13C (‰ PDB)

Figure 2.5

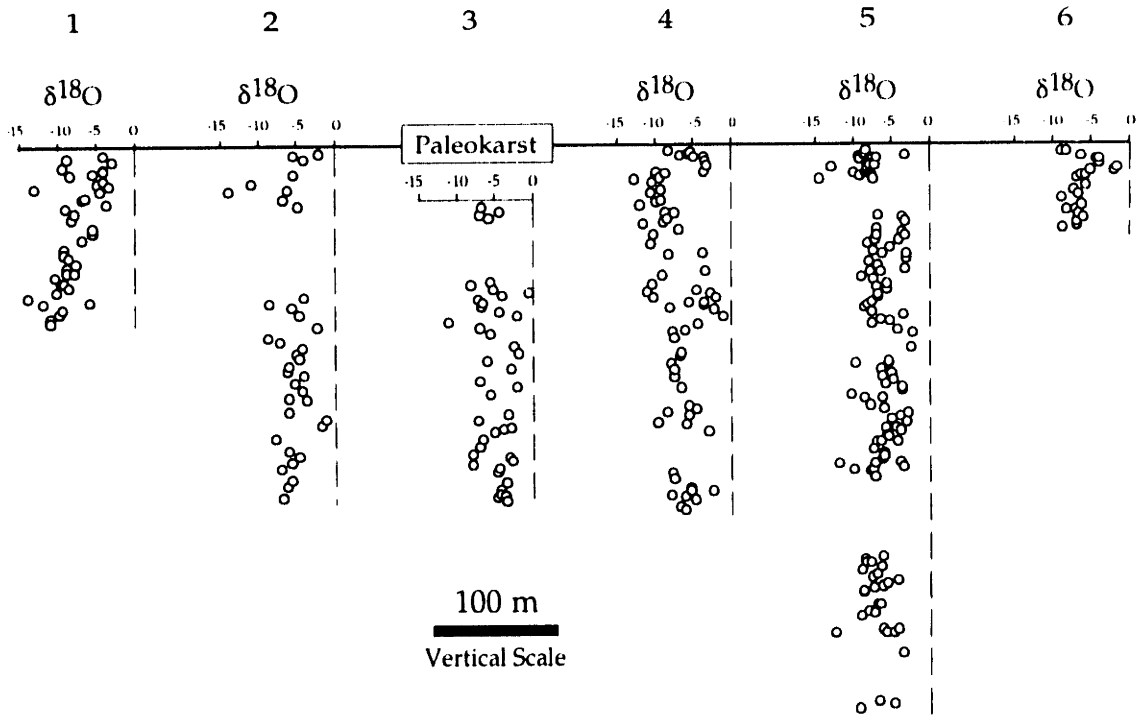
1
2
3
4
5
6
δ18O
δ18O
δ18O
δ18O
δ18O
-15 -10 -5 0
Paleokarst
100 m
Vertical Scale

Figure 2.6

Chapter 3

Chemostratigraphic and Sequence Stratigraphic Constraints on Vendian-Cambrian Basin Dynamics, Northeast Siberian Craton[2]

[2]Pelechaty, S.M., Grotzinger, J.P., Kashirtsev, V.A., and Zhernovsky, V.P., 1996, Chemostratigraphic and sequence stratigraphic constraints on Vendian-Cambrian basin dynamics, northeast Siberian craton: Journal of Geology, v. 104, p. 543-563.

ABSTRACT

$\delta^{13}C$ chemostratigraphic and sequence stratigraphic data from terminal Vendian and earliest Cambrian strata of northeast Siberia are used to constrain the history of regional basin development. These boundary strata consist of 300 to 500 m of latest Vendian age carbonate ramp deposits and less than 100 m of Nemakit Daldyn age siliciclastic shelf deposits; the two successions are separated by a regional paleokarst unconformity. Six $\delta^{13}C$ chemostratigraphic profiles of the carbonates exhibit patterns of secular variation similar to those in coeval strata, with allowances for local diagenetic and tectonic effects. Isotopic profiles are used to recognize time lines (chemo chrons) within individual depositional sequences and to illustrate the geometry of stratigraphic units, and variation in subsidence and stratigraphic completeness across the basin. The Vendian Khorbosuonka Group and correlative deposits are divided into three depositional sequences (1-3) that record sedimentation from ca. 555 to 543 Ma in a gently subsiding east facing passive margin basin. On the basis of chemostratigraphy, outer ramp strata were progressively uplifted and eroded to the north, forming a regionally extensive paleokarst. Unconformity development was associated with felsic volcanism and is considered to reflect the onset of regional rift related uplift that continued to early Tommotian time (530 Ma). Differential uplift produced a transient reversal in depositional slope creating a local south facing basin during onlap of Nemakit Daldyn age shelf strata (sequence 4). Continued synsedimentary tectonism is marked by the presence of bimodal volcanic rocks interbedded with shelf deposits and truncation of the sequence to the north. Overlying Tommotian age limestones provide evidence for restoration of a northerly depositional gradient by southward onlap of the exposed shelf. Tommotian and younger age limestones are interpreted to represent a postrift phase of subsidence (flexural and/or thermal) related to decay of thermal anomalies. Regional stratigraphic evidence suggests that rifting developed across the northern margin of Siberia during the Early Cambrian.

INTRODUCTION

We present a chronostratigraphic study of latest Neoproterozoic (Vendian) and Early Cambrian strata using combined carbon isotope chemostratigraphy and sequence stratigraphy. This integrated stratigraphic approach is shown to be important for high resolution, intrabasinal correlation of marine carbonate strata of any age and is comparable to stratigraphic studies of Phanerozoic sedimentary basins. Recently, most studies of Vendian to Cambrian age strata utilize carbon isotope chemostratigraphy for intercontinental correlation (see summary articles by Ripperdan 1994 and Kaufman and Knoll 1995). Less commonly, chemostratigraphic approaches are used for intrabasinal correlation (Knoll et al. 1986, 1995a; Braiser et al. 1993; Pell et al. 1993; Burns and Matter 1993), and few studies have fully integrated isotope geology with diagenetic, sedimentologic and sequence stratigraphic studies (Pelechaty and Grotzinger 1993; Pelechaty et al. 1995, 1996; Knoll et al. 1995a). Recent geochronological work has calibrated this chronostratigraphy in absolute time (Bowring et al. 1983; Grotzinger et al. 1995) and now provides essential constraints on the rates of terminal Proterozoic geologic processes.

Within a coarsely resolved biostratigraphic framework, sequence stratigraphy serves as an important method for time stratigraphic analysis of Proterozoic sedimentary basins (Christie-Blick et al. 1988, 1995). Unconformities serve to approximate time lines that partition strata into chronostratigraphic units (Vail et al. 1984; Christie-Blick 1991). However, the temporal resolution of sequence stratigraphy is generally confined to the scale of sequences. Distinct isotopic shifts, however, can be correlated as time lines (chemo chrons) to further divide depositional sequences. Thus, by combining $\delta^{13}C$ chemostratigraphy with sequence stratigraphic correlations, additional time lines can be recognized in carbonate dominated sedimentary

basins more accurately than offered exclusively by sequence stratigraphic methods (Pelechaty et al. 1996).

The goal of this study is to integrate chemostratigraphy and sequence stratigraphy in the subsidence analysis of a Vendian to Cambrian age sedimentary basin in northeast Siberia. These sections contain a wealth of biostratigraphic, sedimentologic, and chemostratigraphic information necessary for time stratigraphy (Shapovalova and Shpunt 1982; Sokolov and Fedonkin 1984; Khomentovsky 1986, 1990; Missarzhevsky 1989a, 1989b; Sokolov et al. 1989; Shpunt and Shamshina 1989; Shenfel 1991; Knoll et al. 1995a; Pelechaty et al. 1996). Radiometric dates from northeast Siberia (Bowring et al. 1993), and Namibia (Grotzinger et al. 1995) also provide tight constraints on the age of Vendian and Cambrian strata in northern Siberia. Recently, Pelechaty et al. (1996) presented detailed $\delta^{13}C$ profiles for these sections. The effects of diagenetic and intrabasinal processes on the $\delta^{13}C$ variations were investigated, and the profiles were shown to exhibit secular variations in $\delta^{13}C$ that compare well with the proposed global standard (Knoll and Walter 1992). This study integrates this new $\delta^{13}C$ chemostratigraphic data within a sequence stratigraphic framework, and presents detailed descriptions of facies and their lateral variation across the Olenek uplift and Kharaulakh Mountains. Furthermore, the sedimentologic and chemostratigraphic data are used to constrain the basin subsidence history of the northern part of the Siberian craton during Vendian to Cambrian time. This work also provides stratigraphic constraints on the plate tectonic history of the Siberian craton at this time (Pelechaty 1996).

REGIONAL GEOLOGY OF THE SIBERIAN CRATON

Age Constraints

The Khorbosuonka Group is latest Vendian in age. The group contains Ediacaran soft bodied metazoan fossils in the Khatyspyt Formation (Sokolov and Fedonkin 1984; Karlova 1987; Vodanjuk 1989; Missarzhevsky 1989a; Knoll et al. 1995a), and exhibits $\delta^{13}C$ profiles similar to other latest Vendian intervals (Knoll and Walter 1992; Narbonne et al. 1994; Kaufman and Knoll 1995; Knoll et al. 1995a). The $\delta^{13}C$ profiles contain a lower positive excursion to +6 ‰ PDB, an interval of relatively steady isotopic values ranging between -1 and +2 ‰, and an upper negative excursion at the top of the Khorbosuonka Group with values to -4 ‰. Knoll et al. (1995a) correlated the positive isotopic excursion characterizing the Mastakh and lower Khatyspyt formations of the lower Khorbosuonka Group with a similar positive isotopic excursion in the Ediacaran bearing Zaris Formation in the lower Nama Group, Namibia. U-Pb radiometric dates from volcanic ash beds interlayered with sedimentary rocks of the Nama Group provides a temporal calibration for the isotopic profiles (Grotzinger et al. 1995). The top of the positive excursion is 549 Ma, and the base of the negative excursion immediately beneath the Vendian-Cambrian boundary is conservatively estimated to be no older than about 544 Ma; the Precambrian-Cambrian boundary and top of the negative excursion is constrained to be approximately 543 Ma (Grotzinger et al. 1995). The base of the Khorbosuonka Group is taken to be ca. 555 Ma based on conservative sediment accumulation rates by Pelechaty et al. (1996), and thus, the Khorbosuonka and correlative units in this area are considered to span a maximum of the lastest 10 m.y. of Vendian time.

The Vendian deposits are overlain by earliest Cambrian sedimentary strata. Their ages are constrained paleontologically (Sokolov and Fedonkin 1984;

Missarzhevsky 1989a; Khomentovsky and Karlova 1993; Bowring et al. 1993; Knoll et al. 1995a).

Paleogeography

The present day Siberian craton covers an extensive region nearly 4.4 million km^2 in area in eastern Russia. Orogenic belts define the margins of the craton. Notably, the Baykalide collisional orogenic belt on the western and southern margins of the craton was active during Vendian to Cambrian time (Khain et al. 1985; Zonenshain et al. 1990; figure 1). Vendian strata are flat lying in the interior of the craton but are deformed in the bordering orogenic belts (Khain et al. 1985). Strata are exposed along river valleys and have been intersected in drill cores located in oil and gas exploration areas near the mouth of the Lena River and in southern Siberia (i.e. Lena-Tunguska; Fig. 3.1).

Vendian strata form an unconformity bounded interval of sedimentary rocks bounded below by a significant angular unconformity, and above by an equally extensive disconformity. The Vendian section is less than 500 m thick in the interior of the craton but is up to 1500 m thick along the margins of the craton (Bobrov 1979; Meyerhoff 1980; Khomentovsky 1986, 1990). Most of Siberia was covered by Vendian sediments except in a few regions, notably the Aldan shield; a prominent highland that was transgressed and overlain by only a thin succession (< 200 m) of sedimentary deposits during latest Vendian time (Khain et al. 1985; Khomentovsky 1990).

Vendian deposits form at least three major facies belts that trend roughly north to south across the craton (Bobrov 1979; Khomentovsky 1986, 1990; Surkova 1987; Grosman and Zhernovsky 1989; Shenfel 1991; Fig. 3.1): a western siliciclastic belt; a central carbonate and evaporite belt; and an eastern carbonate belt. The siliciclastic facies belt contains interbedded conglomerates, sandstones and shales interpreted to represent continental molasse deposits that were shed eastwards (present day

coordinates) from the ancient Baykalide mountains into an adjacent foredeep (Khain et al. 1985; Zonenshain et al. 1990). These deposits thin to the east across the craton where they occur associated with sequence boundaries intercalated with carbonate and evaporite deposits. The central carbonate and evaporite facies belt is characterized by bedded carbonates and sabhka related evaporites (Kuznetsov and Suchy 1992). This belt grades eastwards into the carbonate facies belt dominated by normal marine carbonates with uncommon siliciclastics in the Olenek uplift, Kharaulakh Mountains, and in southeastern Siberia (Magaritz et al. 1986, 1991; Khomentovsky 1990; Shenfel 1991; Pelechaty and Grotzinger 1993; Knoll et al. 1995a; Pelechaty, unpub. data).

Paleomagnetic data show that during Vendian time, the Siberian craton was geographically inverted and located at low latitudes (between 5° and 30°) of the southern hemisphere (Khramov et al. 1981; McKerrow et al. 1992). The low latitude position of Siberia is also supported sedimentologically by the extensive development of evaporites and carbonates. With respect to the reconstructed position of Siberia, the Baykalide mountains formed the eastern edge of the Siberian craton from which river systems transported coarse siliciclastic sediments to the west. The presence of sabhka deposits next to the Baykalides at this time suggests that an arid climate developed in this region as an orogenic rainshadow (i.e. Hoffman and Grotzinger 1993). This is consistent with predicted northeasterly tradewinds (present day coordinates) based on paleomagnetic data.

NORTHEAST SIBERIA: SEDIMENTOLOGY AND DEPOSITIONAL FACIES

Geologic Setting and Stratigraphic Nomenclature

Vendian and Cambrian deposits of the carbonate facies belt are exposed in the Olenek uplift and Kharaulakh Mountains region of northeastern Siberia (Figs. 3.1 and

3.2). In the Olenek area, strata dip gently in all directions from the center of the uplift, while strata in the Kharaulakh Mountains are folded into large north to south trending anticlines of the Verkoyansk fold belt. The datum for six stratigraphic sections is established using the base of wide spread Tommotian age, reddish hyolithid limestones (Fig. 3.3). In the southern Olenek at sections 2 and 3 the Kessyusa Formation is poorly exposed for detailed stratigraphic studies. Here, its thickness is based on regional mapping reported by Khomentovsky (1990).

Below the datum, Vendian and Cambrian deposits consist of two distinctive sedimentary packages separated by a regional paleokarst unconformity, which marks the Vendian-Nemakit Daldyn (ND) boundary. The unconformity is underlain by carbonate strata of the Khorbosuonka Group in the Olenek uplift, and the Kharayutekh Formation in the Kharaulakh Mountains (Figs. 3.2 and 3.3). ND age strata overlying the unconformity consist of siliciclastic deposits of the Kessyusa Formation in the Olenek uplift. In the Kharaulakh Mountains, the Tyuser Formation overlies Vendian carbonates and is informally divided into lower and upper members. Siliciclastic deposits of the lower member are unfossiliferous but are considered to be ND in age (Missarzhevsky 1989a, 1989b), while the upper member contains Tommotian age fauna, and is lithostratigraphically correlated with the Erkeket Formation above the Kessyusa Formation in the Olenek area (Repina et al. 1974; Ogurtsova 1975; Rudavskaya and Vasileva 1987; Valkov 1987; Meshkova et al. 1987; Bokova and Vasilyeva 1990). The Kessyusa-Erkeket contact is a paleokarst while the lower-upper member contact of the Tyuser Formation appears conformable.

The Khorbosuonka Group is less than 320 m thick in the Olenek area. It comprises three formations, including in ascending order (Sokolov and Fedonkin 1984; Khomentovsky 1990): the Mastakh Formation, less than 50 m of conglomerates, sandstones and dolostones; the Khatyspyt Formation, up to 180 m of black, bituminous limestones; and the Turkut Formation, 80 to 300 of buff colored dolostones. The

Mastakh Formation pinches out towards the southern Olenek area where the Turkut Formation forms the entire Khorbosuonka Group (Khomentovsky 1990). At the Dyapanskaya 1 well located between the Olenek uplift and Kharaulakh Mountains, the Khorbosuonka Group is 465 m thick (Mastakh, 65 m; Khatyspyt, 169 m; Turkut, 230 m; Surkova, 1987). The correlative Kharayutekh Formation comprises 480 m of mixed sandstones, bituminous limestones and dolostones. The base of the formation is not exposed at section 6. These rocks are divided into lower, middle and upper members that have been individually correlated with the Mastakh, Khatyspyt, and Turkut formations, respectively, in the Olenek area (Shapovalova and Shpunt 1982; Khomentovsky 1990).

The Kessyusa Formation is dominated by siliciclastic deposits and minor limestones and volcanic rocks (Repina et al. 1974; Valkov 1987; Shpunt and Shamshina 1989; Shpunt 1992; Bowring et al. 1993; Khomentovsky and Karlova 1993; Vidal et al. 1995; Knoll et al. 1995a). The formation thins to the northeast; it is 100 m thick along the Olenek River, 50 m thick at the Khorbosuonka River, and 30 m thick in the Kharaulakh Mountains. The ND-Tommotian stage boundary occurs in the upper part of the Kessyusa Formation in the Olenek uplift, and in the lower Tyuser Formation at the first occurrence of Tommotian age fauna (Repina et al. 1974; Ogurtsova 1975; Rudavskaya and Vasileva 1987; Valkov 1987; Moshkova et al. 1987; Missarzhevsky 1989a, 1989b; Bokova and Vasilyeva 1990; Bowring et al. 1993; Vidal et al. 1995; Knoll et al. 1995a; Fig. 3.3).

Vendian strata: Khorbosuonka Group and Kharayutekh Formation

The Vendian strata are interpreted to record sedimentation on carbonate ramps composed of at least four major depositional facies, including, tidal flat, lagoon, shoal and distal ramp. The carbonates are intercalated with minor fluvial and marine siliciclastic rocks at the bases of sections (Fig. 3.3). The strata thicken eastward from

the southern Olenek. This section expands upon previous descriptions of the facies and their regional variation in northeast Siberia (Krasilshchikov and Biterman 1970; Sokolov and Fedonkin 1984; Khomentovsky 1986, 1990; Shenfel 1991; Bowring et al. 1993; Pelechaty and Grotzinger 1993; Vidal et al. 1995; Knoll et al. 1995a; Pelechaty et al. 1995, 1996).

Siliciclastic Fluvial and Marine Facies

Siliciclastic deposits mark the base of the Turkut Formation in the southern Olenek (sections 2 and 3), while two separate siliciclastic units are developed to the north (section 4) at the bases of the Mastakh and Khatyspyt formations, and at section 5, where they comprise two siliciclastic to carbonate units (Fig. 3.3); an erosional surface marks the top of the lower unit (Khomentovsky 1990).

Reddish, quartz pebble conglomerates, sandstones and shales up to 10 m thick are developed at the base of the Mastakh Formation at section 4 (Figs. 3.3 and 3.4a). Units are thin to medium bedded, and are discontinuous both on a meter scale in outcrops and regionally along the Khorbosuonka River valley. Beds exhibit planar stratification, and simple and compound trough, and planar tabular cross bedding. Sandstones are locally current ripple laminated. Measurements of the thicker cross beds indicate northeast directed paleoflow (Fig. 3.3).

The red beds are interpreted as simple and complex channel floor dunes that accumulated in a braided river environment (Walker and Cant 1984). The regionally discontinuous nature of these deposits at section 4 may reflect either truncation of continuous, sheet like deposits, or the localization of fluvial sediments within incised valleys. Unpublished seismic data (courtesy of Maxus Energy Corp.) from this region shows significant antecedent relief along the basal Vendian unconformity, and suggests that deposition was probably confined to preexisting valleys.

The base of the Khatyspyt and Turkut formations in the southern Olenek is represented by massive conglomeratic units less than a few meters thick, and thin to medium bedded sandstones, which are trough and hummocky cross bedded (Fig. 3.4b). Sandstones are current rippled where they are thinly intercalated with shales. The lower part of section 5 contains intercalated cross bedded, glauconitic sandstones, desiccation cracked shales and stromatolitic dolostones (Fig. 3.3).

Collectively, these rocks record deposition in at least two marine settings: a tidal flat setting as shown by the occurrences of intercalated sandstones and mudcracked shales; and a storm influenced shelf setting as evidenced by occurrences of hummocky cross bedded sandstones and glauconitic sandstones (Hamblin and Walker 1979; Knoll et al. 1995a).

Tidal flat Facies

Stratigraphically, the tidal flat facies has its thickest development at sections 2 and 3 in the upper Turkut Formation, and forms the upper Mastakh Formation at section 4 (Fig. 3.3).

The tidal flat facies consist of very thin to thin bedded, buff colored dolomitic microbial laminites, packstones, grainstones and minor mudstones. The microbial laminites are finely laminated, which produces thin plates in weathered outcrops; individual laminae are crinkly, uneven, and locally form digitate stromatolites. Microbial laminites are typically desiccation cracked (Fig. 3.4c) and occur with laminated and current rippled clastic carbonates. Intraformational breccias locally truncate microbial units. The clastic carbonates are very fine to medium grained and consist variably of ooids, rip-up clasts of microbial laminites, intraclasts and oncoids. Oolites appear to be confined to tidal flat facies and have not been observed in other ramp facies. White cauliflower chert nodules have been described in the Mastakh Formation, and are considered to record the former presence of anhydrite (Knoll et al. 1995a).

The tidal flat deposits record deposition on flats dominated by microbial mats and periods of subaerial exposure and desiccation. This setting was episodically evaporitic and the site of calcium sulfate precipitation. Moderately high energy tidal and/or storm events intermittently deposited clastic carbonate sediments onto flats. Ooids and intraformational breccia clasts are restricted to tidal flat facies and most likely formed on tidal flats, while oncolites may have formed in outer shoal environments (see below) and then were transported onto tidal flats.

Lagoon Facies

This facies occurs as 20 to 40 m thick units intercalated with other proximal ramp facies (Figs. 3.3 and 3.5). It is characterized by thin to medium bedded stromatolitic dolostones, which form low relief, laterally linked domes 50 to 200 cm in diameter and up to 40 cm in height (Fig. 3.4d). Locally, domes may be elongate in form. Internally, domes exhibit either columnar or wavy laminae. Columnar laminae form columns less than 1 cm in width and a few 10's of cm's in height, and tend to be oriented perpendicular to the bases of beds and diverge upwards to the tops of beds. The surface texture of domes reflects internal lamination: smooth surfaced domes tend to be internally smoothly laminated while pustular surfaced domes are columnar laminated. Biostromes account for approximately 80 to 90 % of the facies; remaining deposits consist of rudstones, grainstones, packstones and mudstones. The clastic carbonates form current ripple laminated layers that drape domes. All the dolostones are parted by millimeter thick, green shale seams.

A shallow water origin for this facies is indicated by its association with tidal flat and shoal facies carbonates. The biostromal dolostones are interpreted to be quiet water deposits that formed in restricted, low energy lagoons inboard of carbonate shoals (see below; Kerans 1982). The mudstones, shales and the nonelongate aspect of most stromatolitic domes attest to predominately quiet water depositional conditions. This

setting, however, was probably influenced by occasional high energy depositional events as indicated by the presence of coarser clastic carbonate sediments, probably derived from nearby shoals, and the elongation of some stromatolitic domes (Pelechaty and Grotzinger 1989).

Shoal Facies

The shoal facies occurs interbedded with other proximal ramp deposits across the Olenek, and intercalated with distal ramp facies at sections 5 and 6 (Figs. 3.3 and 3.5).

This facies consists of intraclastic and oncolitic rudstones (Fig. 3.4e), grainstones and packstones, and minor mudstones. These deposits are thin to medium bedded and are typically amalgamated along sharp, irregular bases with cm's of scoured relief. Coarser deposits are variably trough cross bedded (Fig. 3.4f) with bedsets less than 50 cm thick, planar and current ripple laminated, or massive. Mudstones are typically massive. They occur as thin interbeds, lenses, mud flasers draping trough foresets, and rip-up clasts at the bases of coarser sedimentary beds.

Clastic carbonate grains range from very fine to granule in size. The coarsest beds are oncolitic. With increasing grain size, the morphology of oncoids is more complex: fine grainstones and packstones contain coated grains (i.e. an intraclast with a single isopachous micrite layer), while coarser grainstones are characterized by multicoated grains (i.e. several micrite layers coating an intraclast), and very coarse grainstones and rudstones have grapestone textures (i.e. several nuclei coated by multilayered micrite). The nuclei of grapestones variably include intraclasts, coated grains, and multicoated grains. The micritic laminations for all these grains vary in thickness around individual intraclast nuclei, exhibit truncation features and display asymmetric accretion patterns characteristic of other oncoids (Peryt 1983).

The coarse clastic carbonates are interpreted as traction deposits as shown by the predominance of trough cross beds, current ripples and erosional bases of beds

(Southard and Boguchwal 1990), and probably formed extensive sand and gravel shoals on platforms (i.e., Loreau and Purser 1973). Muds were probably deposited during intermittent periods of quiescence and then reworked during high energy events into sand size intraclasts. Sediment occasionally was transported landwards into lagoons and onto tidal flats during storms and/or tides. Intraclasts formed nuclei for microbially related precipitation and accretion of carbonate. Variations in the grain size of oncoids may reflect the interplay between depositional energy, supply of intraclasts as nuclei and residence time of sediment particles in the active sediment layer (Sumner and Grotzinger 1993).

Distal Ramp Facies

The distal ramp facies thicken to the northeast. It occurs as thin dolostones and limestones at sections 1, 2, and 3, and as thicker black limestones at sections 4, 5, and 6 (Figs. 3.3 and 3.4g).

The distal ramp facies is characterized by fine grained calcitic and dolomitic mudstones and wackestones. Limestones are characteristically black, highly bituminous deposits that exhibit a strong fetid odor. These deposits are considered significant hydrocarbon producing source rocks on the Siberian platform (Chersky 1986; Bolshakov 1987; Sokolov et al. 1989; Kashirtsev et al. 1993). Ediacaran body fossils are associated with the black limestones of this facies (Sokolov and Fedonkin 1984; Vodanjuk 1989; Sokolov et al. 1989; Knoll et al. 1995a). Dolostones are buff colored and non bituminous. Both limestones and dolostones are thin to medium bedded, and either finely laminated (Fig. 3.4g), massive, or nodular. Bedding is typically even, and locally exhibits pinch and swell structures related to postdepositional compaction. Laminae may show millimeter scale fining upward, silt to mud couplets. Beds exhibit small scale flutes and gutter casts, and soft sediment deformation features, including local slump related structures (Fig. 3.4h). Microbially laminated carbonate is

developed locally in the southern Olenek where the Khorbosuonka Group is dominated by shallow water carbonates. Wackestones tend to be thicker than mudstones, and occur as massive units with mudstone rip-ups and sharp, erosive bases.

These carbonates indicate that deposition occurred below storm wave base. Local microbial dolostones in the southern Olenek suggest that upper distal ramp facies developed within the photic zone. The limestones contain sedimentary organic carbon (<1%; Knoll et al. 1995a) indicating that the distal ramp was anoxic, at least at the sediment-water interface, and associated with relatively high rates of organic sediment accumulation (North 1990). The finely laminated, graded mudstones are interpreted as distal turbidites whereas the ungraded units are interpreted to record hemipelagic sedimentation (Cook and Mullins 1983). Flutes and gutter casts provide further evidence that turbulent flows occurred in this setting. The massive wackestones are interpreted as rapidly emplaced debris flow deposits based on the presence of their sharp erosive bases, and the disrupted nature of underlying beds. Erosional surfaces and slumps indicate that the distal ramp occasionally experienced failure resulting in the remobilization of sediment and generation of sediment gravity flows (Cook and Mullins 1983). Coarse, shallow water sediments are not present in the distal ramp facies, which indicates that very little sediment was derived from the platform. This suggests that the mudstones of this facies represent accumulation of mud that originally precipitated in the water column (Sami and James 1994).

Vendian-Nemakit Daldyn Unconformity

The Vendian-ND boundary generally coincides with a regionally extensive paleokarst unconformity developed across northern Siberia (Khomentovsky 1986, 1990; Pokrovsky and Venagradov 1991; Pokrovsky and Missarzhevsky 1993; Knoll, et al. 1995b). In northeast Siberia, the paleokarst shows up to 20 m of erosional relief.

It is associated with shallow sinkholes, potholes, surface karren (section C; Fig. 3.5), terra rossa soil and decimeter size, sandstone filled caves (Fig. 3.6a) developed beneath the main surface of erosion (Pelechaty and Grotzinger 1993; Pelechaty et al. 1996).

Early Cambrian Strata: Kessyusa and (Lower Member) Tyuser Formations

Early Cambrian time is represented by siliciclastic rocks and minor carbonates and volcanic rocks that collectively thin towards the northeast (Fig. 3.3). This section summarizes previous descriptions of these deposits (Repina et al. 1974; Valkov 1987; Shpunt and Shamshina 1989; Missarzhevsky 1989b; Shpunt 1992; Bowring et al. 1993; Knoll et al. 1995a) and presents the stratigraphic variability of these formations.

Siliciclastic Fluvial and Marine Facies

This facies includes conglomerates, sandstones and shales. In the Olenek uplift, quartz pebble conglomerates form fluvial deposits several meters thick that drape and fill antecedent karstic topography. At section 5, fluvial beds sharply overlie hummocky cross stratified sandstones. They occur as thick bedded, boulder conglomerates with clasts of rhyolite (99%) and subordinate basalt (Bowring et al. 1993). They are unidirectionally trough cross bedded and interfinger with marine sandstones and shales.

The marine deposits consist of interbedded sandstones and shales. Sandstones form thin to medium bedded amalgamated units in the lower and upper parts of the Kessyusa Formation, and at the base of the lower member of the Tyuser Formation (Fig. 3.3). Sandstones exhibit trough and hummocky cross bedding, and current ripple lamination. Beds are also bioturbated (Fig. 3.6b) and locally contain abundant glauconite. Shales are typically recessive in outcrop and poorly exposed. Collectively,

these deposits have been interpreted to indicate deposition on the outer shoreface of a storm influenced siliciclastic shelf (Knoll et al. 1995a).

Limestones: Calcrete and Marine Facies

Minor limestones occur as traction deposits and calcretes. The traction deposits are thin to medium bedded, trough cross stratified oolitic grainstones. Oolitic beds everywhere gradationally overlie sandstones to cap the Kessyusa Formation in the Olenek uplift; their tops are marked by a paleokarst at the top of the formation. They contain glauconite and have been interpreted to represent isolated carbonate sand shoals that developed on a high energy siliciclastic dominated shelf (Knoll et al. 1995a).

Calcretes are developed at the tops of scoured pillowed basalts at section 6 (Figs. 3.3 and 3.6c). The calcretes consist of laminated, accretionary micritic crusts that fill fractures in basalts and mantle the tops of the flows. They resemble other examples of Proterozoic calcretes (Pelechaty and James 1991). Pebbles of basalt and rhyolite occur cemented in calcretes and in sandstones above the calcretes (Fig. 3.6d).

Igneous Rocks

Volcanic breccias and associated diatremes occur in the Olenek uplift, while pillowed basalts and rhyolitic conglomerates occur at sections 5 and 6 (Shpunt and Shamshina 1989; Bowring et al. 1993). Horizons of volcanic breccia in the lower Kessyusa Formation at section 4 contain pumice fragments with zircons that have yielded an upper intercept age of 543.8+5.1/-1.3 Ma (Bowring et al. 1993). Compositionally similar diatremes (Fig. 3.6e) cross cut the upper Turkut Formation in the same area and have been reported by Shpunt and Shamshina (1989) to be cut by the Vendian-ND unconformity. Due to the lithologic similarity between the diatremes and the extrusive breccias, however, injection of diatremes probably continued to Early Cambrian time.

The rhyolite clasts have been interpreted as eroded remnants of volcanic or shallow intrusive bodies (Bowring et al. 1993). Zircons from the boulders at section 5 yield an U-Pb age of 534.6±0.5 Ma (Bowring et al. 1993). Pillowed basalts at section 6 are 2 to 7 m in thickness; they display well preserved pillow margins, chilled basal contacts and amygdules along their tops. The observation of coexisting felsic and mafic clasts in fluvial deposits at section 5 and within calcretes at section 6 provide sedimentologic evidence for coeval bimodal volcanism in the Kharaulakh Mountains.

Tommotian Strata: Erkeket and (Upper Member) Tyuser Formations.

Tommotian strata form the base of 700 to 800 m of limestones unconformably overlying the Kessyusa and correlative formations (Fig. 3.3). The base of the Tommotian is marked by 1 to 3 m of pebbly sandstones in the Olenek, and 1 to 2 m of bioturbated sandstones and sandy limestones to the northeast. These units are overlain by thin bedded, maroon colored mudstones, wackestones and hyolithid packstones (Fig. 3.6f). The limestones are shallow water deposits that onlapped the Kessyusa shelf during a rise in relative sea level (Knoll et al. 1995a).

INTEGRATED SEQUENCE STRATIGRAPHY AND $\delta^{13}C$ CHEMOSTRATIGRAPHY

Pelechaty et al. (1996) provided a $\delta^{13}C$ chemostratigraphic framework and detailed discussion of the geochemical and diagenetic aspects of these $\delta^{13}C$ profiles for the Vendian sections in northeast Siberia. Their results are summarized herein and incorporated into a sequence stratigraphic analysis of these same strata.

$\delta^{13}C$ Chemostratigraphic Constraints

The $\delta^{13}C$ profiles exhibit at least three major secular isotopic carbon anomalies, and following the nomenclature of Pelechaty et al. (1996) include from oldest to youngest (see inset; Fig. 3.3): (1) a P interval, a positive carbon isotope excursion with values up to +6 ‰; (2) an intermediate I interval with relatively little variation in isotopic carbon values ranging between -1 and +2 ‰; and (3) a N interval, a prominent negative excursion with values that decrease to -4 ‰ at the top of the Vendian. The isotopic profiles are used to construct time lines or chemo chrons (Figs. 3.3 and 3.7) by correlating the top of the P interval (chemo chron 1) and the base of the N interval (chemo chron 2).

The most complete $\delta^{13}C$ record occurs at section 4 (Fig. 3.3) with the P interval expressed in the Mastakh and lower Khatyspyt formations, the I interval in the upper Khatyspyt and lower Turkut formations, and the N interval at the top of the Turkut Formation (Knoll et al. 1995a). The P interval is present across the Olenek area in the Khatyspyt Formation at section 1 and in the lower Turkut Formation at sections 2 and 3. In the lower 80 m of section 5, a few data points are considered to represent the P interval. The I interval is present across northeast Siberia and systematically thickens to the northeast from 75 m at section 1 to at least 420 m at section 5; the N interval is not preserved here, so the complete thickness of the I interval is unknown. The isotopic values at section 6 have been interpreted to represent a diagenetically altered I interval based on the covariance between $\delta^{13}C$ and $\delta^{18}O$ (Pelechaty et al. 1996). The N interval is well developed locally at sections 1 and 4.

Sequence Stratigraphic Correlation

The Vendian and Cambrian deposits are partitioned into at least five depositional sequences based on the recognition of unconformities, vertical stacking patterns of facies and $\delta^{13}C$ chemostratigraphic constraints (Fig. 3.7).

Sequence 1

The Mastakh Formation at section 4 forms a single, unconformity bounded depositional sequence (Knoll et al. 1995a; Fig. 3.7). The sequence at this location consists of lowstand fluvial conglomerates and transgressive to highstand tidal flat dolostones. Isotopically, sequence 1 is characterized by rising positive $\delta^{13}C$ values of the P interval. As proposed by others (Shapovalova and Shpunt 1982; Khomentovsky 1990), the Mastakh Formation is considered to correlate with the lower unconformity capped siliciclastic to carbonate unit (parasequence) at section 5. There is no evidence of exposure at the top of the overlying siliciclastic to carbonate parasequence. Sequence 1 pinches out toward the southern Olenek area.

Sequence 2

The sequence is represented by the lower Turkut Formation at sections 2 and 3, parts of the Khatyspyt Formation at sections 1 and 4, and the middle member of the Kharayutekh Formation at section 5; and, isotopically, by the upper P and lower I intervals (Fig. 3.7).

At section 2, the top of sequence 2 is marked by a paleokarst in the middle of the Turkut Formation above an interval of shoal facies carbonates that exhibit well developed karstic porosity. The same stratigraphic horizon at section 3 does not exhibit obvious karstic features. At section 5, the top of sequence 2 is defined as a sharp

transition between distal ramp limestones and overlying shoal facies dolostones. This surface is considered to represent an abrupt downward shift in facies that formed in response to a drop in sea level (Van Wagoner et al. 1988) that did not lead to exposure of the platform at this section. The correlative sequence boundary is not obvious at sections 1 and 4. Here, the boundary may be a subtle unconformity or correlative conformity in distal ramp facies of the Khatyspyt Formation. The sequence boundary is tentatively placed at the level of a discrete black shale unit in the lower Khatyspyt Formation at section 4 (Fig. 3.7), which is considered to represent background sedimentation during a sea level lowstand. Thus, the Khatyspyt and Turkut formations are divided into two sequences, as opposed to a single, shallowing upward sequence as suggested by Knoll et al. (1995a). At section 1, because of the gradational upward shallowing from distal to proximal facies (Fig. 3.5), the sequence boundary is placed below this transition in the I interval.

Sequence 2 is partitioned into transgressive and highstand systems tracts. Interpreted transgressive deposits occur at the base of the sequence as marine sandstones and shales in the Olenek uplift, and as the upper siliciclastic to carbonate parasequence at section 5 (Fig. 3.7). These lowermost transgressive deposits are sharply overlain by distal ramp facies along a distinctive flooding surface (fs 1), which is confidently correlated across northeast Siberia. It marks the first significant flooding event in this region. The sequence is dominated by transgressive to highstand proximal ramp facies in the southern Olenek; they form two shallowing upward parasequences separated by a flooding surface (fs2) present only in this area. Distal ramp facies are mainly developed at sections 1, 4 and 5.

Sequence 3

Sequence 3 is a truncated sequence. It is represented by most of the Turkut Formation at sections 1, 2 and 3, the upper Khatyspyt and Turkut formations at section

4, the upper member of the Kharayutekh Formation at sections 5 and 6, and isotopically by the upper I and N intervals (Fig. 3.7).

The sequence is partitioned into lowstand, transgressive, and highstand system tracts. Shoal facies dolostones at the base of the sequence at section 5 and in the lower part of section 6 are considered to represent a lowstand sedimentary wedge that formed following an abrupt basinward shift in facies following a drop in relative sea level. These deposits are absent in the Olenek uplift and may correspond in time with the upper boundary of sequence 2 at sections 2 and 3. The lowstand deposits at sections 5 and 6 are sharply overlain by distal ramp facies along a flooding surface (fs 3; Fig. 3.7), which is correlated with another prominent flooding surface in the southern Olenek where it coincides with the top of sequence 2. Overlying this surface, interpreted transgressive to highstand deposits record gradual shoaling to sea level towards the top of the Vendian. The sequence is capped by the Vendian-ND paleokarst unconformity. On the basis of chemostratigraphy, the Vendian strata are truncated to the east from sections 4 to 6 (Fig. 3.7).

Sequence 4

The Kessyusa Formation forms a single, unconformity bounded depositional sequence at section 4 (Knoll et al. 1995a). They partitioned the sequence at this location into four parasequences, interpreted to record highstand sedimentation based on the absence of net long term variation in parasequence thickness and grain size. Poor outcrop exposures of the sequence elsewhere in the Olenek area has prohibited the recognition of similar parasequences.

The top of sequence 4 in the Olenek area is a paleokarst surface that formed during exposure of the Kessyusa shelf. This boundary correlates with one of two possible stratigraphic surfaces at sections 5 and 6: (1) the base of coarse fluvial conglomerates at section 5 and its correlative surface at the base of marine sandstones at

section 6; or (2) the contact between the lower and upper members of the Tyuser Formation (Fig. 3.7). The top of the lower member does not show evidence for exposure, however, the conglomerates incise outer shoreface, hummocky cross bedded sandstones, and signify a major drop in relative sea level, and is thus chosen to mark the base of sequence 5. This correlation illustrates pronounced thinning of sequence 4 to the northeast.

Sequence 5

The Erkeket Formation and part of the Tyuser Formation form the base of a separate depositional sequence. The lower part of sequence 5 consists of mainly siliciclastic rocks interpreted to be transgressive deposits. At section 6, they form two parasequences composed of lower bioturbated sandstones, pillowed basalts and capping calcretes. Correlative parasequences are not obvious at section 5. These deposits thin to the Olenek area where thin conglomerates overlie the sub-Erkeket paleokarst. Reddish limestones overlie these deposits along a distinct flooding surface and form the base of 700 to 800 m of limestones considered to reflect prolonged quiet water highstand sedimentation (Knoll et al. 1995a).

DISCUSSION

Subsidence of the Northeast Siberian Craton

A time versus space diagram (c.f. Wheeler 1958) is constructed to help illustrate the differential motions of the northeast Siberian craton during Vendian to Cambrian time (Fig. 3.8). Three distinct periods of sedimentation separated by major unconformities are recognized: (1) Vendian age carbonate ramp development (sequences 1, 2, and 3) in an east facing basin; (2) ND age siliciclastic shelf development

(sequence 4) in a south facing basin; and (3) post-ND age carbonate sedimentation (base of sequence 5) in a north facing basin.

The first three sequences (1-3) reflect deposition in a gently subsiding, east facing basin from ca. 555-543 Ma (Fig. 3.8). Sequence 1 is interpreted to represent the westward onlap of a thin, shallow water platform prior to 549 Ma. As suggested by Khomentovsky (1990), sequence 1, which consists of the Mastakh Formation in the Olenek area, is shown to be erosionally truncated to the west.

Sequence 2 reveals a complete shallow to deep water ramp transition in northeast Siberia. The basal transgressive siliciclastic rocks probably onlapped the older sequence to the west as indicated by concomitant thinning of the sequence and lateral transition from distal to proximal ramp facies in a westward direction. Ramp progradation probably occurred towards sections 5 and 6 from the southern Olenek based on regional $\delta^{13}C$ correlations. Chemo chron 1 demonstrates that distal ramp facies young to the east (Fig. 3.7). Distal ramp sedimentation occurred at sections 1 and 4 during P interval time but did not start until after P interval time at section 5 and possibly at section 6 (fs 1; Fig. 3.8). This correlation nicely illustrates stratigraphic downlap to the east. By the end of sequence 2 time, distal ramp sedimentation developed across northeast Siberia while shallow water conditions were confined to the southern Olenek (sections 2 and 3; Fig. 3.8). A drop in relative sea level culminated in subaerial exposure and erosion of the ramp in the southern Olenek uplift, and a basinward shift in shallow water deposition to the east with the formation of a lowstand sedimentary wedge at sections 5 and 6 at the start of sequence 3 time. Subsequent flooding of the craton led to extensive distal ramp sedimentation. By the end of sequence 3 time, however, shallow water conditions extended across most of northeast Siberia following widespread shoaling.

The Vendian-ND paleokarst represents a major drop in relative sea level, subaerial exposure, and erosion of Vendian carbonates. The paleokarst progressively

truncates the Vendian to the northeast towards the outer part of the basin, implying that the paleokarst formed in response to tectonic tilting of the craton. Significant unconformities at the Vendian-Cambrian boundary also are developed at other sections across Siberia (Khomentovsky 1990; Pelechaty, unpub. data), and within other basins, such as in Namibia (Saylor et al. 1995), western North America (Narbonne et al. 1994; Ross et al. 1995; Runnegar et al. 1995), Australia (Christie-Blick et al. 1995; Jenkins 1995; Walter et al. 1995), and Greenland and Svalbard (Fairchild and Hambrey 1995). Thus, the paleokarst in northeast Siberia may also reflect a drop in eustatic sea level, in addition to local tectonism.

Similar to the Vendian-ND paleokarst, the unconformity at the top of sequence 4 truncates ND age strata to the north and implies that tectonic uplift persisted during deposition of the ND shelf sequence from 543 to 530 Ma (Fig. 3.8). Facies of sequence 4 deepen to the southwest suggesting that deposition occurred in a local south facing basin. The shelf sequence is shown to onlap the Vendian platform to the north, which implies a diachronous age for basal strata of sequence 4. At the close of the ND, the Kessyusa shelf became exposed during a lowering in relative sea level. The sequence at sections 5 and 6 is shown to be truncated by valley fill deposits that incise outer shoreface strata, and is interpreted to reflect continued tectonic uplift in this region. This interpretation is further supported by the presence of bimodal volcanic rocks at sections 5 and 6. Using available biostratigraphic data (Missarzhevsky 1989a; Bowring et al. 1993; see inset A of Fig. 3.8), the shelf was first uplifted and exposed at sections 5 and 6 at the start of fossil stage 5, while the shelf remained submerged and sedimentation continued in the Olenek area. The unconformity appears to be diachronous in time, decreasing in age to the Olenek area. Restoration of a northerly tilt resulted in the formation of a north facing basin. The sequence 4 shelf became exposed in the Olenek at the start of fossil stages 6 and 7, following initial onlap of the craton at sections 5 and 6 from the north.

This onlap is interpreted to signal the onset of subsidence in this region at approximately 530 Ma following a prolonged period of volcanic activity and uplift.

Implications for Vendian to Cambrian Rifting in Northern Siberia

The Vendian sequences form part of a passive margin succession that developed along the eastern edge of the Siberian craton during Neoproterozoic time (Khain 1985; Zonenshain et al. 1990). On the basis of evidence for sporadic tectonic tilting and bimodal volcanism, the post-Vendian sequences in northeast Siberia are interpreted to reflect the influence of mild (i.e., far field effects) continental extension along the northeastern margin of the craton. Uplift in response to convergent tectonics is considered unlikely because deformation is limited to regional tilting and local high angle faulting, and there is no evidence of foreland basin style sedimentation (i.e. flysch, molasse; Allen et al. 1986), or associated fold and thrust belt. Although there also is no indication of large scale rifting preserved in outcrop in northeast Siberia (i.e. deep, fault bounded basins, abundant volcanic rocks), such rifting may have been located several hundred's of km's to the north where no Vendian and Cambrian rocks are presently exposed. The proposed rift sequence in northeast Siberia is thin and contains only a few volcanic rocks, however, such a sedimentary record may represent rift related processes, including thermally driven uplift (i.e. DeCharpal et al. 1978; Steckler et al. 1988) followed by postrift subsidence in a region of relatively unstretched upper crust along the flank of an active rift zone (i.e. rift shoulder; Bally and Snelson 1980; Steckler 1985; Bond et al. 1989).

Extension in northeast Siberia is suggested to have started at least by 543 Ma culminating in differential uplift and erosion of the Vendian platform. Episodes of rift related uplift may have started earlier at the close of Vendian time with injection of diatremes in the Olenek area, and the replacement of deep ramp facies by more proximal

ramp facies at section 5 (Figs. 3.8 and 3.9). Uplift continued until ca. 530 Ma, at which time volcanism ceased and the region likely underwent passive subsidence and open marine carbonate sedimentation. The proposed rifting probably lasted nearly 15 Ma. The main phase of rift related uplift probably occurred during ND time (Figs. 3.9b and 3.9c). Rifting was associated with tilting of the craton to form a south facing depocenter that received abundant siliciclastic sediments, and volcanic activity marked by intrusion of diatremes, and extrusion of volcanic breccias, rhyolites and basalts. Uplift probably continued until 530 Ma as suggested by the observed truncation of sequence 4 in the Kharaulakh Mountains (Fig. 3.9d). Bodies of hypabyssal intrusive or extrusive rhyolites may have been uplifted at this time during high angle faulting (Bowring et al. 1993), and then eroded and transported by rivers that incised underlying sedimentary deposits.

The onset of differential subsidence (i.e. flexural and/or thermal) is proposed to coincide closely with the beginning of Tommotian time and development of a sedimentary basin characterized by northerly increasing subsidence (Fig. 3.9e). In northeast Siberia, the Early to Late Cambrian age section is truncated and unconformably overlain by Permian sandstones, and so the record of proposed postrift sedimentation is incomplete; at a maximum, 25 Ma of postrift sedimentation is represented assuming an age of 505 Ma for the Cambrian-Ordovician boundary (Harland et al. 1989).

The interpreted rifting in northeast Siberia may have developed across the northern margin of the Siberian craton. The Vendian-ND paleokarst also occurs on the western (Fig. 3.1; Knoll et al. 1995b) and eastern (Pelechaty, unpub. data) margins of the Anabar uplift and suggests that exposure and erosion of the Vendian carbonates extended across the north. Occurrences of felsic and mafic volcanic rocks in the Anabar area of reportedly Vendian age (Shpunt 1988, 1992) also indicates that paleokarst development coincided with volcanism, as shown by this study in northeast Siberia.

Throughout the Siberian platform the Vendian-Cambrian unconformity is a significant boundary that marks a pronounced change in lithology, depositional style, and fossil content. The relative amount of erosion on the unconformity can be estimated by the degree of preservation of the sub-Cambrian isotopic excursions (i.e. the negative excursion) immediately beneath the unconformity. Across northern Siberia, including the western Anabar uplift (Pokrovsky and Venagradov 1991; Pokrovsky and Missarzhevsky 1993; Knoll et al. 1995b) and northeast Siberia (Knoll et al. 1995a; this study) the negative excursion is either completely missing or only the lower part is preserved (i.e. values decrease upsection; Fig. 3.10). In contrast, complete negative excursions are observed within Vendian carbonates beneath the sub-Cambrian unconformity to the south. In the Turukhansk area in western Siberia, a full negative excursion occurs in Vendian carbonates of the Platonovskaya Formation (Bartley et. al. in prep). Similarly, Vendian carbonates at the Dvortsy section on the Aldan River, southern Siberia, exhibit the upper part of the negative excursion (i.e. values increase upsection; Magaritz et al. 1986, 1991). A complete negative excursion is also observed within the upper part of the Vendian Tennovskaya Formation at a section located on the Lena River near the mouth of the Patom River (Fig. 3.10; Pelechaty, unpub. data). On the basis of the correlation of sub-Cambrian isotopic profiles across the Siberian platform, the sub-Cambrian unconformity in the north is considered to be associated with significant truncation of Vendian carbonates. This pattern of erosion in the north is interpreted to reflect the regional development of a broad, thermally elevated rift shoulder along the craton's northern margin; it is inferred that an early Cambrian age active rift zone was positioned farther to the north.

CONCLUSIONS

(1) The $\delta^{13}C$ excursions observed in Vendian carbonates of northeast Siberia appear to be concordant with the time stratigraphic framework independently established by sequence stratigraphic methods. An important implication of this observation is that the isotopic shifts seem to be temporally equivalent geochemical events at least at the scale of individual depositional sequences. Although this conclusion is implicit in previous studies that account for isotopic fluctuations in carbonates through variability in global carbon fluxes (Knoll et al., 1986; Kaufman and Knoll, 1995), the stratigraphic relationships documented here independently test and support that conclusion.

(2) Integrated $\delta^{13}C$ chemostratigraphy and sequence stratigraphy is shown to be an effective high resolution chronostratigraphic tool for basin analysis. This integrated approach yields enhanced time stratigraphic resolution at the intrasequence level that enables recognition of stratigraphic onlap and downlap, and evaluation of intrabasinal variations in subsidence and erosion.

(3) The Vendian to Cambrian transition of northeast Siberia records a complex basin history divided into three main episodes: (a) Vendian age carbonate platform development within an east facing basin; (b) Nemakit Daldyn age siliciclastic shelf development in a south facing basin; and (c) post-Nemakit Daldyn age carbonate sedimentation within a restored north facing basin.

(4) The Vendian carbonates represent part of a passive margin sequence that developed along the eastern margin of the Siberian craton during Neoproterozoic time. The observed stratigraphic relationships and occurrence of bimodal volcanic rocks are used to argue that extension occurred in northern Siberia. Extension is proposed to have started no later than 543 Ma, and continued until lower Tommotian time (530 Ma). The interpreted rift sequence is thin and contains only few volcanic deposits but is

considered to represent deposition upon a largely unstretched rift shoulder that developed across the northern margin of the Siberian craton. Extension was marked by uplift and truncation of Vendian strata to the north, reversal in depositional gradient, influx of siliciclastic sediments, bimodal volcanism and possible local faulting. The onset of passive subsidence related to decay of thermal anomalies and/or flexural loading is postulated to have started at 530 Ma coincident with southward flooding of the craton and accumulation of widespread open marine limestones.

REFERENCES

Allen, P.A.; Homewood, P.A.; Williams, G.D., 1986, Foreland basins: An introduction: *in* Allen, P.A., and Homewood, P.A., eds.: Intern. Assoc. Sed. Spec Pub. No. 8, p. 3-12.

Bally, A.W., and Snelson, S., 1980, Realms of subsidence, *in* Miall, A. D., ed., Facts and principles of world petroleum occurrences: Can. Soc. Petro. Geol., Mem. 6, p. 9-94.

Bartley, J.K.; Pope, M.; Knoll, A.H.; Petrov, P.Yu.; Semikhatov, M.A.; and Sergeev, V.N., in prep, A Proterozoic-Cambrian boundary succession from the western Siberian Platform: Stratigraphy, geochemistry, and paleontology: Palaios.

Bobrov, A.K., 1979, Stratigraphy and paleogeography of deposits of the upper Precambrian of southern Yakutia: Yakutsk, Yakutian Book Pub., p. 128 (in Russian).

Bokova, A.R., and Vasilyeva, N.I., 1990, Some new species of skeletal problematics from the Lower Cambrian of the Olenek uplift, *in* Fossil Problematics of the USSR: Moscow, Nauka, p. 28-33 (in Russian).

Bolshakov, Y.A., 1987, Geology and geochemistry of oil and gas, and coal, Yakutia: Yakutsk, Russ. Acad. of Sci., Inst. Geol., Yakutia, 143 p. (in Russian).

Bond, G.C.; Kominz, M.A.; Steckler, M.S.; and Grotzinger, J.P., 1989, Role of thermal subsidence, flexure, and eustasy in the evolution of early Paleozoic passive margin carbonate platforms, *in* Crevello, P. D., Wilson, J. L., Sarg, J. F., and Read, J. F., eds., Controls on carbonate platform and basin development: SEPM Spec. Pub. No. 42, p. 39-61.

Bowring, S.A.; Grotzinger, J.P.; Isachsen, C.E.; Knoll, A.H.; Pelechaty, S.M.; and Kolosov, P., 1993, Calibrating rates of early Cambrian evolution: Science, v. 261, p. 1293-1298.

Braiser, M.D.; Khomentovsky, V.V.; and Corfield, R.M., 1993, Stable isotopic calibration of the earliest skeletal fossil assemblages in eastern Siberia (Precambrian-Cambrian boundary): Terra Nova, v. 5, p. 225-232.

Burns, S.J. and Matter, A., 1993, Carbon isotopic record of the latest Proterozoic from Oman: Eclogae geol. Helv., v. 89, p. 595-607.

Chersky, H.V., 1986, Upper Precambrian-Phanerozoic oil and gas deposits, eastern part of the Siberian platform: Russ. Acad. Sci., Inst. Geol., Yakutia, 123 p. (in Russian).

Christie-Blick, N.; Grotzinger, J.P.; and von der Borch, C.C., 1988, Sequence stratigraphy in Proterozoic successions: Geology, v. 16, p. 100-104.

Christie-Blick, N.; 1991, Onlap, offlap, and the origin of unconformity bounded depositional sequences: Marine Geol., v. 97. p. 35-56.

Christie-Blick, N.; Dyson, I.A.; and von der Borch, C.C., 1995, Sequence stratigraphy and the interpretation of Neoproterozoic Earth history: Precamb. Res., v. 73, p. 3-26.

Cook, H.E., and Mullins, H.T., 1983, Basin Margin Environment, *in* Scholle, P. A., Bebout, D. G., and Moore, C. H., eds., Carbonate Depositional Environments: Tulsa, AAPG Mem. 13, p. 540-617.

DeCharpal, O.; Guennoc, P.; Montadert, L.; and Roberts, D.G., 1978, Rifting, crustal attenuation and subsidence in the Bay of Biscay: Nature, v. 275, p. 706-711.

Fairchild, I.J., and Hambrey, M.J., 1995, Vendian basin evolution in East Greenland and NE Svalbard: Precamb. Res., v. 73, p. 217-233.

Grosman, V.V., and Zhernovsky, V.P., 1989, About upper Precambrian and Cambrian boundary strata in deep wells of western Yakutia, *in* Khomentovsky, V. V., Sovetov, Y. K., Shenfel, V. Y., Yakshen, M. S., and Moryaken, V. B., eds., Late Precambrian and early Paleozoic of Siberia: Actual stratigraphic questions: Hovosibersk, p. 75-106 (in Russian).

Grotzinger, J.P.; Bowring, S.A.; Saylor, B.Z.; Kaufman, A.J., 1995, New biostratigraphic and geochronologic constraints on early animal evolution: Science, v. 270, p. 598-604.

Hamblin, A.P., and Walker, R.G., 1979, Storm dominated shallow marine deposits: The Fernie-Kootney (Jurassic) transition, southern Rocky Mountains: Can. Jour. Earth Sci., v. 16, p. 1673-1690.

Harland, B.W.; Armstrong, R.L.; Cox, A.V.; Craig, L.E.; Smith, A.G.; and Smith, D.G., 1989, A geologic time scale: Cambridge, Cambridge University Press, 263 p.

Hoffman, P.F., and Grotzinger, J.P., 1993, Orogenic precipitation, erosional unloading, and tectonic style: Geology, v. 21, p. 195-198.

Jenkins, R.J.F., 1995, The problems and potential of using animal fossils and trace fossils in terminal Proterozoic biostratigraphy: Precamb. Res., v. 73, p. 51-79.

Kerans, C., 1982, Sedimentology and stratigraphy of the Dismal Lakes Group, Proterozoic, Northwest Territories, Ph.D. thesis, Carleton University, Ottawa, Canada, 304 p.

Karlova, G.A., 1987, First findings of skeletal fauna in the Turkut Formation of the Olenek uplift: Doklady Acad. Sci. USSR, v. 292, p. 204-205 (in Russian).

Kashirtsev, V.A.; Philp, R.P.; Allen, J.; Galvec-Senebalde, A.; Zyeba, E.N.; Chalaya, O.H.; and Andreev, E.N., 1993, Biodegradation of bitumen within bitumenous rocks of the Olenek uplift: Geol. and Geoph., v. 34, p. 44-54 (in Russian).

Kaufman, A.J., and Knoll, A.H., 1995, Neoproterozoic variations in the C isotopic composition of seawater: Stratigraphic and biogeochemical implications: Precamb. Res., v. 73, p. 27-50.

Khain, V.E., 1985, Geology of the USSR: First part. Old cratons and Paleozoic fold belts, Bender, F., Jacobshagen, V., de Jong, J. D., and Lüttig, G., eds.: Berlin,Gebrüder Borntraeger, p. 272.

Khomentovsky, V.V., 1986, The Vendian System of Siberia and a standard stratigraphic scale: Geol. Mag., v. 123, p. 333-348.

Khomentovsky, V.V., 1990, Chapter 5: Vendian of the Siberian Platform, Sokolov, B. S., and Fedonkin, M. A., eds.: Berlin, Springer-Verlag, 2, p. 103-183.

Khomentovsky, V.V., and Karlova, G.A., 1993, Biostratigraphy of the Vendian-Cambrian beds and the lower Cambrian boundary in Siberia: Geol. Mag., v. 130, p. 29-45.

Khramov, A.N.; Petrova, G.N.; and Pechersky, D.M., 1981, Paleomagnetism of the Soviet Union, McElhinny, M. W., and Valencio, D. A., eds.: Am. Geoph. Union Geodyn. Ser., 2, p. 177-194.

Knoll, A.H., and Walter, M.R., 1992, Latest Proterozoic stratigraphy and Earth History: Nature, v. 356, p. 673-678.

Knoll, A.H., Hayes, J.M.; Kaufman, A.J.; Sweet, K.; and Lambert, I.B., 1986, Secular variation in carbon isotope ratios from Upper Proterozoic successions of Svalbard and East Greenland: Nature, v. 321, p. 832-838.

Knoll, A.H., Grotzinger, J.P.; Kaufman, A.J.; and Kolosov, P., 1995a, Integrated approaches to terminal Proterozoic stratigraphy: An example from the Olenek Uplift, northeastern Siberia: Precamb. Res., v. 73, p. 251-270.

Knoll, A.H., Kaufman, A.J.; Semikhatov, M.A.; Grotzinger, J.P.; and Adams, W., 1995b, Sizing up the sub-Tommotian unconformity in Siberia: Geology, v. 23, p. 1139-1143.

Krasilshchikov, A.A., and Biterman, I.M., 1970, Proterozoic group of the Olenek uplift, *in* Markov, F.G., ed., Geology of the USSR Western part of the Yakutian ASSR: Nedra, p. 91-100 (in Russian).

Kuznetsov, V.G., and Suchy, V., 1992, Vendian-Cambrian tidal and sabkha facies of the Siberian platform: Facies, v. 27, p. 285-294 (in Russian).

Loreau, J.P., and Purser, B.H., 1973, Distribution and ultrastructure of Holocene ooids in the Persian Gulf, *in* Purser, B.H., ed., Coated Grains: Berlin, Springer-Verlag, p. 279-328.

Magaritz, M.; Hoser, W.T.; and Kirschvink, J.L., 1986, Carbon isotope events across the Precambrian-Cambrian boundary on the Siberian platform: Nature, v. 320, p. 258-259.

Magaritz, M.; Kirschvink, J.L.; Latham, A.; Zhuravlev, A.Y.; and Rozanov, A.Y., 1991, Precambrian-Cambrian boundary problem: Carbon isotope correlations for Vendian and Tommotian time between Siberia and Morocco: Geology, v. 19, p. 847-850.

McKerrow, W.S.; Scotese, C.R.; and Brasier, M.D., 1992, Early Cambrian continental reconstructions: Jour. Geol. Soc. London, v. 149, p. 599-606.

Meshkova, N.P.; Zhuravleva, I.T.; and Luchinina, V.A., 1987, Lower Cambrian and the lower part of the Middle Cambrian of the Olenek uplift. Problems of paleontology and biostratigraphy in the Lower Cambrian of Siberia and the Far East: Nauka, Novosibersk, p. 194-214 (in Russian).

Meyerhoff, A.A., 1980, Geology and petroleum fields in Proterozoic and Lower Cambrian strata, Lena-Tunguska petroleum province, Eastern Siberia, USSR, *in* Halbouty, M. T.,

ed., Giant oil and gas fields of the decade 1968-1978: Tulsa, OK, AAPG Mem. 30, p. 225-252.

Missarzhevsky, V.V., 1989a, Oldest skeletal fossils and stratigraphy of Precambrian and Cambrian boundary beds: Nauka, v. 221, p. (in Russian).

Missarzhevsky, V.V., 1989b, Stratigraphy of Precambrian-Cambrian boundary deposits: a general model, *in* Drasheninnikov, V. A., ed., Problems of upper Proterozoic and Phanerozoic stratigraphy: Nauka, p. 59-74 (in Russian).

Narbonne, G.M.; Kaufman, A.J.; and Knoll, A.H., 1994, Integrated chemostratigraphy and biostratigraphy of the upper Windermere Supergroup (Neoproterozoic), Mackenzie Mountains, northwestern Canada: Geol. Soc. America Bull., v. 106, p. 1281-1292.

North, F.K., 1990, Petroleum Geology: Boston, Unwin Hyman, 631 p.

Ogurtsova, R.N., 1975, Lontovan acritarchs of the Tommotian stage on the Olenek uplift: Intern. Geol. Rev., v. 19, p. 921-923.

Pelechaty, S.M., and James, N.P., 1991, Dolomitized middle Proterozoic calcretes, Bathurst Inlet, Northwest Territories, Canada: Jour. Sed. Petrology, v. 61, p. 988-1001.

Pelechaty, S.M., and Grotzinger, J.P., 1989, Stromatolite bioherms of the 1.9 Ga foreland basin carbonate ramp, Beechey Formation, Kilohigok basin, Northwest Territiories, *in* Geldsetzer, H.H.J., James, N.P., and Tebbutt, G.E., eds., Reefs, Canada and Adjacent Areas: Can. Soc. Petro. Geol. Mem. 13, p. 93-104.

Pelechaty, S.M., and Grotzinger, J.P., 1993, Correlation of Vendian carbonate rocks between the Olenek uplift and Kharalaukh Mountains, northern Siberia: Geol. Soc. America Prog. with Abs., p. A337.

Pelechaty, S.M., Grotzinger, J.P , and Kaufman, A.J., 1995, Application of combined isotopic carbon chemostratigraphy and sequence stratigraphy for basin analysis: An example from the Vendian-Cambrian interval of northeast Siberia: Geol. Soc. America Prog. with Abs., v. 27, p. A330.

Pelechaty, S.M., Kaufman, A.J.; and Grotzinger, J.P., 1996, Evaluation of $\delta^{13}C$ isotope stratigraphy for intrabasinal correlation: Vendian strata of northeast Siberia: Geol. Soc. America Bull, v. 108, p. 992-1003.

Pelechaty, S.M.,1996, Stratigraphic evidence for the Siberia-Laurentia connection and Early Cambrian rifting: Geology, v. 24, p. 719-722.

Pell, S.D.; McKirdy, D.M.; Jansyn, J.; and Jenkins, R.J.F., 1993, Ediacaran carbon isotope stratigraphy of South Australia: An initial study: Trans. Royal Soc. Austr., v. 117, p. 153-161.

Peryt, T.M., 1983, Classification of coated grains, *in* Peryt, T. M., ed., Coated Grains: New York, Springer-Verlag, p. 3-6.

Pokrovsky, B.G., and Missarzhevsky, V.V., 1993, Isotope correlation of Precambrian and Cambrian of the Siberian platform: Akad. Nauk SSSR, Doklady, v. 329, p. 768-771 (in Russian).

Pokrovsky, B.G., and Venogradov, V.E., 1991, Isotopic composition of strontium, oxygen and carbon in upper Precambrian carbonates of the western area of the Anabar uplift (Kotyikan River): Akad. Nauk SSSR, Doklady, v. 320, p. 1245-1250 (in Russian).

Repina, L.N.; Lazarenko, N.P.; and Meshkova, N.P., 1974, Lower Cambrian biostratigraphy and facies of Kharaulakh: Nauka, Moscow, (in Russian).

Ripperdan, R.L., 1994, Global variations in carbon isotope composition during the latest Neoproterozoic and earliest Cambrian: Ann. Rev. Earth Planet. Sci., v. 22, p. 385-417.

Ross, G.M.; Bloch, J.D.; and Krouse, H.R., 1995, Neoproterozoic strata of the southern Canadian Cordillera and the isotopic evolution of seawater sulfate: Precamb. Res., v. 73, p. 71-99.

Rudavskaya, V.A., and Vasileva, N.I., 1987, Archaeocyaths and skeletal problematics in the Vendian, Tommotian, and Adtabanian, *in* Kokoulin, M.L., and Rudavskaya, V.A., eds., Stratigraphy of the Late Precambrian and Early Paleozoic of the Siberian platform: Leningrad, Nauka, p. 51-58 (in Russian).

Runnegar, B.; James, G.; Horodyski, R.J.; Sören, J.; and Knauth, L.P., 1995, Base of the Sauk sequence is a global eustatic event that lies just above the Precambrian-Cambrian boundary: Geol. Soc. America Prog. with Abs., v. 27, p. A330.

Sami, T.T., and James, N.P., 1994, Peritidal carbonate platform growth and cyclicity in an early Proterozoic foreland basin, Upper Pethei Group, Northwest Canada: Jour. Sed. Petrology, v. B64, p. 111-131.

Saylor, B.Z.; Grotzinger, J.P.; and Germs, G.J.B., 1995, Sequence stratigraphy and sedimentology of the Neoproterozoic Kuibus and Schwarzrand Subgroups (Nama Group), southwestern Namibia: Precamb. Res., v. 73, p. 153-171.

Shapovalova, E.G., and Shpunt, B.R., 1982, Chapter 2: Stratigraphy, Shpunt, B. R., Shapovalova, E. G., and Shamshena, E. A., eds: Hovosibersk, Russ. Acad. Sci., 224 p. (in Russian)

Shenfel, V.Y., 1991, Late Precambrian of the Siberian Platform: Novosibersk, Sci. Acad. USSR, 185 p. (in Russian).

Shpunt, B.R., 1988, Continental riftogenesis in the late Precambrian on the Siberian platform: Geotectonics, v. 22, p. 504-510.

Shpunt, B.R., and Shamshina, E.A., 1989, Late Vendian potassic volcanic rocks of the Olenek highlands on the northeast Siberian craton: Doklady Akad. Nauk SSSR, v. 307, p. 678-682.

Shpunt, B.R., 1992, Tectonic settings for Neogaea magnatism in the eastern Siberian platform: Geotectonics, v. 26, p. 214-227.

Sokolov, B.S., and Fedonkin, M.A., 1984, The Vendian as the Terminal System of the Precambrian: Episodes, v. 7, p. 12-19.

Sokolov, B.S., Egorov, V.A.; Nakaryakov, V.D.; Bitner, A.K.; Zhukovin, Y.A.; Kuznetzov, L.L.; Skorobogatikh, P.P.; and Zakharyan, A.Z., 1989, Geological and geophysical

conditions of formation of oil and gas bearing deposits in the ancient rocks of eastern Siberia, Walter, M. R., ed.: Moscow, Moscow University Press, 173 p.

Southard, J.B., and Boguchwal, L.A., 1990, Bed configurations in steady unidirectional water flows. Part 2. Synthesis of flume data: Jour. Sed. Petrology, v. 60, p. 658-679.

Steckler, M.S., 1985, Uplift and extension of the Gulf of Suez: Indication of induced mantle convection: Nature, v. 317. p. 135-139.

Steckler, M.S., Watts, A.B.; and Thorne, J.A., 1988, Subsidence and basin modeling at the U.S. Atlantic passive margin, *in* Sheridan, R. E., and Grow, J. A., eds.: Geol. Soc. America, No. 1-2, p. 399-416.

Sumner, D.Y., and Grotzinger, J.P., 1993, Numerical modeling of ooid size and the problem of Neoproterozoic giant ooids: Jour. Sed. Petrology, v. 63, p. 974-982.

Surkova, V.S., 1987, Megacomplexes and structures of the Earth's crust: Petroleum provinces of the Siberian platform: Nedra, Moscow, 204 p. (in Russian).

Van Wagoner, J.C.; Posamentier, H.W.; Mitchum, R.M.; Vail, P.R.; Sarg, J.F.; Loutit, T.S.; and Hardenbol, J., 1988, An overview of the fundamentals of sequence stratigraphy and key definitions, *in* Sea level Changes: An integrated approach: SEPM, Spec. Pub. 42, p. 39-46.

Vail, P.R.; Hardenbol, J.; and Todd, R.G., 1984, Jurassic unconformities, chronostratigraphy, and sea level changes from seismic stratigraphy and biostratigraphy, *in* Schlee, J. S., ed., Interregional unconformities and hydrocarbon accumulations: AAPG Mem. 36, p. 129-144.

Valkov, A.K., 1987, Biostratigraphy of the lower Cambrian of the east Siberian Platform: Moscow, Moscow Science, 136 p. (in Russian).

Vidal, G.; Moczydlowska, M.; and Rudavskaya, V.R., 1995, Constraints on the early Cambrian radiation and correlation of the Tommotian and Nemakit Daldynian regional stages of eastern Siberia: Jour. Geol. Soc. London, v. 152, p. 499-510.

Vodanjuk, S.A., 1987, Soft bodied metazoan remains of the Khatyspyt Formation, Olenek uplift, *in* Khomentovsky, V.V., Sovetov, Y.K., Shenfel, V.Y., Yaksher, M.C., and Moryaken, V.B., eds.: Late Precambrian and early Paleozoic of Siberia: Questions of Stratigraphy: Novosibersk, Russ. Acad. Sci., p. 61-74 (in Russian).

Walker, R.G., and Cant, D.J., 1984, Sandy fluvial systems, *in* Walker, R. G., ed., Facies Models: Geosci. Can., p. 71-90.

Walter, M.R.; Veevers, J.J.; Calver, C.R.; and Grey, K., 1995, Neoproterozoic stratigraphy of the Centralian Superbasin, Australia: Precamb. Res., v. 73, p. 173-195.

Wheeler, H.E., 1958, Time stratigraphy: AAPG Bull., v. 42, p. 1047-1063.

Zonenshain, L.P., Kuzmin, M.I. and Natapov, L.M., 1990, Geology of the USSR: A plate tectonic synthesis, *in* Page, B. M., ed.: Washington, D.C., Am. Geoph. Union, No. 21, 17-26 p.

LIST OF FIGURES

upper Turkut Formation at section 4; knife for scale; (F) Thin bedded, Tommotian age limestones of lower Erkeket Formation along Olenek River; hammer for scale.

Figure 3.7
Sequence stratigraphic correlation of Vendian and Cambrian strata. Letters: R, Riphean; V, Vendian; ND, Nemakit Daldyn; T, Tommotian; S, sequence; c, calcretes. U-Pb ages from Bowring and others (1993). Depositional gradients based on thickness and facies variations from outcrop and unpublished seismic and wire line log data (courtesy of Maxus Energy Corp.). See Fig. 3.3 for facies patterns.

Figure 3.8
Time versus space diagram. See Fig. 3.2 for location of sections. Age constraints: (a) estimated maximum age for basal Vendian strata; (b) 549 Ma as chemo chron 1, (c) 544 Ma as chemo chron 2, and (d) 543 Ma for the Vendian-Cambrian boundary (b, c, and d from Grotzinger et al. 1995); (e) an U-Pb age of 543+5.1/-1.3 Ma from Bowring et al. (1993); and stage boundaries (f) Tommotian and (g) Atdabanian from Bowring et al. 1983. Letters: R, Riphean; V, Vendian; ND, Nemakit Daldyn; T, Tommotian; A, Atdabanian; fs, flooding surface. Coded bar shows the isotopic intervals P (black), I (hashured) and N (white). Inset A shows diachronous sequence boundary (dark line) between sequences 4 and 5 from sections 4 to 5 based on fossil zones summarized by Knoll et al. (1995a).

Figure 3.9
Proposed tectonic history of the Vendian-Cambrian basin in northern Siberia.

Figure 3.10
Regional correlation of sub-Cambrian isotopic carbon profiles in Siberia. Only the N and upper I intervals are shown. Correlation illustrates pronounced erosion of uppermost Vendian strata beneath the sub-Cambrian unconformity in northern Siberia. Refer to Figs. 3.1 and 3.2 for location of sections: T, Turikhansk region (Bartley et al. in prep); A, western Anabar (Knoll et al. 1995b); 1, 2, 3, 4 and 5, northeast Siberia (this study); L, Lena River, southern Siberia (Pelechaty, unpub. data); D, Aldan River (Magaritz et al. 1986).

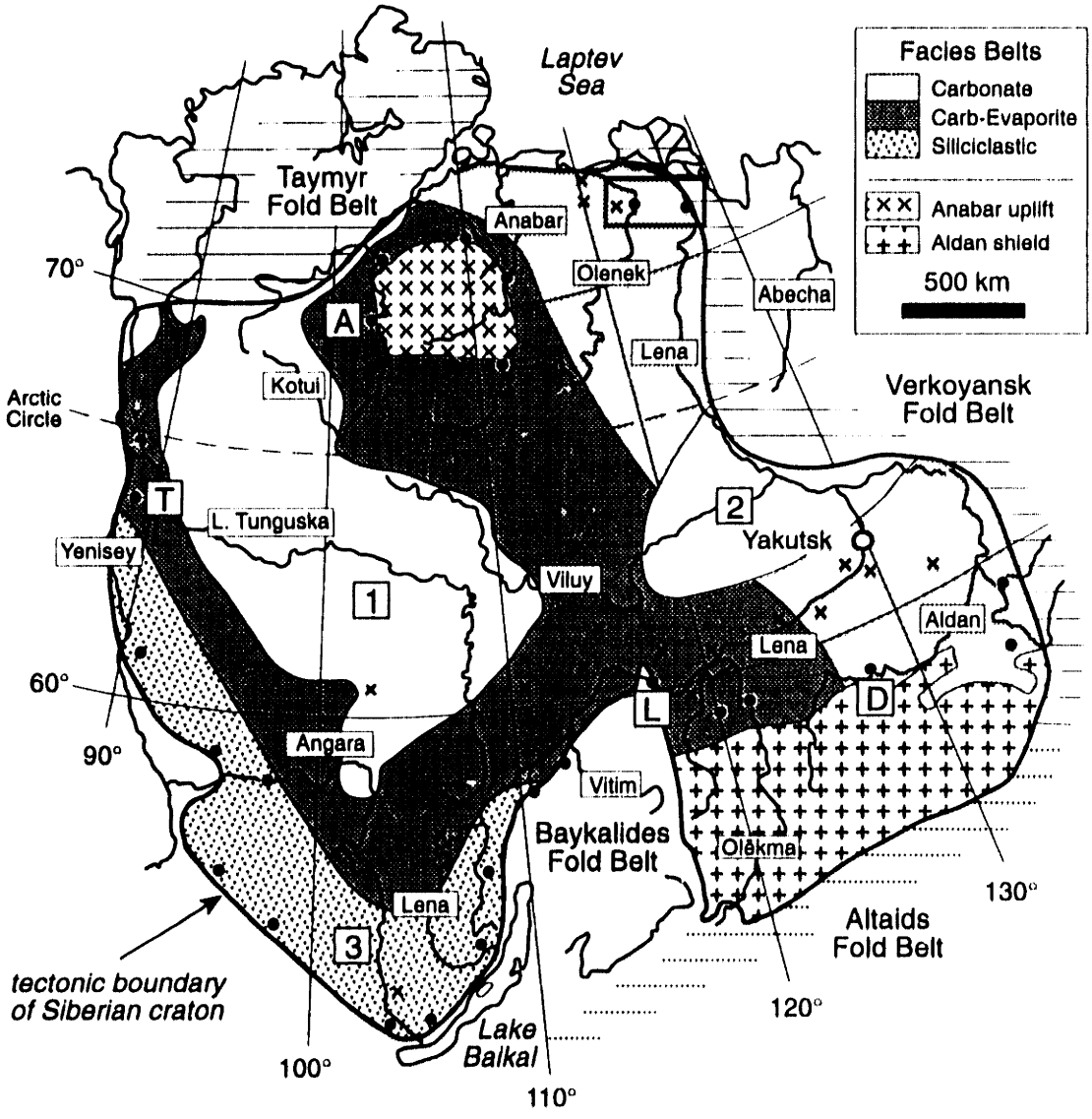
Facies Belts
Carbonate
Carb-Evaporite
Siliciclastic
Anabar uplift
Aldan shield
500 km
Laptev Sea
Taymyr Fold Belt
Anabar
Olenek
Abecha
Lena
Verkoyansk Fold Belt
Kotui
Arctic Circle
70°
A
T
L. Tunguska
Yenisey
1
2
Yakutsk
Viluy
Aldan
Lena
60°
90°
Angara
L
D
Vitim
Baykalides Fold Belt
Olekma
130°
Lena
3
Altaids Fold Belt
tectonic boundary of Siberian craton
120°
Lake Baikal
100°
110°

Figure 3.1

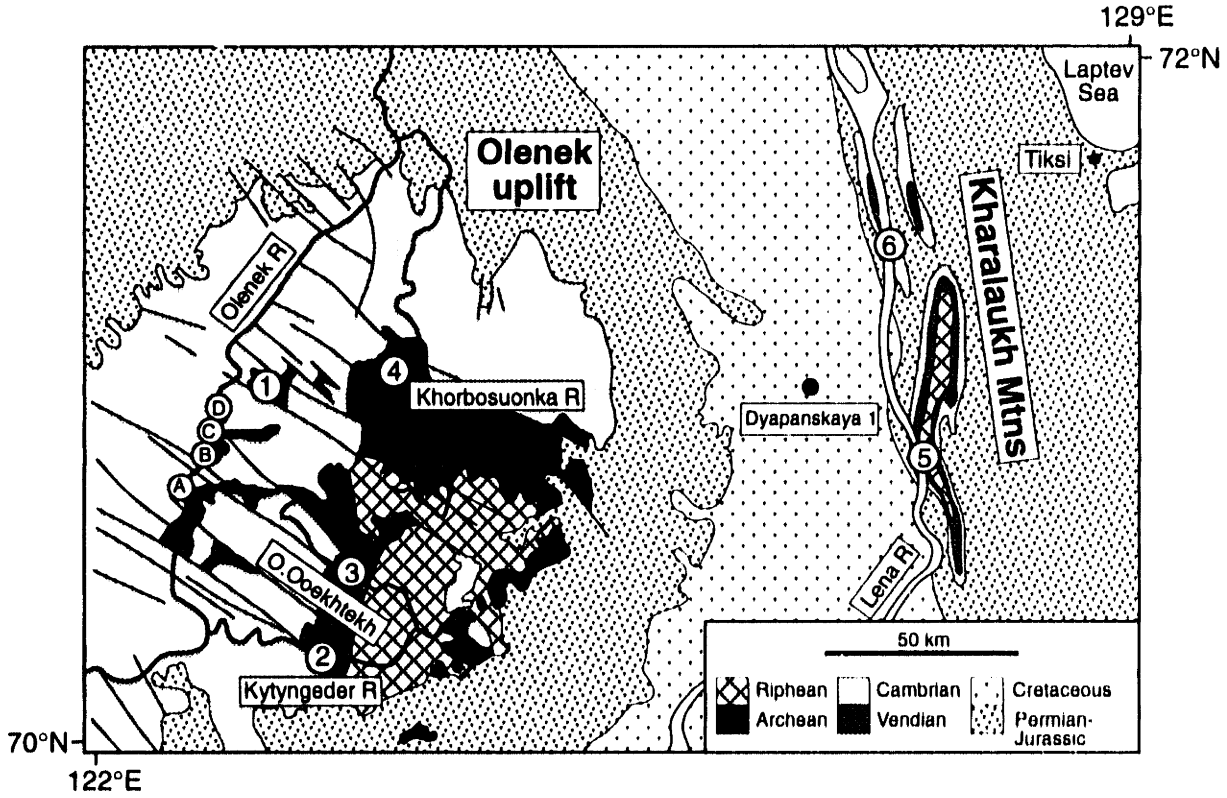
129°E
72°N
Laptev Sea
Tiksi
Olenek uplift
Olenek R.
Khorbosuonka R.
Kharalaukh Mtns
Dyapanskaya 1
Lena R.
O.Oosekhtekh
Kytyngeder R.
70°N
122°E
50 km
Riphean
Archean
Cambrian
Vendian
Cretaceous
Permian-Jurassic

Figure 3.2

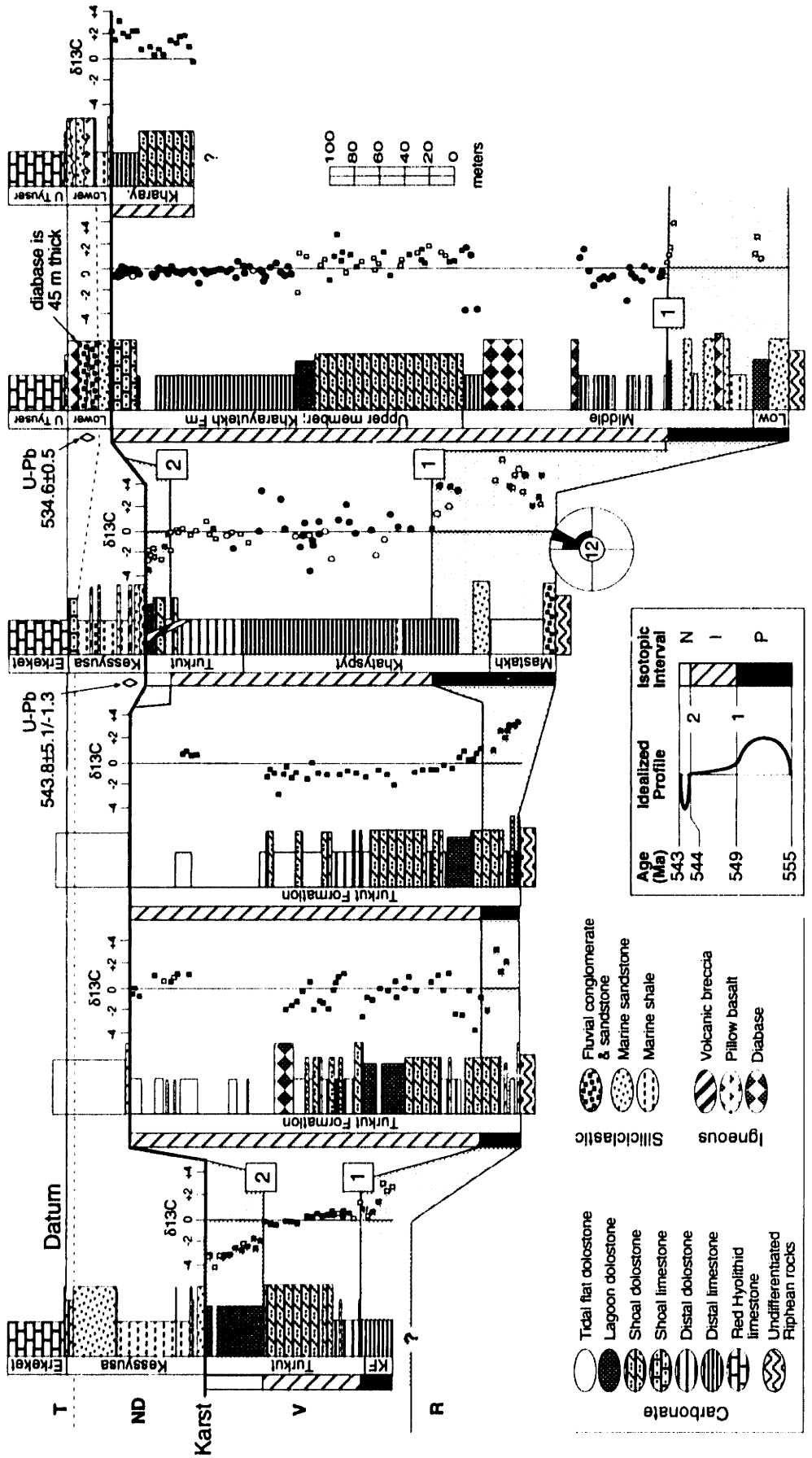
Datum
Karst
T
ND
V
R
δ13C
meters
100
80
60
40
20
0
diabase is 45 m thick
U-Pb 534.6±0.5
U-Pb 543.8±5.1/-1.3
Khabray
Upper member: Khrayulekh Fm
Middle
Low
U Tyuser
Lower
Erkeket
Kessyusa
Turkut
KF
Khatyspyt
Mastakh
Turkut Formation
Carbonate
Tidal flat dolostone
Lagoon dolostone
Shoal dolostone
Shoal limestone
Distal dolostone
Distal limestone
Red Hyolithid limestone
Undifferentiated Riphean rocks
Siliciclastic
Fluvial conglomerate & sandstone
Marine sandstone
Marine shale
Igneous
Volcanic breccia
Pillow basalt
Diabase
Isotopic interval
Idealized Profile
Age (Ma)
543
544
549
555
N
I
P

Figure 3.3

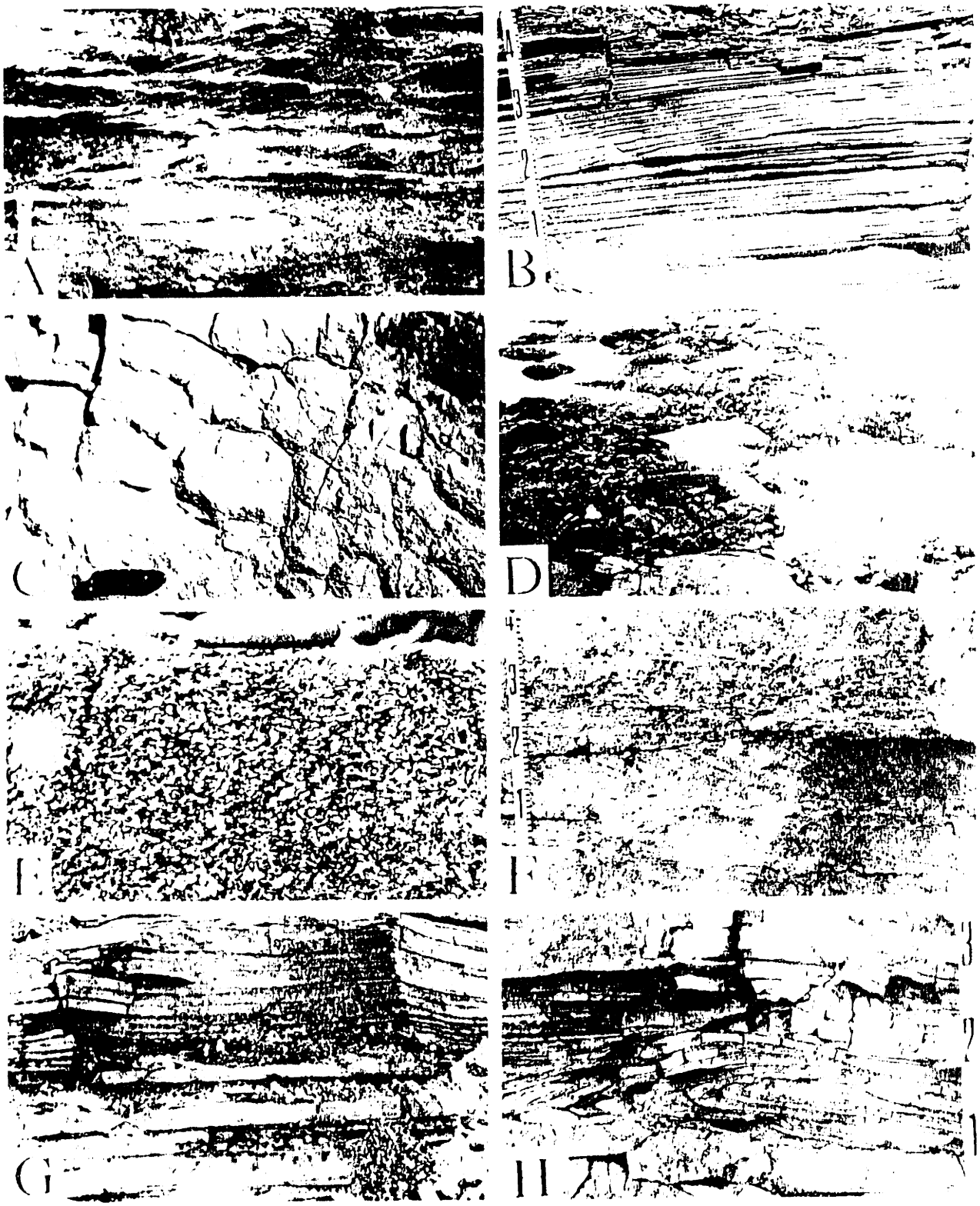

Figure 3.4

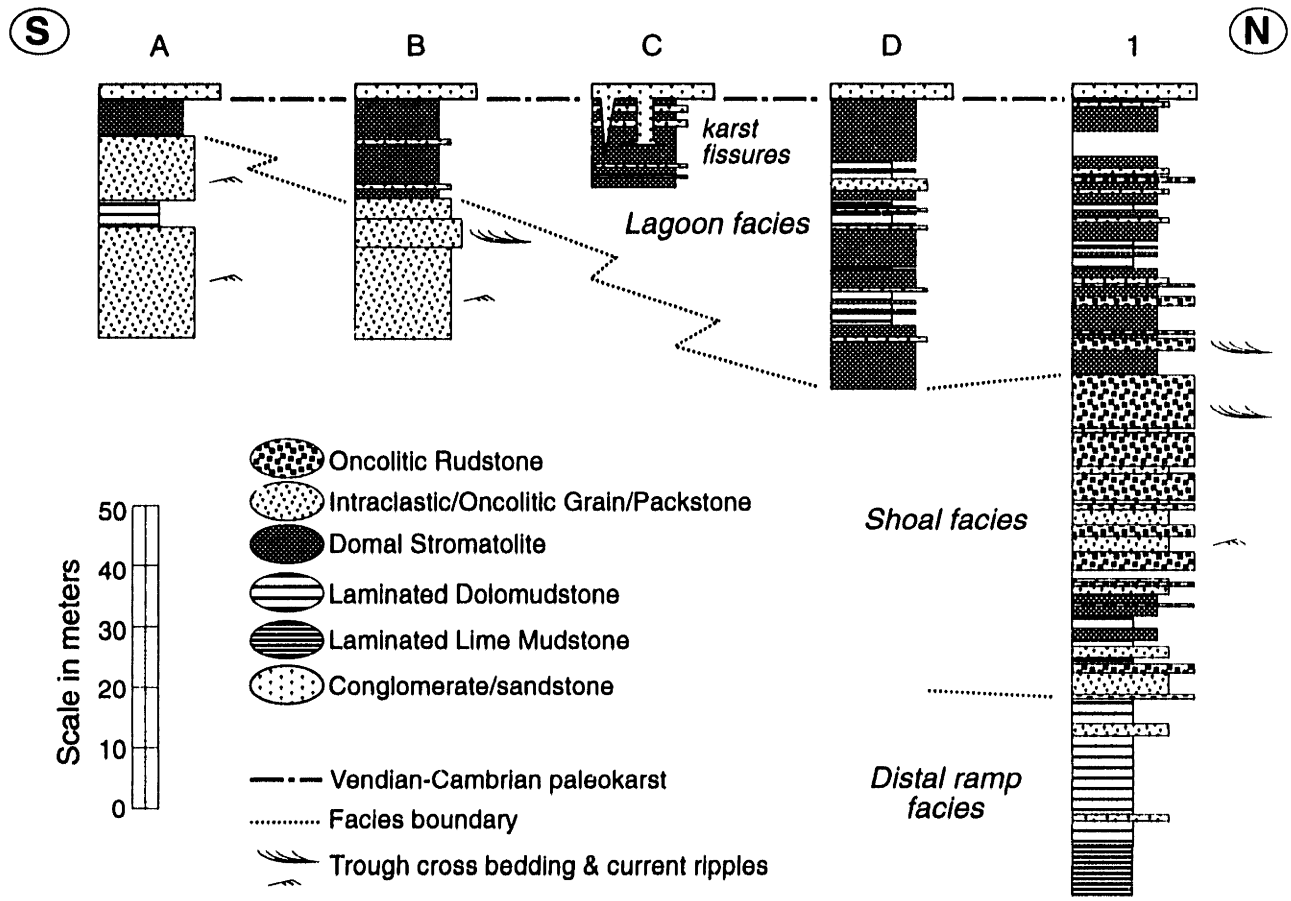
S
A
B
C
D
1
N
karst fissures
Lagoon facies
Shoal facies
Distal ramp facies
Oncolitic Rudstone
Intraclastic/Oncolitic Grain/Packstone
Domal Stromatolite
Laminated Dolomudstone
Laminated Lime Mudstone
Conglomerate/sandstone
Vendian-Cambrian paleokarst
Facies boundary
Trough cross bedding & current ripples
Scale in meters
50
40
30
20
10
0

Figure 3.5

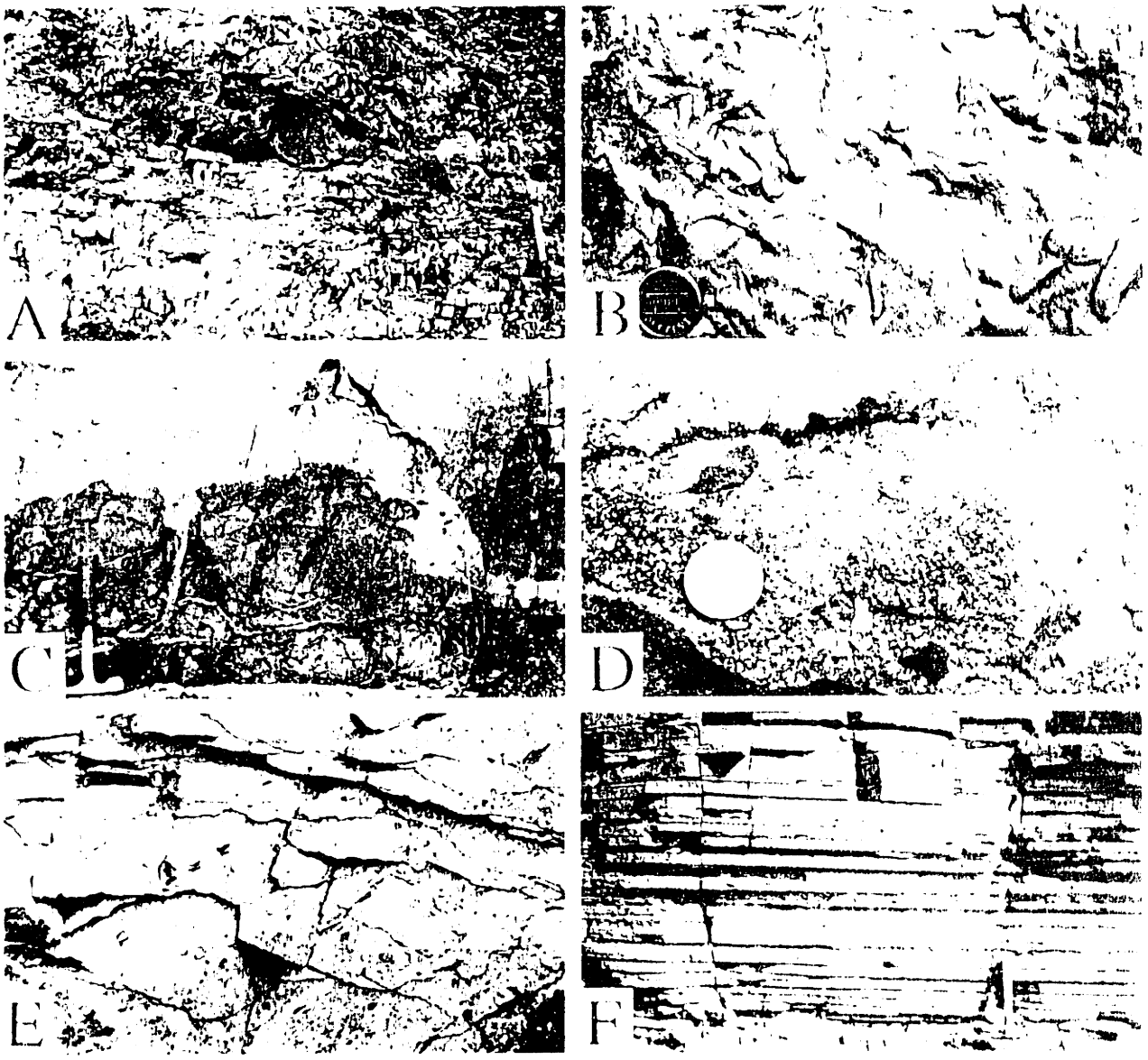

Figure 3.6

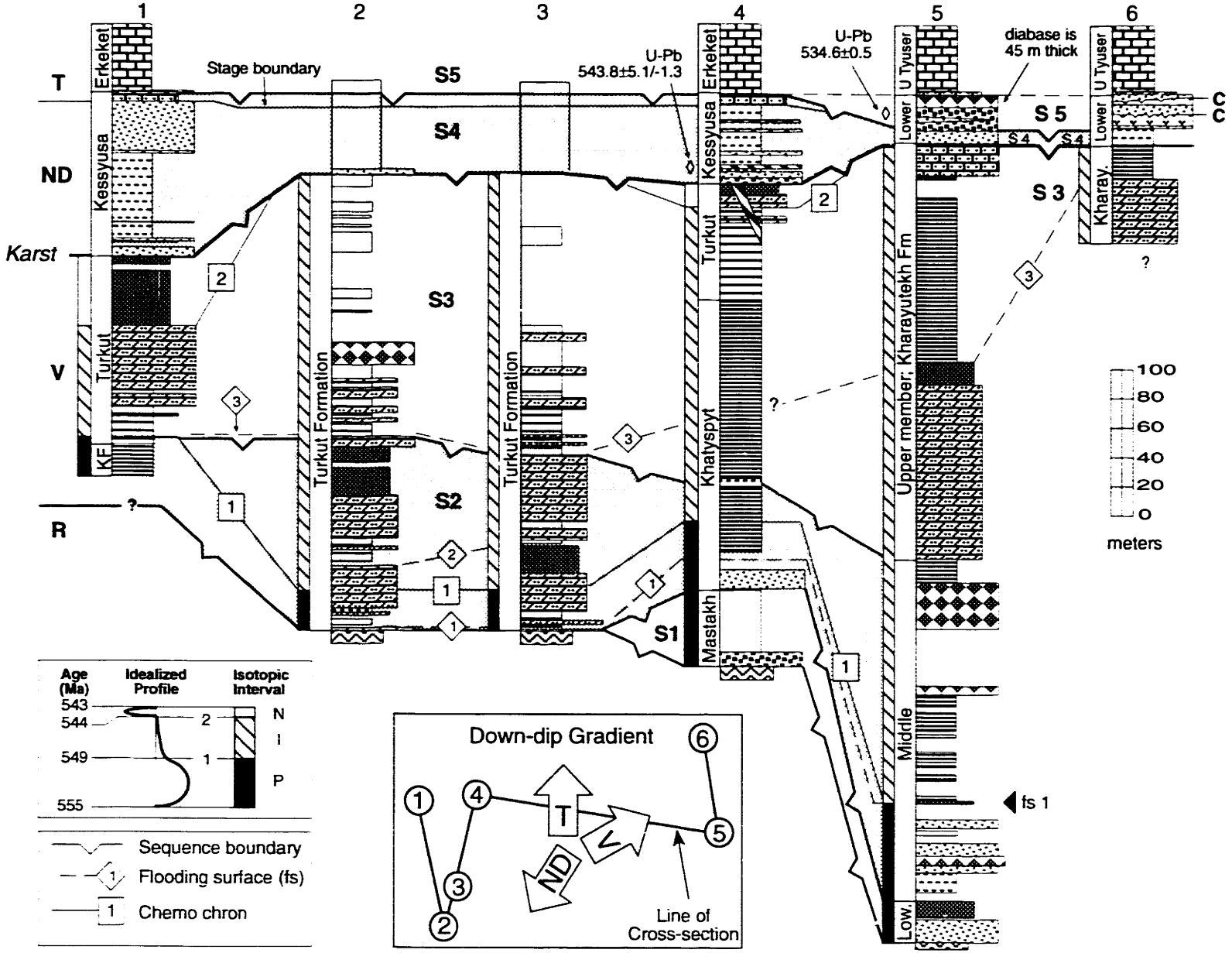
1
2
3
4
5
6
T
ND
Karst
V
R
Erkeket
Kessyusa
Turkut
KF
Stage boundary
S5
S4
S3
S2
S1
Turkut Formation
U-Pb
543.8±5.1/-1.3
U-Pb
534.6±0.5
diabase is
45 m thick
Khatyspyt
Mastakh
Upper member; Kharayutekh Fm
Middle
Low.
U Tyuser
Lower
Kharay.
S 5
S 4
S 3
fs 1
100
80
60
40
20
0
meters
Age (Ma)
Idealized Profile
Isotopic Interval
543
544
549
555
N
I
P
Sequence boundary
Flooding surface (fs)
Chemo chron
Down-dip Gradient
Line of Cross-section

Figure 3.7

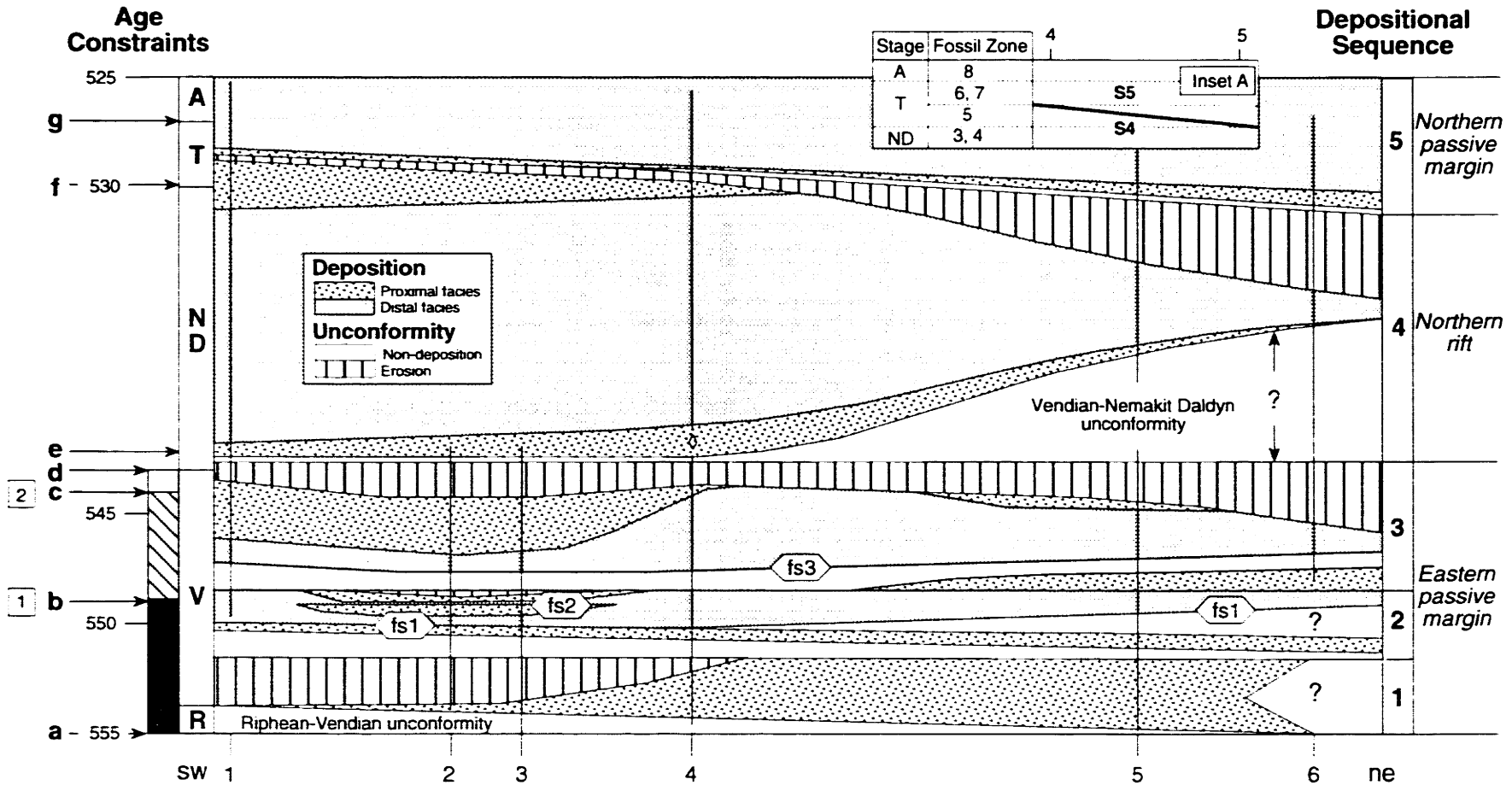
Age Constraints
Depositional Sequence
525
g
A
T
f - 530
N
D
e
d
c
545
b
V
550
a - 555
R
Riphean-Vendian unconformity
Stage
Fossil Zone
A
8
T
6, 7
5
ND
3, 4
Inset A
S5
S4
4
5
Deposition
Proximal facies
Distal facies
Unconformity
Non-deposition
Erosion
Vendian-Nemakit Daldyn unconformity
?
fs3
fs2
fs1
fs1
?
?
5
Northern passive margin
4
Northern rift
3
2
Eastern passive margin
1
SW
1
2
3
4
5
6
ne

Figure 3.8

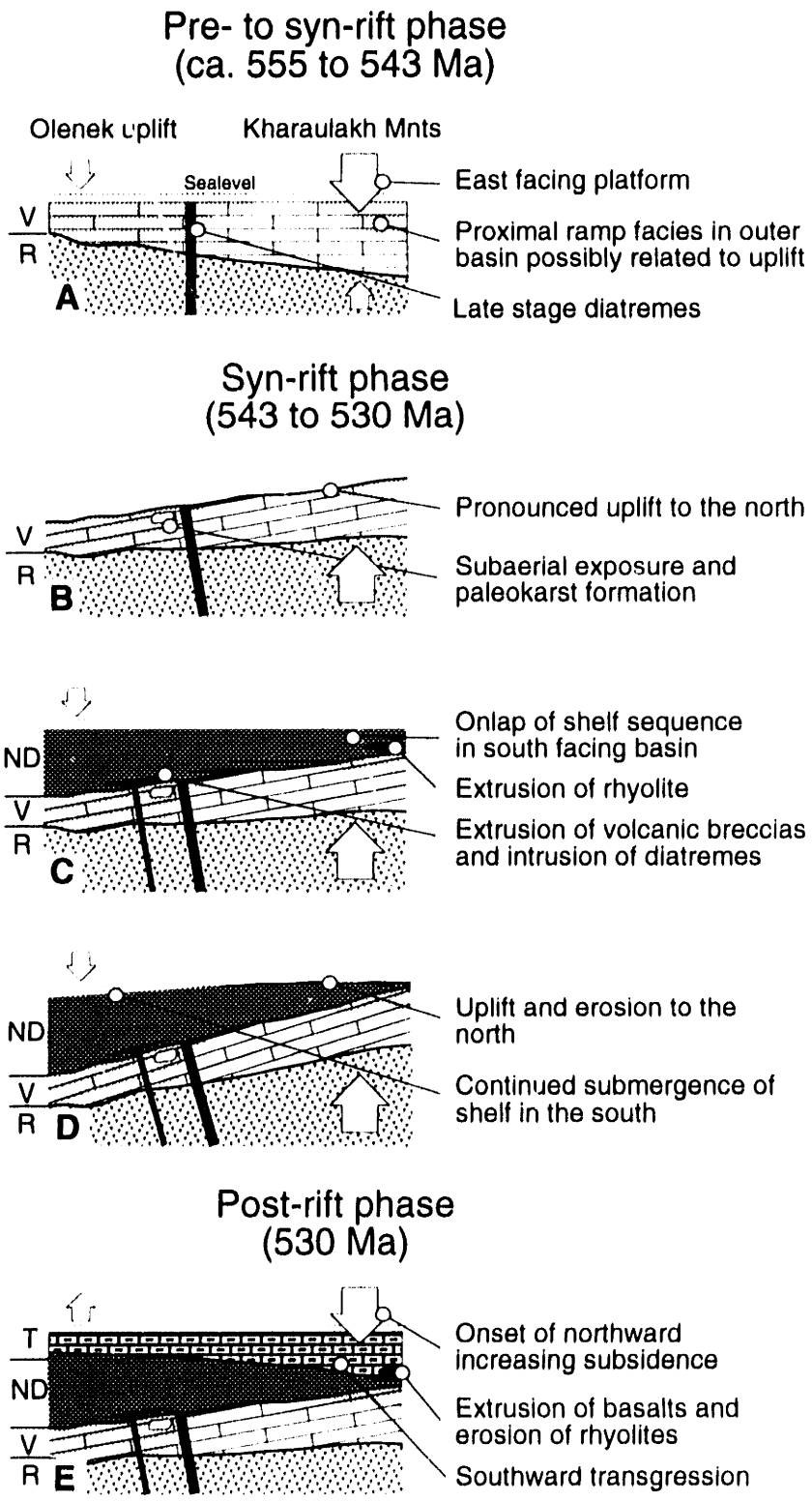
Pre- to syn-rift phase
(ca. 555 to 543 Ma)
Olenek uplift
Kharaulakh Mnts
Sealevel
V
R
A
East facing platform
Proximal ramp facies in outer basin possibly related to uplift
Late stage diatremes
Syn-rift phase
(543 to 530 Ma)
V
R
B
Pronounced uplift to the north
Subaerial exposure and paleokarst formation
ND
V
R
C
Onlap of shelf sequence in south facing basin
Extrusion of rhyolite
Extrusion of volcanic breccias and intrusion of diatremes
ND
V
R
D
Uplift and erosion to the north
Continued submergence of shelf in the south
Post-rift phase
(530 Ma)
T
ND
V
R
E
Onset of northward increasing subsidence
Extrusion of basalts and erosion of rhyolites
Southward transgression

Figure 3.9

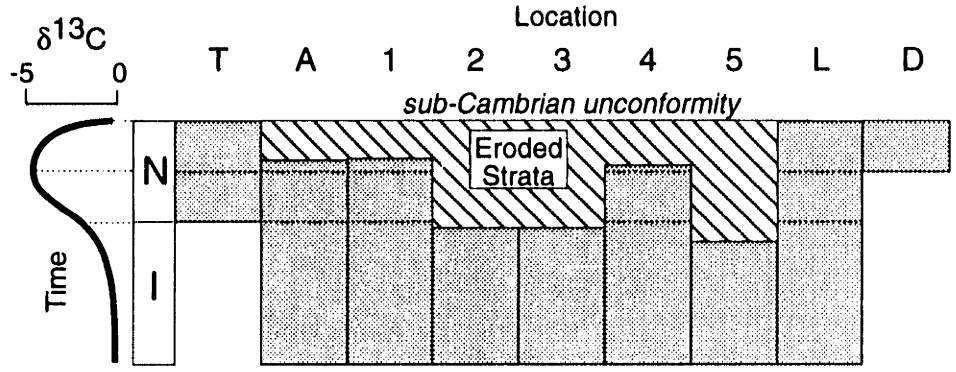
Location
δ13C
-5
0
T
A
1
2
3
4
5
L
D
sub-Cambrian unconformity
Eroded Strata
N
I
Time

Figure 3.10

Chapter 4

Stratigraphic evidence for the Siberia-Laurentia connection and Early Cambrian rifting[3]

[3]Pelechaty, S.M., 1996, Stratigraphic evidence for the Siberia-Laurentia connection and Early Cambrian rifting: Geology, v. 24, p.719-722.

ABSTRACT

Vendian to Cambrian age sediments of the northern Siberian craton record Early Cambrian rifting from ~543 to 530 Ma and onset of regional thermal subsidence in early Tommotian time. A similar tectonic history in the Franklinian basin of northern Canada and Greenland supports the possibility that both basins formed conjugate margins. This correlation constrains both the configuration of the Siberia-Laurentia connection, also supported by paleomagnetic and paleoclimatic data from Siberia, and timing of continental breakup, which is further supported by regional trilobite biostratigraphy. Prior to breakup, Siberia and Laurentia formed a coherent continent that rifted from a western landmass (Australia-Antarctica-India-South China) at ~720 Ma, forming a continuous passive margin along western Siberia-Laurentia. Nearly orthogonal to this margin, the 723 Ma Natkusiak volcanic rocks and Franklin dike swarm in northern Canada are suggested to represent a failed rift that extended into Siberia-Laurentia. Subsequent Early Cambrian separation of Siberia-Laurentia was possibly influenced by crustal heterogeneity created by the failed rift.

INTRODUCTION

Neoproterozoic to Early Cambrian time was a period of widespread continental breakup (Bond et al., 1984; Hoffman, 1991; Moores, 1991). Due to poor geologic constraints from Siberia, the position of the Siberian craton in the Neoproterozoic supercontinent has been uncertain. Many hypotheses connecting Siberia to Laurentia

have been proposed. On the basis of geologic and paleoclimatic data, Sears and Price (1978) and Piper (1982) connected Siberia to southwest Laurentia, while Scotese and McKerrow (1990) connected Siberia to northeast Laurentia east of Greenland. Neither models are consistent with regional correlation of Precambrian provinces, which led Hoffman (1991) and Condie and Rosen (1994) to suggest that Siberia was connected to northern Laurentia but with disagreement on the precise relative position. Hoffman (1991) correlated the Thelon-Taltson magmatic zone in northwest Canada with the Aldan and Anabar shields of Siberia, linking northern Siberia to Laurentia. Condie and Rosen (1994) concluded that eastern Siberia was attached to Laurentia on the basis of a revised correlation of the Thelon-Taltson zone with the Akitkan fold belt. New stratigraphic studies of Vendian-Cambrian strata in northern Siberia by Pelechaty et al. (1996a) do not support the paleogeographic reconstruction of Condie and Rosen (1994) but rather are in agreement with a northern Siberian connection first proposed by Hoffman (1991). This configuration, however, may not be inconsistent with the correlation of orogenic belts made by Condie and Rosen (1994).

On the basis of the 723 Ma Franklin magmatic event in northern Canada (Heaman et al., 1992), Condie and Rosen (1994) suggested that Siberia and Laurentia rifted during the Neoproterozoic. This paper shows that the sedimentary basin in northern Siberia documented by Pelechaty et al. (1996a) correlates with the early Paleozoic Franklinian basin in northern Canada and Greenland and constrains the timing of rifting of Siberia and Laurentia to the Early Cambrian. In this reconstruction, it is postulated that an older rift margin defined the western edge of Siberia-Laurentia prior to Early Cambrian separation, and that the 723 Ma Franklin dike swarm in northern Canada represents a failed rift arm.

SIBERIAN STRATA AND TECTONIC CORRELATION WITH LAURENTIA

A thin succession (<600 m) of late Vendian to Early Cambrian strata in northern Siberia provides evidence for nonuniform extension from 543 to 530 Ma, followed by thermal subsidence in the early Tommotian (Pelechaty et al., 1996a). Onset of rift-related uplift created a regional paleokarst unconformity at the Vendian-Cambrian boundary observed in sections bordering the Anabar shield, Olenek uplift, and Kharaulakh Mountains (Figs. 4.1A and 4.1B). The paleokarst bevels underlying Vendian strata to the north. In northeast Siberia, this unconformity defines the top of a 300- to 500-m-thick succession of latest Vendian (~555-543 Ma) ramp carbonates and minor siliciclastic sediments (area 1 in Fig. 4.2). The Khorbosuonka Group represents part of an east-facing passive margin on the eastern side of the craton (Khain et al., 1985). Correlation of carbon isotope profiles of the Khorbosuonka carbonates (Pelechaty et al., 1996b) suggests that thermal doming resulted in progressive truncation of the outer platform to the north beneath the sub-Cambrian paleokarst (area 2 in Fig. 4.2). Volcanism coeval with uplift of the platform in northern Siberia is evidenced by felsic diatremes truncated by the unconformity, and volcanic breccias interbedded with Early Cambrian (Nemakit-Daldyn) sediments directly overlying the paleokarst in the Olenek (area 3 in Fig. 4.2). The best estimate of the timing of initial rifting is a U-Pb age of 543 Ma from the volcanic breccias (Bowring et al., 1993).

Overlying the paleokarst, Nemakit-Daldyn strata consist of <100 m of interbedded conglomerates, sandstones, shales, and rare limestones and volcanic rocks (area 4 in Fig. 4.2). The deposits are interpreted to reflect continental extension, including uplift, influx of clastics, and rare volcanism and faulting. In northeast Siberia, these sediments were deposited in a local southwest-facing basin (arrows in Fig. 4.1A), recording a nearly 180° change in depositional gradient from latest Vendian time as the result of uplift to the north. Effects of uplift continued into early Tommotian

time as seen by truncation of Nemakit-Daldyn strata to the north, and occurrences of bimodal volcanic rocks overlying these strata in the Kharaulakh Mountains (area 5 in Fig. 4.2). The volcanic rocks consist of reworked rhyolite clasts in fluvial conglomerates and several thick-bedded pillowed basalts, which are capped by calcretes with cemented pebbles of basalt and rhyolite. Overlying with unconformity, Tommotian age limestones of the Erkeket Formation and correlative units in northern Siberia record regional flooding of the craton (area 6 in Fig. 4.2). On the basis of biostratigraphic correlations in northeast Siberia, onlap occurred from north to south in a northward-subsiding basin during initial stages of postrift subsidence (<530 Ma; Pelechaty et al., 1996a).

The early Paleozoic Franklinian basin in northern Canada and Greenland (Fig. 4.3) records a similar Early Cambrian tectonic history (Trettin, 1991). The basin overlies Neoproterozoic strata along a regional sub-Cambrian unconformity. The oldest exposed deposits of the Franklinian basin are Atdabanian in age and consist of (<1200 m) clastics and carbonates of the Kennedy Channel (Canada) and Skagen (Greenland) formations. The deposits onlap basement from north to south and are interpreted to reflect late synrift subsidence (Long, 1989). These deposits are conformably overstepped by mainly platform carbonates (<1000 m) of the Ella Bay (Canada) and Portfjeld (Greenland) formations, interpreted as late synrift to possibly early passive margin sediments (Long, 1989). At the close of Atdabanian time, a significant drop in sea level resulted in exposure and karstification of the upper carbonates. This erosion surface is overlain by clastics of the Ellesmere Group and is interpreted as a breakup unconformity (Long, 1989).

Trettin (1989) proposed that the Franklinian basin developed in response to emplacement of the 723 Ma Natkusiak volcanic rocks and Franklin dike swarm. However, there is no record of a Neoproterozoic rift sequence across the northern margin of Laurentia. Furthermore, a Neoproterozoic rifting event does not explain the

observed record of thermal subsidence from Early Cambrian to Silurian time in the Franklinian basin; only a minor thermal anomaly would still exist in the early Paleozoic if rifting occured at ~720 Ma. Several observations, however, suggest that rifting probably occurred later during terminal Neoproterozoic to earliest Cambrian time (Surlyk and Hurst, 1984; Sonderholm and Jepsen, 1991). Rift-related thermal uplift in northern Laurentia probably is represented by the sub-Cambrian unconformity at the base of the Franklinian basin. Runnegar (1995) suggested that the sub-Cambrian unconformity represents a major eustatic sea level drop; however, in northwest Canada, the unconformity truncates nearly 2 km of Windermere Group strata to the northeast (Ross, 1991) and suggests that tectonic uplift was also a significant factor in unconformity development in northern Canada. In north Greenland, rifting is also represented by local block faulting, which appears to have influenced Early Cambrian facies patterns in the Franklinian basin (Surlyk and Hurst, 1984). On a regional scale, however, there is limited evidence of continental extension. According to arguments by Levy and Christie-Blick (1991) for the western United States, the lack of appreciable evidence for upper crustal extension in northern Laurentia and Siberia may reflect nonuniform extension. Alternatively, the observed subsidence in northern Laurentia and Siberia may have formed by flexural loading of the lithosphere inboard of the hinge zone by passive loading outboard of the hinge zone.

On the basis of similarities in timing and tectonic origin, the Early Cambrian basins in northern Siberia and Laurentia are interpreted to be conjugate continental margins (Fig. 4.3). Paleomagnetic data (Khramov et al., 1981) and regional Vendian-Cambrian facies patterns across the Siberian craton (summarized by Pelechaty et al., 1996a) show that Siberia was geographically inverted and located at low latitudes of the southern hemisphere. Laurentia is interpreted to have been at similar low latitudes (Dalziel, 1992), consistent with correlation of the basins. An Early Cambrian age for rifting is also supported by regional trilobite biostratigraphic correlations by Palmer

and Repina (1993). They show that trilobite fossils on the two continents were similar in the earliest Cambrian (i.e., genera of *Fallotaspididae*) but diverged into separate endemic populations at the close of the Atdabanian, reflecting isolation of Siberia and Laurentia.

The difference in the timing of initial thermal subsidence between the basins in Siberia (<530 Ma; Tommotian; Pelechaty et al., 1996a) and Laurentia (~525 Ma; Atdabanian; Long, 1989) is a maximum of 5 m.y. and may reflect that rifting propagated diachronously from west to east (Fig. 4.3).

NEOPROTEROZOIC RIFTING IN WESTERN SIBERIA-LAURENTIA

The western margin of Laurentia underwent a period of continental extension during latest Neoproterozoic time, resulting in block faulting, clastic sedimentation, and magmatism. In northwest Canada, rifting probably started no later than ~720 Ma with deposition of the lower Windermere Group (Ross, 1991; Ross et al., 1995). The upper Windermere Group (i.e., post-Shezal Formation strata) over-steps the rift sequence and is considered to represent postrift thermal subsidence that continued to the end of Vendian time.

Neoproterozoic rifting also occurred along the present-day eastern margin of Siberia (Khain et al., 1985) but the precise age of rifting is unknown (Fig. 4.1A). Seismic profiles from the Olenek uplift area in northeast Siberia show pre-Vendian strata as continuous reflectors that onlap eastward-dipping faulted basement. Condie and Rosen (1994) reported occurrences of diabase dikes from the Aldan shield in southeast Siberia with unpublished ages of 763 Ma and 628 Ma. They consider the dikes to reflect rift-related magmatism, suggesting that similar age rifting occurred on both continents, which may have lead to opening of the proto-Pacific Ocean (Ross, 1991). Although the age of rifting in Siberia is poorly constrained, both continents record correlative

passive margin sequences. Consistent with latest Neoproterozoic rifting, latest Vendian (~555-543 Ma) strata in eastern Siberia record eastward-increasing differential subsidence (Figs. 1 and 2), indicating that decay of thermal anomalies continued to the end of the Vendian as observed in western North America. Regional biostratigraphic and chemostratigraphic correlations show that the Khorbosuonka Group correlates with nearly 2000 m of upper Windermere Group strata (Knoll et al., 1995). This correlation supports the notion that temporally-equivalent passive margins developed along the reconstructed western edges of Siberia and Laurentia at this time (Fig. 4.4). The relatively condensed Vendian section in Siberia possibly records lower subsidence rates of an inner flexural wedge (Bond et al., 1989). This correlation also shows that the Siberian section is considerably younger than latest Neoproterozoic diamictites in Canada and elsewhere, and explains the absence of correlative glacial deposits in Siberia. However, such diamictites may occur farther basinward where older Vendian strata are likely buried beneath the Verkoyansk fold belt (Fig. 4.1A).

In accordance with the proposed Siberia-Laurentia fit, it appears that a spatially continuous continental rift margin defined the western edge of Siberia-Laurentia during latest Neoproterozoic time (Fig. 4.4). The 723 Ma Franklin dike swarm in northern Canada is nearly orthogonal to the orientation of this continental margin. The Franklin magmatic event, also including basalts of the Natkusiak Formation on Victoria Island, may represent a failed rift arm that propagated into Siberia-Laurentia. However, there is no evidence of associated small, fault-bounded basins with terrestrial sediments, possibly because of sub-Cambrian erosion in northern Canada. The interpreted failed rift likely generated little subsidence in northern Canada, thus reducing the preservation potential for glacial deposits. This scenario may explain the absence of latest Neoproterozoic diamictites in the Minto Arch area, Victoria Island (G. M. Young, pers. commun., 1996). The strikingly similar orientation of the dikes with the younger Franklinian basin indicates that dike emplacement may have created a zone of crustal

weakness (Fig. 4.3), which was later reactivated during the separation of Siberia and Laurentia.

The conjugate to western Laurentia was probably Antarctica-Australia-India (Moores, 1991) but others also include the South China block in this western landmass (Eisbacher, 1985; Li et al., 1995; Fig. 4.4A). In the reconstruction of Li et al. (1995), South China is wedged between Laurentia and Australia based on the correlation of 1.9-1.4 Ga crust of Cathaysia in southern China and the Priest River Complex in the southwestern United States, thus providing a potential source area of the appropriate age for detrital zircons in the lower Belt Supergroup (Ross et al., 1992). Considering similar rifting ages in South China and Siberia, the northern part of South China in this reconstruction may also have been connected to Siberia (Fig. 4.4A). Another proposed scenario places South China farther north next to Siberia (Fig. 4.4B). This fit is consistent with studies that support an Australia-Laurentia connection based on regional stratigraphic correlations (Young, 1992), paleomagnetic data (Powell et al., 1993) and isotopic mapping (Borg and DePaolo, 1994). This scenario implies that the source for detrital zircons in the Belt Supergroup was basement blocks of south-central Australia (Ross et al., 1992). The Cathaysian block contains a core of >2.5 Ga crust, with evidence of additional crustal growth at 1.8 Ga and 1.4-1.2 Ga, and metamorphic ages of 1.9-1.7 Ga and ~1.0 Ga, the latter related to collision of the Yangtze and Cathaysia blocks (Li et al., 1995 and references therein). Although composed of older continental crust (3.5 to 3.0 Ga), the Aldan shield in southeastern Siberia does exhibit similar ages of metamorphism (2.4-1.7 Ga), and magmatism (i.e., 1.9-1.7 Ga granitoids), including circa 1.0 Ga granite stocks (Grenville age; Khain et al., 1985), coeval with the South China block, supporting such a connection. Nevertheless, additional geochronologic and geologic constraints are needed to test a South China-Siberia fit.

Finally, the proposed Siberia-Laurentia fit predicts that the present-day northwest corner of Siberia was connected to Barentsia and Arctic Alaska-Chukotka (Fig.

4.4A), which record rift-related magmatism at ~680 Ma (Patrick and McClelland, 1995). A late Riphean rift sequence with poorly constrained ages in the Taymyr region may support this notion (Khain et al., 1985).

REFERENCES

Bond, G. C., Nickeson, P. A., and Kominz, M. A., 1984, Breakup of a supercontinent between 625 Ma and 555 Ma: New evidence and implications for continental histories: Earth and Planetary Science Letters, v. 70, p. 325-345.

Bond, G. C., Kominz, M. A., Steckler, M. S. and Grotzinger, J. P., 1989, Role of thermal subsidence, flexure, and eustasy in the evolution of early Paleozoic passive-margin carbonate platforms, *in* Crevello, P. D., Wilson, J. L., Sarg, J. F., and Read, J. F., eds., Controls on carbonate platform and basin development: Society of Economic Paleontologists and Mineralogists Special Publication, 44, p. 39-61.

Borg, S. G. and DePaolo, D. J., 1994, Laurentia, Australia, and Antarctica as a Late Proterozoic supercontinent: Constraints from isotopic mapping: Geology, v. 22, p. 307-310.

Bowring, S. A., Grotzinger, J. P., Isachsen, C. E., Knoll, A. H., Pelechaty, S. M. and Kolosov, P., 1993, Calibrating rates of Early Cambrian evolution: Science, v. 261, p. 1293-1298.

Condie, K. C. and Rosen, O. M., 1994, Laurentia-Siberia connection revisited: Geology, v. 22, p. 168-170.

Dalziel, I. W. D., 1992, On the organization of American plates in the Neoproterozoic and the breakup of Laurentia: GSA Today, v. 2, p. 237, 240-241.

Eisbacher, G. H., 1985, Late Proterozoic rifting, glacial sedimentation, and sedimentary cycles in the light of Windermere deposition, western Canada: Palaeogeography, Palaeoclimatology, Palaeoecology, v. 51, p. 231-254.

Heaman, L. M., LeCheminant, A. N., and Rainbird, R. H., 1992, Nature and timing of Franklin igneous events, Canada: Implications for a Late Proterozoic mantle plume and the break-up of Laurentia: Earth and Planetary Science Letters, v. 109, p. 117-131.

Hoffman, P. H., 1991, Did the breakout of Laurentia turn Gondwanaland inside out?: Science, v. 252, p. 1409-1413.

Khain, V. E., 1985, Geology of the USSR: Part 1. Old cratons and Paleozoic fold belts: Berlin, Gebrüder Borntraeger, 272 p.

Khomentovsky, V. V., 1990, Chapter 5: Vendian of the Siberian Platform, *in* Sokolov, B. S., and Fedonkin, M. A., eds.: The Vendian System: Moscow, Nauka, p. 103-183.

Knoll, A. H., Grotzinger, J. P., Kaufman, A. J. and Kolosov, P., 1995, Integrated approaches to terminal Proterozoic stratigraphy: An example from the Olenek Uplift, northeastern Siberia: Precambrian Research, v. 73, p. 251-270.

Khramov, A. N., Petrova, G. N., and Pechersky, D. M., 1981, Paleomagnetism of the Soviet Union, McElhinny, M. W. and Valencio, D. A., eds.: American Geophysics Union Geodynamics Series 2, p. 177-194.

Levy, M., and Christie-Blick, N., 1991, Tectonic subsidence of the early Paleozoic passive continental margin in eastern California and southern Nevada: Geological Society of America Bulletin, v. 103, p. 1590-1606.

Li, Z.-X., Zhang, L., and Powell, C. M., 1995, South China in Rodinia: Part of the missing link between Australia-East Antarctica and Laurentia?: Geology, v. 23, p. 407-410.

Long, D. G. F., 1989, Ella Bay Formation: Early Cambrian shelf differentiation in the Franklinian basin, central eastern Ellesmere Island, Arctic Canada: Canadian Journal of Earth Sciences, v. 26, p. 2621-2635.

Moores, E. M., 1991, Southwest U.S.-East Antarctic (SWEAT) connection: A hypothesis: Geology, v. 19, p. 425-428.

Palmer, A. R. and Repina, L. N., 1993, Through a glass darkly: Taxonomy, phylogeny, and biostratigraphy of the Olenellina: The University of Kansas Paleontological Contributions, v. 3, 35 p.

Patrick, B. E., and McClelland, W. C., 1995, Late Proterozoic granitic magmatism on Seward Peninsula and a Barentian origin for Arctic Alaska-Chukotka: Geology, v. 23, p. 81-84.

Pelechaty, S. M., Grotzinger, J. P., Kashirtsev, V. A., and Zhernovsky, V. P., 1996a, Chemostratigraphic and sequence stratigraphic constraints on Vendian-Cambrian basin dynamics, Northeast Siberian craton: Journal of Geology, v. 104, p. 543-564.

Pelechaty, S. M., Kaufman, A. J., and Grotzinger, J. P., 1996b, Evaluation of $\delta^{13}C$ isotope stratigraphy for intrabasinal correlation: Vendian strata of the Olenek uplift and Kharaulakh Mountains, Siberian platform, Russia: Geological Society of America Bulletin, v. 108, p. 992-1003.

Piper, J. D. A., 1982, The Precambrian palaeomagnetic record: the case for the Proterozoic supercontinent: Earth and Planetary Science Letters, v. 59, p. 61-89.

Powell, C. M., Li, Z. X., McElhinny, M. W., Meert, J. G., and Park, J. K., 1993, Paleomagnetic constraints on timing of the Neoproterozoic breakup of Rodinia and the Cambrian formation of Gondwanaland: Geology, v. 21, p. 889-892.

Ross, G. M., 1991, Tectonic setting of the Windermere Supergroup revisited: Geology, v. 19, p. 1125-1128.

Ross, G. M., Parrish, R. R. and Winston, D., 1992, Provenance and U-Pb geochronology of the Mesoproterozoic Belt Supergroup (northwestern United States): Implications for age of deposition and pre-Panthalassa plate reconstructions: Earth and Planetary Science Letters, v. 113, p. 57-76.

Ross, G. M., Block, J. D., and Roy Krouse, H., 1995, Neoproterozoic strata of southern Canadian Cordillera and the isotopic evolution of seawater sulfate: Precambrian Research, v. 73, p. 71-99.

Runnegar, B., 1995, Base of the Sauk sequence is a global eustatic event that lies just above the Precambrian-Cambrian boundary: Geological Society of America Abstracts with Programs, v. 27, no. 6, p. A330.

Scotese, C. R., and McKerrow, W. S., 1990, Revised world maps and introduction, *in* McKerrow, W.S., and Scotese, C. R., eds., Palaeozoic palaeogeography and biogeography: Geological Society of America Memoir 2, p. 1-21.

Sears, J. W., and Price, R. A., 1978, The Siberian Connection: A case for Precambrian separation of the North American and Siberian cratons: Geology, v. 6, p. 267-270.

Sonderholm, M., and Jepsen, H. F., 1991, Proterozoic basins in North Greenland: Bulletin Gronlands Geology Unders, v. 160, p. 49-69.

Surlyk, F., and Hurst, J. M., 1984, The evolution of the early Paleozoic deep-water basin of North Greenland: Geological Society of America Bulletin, v. 95, p. 131-154.

Trettin, H. P., 1989, The Arctic Islands, *in* Bally, A. W., and Palmer, A. R., eds., Geology of North America: Boulder, Colorado, Geological Society of America, v. A, p. 349-370.

Trettin, H. P., 1991, Tectonic framework, *in* Trettin, H. P., ed., Geology of the Innuitian Orogen and Arctic Platform of Canada and Greenland: Geological Survey of Canada, Geology of Canada, No. 3, p. 57-66.

Young, G. M., 1992, Late Proterozoic stratigraphy and the Canada-Australia connection: Geology, v. 20, p. 215-218.

LIST OF FIGURES

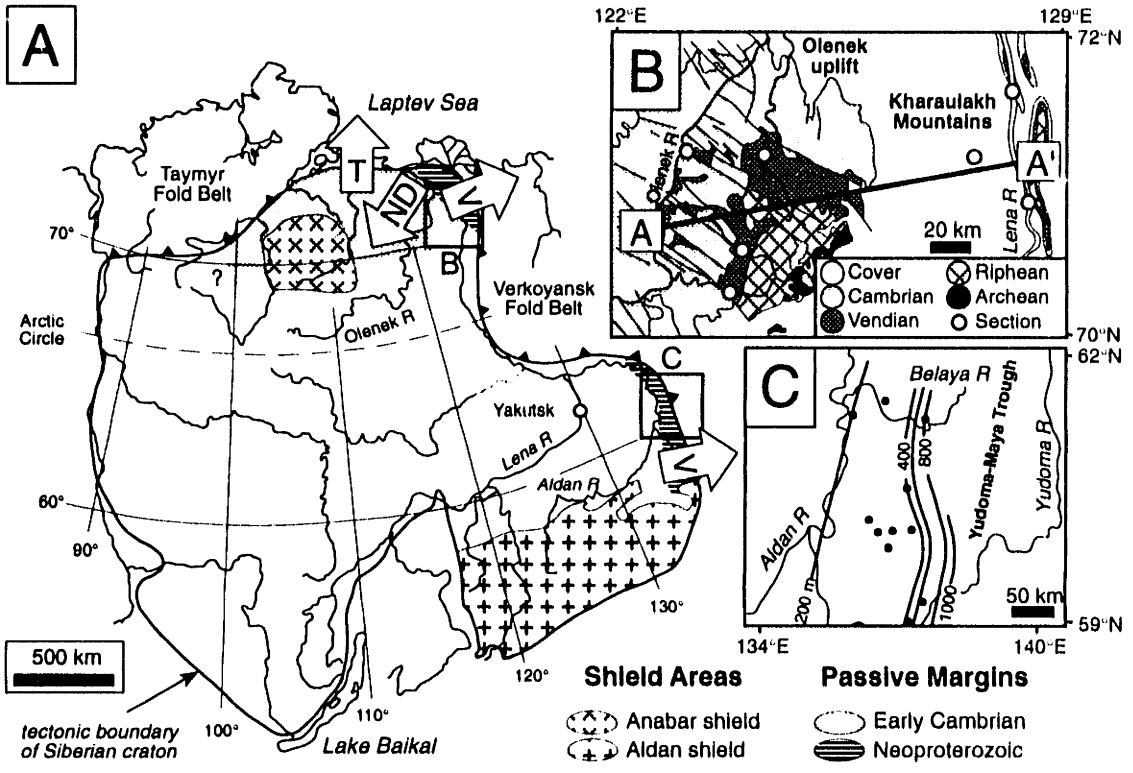
A
Laptev Sea
Taymyr
Fold Belt
T
ND
V
B
Verkoyansk
Fold Belt
70°
Arctic
Circle
Olenek R
?
60°
90°
Yakutsk
Lena R
Aldan R
C
130°
120°
110°
100°
500 km
tectonic boundary
of Siberian craton
Lake Baikal
122°E
129°E
72°N
B
Olenek
uplift
Kharaulakh
Mountains
A'
Olenek R
A
20 km
Lena R
Cover
Cambrian
Vendian
Riphean
Archean
Section
70°N
62°N
C
Belaya R
400
800
Yudoma-Maya Trough
Yudoma R
Aldan R
200 m
1000
50 km
59°N
134°E
140°E
Shield Areas
Anabar shield
Aldan shield
Passive Margins
Early Cambrian
Neoproterozoic

Figure 4.1

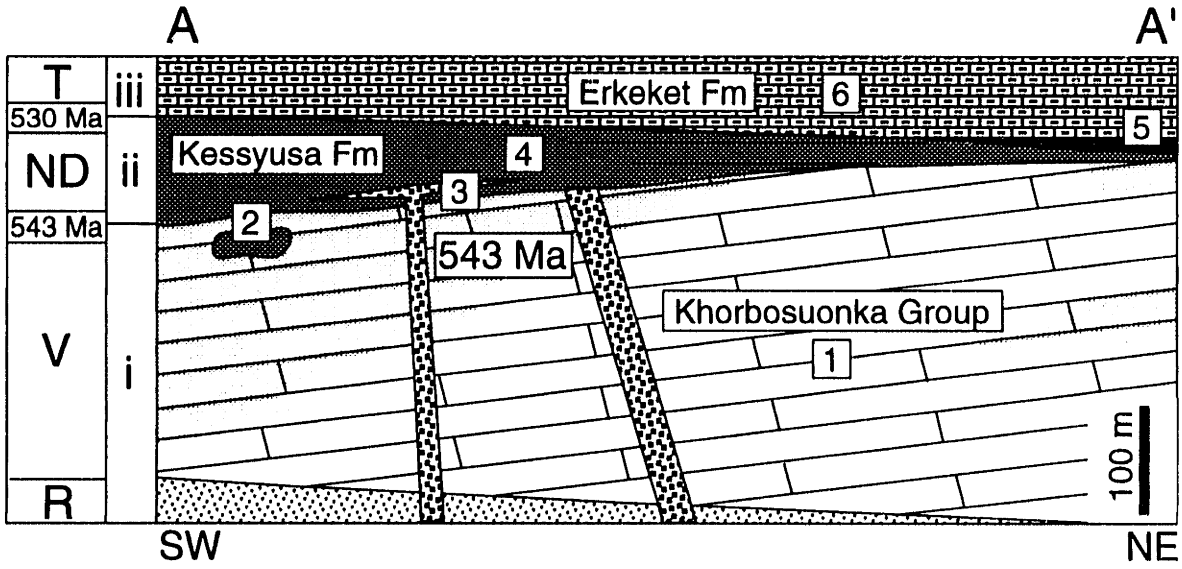
A
A'
T
530 Ma
ND
543 Ma
V
R
iii
ii
i
Erkeket Fm
6
5
Kessyusa Fm
4
3
2
543 Ma
Khorbosuonka Group
1
100 m
SW
NE

Figure 4.2

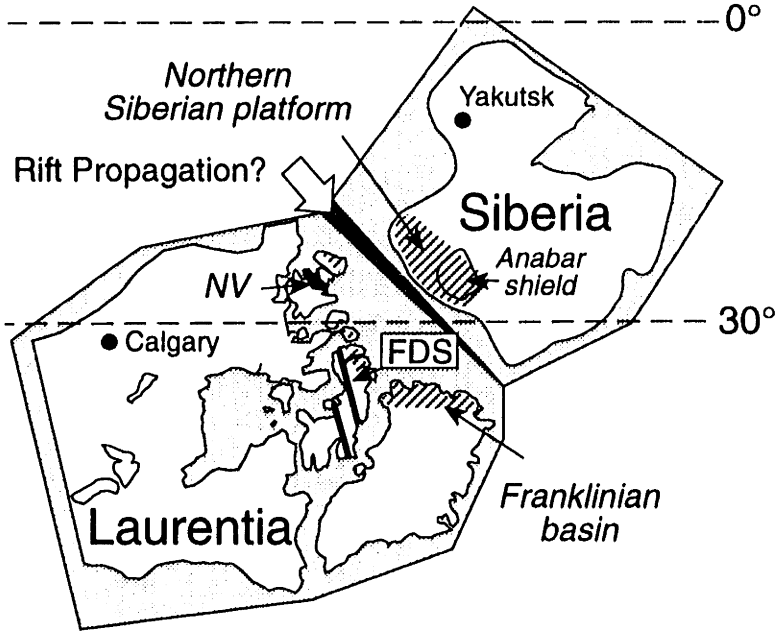
0°
Northern
Siberian platform
Yakutsk
Rift Propagation?
Siberia
Anabar
shield
NV
30°
Calgary
FDS
Laurentia
Franklinian
basin

Figure 4.3

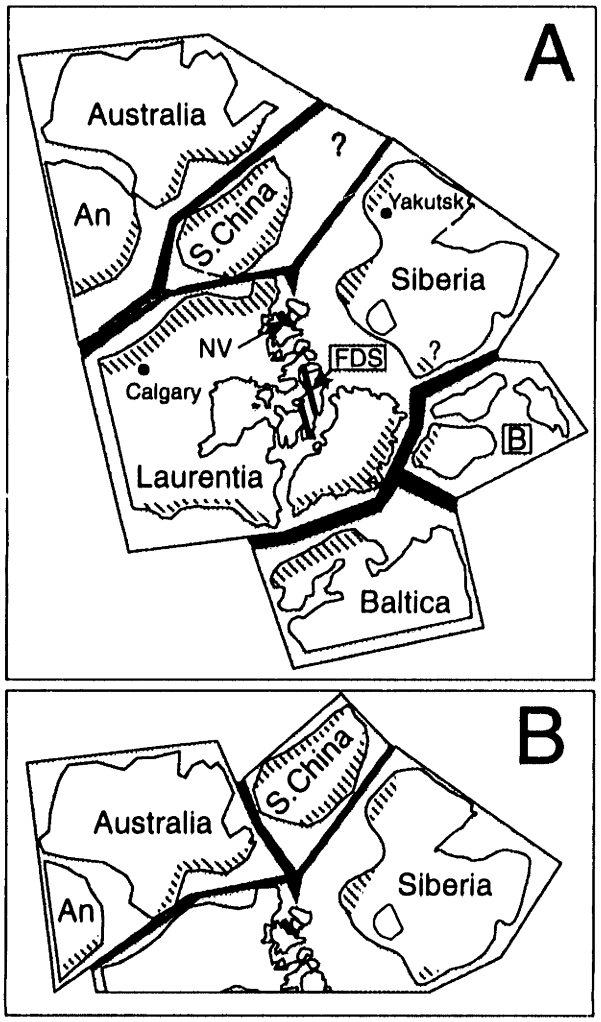
A
Australia
?
An
S.China
Yakutsk
Siberia
NV
FDS
?
Calgary
B
Laurentia
Baltica
B
S.China
Australia
Siberia
An

Figure 4.4

Chapter 5

Vendian Chronostratigraphy Of The South Siberian Platform (Nokhtuisk Section) And Implications For Eustasy

ABSTRACT

Integrated $\delta^{13}C$ chemo- and sequence stratigraphy is developed for a succession of Vendian age strata on the soutnern margin of the Siberian platform. Regional correlation reveals the development of three cratonic stratigraphic sequences on the Siberian platform that partition Siberia's Vendian System into high resolution (< 5 Ma) time slices (i.e. third-order cycles). The Siberian sequences form a larger, second-order sequence. On the basis of global chemostratigraphy, the second-order sea level cycle represents the youngest of two possible eustatic second-order cycles that span the latest 60 Ma of terminal Neoproterozoic time. Evidence for repeated expansion and retreat of glaciers during this time provides a plausible mechanism for Siberia's cratonic sequences but effects due to sea floor spreading are invoked as the major mechanism for the second-order sea level fluctuations.

INTRODUCTION

A time scale for terminal Neoproterozoic history is emerging as the result of carbon isotope chemostratigraphy and its utility for interbasinal and global correlation (Knoll and Walter 1992; Kaufman and Knoll 1995; Pelechaty, et al. 1996b; Saylor 1996; Saylor, et al. in review). Chemostratigraphy in conjunction with additional stratigraphic tools including sequence stratigraphy has provided an unprecedented method for correlation of Neoproterozoic sedimentary sequences that are poorly constrained by biostratigraphy and has now been adopted in studies of Phanerozoic carbonate stratigraphy (Vahrenkamp 1996).

In this paper, I document the depositional and carbon isotope history of a thick, allochthonous succession of Vendian and Early Cambrian deposits (Nokhtuisk section) along the southern margin of the Siberian platform. A detailed chronostratigraphy of the Nokhtuisk section is developed following a detailed facies, geochemical and sequence stratigraphic analysis of the Vendian deposits. In an attempt to develop a regional, high resolution chronostratigraphic model for the Vendian System of the Siberian platform, the results of this study are compared with a chronostratigraphy established for coeval strata in northeast Siberia (Pelechaty, et al. 1996a; 1996b). Regional correlation of Vendian strata reveals the development of three major depositional sequences. These sections are compared with key sections world-wide to investigate the origin of these and other global stratigraphic patterns.

GEOLOGICAL SETTING

The Nokhtuisk section includes an allochthounous succession of Vendian rocks that were thrust northward onto the southern edge of the Siberian platform during development of the Early Paleozoic Predpatom fold and thrust belt (Nikulin 1970). The section includes deep water siliciclastic and carbonate facies and is located only 10's of km's from wells that penetrate coeval paraautochthonous sabkha and associated shallow water facies. Collectively, the Vendian Zherba and Tinnaya formations are 680 m thick and are superbly exposed along the northern shoreline of the Lena River near the mouth of the Bolshoi Patom River and village of Nokhtuisk (Fig. 5.1).

The Nokhtuisk section is a composite of two closely spaced partial sections distributed across a single fold. The Riphean Chencha and basal Zherba formations crop out on the northern flank of the Ura Anticline while the upper Zherba, Tinnaya and Cambrian Nokhtuisk formations crop out on its southern limb (Fig. 5.2). The Chencha-Zherba contact at the southern exposure allows correlation of both sections, which

collectively form a nearly complete column of Vendian deposits; only an interval through the middle 80 m of the Zherba Formation is covered; this interval crops out only to the south along the Maly and Bolshoi Patom rivers (Khomentovsky 1986; 1990).

The Zherba Formation is 350 m thick and consists of a lower interval of siliciclastic sediments and an upper interval of limestones. Lithologically, the Zherba Formation gradationally overlies limestones of the Chencha Formation. Many workers regard this interbedding as evidence for a conformable relationship between the Riphean and Vendian systems. They mark the base of the Vendian at the level of the lowermost sandstone in this interval (Bobrov 1979; Khomentovsky 1990). Others interpret an unconformity between the Chencha and Zherba formations based on observations from the western flank of the Aldan shield to the west where clastics of the Zherba Formation rest with angular unconformity on Riphean carbonates (Shenfel and Yakshin 1975; Shenfel 1991). On this basis, they place the Chencha-Zherba formational boundary at the top of the stratigraphically highest carbonate bed at the Nokhtuisk section. Results from this study recognize an erosion surface at this level, in agreement with the stratigraphic interpretation of Shenfel and others. As defined by Khomentovsky (1990) and Shenfel (1991), the overlying Tinnaya Formation is 330 m thick and is dominated by carbonate conglomerates. It unconformably overlies the Zherba Formation (Avdeeva 1983) and in turn is sharply overlain by the Cambrian Nokhtuisk Formation; a 300 m thick succession of varicolored sandstones, shales and carbonates. The formation grades upward into 180 m of gray dolostones of the Macha Formation (Shenfel 1991).

Because they lack fossils suitable for biostratigraphy, existing age constraints for strata of the Nokhtuisk section are based on regional lithostratigraphic correlation with fossiliferous sections elsewhere in southern Siberia. Bobrov (1964) and Kolosov (1975) place the sub-Tommotian boundary at the base of the Nokhtuisk Formation, which they consider to be equivalent to varicolored rocks of the Tommotian Petrosvet Formation along the Aldan River. Subsequent studies place the sub-Tommotian boundary

higher in the Nokhtuisk Formation and in the Macha Formation on the basis of other lithostratigraphic schemes (citations in Shenfel 1991). On the basis of carbon isotope chemostratigraphy, Sochava, et al. (1996) place the sub-Tommotian boundary approximately 200 m above the basal Nokhtuisk contact and the Vendian-Cambrian boundary at the contact between the Tinnaya and Nokhtuisk formations. This study improves upon the sparsely defined isotopic record presented by Sochava, et al. (1996) but confirms their regional stratigraphic interpretations.

DEPOSITIONAL FACIES

Chencha Formation

The upper 140 meters of the Chencha Formation consists mainly of gray limestones and minor interbedded orange dolostones and clastics in the upper 15 m of the formation (Figs. 5.3 and 5.4a). The gray limestones are formed of oolitic grainstones, mudstones and stromatolites. Medium bedded oolites exhibit planar and ripple cross stratification (Fig. 5.4b). They truncate underlying deposits and have basal lags with pebbles of oolite, dolomudstone and rare stromatolite fragments. Buff dolomudstones contrast with the gray oolites and occur as thin interbeds and lenses. Stromatolites have internal digitate lamination and form meter-thick biostromes and bioherms encased in the oolites (Fig. 5.4c). Locally, white "cauliflower" cherts occur in the biostromes.

In the upper 15 m of the formation, the dolostones show an upward change in color from buff to orange. The lowermost siliciclastics are marked by 2 m of poorly exposed green silty shales and rippled sandstones, followed by 3 m of rippled and cross stratified glauconitic sandstones and minor dolomudstones and thin conglomerate beds. Above this level, orange stromatolitic dolostones occur as medium scale beds associated with rare siltstones and sandstones. The stromatolites are interbedded with grainstones,

tepee carbonates (Fig. 5.4d), intraformational breccias, and edgewise conglomerates. Two erosion surfaces truncate the dolostones in the upper 1.5 m of the formation. The surfaces are coated by black chert and green glauconite, which also occur as clasts in overlying sandstones. The upper surface exhibits up to 50 cm of relief and is associated with sandstone- and siltstone-filled fissures and small cavities that cut the dolostones (Figs. 5.4e and 5.4f). The upper dolostone bed also contains cm-size bladed crystals of anhydrite embedded in the upper part of the dolostone layer.

The upper Chencha Formation is interpreted to represent a shallow water platform comprised of high energy shoals and isolated, low relief stromatolite reefs. The "cauliflower" cherts are interpreted to represent silicified anhydrite clusters and resemble those described in the Mastakh Formation in northern Siberia (Knoll, et al. 1995a). They indicate that some biostromes formed in restricted lagoons located inboard of oolitic shoals where depositional conditions were occasionally evaporitic. The interbedded clastics and carbonates at the top of the formation may represent similar water depths. The erosion surfaces capping the formation probably signify hiatuses in deposition and are interpreted to represent karst profiles associated with surface karren and shallow caverns. The discoloration of the dolostones at this locality is common to many paleokarst profiles and may be related to staining by terra rossa (Estaban and Klappa 1983). Alternatively, the presence of chert and glauconite along these surfaces indicate development of marine hardgrounds, however, such coatings may also have formed during marine transgression of a karst landscape. Regardless, a stratigraphic break is interpreted to separate Riphean and Vendian strata at this section.

Zherba Formation

The Zherba Formation is divided into four lithologic units, including in ascending order; sandstone, lower turbidite, bituminous carbonate, and upper turbidite units (Fig. 5.3).

Sandstone Unit (SU)

The sandstone unit represents 140 m (38 to 280 m; Fig. 5.3) of thin to medium bedded glauconitic sandstones and very minor conglomerates, siltstones and shales. Sandstones occur as tabular beds. Thicker beds are parted by 1 to 2 cm thick green shale seams, which may be truncated laterally where sandstones occur as amalgamated units. The thinner beds occur in recessive intervals intercalated with siltstones and shales. Sandstones are sharp-based with up to 40 cm of relief along the bases of thicker beds, and contain abundant cm-size shale chips, which may also occur throughout a single bed. Soft sediment deformation is common as exemplified by ball-and-pillow and dish structures at the tops of beds. The sandstones are planar to current ripple laminated to trough cross stratified (Figs. 5.5a and 5.5b). Locally, the thin sandstones have massive or planar laminated bases and current rippled tops. In the upper part of the unit, fine sandstones exhibit planar to hummocky cross stratification. The unit also contains minor meter-thick cross stratified pebble conglomerates.

The sandstone unit is interpreted to represent a succession of storm-influenced shelf deposits. Their marine origin is supported by occurrences of glauconite-bearing sandstones and hummocky cross stratified sandstones in the upper part of the unit (e.g. Hamblin and Walker 1979). The sandstones reveal evidence of both proximal and distal shelf storm sedimentation; the thicker sandstones indicate sedimentation in more proximal reaches of the shelf whereas intervals of thinly interbedded sandstones, siltstones and shales are interpreted as distal shelf turbidites.

Lower Turbidite Unit (LTU)

This unit is at least 40 m thick (360-400 m Fig. 5.3). Its lower contact is covered, and its upper contact is arbitrarily chosen at the uppermost siliciclastic bed. The unit consists of an equal proportion of cm-bedded sandstones, siltstones, and shales and minor carbonates, which increase in abundance up section (Fig. 5c). The sandstones are fine grained, sharp-based, and are either massive, planar laminated or ripple cross laminated, and grade upward into siltstones and shales. The carbonates occur as massive dark gray dolostones and black bituminous lime mudstones.

The deposits of this unit are interpreted to be distal turbidites that accumulated below storm wave base (e.g. Walker 1984). Sandstones were deposited by traction currents along the sea floor producing scoured relief at the bases of beds and planar and ripple cross stratification. Deceleration of flow events led to deposition of finer siliciclastic sediment and formation of fining upward sandstone to siltstone to shale triplets.

Bituminous Carbonate Unit (BCU)

The bituminous carbonate unit includes 20 m (400-420 m; Fig. 5.3) of thinly bedded black bituminous limestones, dolostones and shaley dolostones (Fig. 5d). The carbonates are either finely laminated, with individual laminae characterized by silt to mud fining-upward couplets, or sharp-based massive beds. The carbonates exhibit slump features, low angle truncation surfaces and concretions.

Deposits of the bituminous carbonate unit are interpreted as distal ramp facies, including turbidites (laminated beds) and debris flows (massive beds), which show evidence for slope failure and generation of slump features. These deposits greatly resemble the bituminous carbonates of the Khatyspyt and Kharayutekh formation in northeast Siberia (Knoll, et al. 1995a; Pelechaty, et al. 1996b).

Upper Turbidite Unit (UTU)

This unit is nearly 70 m thick (ca. 420-486 m; Fig. 5.3) and sharply overlies the bituminous carbonates (Figs. 5.5e and 5.5f). The upper turbidite unit consists of varicolored limestones, dolostones and minor sandstones, siltstones, and shales. The lower 15 m of the unit resembles the clastics of the lower turbidite unit. They grade upward into red, gray and rare buff carbonates. The carbonates are arranged into thin (5-10 cm) fining-upward units with sharp-based, silty to fine grained limestones grading upward into recessive red lime mudstones and rare buff dolomudstones (Fig. 5.5e). The gray limestones are variably massive, planar and ripple cross laminated and form ball-and-pillow structures and starved ripples in the red limestones. The upper 10 m of the unit contains mixed clastics and carbonates (Figs. 5.3 and 5.6a). A 50 cm thick cross stratified quartz pebble and intraclast conglomerate marks the base of this interval (Fig. 5.6b). It grades upward into rippled fine sandstones and limestones similar to those in the lower unit. The carbonates are intercalated with stromatolites, including two discrete horizons of black silicified bioherms (Fig. 5.6c) and a thick biostromal bed capping the Zherba Formation (Fig. 5.6d). The silicified bioherms are elongate in plan ($\leq$ 1 m long and 40 cm wide) and exhibit a well developed axial ridge that parallels neighboring bioherms. The capping biostrome is wavy laminated and exhibits symmetric domes along a well exposed bedding surface. The stromatolite is cut by smooth, shallow fissures less than a few cm's deep that are filled with red silty shales of the overlying Tinnaya Formation (Fig. 5.6e).

The thinly bedded clastics and carbonates of this unit are interpreted as distal turbidite deposits. The unit reveals an overall shallowing to sea level towards the top of the unit where the carbonate turbidites occur interstratified with conglomerates, sandstones and stromatolites. The fractures at the top of the biostrome are interpreted as karst dissolution features The conspicuous smooth nature of the fractures suggest

that corrosion of the carbonate bed may have occurred beneath a sediment mantle (e.g. Bogli 1980).

Tinnaya Formation

The Tinnaya Formation is 330 m thick and is dominated by carbonate breccias (Bobrov 1979; Khomentovsky 1990; Shenfel 1991), however, most of the "breccias" contain rounded clasts and are herein described as carbonate conglomerates. The formation is divided into four lithologic units, including in ascending order (Fig. 5.3): quartz conglomerate, chip conglomerate, raft conglomerate, and rudstone units.

The upper three units contain abundant carbonate conglomerates. These conglomerates are described following the classification scheme used by James and Stevens (1986) for similar carbonate conglomerates of the Cow Head Group in western Newfoundland. Three major conglomerate types are recognized: chip conglomerates which contain cm-size equant clasts; plate conglomerates characterized by plate-like clasts that are a few cm's thick and 10's of cm's in length; and raft conglomerates containing meter-scale tabular blocks of bedded carbonates.

Quartz Conglomerate Unit (QCU)

The QCU is 14 m thick (ca. 486-500 m; Fig. 5.3). The lower 0.7 m consists of varicolored (red, green, gray and yellow) and crudely stratified silty shale, which drapes stromatolitic and karstic topography (Figs. 5.6a and 5.6d). The shale is sharply overlain by a 4 m thick trough cross bedded, quartz pebble conglomerate (Fig. 5.6f). Above the conglomerate, the unit consists of thinly bedded trough cross bedded and ripple cross laminated pebble conglomerates, sandstones and minor shales. The cross bedding in the conglomerates and sandstones are unidirectional. The top of the unit is marked by a 2 m thick interval of thinly bedded rippled and stromatolitic dolostones.

The lower shales are interpreted to represent terra rossa associated with the underlying karstic surface (e.g. Estaban and Klappa 1983). The unidirectionally cross stratified conglomerates and sandstones may represent fluvial deposits (e.g. Walker and Cant 1984), however, in the absence of other diagnostic features, it is difficult to rule out a shallow marine origin for the clastics. Even the stromatolites at the top of the unit may have formed in small lakes on a braid plain or in a shallow marine setting.

Chip Conglomerate Unit (LCCU & UCCU)

The chip conglomerate unit is 170 m thick (500-670 m; Fig. 5.3). It is gradationally overlain by the raft conglomerate unit and is separated into two subunits; a lower subunit (LCCU) dominated by thin bedded (< 50 cm) conglomerates (Fig. 5.7a) and an upper subunit (UCCU) characterized by thicker (up to 1 m), coarser conglomerates (Fig. 5.7b). The boundary between the two subunits is marked by 10 m of quartzose sediments, including 10 to 20 cm thick fine sandstones, siltstones and quartz-bearing carbonate conglomerates, which contain clasts of carbonate mudstone, as well as sandstone and oolite.

The LCCU is dominated by limestone conglomerates and associated minor lime mudstones, dolomudstones, grainstones and shales. The chip conglomerates primarily contain cm-size clasts (Figs. 5.7c and 5.7d) and lesser amounts of larger plates and rafts in the upper part of the subunit. A similar transition occurs over a thicker stratigraphic interval from the UCCU to the raft conglomerate unit. Beds are chaotic (Fig. 5.7e), clast supported and have a carbonate mud matrix. They are massive and only locally are they crudely inversely graded with larger plates and rafts at the tops of chip conglomerates. Beds have sharp lower and upper contacts (Fig. 5.7f). The conglomerates of the entire unit are generally limestone and less commonly dolostone or of mixed lithology. For the latter, conglomerates are composed of dolostone clasts in a lime mud matrix or visa-versa. The conglomerates consist predominately of lime

mudstone and dolomudstone clasts with rare exotic clasts of stromatolite and grainstone located in conglomerates in the upper part of the LCCU. Conglomerates are parted by carbonate mud or shale, and interstratified with thicker intervals of black bituminous lime mudstones and buff dolomudstones (Fig. 5.7f). The bedded carbonates are finely laminated and resemble the lithoclasts in conglomerates. Minor grainstones and rudstones in the unit show ripple cross bedding and slump features, which are also developed in the bedded carbonate mudstones.

Raft Conglomerate Unit (RCU)

The raft conglomerate unit is 120 m thick (670-790; Fig. 5.3). In addition to containing chip conglomerates, the unit is characterized by abundant raft conglomerates associated with meter-scale tabular clasts (Figs. 5.8a to 5.8d). Platy clasts and rafts are typically oriented subparallel to bedding and occur in finer chip conglomeratic material (Fig. 5.8c). Rafts, which are composed of bedded lime mudstones and dolostones, tend to be folded in conglomerate beds (Fig. 5.8c and 8d), or broken along their lengths to form "trains" of smaller plates and rafts. Individual rafts may measure several meters in thickness and extend laterally beyond the limits of the outcrop. Such intervals of lime mudstone are interpreted as rafts on the basis of their bedding contacts, which tend to be truncated and show evidence of erosion and transport, and internal deformation, including small scale folds, faults and *in situ* breccia. Locally, large folded rafts can be traced laterally into chaotic plate and chip conglomerates (Fig. 5.8b). Other intervals of lime mudstones and dolomudstones appear to be *in situ* depositional units (Fig. 5.8e). The mudstones at the bases of these intervals onlap underlying sediments, while their upper contacts are either concordant with, or truncated by carbonate conglomerates. In the upper part of the unit, conglomerates consist of rafts made of lime mudstones interbedded with either fine grainstones or stromatolitic layers.

Rudstone Unit (RU)

This unit is nearly 30 m thick (790-820 m; Fig. 5.3). It gradationally overlies the raft conglomerate unit to cap the Tinnaya Formation and is sharply overlain by clastics of the Nokhtuisk Formation (Fig. 5.8g). The rudstone unit contains a variety of carbonates, including rudstones, grainstones and packstones, fine chip conglomerates with cm-size clasts, stromatolites, and fetid dolomudstones. Grainstones and packstones are intraclastic to oolitic and trough cross stratified. The dolomudstones occur as finely laminated to massive beds containing floating chips of carbonate, which are thinly interstratified with beds and lenses of chip conglomerates. The very top of the unit is represented by a 2 m thick chaotic chip conglomerate with gray limestone clasts set in a pervasive dolomitic matrix (Fig. 5.8h). The clasts protrude above the top surface of the bed and are draped by clastic sediments of the overlying Nokhtuisk Formation.

Interpretation of Carbonate Conglomerates

The carbonates of the Tinnaya Formation are interpreted to represent a variety of depositional processes that occurred within a slope environment, including fall out of suspended mud, slumping, debris flows and turbidity currents. These deposits greatly resemble slope conglomerates of the Cambro-Ordovician Cow Head Group of western Newfoundland (James and Stevens 1986) and the Cambro-Ordovician Hales Limestone of Nevada (Cook and Taylor 1977). The Tinnaya Formation conglomerates most likely represent sedimentation on a distally steepened ramp (i.e. depositional margin of James and Stevens 1986) as opposed to accumulation of carbonate debris downdip of a rimmed platform (i.e. bypass margin of James and Stevens 1986) on the basis of: (1) the abundance of deep water clasts and the absence of large blocks of reefal material within conglomerates; and (2) the intercalation of conglomerates with shallower water deposits in the upper part of the formation, including stromatolitic biostromes and cross stratified oolitic grainstones.

The carbonates illustrate in vertical succession, progressive deformation related to increase transport of carbonate sediment in a down slope direction: (1) *in situ* bedded bituminous limestones that show no evidence of transport; (2) bedded limestones that show evidence for *in situ* deformation, including small scale folding, brecciation and faulting; (3) internally deformed (i.e. folded) bedded limestones that can be traced laterally into conglomerates; (4) large rafts of bedded limestones encased in conglomeratic material; and (5) chaotic platy and chip conglomerates. Cook and Taylor (1977) observed a similar spectrum of deposits in Nevada and interpreted them to record a progressive loss in cohesion. Deformation began with the development of slumps. Once shear stress was exceeded, slumps could break into fragments, entrain water and mud, and evolve into debris flows. In a summary study of slope environments, Cook and Mullins (1983) outlined four main stages for the progressive deformation of slope sediment with increased down slope transport. They suggest that folding begins in the basal layers of slump masses, and with transport, folds grow to deform the entire mass. With increasing transport, progressive deformation leads to oversteepening of folds and brecciation, which begins in the basal layer and extents through the entire mass generating both chaotic conglomerates and conglomerates composed of subparallel clasts. Observations from the Tinnaya Formation support this model.

The platy and chip conglomerates exhibit many of the characteristics of debris flows (Cook and Taylor 1977; Cook and Mullins 1983; Hiscott and James 1984), including: (1) flat, sharp bases with only minor evidence of erosion; (2) poor clast fabric (chaotic) to subparallel arrangement of tabular (i.e. plates and rafts) clasts; and (3) entrainment of very large clasts, that in some cases occur in the upper parts of beds and protrude upwards above the surrounding bed surface indicative of flows associated with matrix strength and buoyancy. Because of limited exposures of the conglomerates, it is not possible to delineate the geometry of beds and therefore it is not known whether

the conglomerates were deposited as sheets that blanketed the sea floor or as channels that incised underlying slope muds.

The stratified and cross bedded conglomerates, rudstones, and grainstones are interpreted to represent turbidity currents. They contain abundant clasts of shallow water affinity and suggest that turbidity currents initiated on the shallow outer platform by spontaneous flow initiation. Turbidity currents may have been generated during storms, which led to basinward movement of sediment laden, gravity induced currents. Several workers have identified contourites within similar slope settings; however, the Tinnaya Formation deposits are poorly sorted and do not resemble well washed grainstones that have been interpreted as contourites by Cook and Taylor (1977).

The majority of this section is composed of slumps and debris flows indicating that gravity induced failure was an important depositional process within this slope environment. The majority of the debris flows consist of deep water lithoclasts, illustrating that most of the resedimented material was sourced from the upper slope. Some deposits, however, contain shallow water lithoclasts (Fig. 5.8f) and show that sediment was occasionally sourced from the shallow water platform. On the basis of these shallow water lithoclasts, the platform margin during this time was probably a series of ooid sand shoals and low relief stromatolitic bioherms that graded basinward into organic rich muds along an oversteepened slope profile.

Nokhtuisk Formation

The basal 80 m of the Nokhtuisk Formation is dominated by clastic red beds with cm-scale interbedded sandstones, siltstones and shales and minor dolostones (Fig. 5.9a). The sandstones are planar to ripple cross laminated and grade upward into siltstones and shales (Figs. 5.9b and 5.9c), which are typically laminated and exhibit well developed polygonal desiccation cracks (Figs. 5.9d and 5.9e). The dolostones occur as oolitic

grainstones, massive mudstones, tepee beds and domal stromatolites (Fig. 5.9f). Dolostones also form conglomerates and clasts at the bases of sandstones.

The basal Nokhtuisk Formation contains a succession of siliciclastic and carbonate deposits that reflect deposition within shallow water with repeated episodes of subaerial exposure. Such conditions are common on coastal mud flats of all ages (Klein 1977; Weimer, et al. 1982).

SEQUENCE STRATIGRAPHIC ANALYSIS

The Vendian is considered to display at least three depositional sequences, which are recognized by the vertical distribution of unconformities, siliciclastic detritus and depositional facies. The Zherba Formation is bounded by significant erosion surfaces and is interpreted to represent a single depositional sequence (sequence 1). Regional stratigraphic work by Khomentovsky (1990) shows a gradational relationship between the sandstones unit (SU) and overlying finer clastics of the lower turbidite unit. This observation is used to indicate that the Zherba Formation contains an assemblage of relatively conformable deposits bounded by major unconformities. Sequence 1 is divided into transgressive and highstand systems tracts. The transgressive systems tract is represented by the sandstone, lower turbidite and bituminous carbonate units. Together, they record an overall deepening of facies and reduction of siliciclastic detritus up section. The bituminous carbonate unit may represent an interval of maximum flooding and conditions of starved siliciclastic sedimentation in response to a maximum landward shift of clastic coastal depositional systems. The highstand systems tract records gradual shallowing during deposition of the upper turbidite unit. The two siliciclastic-to-carbonate cycles at the top of the sequence are interpreted as parasequences. They are sharp based, show a gradation from siliciclastic to carbonate facies, and show a pattern of thinning up section, which may indicate terminal highstand conditions. Continued

shallowing and exposure of the shelf is represented by the paleokarst capping the Zherba Formation.

The carbonate conglomerates of the Tinnaya Formation are considered to represent two additional depositional sequences. Evidence for changes in relative sea level includes vertical changes in conglomerate type and associated facies, clast composition, and partitioning of siliciclastic detritus. Sequence 2 is represented by the quartz conglomerate and lower chip conglomerate units up to the base of the quartz bearing deposits in the center of the LCCU. The basal quartz conglomerates are interpreted as transgressive deposits. They are sharply overlain by transgressive to highstand conglomerates along a marine flooding surface, which marks a pronounced change from shallow to deep water conditions. The chip conglomerates are interpreted to downlap this flooding surface, which is considered to represent a significant interval of nondepcsition. Several observations indicate gradual shoaling from the base to the top of the conglomerates included in sequence 2: (1) the proportion of shallow water lithoclasts increase up section; and (2) an upward increase in clast size and abundance of *in situ* deep water mudstones and proximal conglomerates.

The interbedded quartzose conglomerates, sandstones and siltstones mark the base of sequence 3 and are interpreted to represent a drop in relative sea level and a basinward influx of siliciclastic sediment onto the slope. A return to relatively deep water conditions during the start of sequence 3 time is represented by the absence of shallow water clasts in the overlying conglomerates. Sequence 3 is represented by the upper chip conglomerate, raft conglomerate and rudstone units. The conglomerates of sequence 3 also reveal an overall shoaling in facies up section as indicated by: (1) an increase in the proportion of shallow water clasts in conglomerates; (2) an increase in clast size, *in situ* conglomerates, and rafts; and (3) increase in proportion of *in situ* slope mudstones, rudstones and grainstones and stromatolites. The sequence does not shallow to sea level but reveals an abrupt downward shift in facies across the Tinnaya-

Nokhtuisk formational boundary, which is herein defined to mark the top of sequence 3. The tidal flat clastics of the Nokhtuisk Formation are interpreted to mark the base of an overlying depositional sequence.

ISOTOPIC DATA AND RESULTS

The $\delta^{13}C$ and $\delta^{18}O$ profiles for the Nokhtuisk section are based on over 150 analyses of stratigraphically closely spaced carbonates (this study; shown as circles in Figs. 5.3 and 5.10) and an additional 27 pairs of isotopic values published by Sochava, et al. (1996; shown as squares in Fig. 5.10). Sochava and others also report accompanying major element (Fe, Mn and Sr) compositions, which have been considered in interpreting the diagenetic grade of the sampled carbonates. Selection of carbonate samples for the isotopic analyses follows methods described by Pelechaty, et al. (1996a). Results of this study are summarized in Table 5.1 and Fig. 5.10.

Oxygen Isotope Composition

The carbonates of this section reveal extreme variability in $\delta^{18}O$, ranging between 0 and -20‰ PDB (Fig. 5.10). These data separate into two distinct isotopic groups as shown by this study and the results of Sochava, et al. (1996); the limestones are depleted by varying amounts relative to the dolostones in the section. The Chencha Formation is characterized by values between -7.5‰ (limestones) and -5‰ (dolostones) and are similar to the range of values reported by Pokrovsky and Gertsev (1993) for the same stratigraphic interval. Higher in the section, the upper Zherba Formation is characterized by dolostones with values between 0 and -5‰, and limestones between -4 and -10‰, which become relatively less depleted relative to the dolostones towards the top of the formation. The Tinnaya Formation reveals most

pronounced separation of isotopes by lithology. In general, the limestones have values between -15 and -20‰. They are depleted by as much as 10‰ in $\delta^{18}O$ relative to interbedded dolostones in the upper part of the Tinnaya Formation and dolostones of the lower Nokhtuisk Formation, which all range between -5 and 0‰. A few dolostones, however, exhibit values similar to the limestones near the 600 m level (Fig. 5.10) in the lower part of the Tinnaya Formation.

Carbon Isotope Composition

The carbonates reveal a consistency in $\delta^{13}C$ values through the section, which comprises both limestones, dolostones and a spectrum of depositional facies. At the base of the profile, the carbonates of the Chencha Formation exhibit a slight decline in $\delta^{13}C$ from -9 to -5‰ up section (Pokrovsky and Gertzev 1993). The upper Zherba Formation, however, reveals greater variability in $\delta^{13}C$. Through the lower turbidite unit, dolostones have values between -20 and -15‰, while above this interval, interbedded limestones and dolostones have heavier values but show consistent, high-frequency variation superposed on an overall increasing positive trend from -5 and +3‰ towards the top of the formation. The entire Tinnaya and lower Nokhtuisk formations reveal well defined isotopic variations. They form a first-order negative anomaly with only a few scattered data points (a, b and c in Fig. 5.10). The lower ca. 150 m of the Tinnaya Formation is characterized by decreasing $\delta^{13}C$ values from +1 to -10‰ up section, followed by an overall increase in values to +1‰ in the lower Nokhtuisk Formation. High-frequency, < 5‰ shifts are superposed on this large magnitude negative excursion.

Discussion of Isotopic Results: Secular and Diagenetic Trends

The $\delta^{18}O$ patterns are interpreted to reflect diagenetic trends. Sochava, et al. (1996) considered the extremely depleted limestones of the Tinnaya Formation to record combined effects of burial and meteoric diagenesis, which both lead to isotopic depletion of carbonates (Anderson and Arthur 1983). Sochava, et al. (1996) considered the limestones to record burial diagenesis on the basis of the crystalline texture of some of their limestone samples. Petrographic work during this study shows that the lime mudstones, which constitute the majority of sampled carbonates, are composed of micrite or pseudospar similar to the "unaltered" carbonates of the Khorbosuonka Group (Knoll, et al. 1995a; Pelechaty, et al. 1996a), and appear not to record significant burial alteration. Furthermore, as reported by Sochava, et al. (1996), the limestones have an average Mn/Sr ratio of less than 2, which is commonly considered to reflect minimal alteration (e.g. Brand and Veizer 1980; Kaufman, et al. 1993; Narbonne, et al. 1994; Knoll, et al. 1995a). More likely, the isotopic values of the Tinnaya Formation limestones reflect isotopic alteration by meteoric fluids. The ^{18}O composition of meteoric waters is dominantly influenced by temperature but also by orographic and latitudinal effects (Anderson and Arthur 1983; Siegenthaler 1979 and cited references). The limestones likely record alteration by cold ground water (i.e. glacial melt water) sourced from upper reaches of the Predpatom mountains during the Early Paleozoic, combined with orographic effects leading to isotopically light carbonates. These isotopic values are restricted to the conglomerates suggesting that these limestone were more permeable relative to underlying strata of the Zherba and Chencha formations.

The $\delta^{18}O$ composition of the dolostones is interpreted to reflect dolomitization. The dolomites were probably formed relatively early in the diagenetic history of this

section. Many conglomerates contain dolostone clasts set in a pervasive lime matrix suggesting that dolomitization occurred prior to resedimentation of the slope carbonates. Because dolomite is less susceptible than calcium carbonate to meteoric corrosion (Choquette and James 1988), any "dolomite" signal would most likely be retained during subsequent diagenetic events. Updip of this section, coeval strata consist of sabkha and associated shallow water deposits, which have been detected in petroleum wells in southern Siberia (Grosman and Zhernovsky 1989; Kuznetsov and Suchy 1992). They form part of an extensive arid climatic belt that extended across central Siberia. The enriched $\delta^{18}O$ composition of the dolostones and their stratigraphic proximity to unconformities strongly suggest that they record an "evaporation" signal associated with dolomitizing fluids formed by evaporation of seawater in an intertidal to supratidal setting. On a regional scale, the dolostones of this section are enriched in $\delta^{18}O$ relative to dolostones of the Khorbosuonka Group and correlative rocks in northeast Siberia, which range in $\delta^{18}O$ from -10 to -5‰ (Pelechaty, et al. 1996a). The Vendian carbonates located east of the central arid belt (i.e. the Khorbosuonka Group) do not contain significant evaporites in the shallow water sequences and thus have been considered to reflect relatively humid depositional conditions (Pelechaty, et al. 1996b). These regional climatic variations across the Siberian platform may account for the observed regional differences in the $\delta^{18}O$ composition of the carbonates.

The $\delta^{13}C$ profile (except through the LTU) is interpreted to represent secular change in carbon isotope composition even though most samples appear "altered" according to standard geochemical proxies (i.e. the limestones have $\delta^{18}O < -10$‰ and the dolostones have Mn/Sr > 10; Sochava, et al. 1996). However, despite these signs of diagenetic alteration, several observations suggest that the $\delta^{13}C$ profile retains a primary signal: (1) consistency in $\delta^{13}C$ values preserved in both dolostones and limestones and by a variety of depositional facies; (2) consistency in $\delta^{13}C$ values despite variability in $\delta^{18}O$ and Mn/Sr composition; and (3) the isotopic patterns of this section

can be interpreted in the context of the global standard (Knoll and Walter 1992; see below).

The $\delta^{13}C$ values through the lower turbidite unit (LTU; Figs. 5.3 and 5.10) are anomalously light. In general, the dolostones of this unit become progressively depleted in $\delta^{13}C$ towards the overlying bituminous carbonate unit. Such values are typical of carbonates that have undergone diagenesis in association with oxidation of sedimentary organic matter. Under conditions of anoxia or low dissolved oxygen contents in pore waters, bacterial sulfate reduction gives off isotopically light (down to -30‰) dissolved carbon to the pore waters (Anderson and Arthur 1983; Claypool and Threlkeld 1983), which may then be incorporated into newly formed carbonates (Kocurko 1986). On the basis of similarity of isotopically very light authigenic dolomites collected from anoxic sediments at a DSDP site (Pisciotto and Mahoney 1981), the dolomites of the LTU unit are intepreted to reflect early dolomitization associated with oxidation of interstitial sedimentary organic matter. Although the overlying BCU also contains bituminous carbonates, the sandstones and shales that occur interbedded with the light dolomites most likely provided permeable flow paths for such diagenetic fluids.

DISCUSSION

Stratigraphic Significance of $\delta^{13}C$ Profile

The carbonates of the Nokhtuisk section reveal a complex pattern of isotopic change but despite of this observed complexity, the Nokhtuisk profile appears to conforms with the global standard (Knoll and Walter 1992) with allowances for effects due to basin subsidence and stratigraphic hiatuses. Using a modified carbon isotope chemostratigraphic nomenclature by Pelechaty, et al. (1996a), the Nokhtuisk profile is partitioned into four major isotopic events. In ascending order, the section contains a

negative excursion (N2), a positive excursion (P), an intermediate isotopic interval (I), and a younger negative anomaly (N1). As discussed below, this chemostratigraphic scheme is consistent with regional sequence stratigraphic correlation of strata across Siberia.

The $\delta^{13}C$ composition of the Chencha Formation carbonates are lighter than other known Riphean carbonates of Siberia (Pokrovsky and Missarzhevsky 1993; Knoll, et al. 1995c). They may represent post-Sturtian or even post-Varanger isotopic signatures (Kaufman and Knoll 1995) but in the light of limited data from this interval, their age cannot be confirmed at present.

The high-frequency excursions observed throughout this section are regarded to reflect stratigraphic completeness. Isotopic profiles of shallow water successions (i.e. Magaritz, et al. 1986; Knoll, et al., 1995; Pelechaty, et al. 1996a; Saylor 1996; Saylor, et al. in review) tend to reveal smooth isotopic events without signs of the high-frequency variation as recorded by the Tinnaya Formation. Shallow water sections are inherently associated with abundant high-frequency stratigraphic breaks relative to coeval deep water sections. We regard differences between the isotopic record through the Tinnaya Formation and the smooth excursions observed in coeval shallow water strata as a result of differential preservation: the more complete deep water sections will tend to record more high-frequency variability.

The isotopic events displayed by the Zherba and Tinnaya formations are observed in sub-Cambrian strata throughout Siberia and world wide. The Tinnaya Formation is characterized by a prominent negative excursion similar to other terminal Vendian carbonates (Magaritz, et al. 1986; Narbonne, et al. 1994; Kaufman and Knoll 1995; Knoll, et al. 1995a; 1995b; Pelechaty, et al., 1996b). In the Nokhtuisk section, the negative exursion occupies a greater stratigraphic thickness than other isotopic intervals. Elsewhere, in Namibia (Grotzinger, et al. 1995), northwest Canada (Narbonne, et al. 1994) and northeast Siberia (i.e. Khorbosuonka River section; Knoll,

et al. 1995a), the I interval represents the most stratigraphically important isotopic event relative to the N1 and P intervals. The stratigraphic expression of isotopic excursions may vary across a basin as a function of subsidence and stratigraphic completeness (Pelechaty, et al. 1996a), and at some sections in northeast Siberia, the I and N1 intervals are represented by equally thick intervals of rock. Thus, the prominant N1 shift of the Nokhtuisk profile likely reflects relatively high sediment accumulation rates combined with unlimited accomadation and fewer stratigraphic breaks. In contrast, the stratigraphically compressed I and P intervals reflect lower sediment accumulation, limited accomadation and development of unconformites of relatively shallow water depositional settings.

The N1 excursion provides an anchor for comparison with nearby fossiliferous strata along the Aldan and Lena rivers. This comparison suggests placement of the Vendian-Cambrian boundary (i.e. base of the Nemakit-Daldyn or Manykai stage) at or near the base of the Nokhtuisk Formation as first suggested by Sochava, et al. (1996).

Chronostratigraphy of the Siberian Platform

Regional correlation of Vendian strata of the eastern Siberian platform is based on sequence stratigraphy and reveals the development of three major cratonic stratigraphic sequences. All three sequences are best developed along the margins of the craton and show increasing discontinuity toward the midcraton areas where sections are thinner and less complete as the result of onlap, reduced accommodation and the development of abundant hiatuses (e.g. Wheeler 1958). The assumption that the correlated depositional sequences are coeval depositional events across the Siberian craton is supported by carbon isotope chemostratigraphy.

Sequences 1, 2 and 3 of the Zherba and Tinnaya formations are interpreted to correlate with an identical number of similarly named sequences (see sections 4 and 5;

Pelechaty, et al. 1996b) in northeast Siberia nearly 2000 km to the north on the eastern margin of the platform (Fig. 5.11). In this region, sequence 1 is represented by the lower P interval; sequence 2 includes the upper P and lower I intervals - the P shift is absent at section 5 due to downlap; and sequence 3 includes the upper I interval and locally the N interval. These sequences onlap the craton to the west where only the youngest two sequences (sequences 2 and 3) are represented in the western Olenek area (sections 1, 2 and 3; Fig. 5.11).

The stratigraphic significance of the isotopic shifts of the Nokhtuisk profile are consistent with the above sequence stratigraphic correlation. The isotopic anomaly of the Tinnaya Formation is interpreted to represent a complete N1 interval with both falling and rising limbs of a negative shift. The above sequence stratigraphic constraints imply that the N interval is restricted to sequence 3 and that the isotopic profile through the lower part of the formation (i.e. sequence 2) is part of a separate isotopic event (i.e. I interval). Regional chemostratigraphy of the sequence 3 carbonates provides more precise temporal correlation between the two platform localities and shows that the sequence in the south spans a younger interval of time (Fig. 5.11).

The isotope profile of sequence 2 of the Nokhtuisk section is most likely representative of the I interval, which is characterized by an interval of relatively constant values near 0‰ at many sections of the Siberian platform and world-wide. The sequence also reveals two small negative shifts with magnitudes less than 5‰ (labeled A and B) that are included in the I interval. Although many other sections do not display such isotopic character through the I interval, their absence may simply reflect poor preservation, considering most isotopic records are reported from shallow platform carbonates. A few published $\delta^{13}C$ profiles, however, preserve fragments of similar isotopic variability through the I interval. For example, the P interval of the Kuibis Formation in Namibia leads into a 2‰ negative excursion up section followed by an interpreted I interval represented by +2‰ carbonates of the Schwarzrand Subgroup

(Grotzinger, et al. 1995; Saylor 1996; Saylor, et al. in review). At section 2 in the Olenek area, a similar small negative shift to -4‰ occurs above the P interval at the base of the Turkut Formation (Pelechaty, et al. 1996a). In the western Anabar area, the Staraya Retchka Formation reveals a -3‰ excursion beneath a larger magnitude negative shift interpreted as the N1 interval (Knoll, et al. 1995b). These observations suggest that: (1) the I interval is characterized by an unknown number of high-frequency, low-magnitude excursions centered near 0‰; (2) the profile through sequence 2 is consistent with representing the I interval; and (3) although defined to represent a relatively "invariant" segment of the carbon isotope profile (Pelechaty, et al. 1996a), the I interval should denote an "intermediate" isotopic interval characterized by relatively suppressed isotope shifts between the larger magnitude P and N intervals.

Below this level, the P interval in the Olenek area (section 4; Fig. 5.11) occurs as a large magnitude shift up to +6‰ immediately above and below the boundary between sequences 1 and 2. The isotopic profile across the same boundary at the Nokhtuisk section is also characterized by positive values but of considerably lower magnitude. The absence of such a large magnitude shift at this section, however, may reflect stratigraphic hiatuses represented by parasequence and sequence boundaries at this level, which may have truncated most of the P interval. The isotopic composition of the carbonates beneath this interval provides further support for a P interval at this level in the section. The P interval is presently the oldest recognized isotopic interval preserved in carbonates of the Yudoma Series (i.e. Vendian) of the Siberian platform (Knoll, et al. 1995a) but in other basins this isotopic interval is preceded by isotopically very light carbonates (Kaufman, et al. 1991; Burn.. and Matter 1993; Pell, et al. 1993; Narbonne, et al. 1994; Kaufman and Knoll 1995). The unaltered negative values in the upper part of sequence 1 of the Nokhtuisk section are interpreted to

correlate with the negative shifts of the other sections and is herein named the "N2" interval.

Vendian strata of the Siberian platform can be incorporated into a single chronostratigraphic framework despite the vast geographic separation of sections and regional variability in lithology, depositional facies and tectonic setting. Integrated carbon isotope chemostratigraphy and sequence stratigraphy provides high resolution correlation of Vendian strata and intersequence temporal resolution, which allows recognition of stratigraphic onlap, downlap, erosional hiatuses and regional variations in basin subsidence. Available chronostratigraphic data from the western Anabar (section K), Turukhansk uplift (section T) and Dvortsy section (section D) illustrate relatively brief records of deposition at the close of Vendian (sequence 3) time (Figs. 5.1 and 5.11). The record of deposition at these localities signal late-stage onlap and deposition over paleohighlands of the Siberian craton represented by the Aldan and Anabar shields. The end of the Vendian sedimentary record across the Siberian platform is marked by an unconformity (Pelechaty, et al. 1996b). Recognition of unconformities at this level in a number of basins world wide has been used to interpret this boundary as a eustatic unconformity (Runnegar 1995). Enhanced erosion of Vendian strata in northern Siberia has also been attributed to synchronous development of a rift-shoulder during separation of Siberia and Laurentia in the Early Cambrian (Pelechaty 1996; Pelechaty, et al. 1996b).

The recognition of craton-wide stratigraphic sequences on the Siberian craton appeals to eustasy as a plausible mechanism for their formation. The duration of these sequences can be determined on the basis of global chemostratigraphy with the calibrated carbon isotope profile in Namibia (Grotzingor, et al. 1995). These ages show that the Siberian depositional sequences have a maximum duration of 5 m.y. and likely record third-order sea level fluctuations (Vail, et al. 1984).

The recognition of correlative cycles in other basins provides an important test for eustasy. Correlation of such cycles through the Phanerozoic record are contentious because of poor age constraints (Maill 1992). Carbon isotope geology provides an important constraint for correlation but still the precision of this record is on the order of several millions of years (i.e. I interval is constrained between 544 and 549 Ma; Grotzinger, et al. 1995).

In addition to a third-order cyclicity, the Vendian System of Siberia records a second-order depositional sequence. For example, the Khorbosuonka Group of northeast Siberia records initial flooding of the craton (i.e. Mastakh and lower Khatyspyt formations), followed by gradual shoaling to sea level (upper Khatyspyt and Turkut formations). On the basis of available chemostratigraphy, similar large scale sequences appear in other Neoproterozoic basins. In the following section, we evaluate their global importance as well as their implications for the smaller scale sea level fluctuations recorded on the Siberian platform.

Global Correlation and Implications for Eustasy

Figure 6 illustrates a proposed physical stratigraphic correlation of key terminal Neoproterozoic sections using available global correlations of carbon isotope anomalies and glacial tillites (Kaufman and Knoll 1995; Saylor 1996; Saylor, et al. in review; Kaufman, et al. in review). In the proposed carbon isotope standard of Knoll and Walter (1992), the post-Varanger (600 Ma) sedimentary record up to the Vendian-Cambrian boundary includes a major negative-positive anomaly, followed by an extended interval of moderately positive values and a prominent negative excursion at the sub-Cambrian boundary. The recognition of multiple negative-to-positive excursions in Oman and Canada are used to infer a relatively more complex isotopic record for terminal Neoproterozoic time (Kaufman and Knoll 1995; Kaufman, et al. in review). On

the basis of a revised carbon isotope record and new estimated ages for tillites in Namibia, the terminal Neoproterozoic period contains at least two separate glacial episodes estimated to have occurred between 600 Ma and 565 Ma (Saylor 1996; Saylor, et al. in review; Kaufman, et al. in review).

From this chemostratigraphic scheme and the recognition of multiple tillites, an apparent second-order eustatic cyclicity emerges. It is best illustrated as the two large-scale siliciclastic-to-carbonate packages in the Huqf Group of Oman and its correlative deposits throughout the Middle East, Pakistan and northern India (Fig. 5.12; Gorin, et al. 1982; Hughes Clarke 1988; Husseini and Husseini Brooks 1990; Burns and Matter 1993; Burns, et al. 1994; Peters, et al. 1995). In Oman, the oldest second-order depositional sequence (sequence A; Fig. 5.12) is an unconformity-bounded succession of marine deposits of the Abu Mahara and Khufai formations. Sequence A rests nonconformably on crystalline basement and includes marine sandstones and tillites at its base, which grade upward into sandstones, argillaceous siltstones and dolomitic siltstones near the top of the Abu Mahara Formation. These deposits abruptly pass to bituminous dolomites and then peritidal carbonates of the Khufai Formation. The top of sequence A is marked by a karst erosion surface that is sharply overlain by deposits of sequence B, which is represented by an unconformity-bounded siliciclastic-to-carbonate-to-evaporite package including the Shuram, Buah, and Ara formations.

Deposits equivalent to sequence A in Oman are represented by the Court Formation in Namibia, which records shallowing of sea level between the two tillite horizons. The isotopically equivalent interval in Canada does not show obvious shallowing of sea level but contains a monotonous succession of deep water siliciclastic deposits of the lower Sheepbed Formation above the Icebrook tillite. High subsidence rates in this basin may account for the absence of similar depositional trends at this section. Correlative large scale changes in sea level of sequence B are well recorded by sediments in Oman, China and Siberia (Lambert, et al. 1987; Hughes Clark 1988; this

study). The isotopically equivalent section of the Nama Group does not reveal a clear transgressive-regressive pattern of sea level change. The Nama Group accumulated in an active foreland basin and suggests that this eustatic signal may have been dampened by local tectonically-driven sea level changes.

The terminal Neoproterozoic record reveals multiple tillites and possibly second-and third-order eustatic sequences. Post-glacial transgression has been invoked to interpret records of sea level rise recorded by sediments overlying tillites of pre-Nama Group strata in Namibia (Saylor 1996). Glacioeustasy as a mechanism for the thicker, second-order depositional sequences, however, is less obvious because single deglaciations are difficult to invoke as the cause for major sea level changes that occur over 10's of millions of years. The importance of glacioeustasy at this time is difficult to assess but may be greater than presently known. Assertions have been made of additional tillite horizons in the upper Nama Group (Schwellnus 1942) and in the Early Cambrian sequence (Fersiga Group tillite) of northwest Africa (Bertrand-Sarfati, et al. 1995), suggesting that glacioeustasy was possibly important throughout sequence B time and into the Early Cambrian. The frequency of these glaciations have been suggested by Saylor (1996) to have occurred at 5 m.y. intervals. The coeval third-order sequences of Siberia may well represent such glacioeustatic forcing.

First-order and second-order eustatic cycles of Phanerozoic age record tectonoeustatic changes in sea level related to variations in sea floor spreading during collision and breakup of cratons (Pitman 1978; Bond, et al. 1989; Hallam 1992). Speculation can only be made on the significance of sea floor spreading during terminal Neoproterozoic time because of the absence of oceanic crust to compare with the sea level record. Nevertheless, the duration of the second-order sequences require processes that operate over 10's of millions of years and thus sea floor spreading provides a plausible mechanism for the large scale changes in eustatic sea level, especially during the

Neoproterozoic at a time of wide spread continental breakup (Bond and Kominz 1984; Hoffman 1991; Moores 1991).

Initial transgression of the Siberian platform during the Vendian has been viewed to have occurred well after Varanger deglaciation in northeast Siberia (Knoll, et al. 1995a). Revised global correlation and new age contraints (Saylor 1996; Saylor, et al. in review) demonstrate that the base of the thickest Vendian sections on the platform probably correlate with tillite horizons in China and Namibia suggesting that flooding of the Siberian craton may have occurred in response to deglaciation. Early Cambrian transgression of the Siberian craton may also correspond to a glacial epoch (Bertrand-Sarfati, et al. 1995), however, tectonic processes may equally account for the Siberian transgression. Fragmentation of Siberia and Laurentia in the Early Cambrian (Pelechaty 1996) may represent the final breakup of Rodinia. Geophysical models show that the insulating effects of supercontinents create a geoid high as the result of enhanced mantle convection Gurnis 1988; Gurnis 1990). Early Cambrian transgression of Siberia may reflect the movement of the Siberian craton off of such a geoid as it rifted from Laurentia at this time. Increased sea floor spreading between the Siberian and Laurentian cratons provides an added mechanism for Early Cambrian trangression on other continents (i.e. base of Sauk sequence of North America; Sloss 1963).

CONCLUSIONS

Integrated $\delta^{13}C$ chemo- and sequence stratigraphy yields a high resolution time stratigraphic framework for allochthonous Vendian age deposits of southern Siberia. Vendian strata of the Zherba and Tinnaya formations display three major depositional sequences and the carbonates exhibit $\delta^{13}C$ excursions representative of the global standard (Knoll and Walter 1992) with allowances for subsidence and breaks in the stratigraphic record. Correlation of this section with others on the Siberian platform

reveal the development of three cratonic stratigraphic sequences. They are most complete on the margins of the craton and less complete on the midcraton due to influences of time transgressive onlap, limited accomadation and stratigraphic hiatuses.

Global correlation of the Vendian System of Siberia with other terminal Neoproterozoic successions provide evidence for eustasy by the recognition of correlative, second-order cycles in a number of sedimentary basins world wide (i.e. China, Oman, Namibia and Canada). At least two second-order cycles are recognized and form a physical stratigraphic context for the recognition of multiple tillites (Saylor 1996) and negative-positive $\delta^{13}C$ excursions (Kaufman and Knoll 1995) from the start of Varanger glaciations at 600 Ma to the Precambrian-Cambrian boundary. Evidence of repeated glaciations in Namibia coeval with the Siberian cratonic sequences provide a plausible mechanism for these third-order sea level changes. However, their influence on second-order sea level oscilations is questionable while sea floor spreading related to breakup of the supercontinent Rodinia likely provides a more plausible mechansim.

REFERENCES

Anderson, T.F. and Arthur, M.A., 1983, Stable isotopes of oxygen and carbon and their application to sedimentologicai and paleoenvironmental problems, *in* ed., Stable isotopes in sedimentary geology: SEPM Short Coarse Notes No. 10, p. 1.1-1.151.

Avdeeva, V.E., 1983, Stratigraphy of oil and gas deposits of southwestern Yakutia: (Vendian and Lower Cambrian), *in* ed., Stratigraphy of Late Precambrian and Early Paleozoic of central Siberia: Hovosibersk, USSR Academy of Sciences, p. 73-94.

Bertrand-Sarfati, J., Moussine-Pouchkine, A., Amard, B. and Aït Kaci Ahmaed, A., 1995, First Ediacaran fauna found in western Africa and evidence for an Early Cambrian glaciation: Geology, v. 23, p. 133-136.

Bobrov, A.K., 1964, Geology of the Predbaikal region: Structure and prospectivity of oil and gas: Hayka, v. p. 227 (in Russian).

Bobrov, A.K., 1979, Stratigraphy and paleogeography of deposits of the upper Precambrian of southern Yakutia, Yakutsk, Yakutian Book Publishing, 128 p. (in Russian).

Bogli, J., 1980, Scallops, B. F. Beck, ed.: v. 1, 400 p.

Bond, G.C. and Kominz, M.A., 1984, Construction of tectonic subsidence curves for the early Paleozoic miogeocline, southern Canadian Rocky Mountains: Implications for subsidence mechanisms, age of breakup, and crustal thinning: Geological Society of America Bulletin, v. 95, p. 155-173.

Bond, G.C., Kominz, M.A., Steckler, M.S. and Grotzinger, J.P., 1989, Role of thermal subsidence, flexure, and eustasy in the evolution of early Paleozoic passive-margin carbonate platforms: Controls on carbonate platform and basin development, v. p. 39-61.

Bowring, S.A., Grotzinger, J.P., Isachsen, C.E., Knoll, A.H., Pelechaty, S.M. and Kolosov, P., 1993, Calibrating Rates of Early Cambrian Evolution: Science, v. 261, p. 1293-1298.

Brand, U. and Veizer, J., 1980, Chemical diagenesis of a multicomponent system-1. Trace elements: Journal of Sedimentary Petrology, v. 50, p. 1219-1236.

Brookfield, M.E., 1994, Problems in applying preservation, facies and sequence models to Sinian (Neoproterozoic) glacial sequences in Australia and Asia: Precambrian Research, v. 70, p. 113-143.

Burns, S.J., Haudenschild, U. and Matter, A., 1994, The strontium isotopic composition of carbonates from the late Precambrian (560-540 Ma) Huqf Group of Oman: Chemical Geology, v. 111, p. 269-282.

Burns, S.J. and Matter, A., 1993, Carbon isotopic record of the latest Proterozoic from Oman: Eclogae Geol. Helv., v. 86, p. 597-607.

Choquette, P.W. and James, N.P., 1988, Introduction, *in* N. P. James and P. W. Choquette, ed., Paleokarst: New York, Springer-Verlag, p. 1-24.

Claypool, G.E. and Threlkeld, C.N., 1983, Anoxic diagenesis and methane generation in sediments of the Blake outer ridge DSDP 533, Leg 76: Initial reports of the Deep Sea Drilling Project, v. 76, p.

Cook, H.E. and Mullins, H.T., 1983, Basin Margin Environment, *in* P. A. Scholle, D. G. Bebout and C. H. Moore, ed., Carbonate Depositional Environments: Tulsa, AAPG, Memoir 13, p. 540-617.

Cook, H.E. and Taylor, M.E., 1977, Comparison of continental slope and shelf environments in the Upper Cambrian and Lowest Ordovician of Nevada, *in* H. E. Cook and P. Enos, ed., Deep water carbonate environments: Tulsa, Oklahoma, SEPM Special Publication, 25, p. 51-81.

Estaban, M. and Klappa, C.F., 1983, Subaerial Exposure, *in* P. A. Scholle, D. G. Bebout and C. H. Moore, ed., Carbonate Depositional Environments: Tulsa, AAPG, Memoir 33, p. 1-93.

Gorin, G.E., Racz, L.G. and Walter, M.R., 1982, Late Precambrian-Cambrian sediments of Huqf Group, Sultanate of Oman: American Association of Petroleum Geologists Bulletin, v. 66, p. 2609-2627.

Grosman, V.V. and Zhernovsky, V.P., 1989, About upper Precambrian and Cambrian boundary strata in deep wells of western Yakutia, *in* V. V. Khomentovsky, Y. K. Sovetov, V. Y. Shenfel, M. S. Yakshen and V. B. Moryaken, eds., Late Precambrian and early Paleozoic of Siberia: Actual stratigraphic questions: Hovosibersk, p. 75-106 (in Russian).

Grotzinger, J.P., Bowring, S.A., Saylor, B.Z. and Kaufman, A.J., 1995, Biostratigraphic and geochronological constraints on early animal evolution: Science, v. 270, p. 598-604.

Gurnis, M., 1988, Large scale mantle convection and the aggregation and dispersal of supercontinents: Nature, v. 332, p. 695-699.

Gurnis, M., 1990, Plate-mantle coupling and continental flooding: Geophysical Research Letters, v. 17, p. 623-626.

Hallam, A., 1992, Phanerozoic Sea-Level Changes, New York, Columbia University Press, 266 p.

Hamblin, A.P. and Walker, R.G., 1979, Storm-dominated shallow-marine deposits: the Fernie-Kootney (Jurassic) transition, southern Rocky Mountains: Canadian Journal of Earth Science, v. 16, p. 1673-1690.

Hiscott, R.N. and James, N.P., 1984, Carbonate debris flows, Cow Head Group, western Newfoundland: Journal of Sedimentary Petrology, v. 55, p. 735-745.

Hoffman, P.H., 1991, Did the breakout of Laurentia turn Gondwanaland inside out?: Science, v. 252, p. 1409-1413.

Hughes Clarke, M.W., 1988, Stratigraphy and rock unit nomenclature in the oil-producing area of interior Oman: Journal of Petroleum Geology, v. 11, p. 5-60.

Husseini, M.I. and Husseini, S.I., 1990, Origin of the Infracambrian salt basins of the Middle East, *in* J. Brooks, ed., Classic Petroleum Provinces: London, Geological Society Special Publication, 50, p. 279-292.

James, N.P. and Stevens, R.K., 1986, Stratigraphy and correlation of the Cambro-Ordovician Cow Head Group, western Newfoundland, Geological Survey of Canada, Bulletin 336, 143 p.

Kaufman, A.J., Hayes, J.M., Knoll, A.H. and Germs, G.J.B., 1991, Isotopic compositions of carbonates and organic carbon from upper Proterozoic successions in Namibia: stratigraphic variation and the effects of diagenesis and metamorphism: Precambrian Research, v. 49, p. 301-327.

Kaufman, A.J., Jacobsen, S.B. and Knoll, A.H., 1993, The Vendian record of Sr and C isotopic variations in seawater: Implications for tectonics and paleoclimate: Earth and Planetary Science Letters, v. 120, p. 409-430.

Kaufman, A.J. and Knoll, A.H., 1995, Neoproterozoic variations in the C-isotopic composition of seawater: Stratigraphic and biogeochemical implications: Precambrian Research, v. 73, p. 27-50.

Kaufman, A.J., Knoll, A.H. and Narbonne, G.M., in review, Isotopes, ice ages and terminal Proterozoic Earth history: Nature, v. p.

Khomentovsky, V.V., 1986, The Vendian System of Siberia and a standard stratigraphic scale: Geological Magazine, v. 123, p. 333-348.

Khomentovsky, V.V., 1990, Chapter 5: Vendian of the Siberian Platform, B. S. Sokolov and M. A. Fedonkin]: Berlin, Springer-Verlag, 2, 103-183 p.

Klein, G.D., 1977, Clastic Tidal Flats, Champaign, Illinois, COPCO, 149 p.

Knoll, A.H. and Walter, M.R., 1992, Latest Proterozoic stratigraphy and Earth History: Nature, v. 356, p. 673-678.

Knoll, A.H., Grotzinger, J.P., Kaufman, A.J. and Kolosov, P., 1995a, Integrated approaches to terminal Proterozoic stratigraphy: An example from the Olenek Uplift, northeastern Siberia: Precambrian Research, v. 73, p. 251-270.

Knoll, A.H., Kaufman, A.J., Semikhatov, M.A., Grotzinger, J.P. and Adams, W., 1995b, Sizing up the sub-Tommotian unconformity in Siberia: Geology, v. 23, p. 1139-1143.

Knoll, A.H., Kaufman, A.J., and Semikhatov, M.A., 1995c, The carbon-isotopic composition of Proterozoic carbonates: Riphean successions from northwestern Siberia (Anabar massif, Turukhansk uplift): American Journal of Science, v. 295, p. 823-850.

Knoll, A.H. and Walter, M.R., 1992, Latest Proterozoic stratigraphy and Earth History: Nature, v. 356, p. 673-678.

Kocurko, M.J., 1986, Interaction of organic matter and crystallization of high magnesium calcite, south Lousianna, *in* D. L. Gautier, ed., Roles of organic matter in sediment diagenesis: Tulsa, SEPM, No. 38, p. 13-21.

Kolosov, P.N., 1975, Stratigraphy of upper Precambrian of southern Yakutia: Hayka, v. p. 156.

Kuznetsov, V.G. and Suchy, V., 1992, Vendian-Cambrian tidal and sabkha facies of the Siberian platform: Facies, v. 27, p. 285-294 (in Russian).

Lambert, I.B., Walter, M.R., Wenlong, Z., Songnian, L. and Guogan, M., 1987, Paleoenvironment and carbon isotope stratigraphy of Upper Proterozoic carbonates of the Yangtze Platform: Nature, v. 325, p. 140-142.

Magaritz, M., Hoser, W.T. and Kirschvink, J.L., 1986, Carbon-isotope events across the Precambrian-Cambrian boundary on the Siberian platform: Nature, v. 320, p. 258-259.

Miall, A.D., 1992, Exxon global cycle chart: An event for every occassion?: Geology, v. 20, p. 787-790.

Moores, E.M., 1991, Southwest U.S.-East Antarctic (SWEAT) connection: A hypothesis: Geology, v. 19, p. 425-428.

Narbonne, G.M., Kaufman, A.J. and Knoll, A.H., 1994, Integrated chemostratigraphy and biostratigraphy of the upper Windermere Supergroup (Neoproterozoic), Mackenzie Mountains, northwestern Canada: Geological Society of America Bulletin, v. 106, p. 1281-1292.

Nikulin, V.E., 1970, Main structures of the Baikal-Patom upland and adjacent areas, K. V. Bogolepov, ed.: Moscow, Publishing House Nauka, p. 35-39 (in Russian).

Pelechaty, S.M., 1996, Stratigraphic constraints for the Siberia-Laurentia connection and early Cambrian rifting: Geology, v. p. 719-722.

Pelechaty, S.M., Kaufman, A.J. and Grotzinger, J.P., 1996a, Evaluation of $\delta^{13}C$ isotope stratigraphy for intrabasinal correlation: Vendian strata of the Olenek uplift and Kharaulakh Mountains, Siberian platform, Russia: GSA Bulletin, v. 108, p. 992-1003.

Pelechaty, S.M., Grotzinger, J.P., Kashirtsev, V.A. and Jerinovsky, V.P., 1996b, Chemostratigraphic and sequence stratigraphic constraints on Vendian-Cambrian basin dynamics, Northeast Siberian craton: Journal of Geology, v. 104, p. 543-564.

Pell, S.D., McKirdy, D.M., Jansyn, J. and Jenkins, R.J.F., 1993, Ediacaran carbon isotope stratigraphy of South Australia-an initial study: Transactions of the Royal Society of Australia, v. 117, p. 153-161.

Peters, K.E., Clark, M.E., Gupta, U.D., McCaffrey, M.A. and Lee, C.Y., 1995, Recognition of an Infracambrian source rock based on biomarkers in the Baghewala-1 oil, India: American Association of Petroleum Geologists Bulletin, v. 79, p. 1481-1494.

Pisciotto, K.A. and Mahoney, J.J., 1981, Isotopic survey of diagenetic carbonates, Deep Sea Drilling Project Leg 63, *in* R. S. Yeats and B. U. Haq, ed., Initial Reports DSDR: Washington, U.S. Government Printing Office, 63, p. 595-609.

Pitman, W.C., 1978, Relationship between eustacy and stratigraphic sequences of passive margins: Geological Society of America Bulletin, v. 89, p. 1389-1403.

Pokrovsky, B.G., and Missarzhevsky, V.V., 1993, Isotope correlation of Precambrian and Cambrian of the Siberian platform: Akad. Nauk SSSR, Doklady, V. 329, p. 1245-1250 (in Russian).

Pokrovsky, B.G. and Gertsev, D.O., 1993, Upper Precambrian carbonates with anomalously light carbon isotope composition (South-central Siberia): Lithology and Mineral Resources, v. 1, p. 64-80 (in Russian).

Ross, G.M., 1991, Tectonic setting of the Windermere Supergroup revisited: Geology, v. 19, p. 1125-1128.

Runnegar, B., 1995, Base of the Sauk sequence is a global eustatic event that lies just above the Precambrian-Cambrian boundary: Geological Society of America Abstracts with Programs, v. 27, p. A330.

Saylor, B.Z., 1996, Sequence stratigraphic and chemostratigraphic constraints on the evolution of the terminal Proterozoic to Cambrian Nama basin, Namibia [unpubl. Ph.D. thesis]: Massachusetts Institute of Technology, 193 p.

Saylor, B.Z., Grotzinger, J.P. and Germs, G.J.B., 1995, Sequence stratigraphy and sedimentology of the Neoproterozoic Kuibus and Schwarzrand Subgroups (Nama Group), southwestern Namibia: Precambrian Research, v. 73, p. 153-171.

Saylor, B.Z., Kaufman, A.J., Grotzinger, J.P. and Urban, F., in review, The partitioning of terminal Neoproterozoic time: Constraints from Namibia: Journal of Sedimentary Research.

Schwellnus, C.M., 1942, The Nama tillite in the Klein Kharas mountains, SW Africa: Geologicalt Society of South Africa, v. 12, p. 19-33.

Shenfel, V.Y., 1991, Late Precambrian of the Siberian Platform, Novasibersk, Science Academy of USSR, 185 p. (in Russian).

Shenfel, V.Y. and Yakshin, V.G., 1975, New information on the stratigraphy of Late Proterozoic depostis along the Tokko River basin: Analagous to the Siberian Vendian Complex: Hayka, v. p. 146-151.

Siegenthaler, U., 1979, Stable hydrogen and oxygen isotopes in the water cycle, *in* E. Jäger and J. C. Hunziker, ed., Lectures in Isotope Geology: Berlin, Springer-Verlag, p. 264-273.

Sloss, L.L., 1963, Sequences in the cratonic interior of North America: Geological Society of America Bulletin, v. 74, p. 193-214.

Sochava, A.V., Podkovyrov, V.N. and Vinogradov, D.P., 1996, Variations of carbon and oxygen isotope compositions in Vendian-Lower Cambrian carbonate rocks of the Ura Anticlinorium (southern Siberian platform): Lithology and Mineral Resources, v. 31, p. 248-257.

Vahrenkamp, V.C., 1996, Carbon Isotope stratigraphy of the Upper Kharaib and Shuaiba formations: Implications for the Early Cretaceous evolution of the Arabian Gulf region: American Association of Petroleum Geologists Bulletin, v. 80, p. 647-662.

Vail, P.R., Hardenbol, J. and Todd, R.G., 1984, Jurassic unconformities, chronostratigraphy, and sea-level changes from seismic stratigraphy and biostratigraphy, *in* J. S. Schlee, ed., Interregional unconformities and hydrocarbon accumulations: AAPG Memoir 36, p. 129-144.

Walker, R.G., 1984, Turbidites and associated coarse clastic deposits, 2nd[nd] R. G. Walker, ed.: Toronto, Geoscience Canada Reprint Series 1, 171-188 p.

Walker, R.G. and Cant, D.J., 1984, Sandy fluvial systems, *in* R. G. Walker, ed., Facies Models: Geoscience Canada, p. 71-90.

Weimer, R.J., Howard, J.D. and Lindsay, D.R., 1982, Tidal flats and associated tidal channels, *in* P. A. Scholle and D. Spearing, ed., Sandstone depositional environments: IAS Special Publication, 2, p. 205-224.

Wheeler, H.E., 1958, Time stratigraphy: AAPG Bulletin, v. 42, p. 1047-1063.

LIST OF TABLES

LIST OF FIGURES

Figure 5.8
Conglomerates of the Tinnaya Formation. (A) Raft conglomerate with raft and chip fragments. (B) Raft conglomerate showing raft adjacent to chip conglomerate material. (C) Thick-bedded and folded raft conglomerate beds. (D) Folded raft conglomerate beds. (E) Medium-bedded dolomudstone. (F) Raft conglomerate. Knife for scale rests on blocks of stromatolite. (G) Outcrop of contact between the Tinnaya and Cambrian Nokhtuisk formations. (H) Chip conglomerate capping the Tinnaya Formation. Clast protrude from top of bed and are drapped by clastics of the Nokhtuisk Formation.

Figure 5.9
Deposits of the Cambrian age Nokhtuisk Formation. (A) Red beds: interbedded sandstones (massive beds), siltstones and shales (recessive beds). (B) Trough cross-bedded sandstone. (C) Rippled sandstone separated by siltstone and shale beds. (D) Bedding surface of sandstone showing ripples and mudcracks. (E) Prism cracks developed in siliciclastic sediment. (F) Stromatolitic carbonates interbedded with redbeds. Knife for scale in figures b, c, d, e, and f.

Figure 5.10
Generalized stratigraphic column of the Nokhtuisk section with accompanying carbon isotope and oxygen profiles. Symbols: solid circles (limestone) and open circles (dolostones) are results from this study; and solid squares (limestone) and open squares (dolostones) are results from Sochava, et al. (1996). Refer to text for description of lithologic units given to the left of the stratigraphic column. For comparison, units designated by Bobrov (1964) are shown by roman numerals. SB, sequence boundary; ps, parasequence boundary. Chemochrons refer to a lower negative excursion (N2), a positive excursion (P), an intermediate (I) interval, and an upper negative (N1) isotope anomaly.

Figure 5.11
Proposed regional chemo- and sequence stratigraphic correlation of Vendian sections of the Siberian platform. Refer to Fig. 5.1 for location of sections. Sections, 1, 2, 3, and 4 shown as "O" in Fig. 5.1. Symbols: CC = correlative conformity; dsf = downward shift in facies; P = Platonovka Formation; S. Rechka = Staraya Retchka Formation; Kh = Khatyspyt Formation; Yd = Yudoma Series. Age constraints for carbon isotope standard are from Bowring, et al. (1993) and Grotzinger, et al. (1995) and estimated ages by Saylor (1996). Sections: T from Bartley et al. (unpublished data); K from Knoll, et al. (1995); sections 1, 2, 3, 4 and 5 from Pelechaty, et al. (1996); and D from Magaritz, et al. (1986).

Figure 5.12
Global correlation of terminal Neoproterozoic sections based on chemostratigraphy by Kaufman and Knoll (1995) and correlation of tillites by Saylor (1996). Stratigraphic data: Canada (Narbonne, et al. 1994); Namibia (Kaufman, et al. 1991; Kaufman, et al. 1993; Saylor, et al. 1995; Grotzinger, et al. 1995; Saylor 1996); Oman (Hughes Clarke 1988; Burns and Matter 1993); China (Lambert, et al. 1987; Brookfield 1994); and Siberia (this study). Namibian section: BT = Blaubeker tillite; NT = Naukluft tillite. SB = sequence boundary.

TABLE 5.1. GEOCHEMICAL & PETROGRAPHIC ANALYSES

No.	Height (m)	δ13C (‰ PDB)	δ18O (‰ PDB)	Comment
Chencha Formation				
1	1	-9.0	-8.6	L silt; M*
2	5.5	-9.3	-8.6	L silt; M
3	10	-8.9	-8.4	L silt; M
4	14.5	-8.3	-8.2	L mud; S
5	19	-8.6	-8.8	L mud; M
6	24	-8.4	-7.0	L mud; M
7	28.5	-8.5	-8.0	L mud; M
8	33	-8.4	-8.0	L mud; M
9	35.5	-8.8	-7.7	L mud; M
10	40	-10.4	-7.7	L bmud; M
12	54.5	-8.8	-7.9	L bmud; M
13	59	-7.9	-7.1	L bmud; M
14	64.6	-8.6	-7.6	L bmud; OM
16	75	-7.4	-3.6	D bmud; M
18	87	-7.9	-5.1	D bmud; M
20	96	-7.1	-5.0	D mud; M
22	105	-7.6	-5.2	D mud; M
24	114	-7.0	-5.0	D mud; M
26	123	-6.2	-5.0	D mud; S
27	129.5	-5.5	-3.4	D mud; M
28	134	-4.6	-4.6	D mud, M
Zherba Formation (Sequence 1)				
33	371.5	-8.6	-7.3	L mud; M
34	374.5	-13.3	-2.1	D mud; M
35	377.5	-11.0	-2.0	D mud; NS
36	380.5	-15.4	-2.7	D mud; S
37	383.5	-15.5	-1.7	D mud; M
38	388	-15.8	-2.4	D mud; M
39	391	-19.5	-2.1	D mud; S
40	397	-20.1	-0.2	D grst; M
41	400	-16.9	-6.0	D grst; Mc
42	403	-9.7	-5.8	L grst; Mc
43	406.6	-4.2	-9.4	L grst; Mc
44	410	-3.2	-9.2	L grst; Mc
45	413	-1.8	-8.4	L grst; M
46	416	-2.7	-7.1	L grst; NS
47	419	-1.0	-8.0	L grst; NS
48	422.5	-6.3	-2.3	D grst; Mc
49	425.5	-2.1	-1.2	D grst; NS
51	431.5	-2.9	-1.4	D grst; NS
52	434.5	-2.7	-4.7	L grst; Mc
53	437.5	-4.8	-5.4	L grst; NS
54	441	-1.8	-4.6	L grst; NS
55	444	-1.3	-3.6	L grst; WRx
56	447	-1.4	-4.4	L grst; Mc
57	450	-1.5	-4.7	L grst; Mc
59	456.5	-2.2	-4.5	L grst; Mc
60	459	-1.1	-4.4	L strom; M
61	462	0.3	-4.2	L grst; Mc
62	465	0.4	-1.6	D grst; M
65	474	2.2	-4.7	L grst; M
67	480.5	1.8	-5.9	L grst; M
69	483.5	1.3	-1.9	D grst; M
71	486.5	2.1	-3.1	D strom; M
72	488	1.4	-1.8	D grst; Mc
Lower Tinnaya Formation (Sequence 2)				
73	498.5	0.9	-3.2	D mud; M
74	502.5	-0.4	-6.7	D mud; M
75	505	-2.6	-19.8	L bx; M
77	509.5	2.4	-19.4	L bx; M
78	512.5	-2.9	-18.6	L bx; M
80	520.5	-2.9	-19.8	L grst; M
81	524.5	-1.6	-17.5	L bx; M
82	527.5	-3.2	-17.2	L bx; M
84	531.5	-1.9	-16.5	L bx; M
85	534.5	-0.2	-17.9	L grst; WX
86	537.5	-0.9	-19.1	L grst; M
87	540.5	0.3	-14.0	L bio; M
88	544	-0.2	-19.3	L grst; M
90	552.5	-0.5	-9.4	D grst, M
91	556.5	-1.2	-18.5	L strom; M
92	560	-1.2	-17.3	L strom; M
93	561.5	-1.1	-18.4	L silt; M
94	564	-0.9	-20.0	L silt; M
95	567	-2.3	-19.3	L bio; M
97	569	-4.5	-19.8	L bsilt; M
98	572	-4.8	-19.9	L bmud; M
99	574.5	-3.9	-19.5	L bmud; M
100	578	-2.0	-19.0	L bmud; M
101	581	-1.8	-15.4	D bmud; M
Upper Tinnaya Formation (Sequence 3)				
102	584	-2.9	-16.1	D bmud; M
103	585	-4.2	-17.0	L bmud; M
104	589	-6.5	-16.6	D grst; S
106	595	-2.9	-19.4	L bmud; M
107	598	-3.8	-19.1	L bmud; M
108	601	-2.7	-16.5	D bmud; M
109	604	-4.2	-17.7	D bmud; M
110	610	-4.1	-15.4	D mud; M
111	613	-6.1	-17.3	L mud; M
112	616	-6.3	-16.8	D bx; S
113	619	-7.9	-17.3	L mud; M
119	627	-7.3	-18.4	L mud; M
120	629	-8.9	-17.5	L mud; S
121	633.5	-6.0	-19.5	L mud; M
122	641.5	-4.7	-19.7	L mud; M
123	644.5	-2.9	-15.9	L mud; M
124	651	-5.9	-18.7	L mud; M
125	653.5	-5.2	-17.0	L mud; M
126	665	-6.3	-19.3	L mud; M
127	672.5	-6.0	-19.5	L mud; M
128	675.5	-5.6	-17.2	L mud; M
129	680	-7.8	-19.5	L mud; M
130	684.5	-4.3	-19.7	L mud; M
131	687.5	-4.4	-17.3	L mud; M
132	691	-3.6	-17.7	L mud; M
133	694	-4.7	-15.2	L mud; M
135	700	-4.9	-15.7	L mud; M
136	704	-4.5	-1.5	D mud; M
138	710.5	-5.0	-0.3	D mud; M
139	712	-6.0	-1.3	D mud; M
140	715	-5.5	-1.0	D mud; M
141	719	-9.3	-1.0	D grst; BS
142	722	-6.8	-1.2	D grst; NS

No.	Height (m)	δ13C (‰ PDB)	δ18O (‰ PDB)	Comment
143	725	-6.5	-0.5	D grst; S
144	728.5	-6.0	-17.4	L grst; BS
145	731.5	-4.1	-0.9	D grst; MC
146	736	-3.3	-1.1	D grst; WX
147	740	-3.3	-1.0	D grst; MC
150	746	-3.1	-1.9	D grst; BS
151	749.5	-3.8	-4.6	D grst; BS
153	755.5	-3.1	-2.4	D grst; MC
154	759.5	-3.5	-1.5	D grst; S
155	762.5	-4.2	-3.8	D grst; MC
156	765.5	-7.4	-2.9	D grst; MC
157	768.5	-8.0	-2.6	D grst; S
158	771	-7.0	-2.3	D grst; MC
159	773.5	-3.8	-15.0	L grst; MC
161	779	-3.3	-18.4	L grst; S
162	781.5	-3.2	-15.7	L grst; MC
163	785.5	-3.9	-18.1	L grst; MC
164	788.5	-2.4	-3.0	D grst; S
165	790.5	-2.6	-14.9	L grst; MC
166	793.5	-2.6	-3.0	D grst; MC
167	795.5	-2.8	-2.6	D mud; NS
170	798.5	-2.3	-3.6	D mud; NS
173	803.5	-3.9	-17.0	L mud; M
174	808.5	-3.1	-20.4	L mud; M
175	810	-2.7	-19.2	L grst; MC
176	812	-3.3	-20.5	L mud; M
179	815	-2.7	-20.1	L mud, S
Nokhtuisk Formation				
182	818.5	-2.3	-20.2	L mud; M
184	824	-4.4	-4.1	D mud; M
185	827	-3.7	-2.7	D mud; M
187	832	-4.2	-3.4	D mud; M
188	845	-1.3	-3.7	D grst; MC
189	852	-0.8	-3.8	D grst; MC
191	855.5	0	-4.0	D grst; MC
193	864	0.6	-3.2	D grst; WX
194	868	0	-3.4	D grst; WX
195	872	0.6	-3.4	D grst; WX
196	882.5	-1.6	-3.8	D grst; MC
197	885.5	-0.5	-4.0	D grst; MC
199	891	-2.3	-3.1	D strom; M
201	898.5	-0.3	-4.4	D strom; M
202	901.5	-0.2	-4.8	D strom; M
203	905	1.3	-6.0	D strom; M

*Symbols used for petrographic descriptions: (lithology) D, dolostone; L, limestone; (sediment type) grst, grainstone; pkst, packstone; silt, siltstone; mud, mudstone; bmud, bituminous mudstone; strom, stromatolite; bio, biolaminite; (microscopic component) M, micrite; OM, micrite with abundant sedimentary organic matter; NS, neomorphic spar; MC micritic clast; S, void-filling spar; BS, baroque spar; WX, whole rock sample.

†Not determined

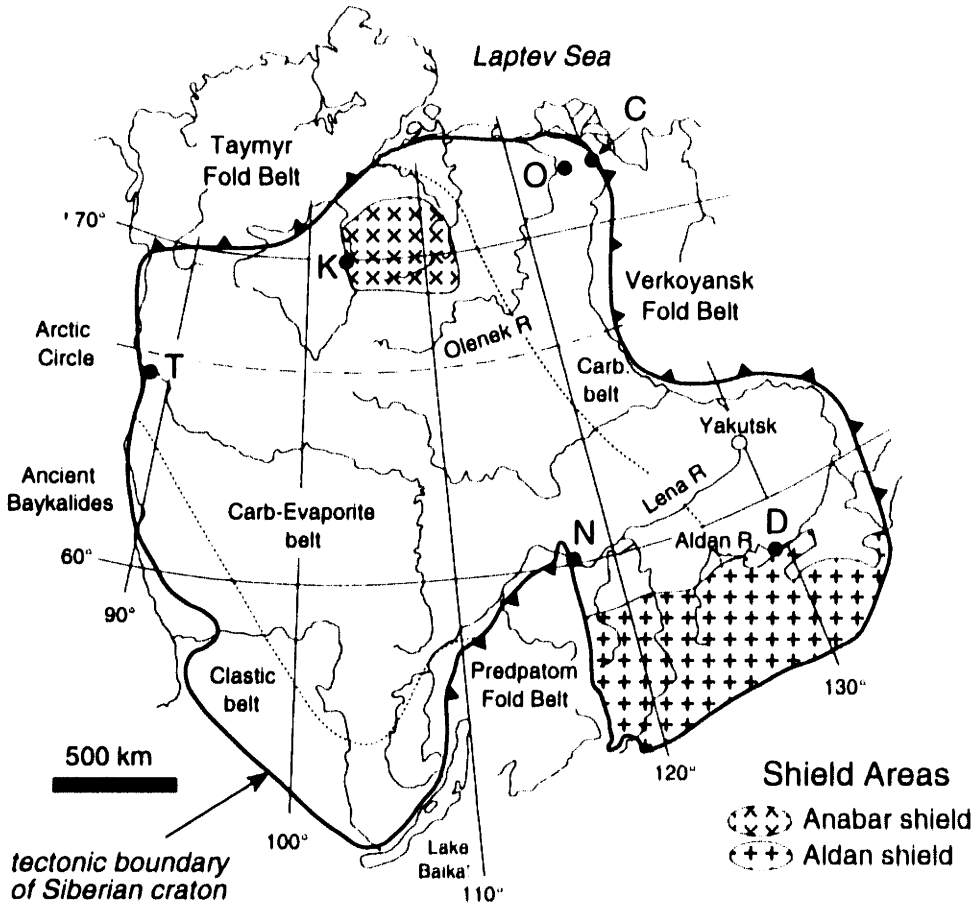
Laptev Sea
C
O
Taymyr
Fold Belt
70°
K
Verkoyansk
Fold Belt
Arctic
Circle
T
Olenek R
Carb.
belt
Yakutsk
Ancient
Baykalides
Carb-Evaporite
belt
Lena R
N
Aldan R
D
60°
90°
Clastic
belt
Predpatom
Fold Belt
130°
500 km
120°
Shield Areas
Anabar shield
Aldan shield
tectonic boundary
of Siberian craton
100°
Lake
Baika
110°

Figure 5.1

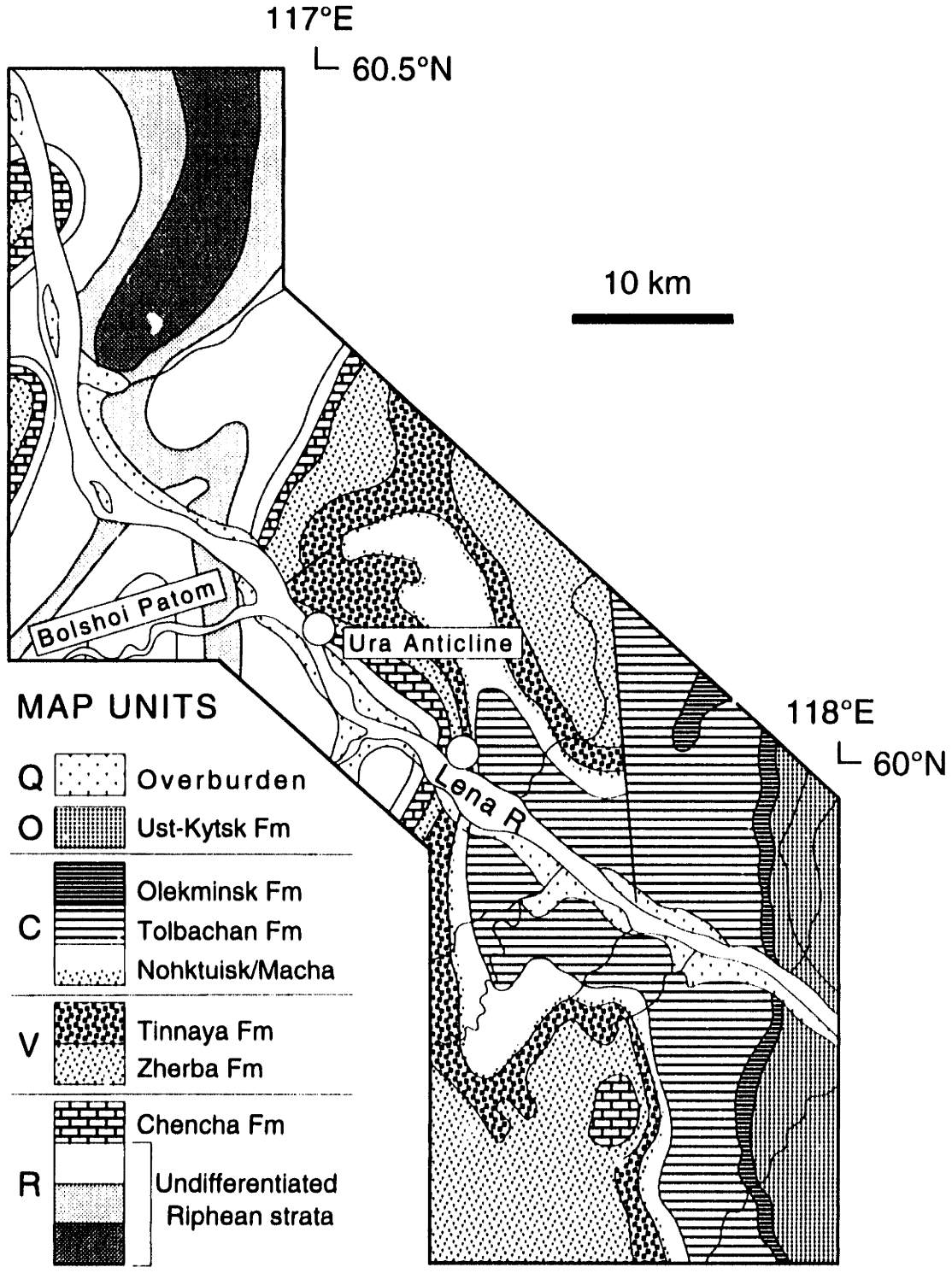
117°E
60.5°N
10 km
Bolshoi Patom
Ura Anticline
Lena R.
118°E
60°N
MAP UNITS
Q
Overburden
O
Ust-Kytsk Fm
C
Olekminsk Fm
Tolbachan Fm
Nohktuisk/Macha
V
Tinnaya Fm
Zherba Fm
R
Chencha Fm
Undifferentiated
Riphean strata

Figure 5.2

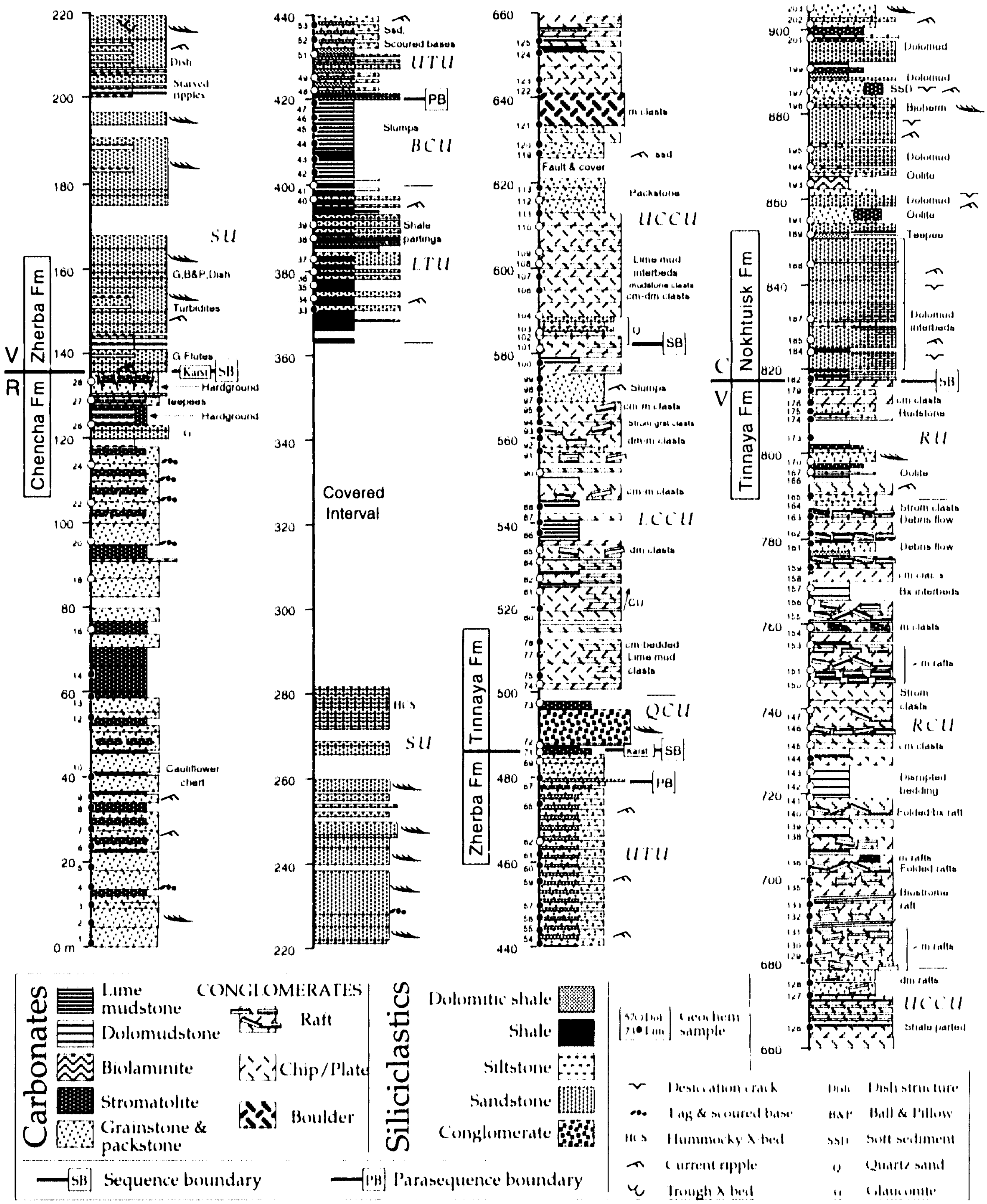
Chencha Fm
Zherba Fm
Tinnaya Fm
Nokhtuisk Fm
Covered Interval
SU
UTU
BCU
LTU
UCCU
LCCU
QCU
RU
RCU
Sequence boundary
Parasequence boundary
Carbonates
Lime mudstone
Dolomudstone
Biolaminite
Stromatolite
Grainstone & packstone
CONGLOMERATES
Raft
Chip/Plate
Boulder
Siliciclastics
Dolomitic shale
Shale
Siltstone
Sandstone
Conglomerate
Geochem sample
Desiccation crack
Lag & scoured base
Hummocky X bed
Current ripple
Trough X bed
Dish structure
Ball & Pillow
Soft sediment
Quartz sand
Glauconite

Figure 5.3

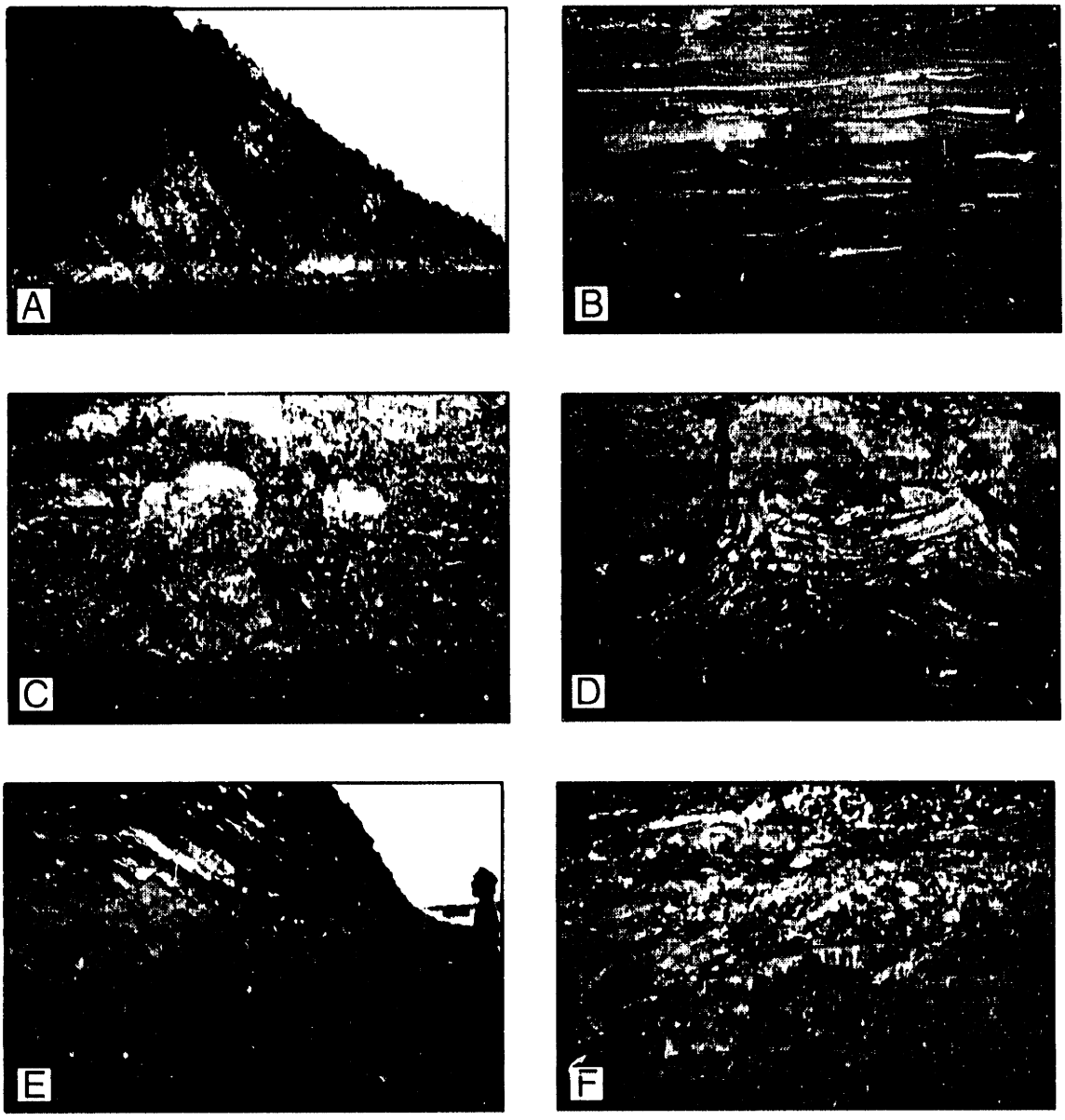

Figure 5.4

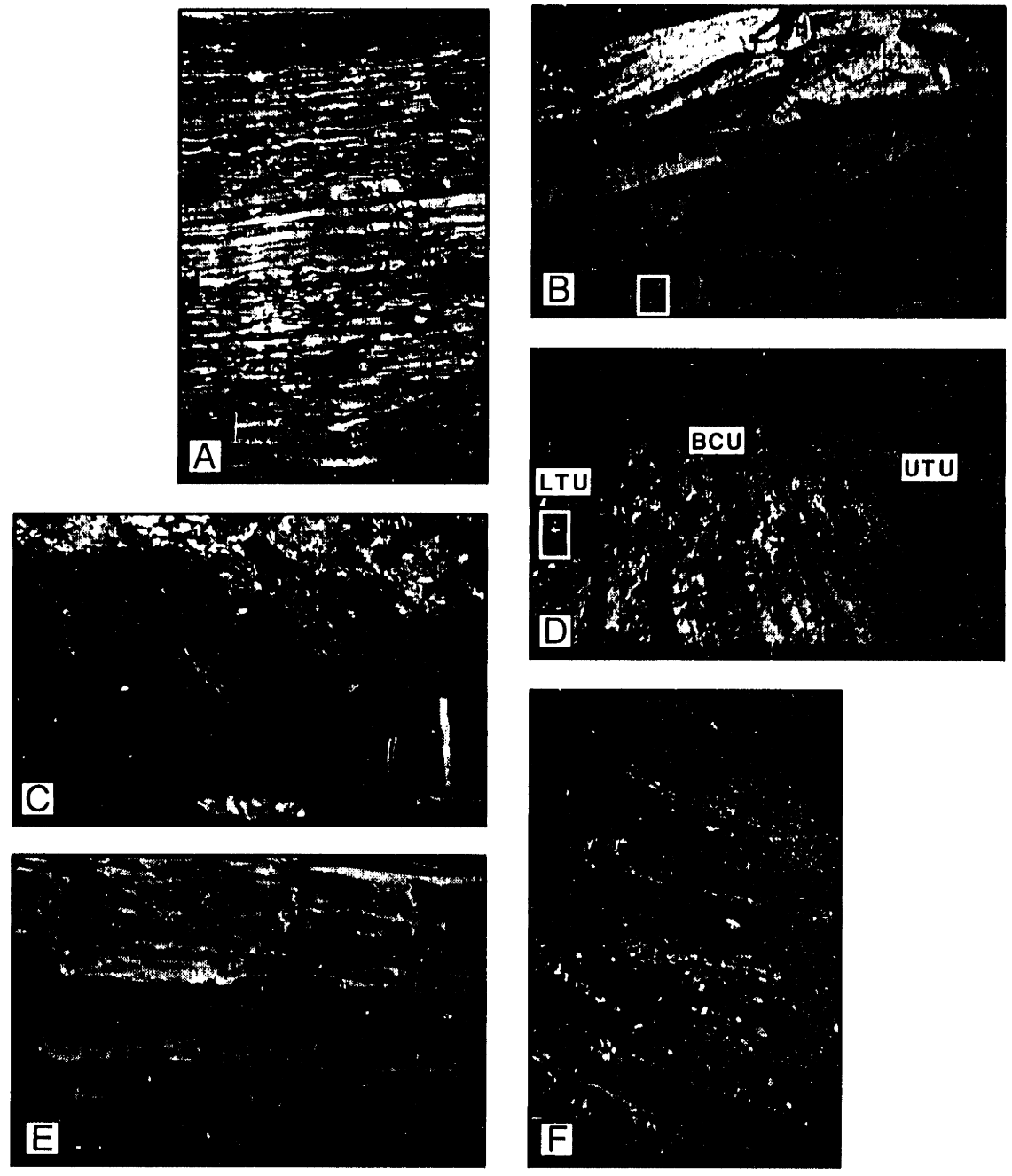

Figure 5.5

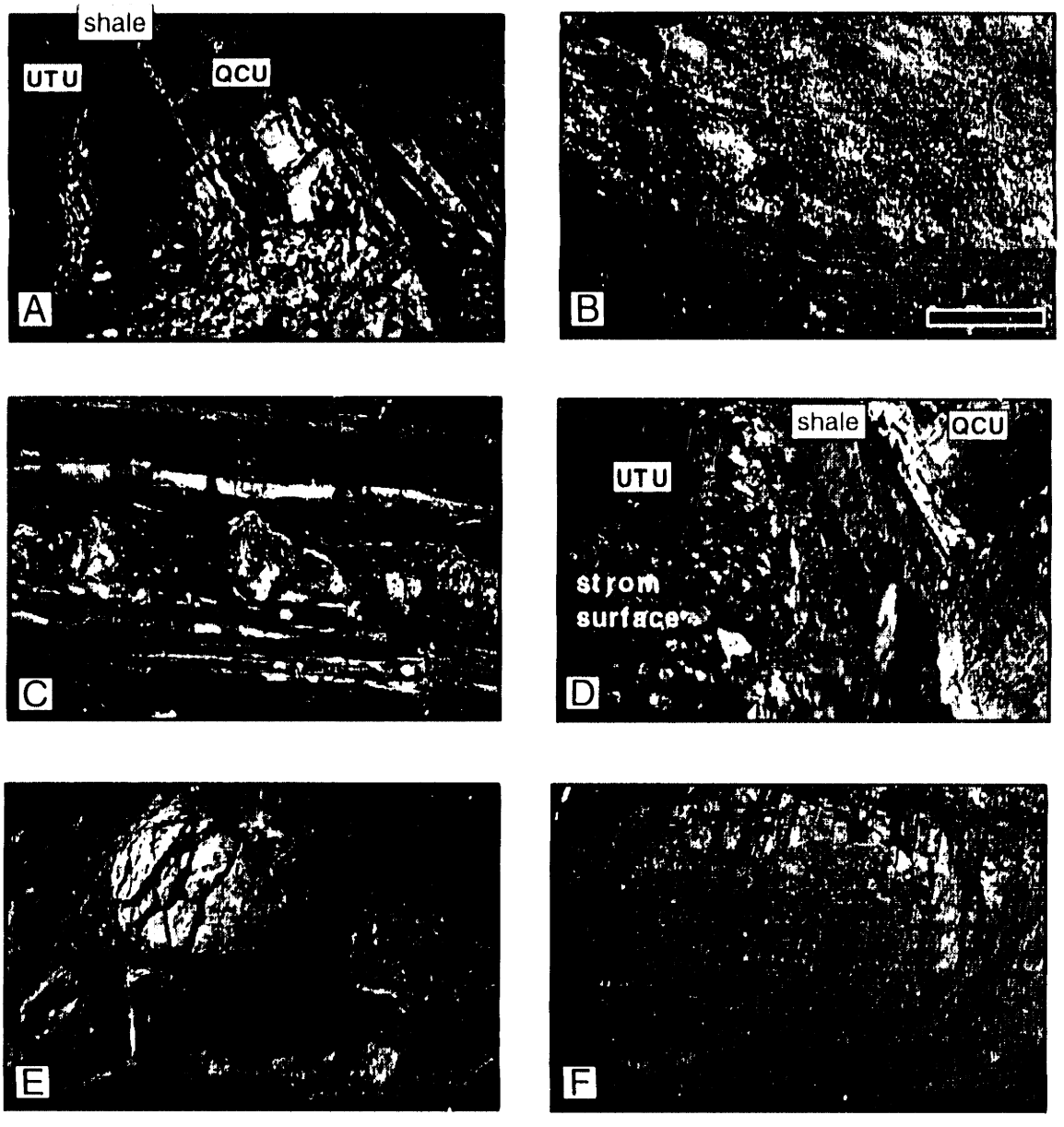

Figure 5.6

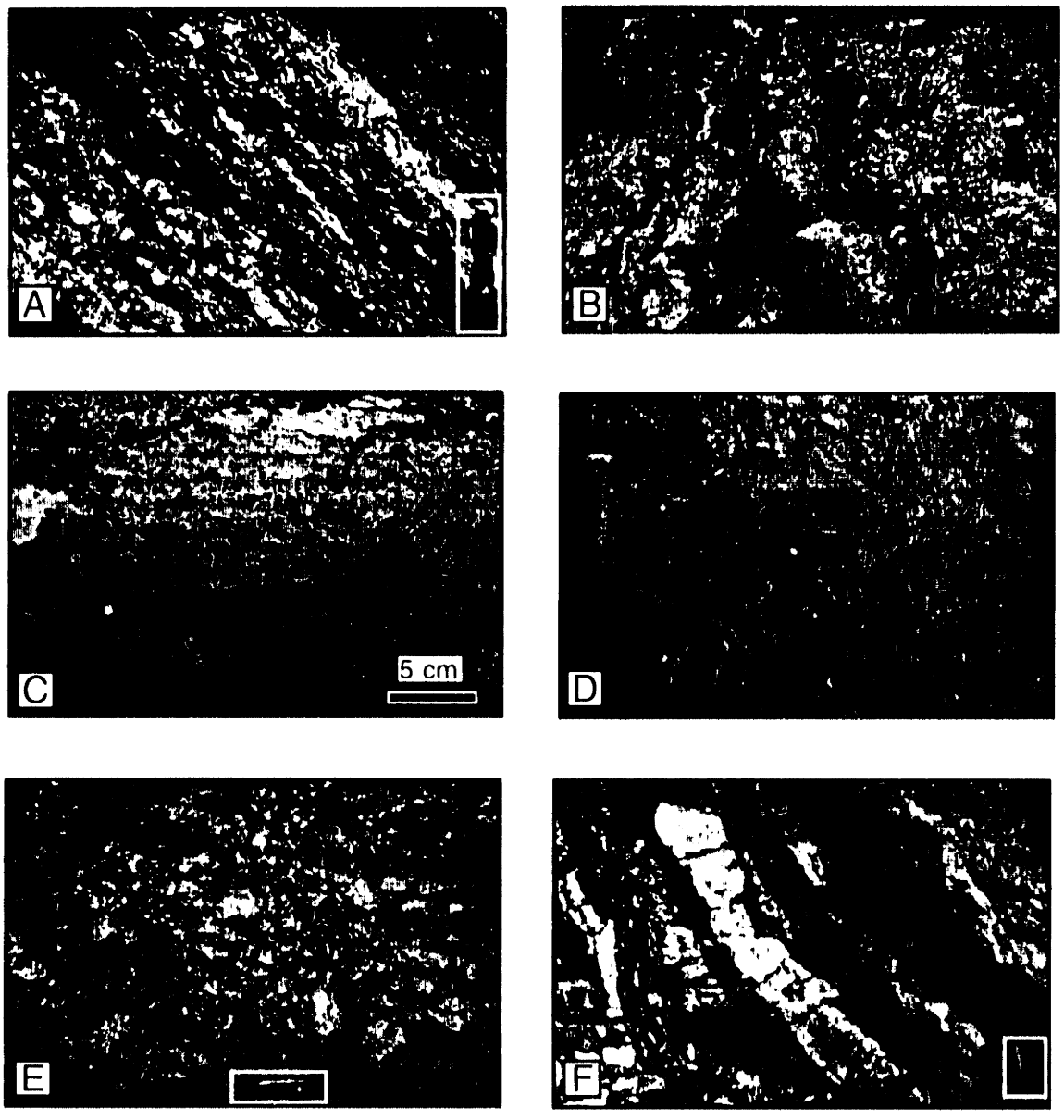

Figure 5.7

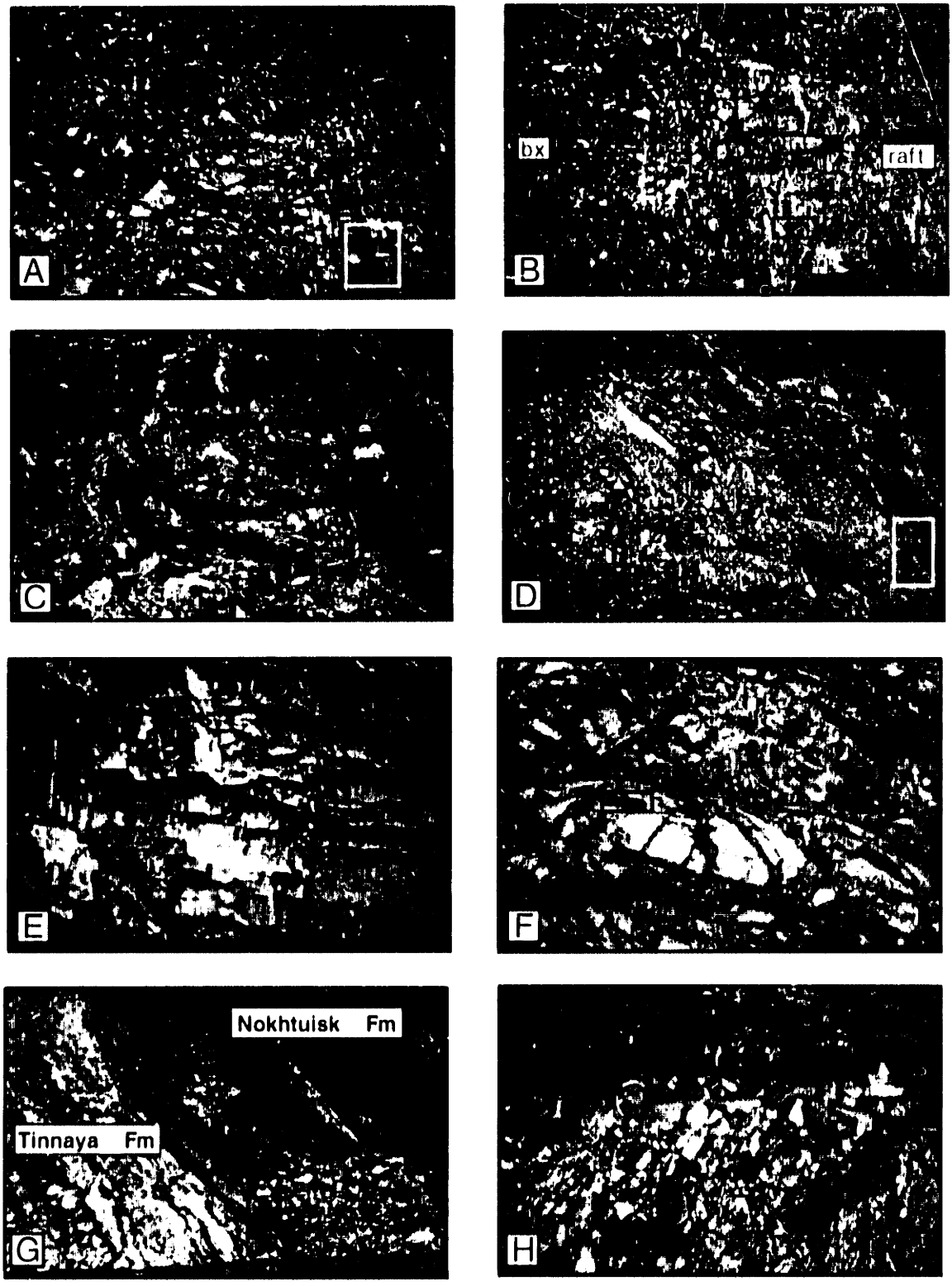

Figure 5.8

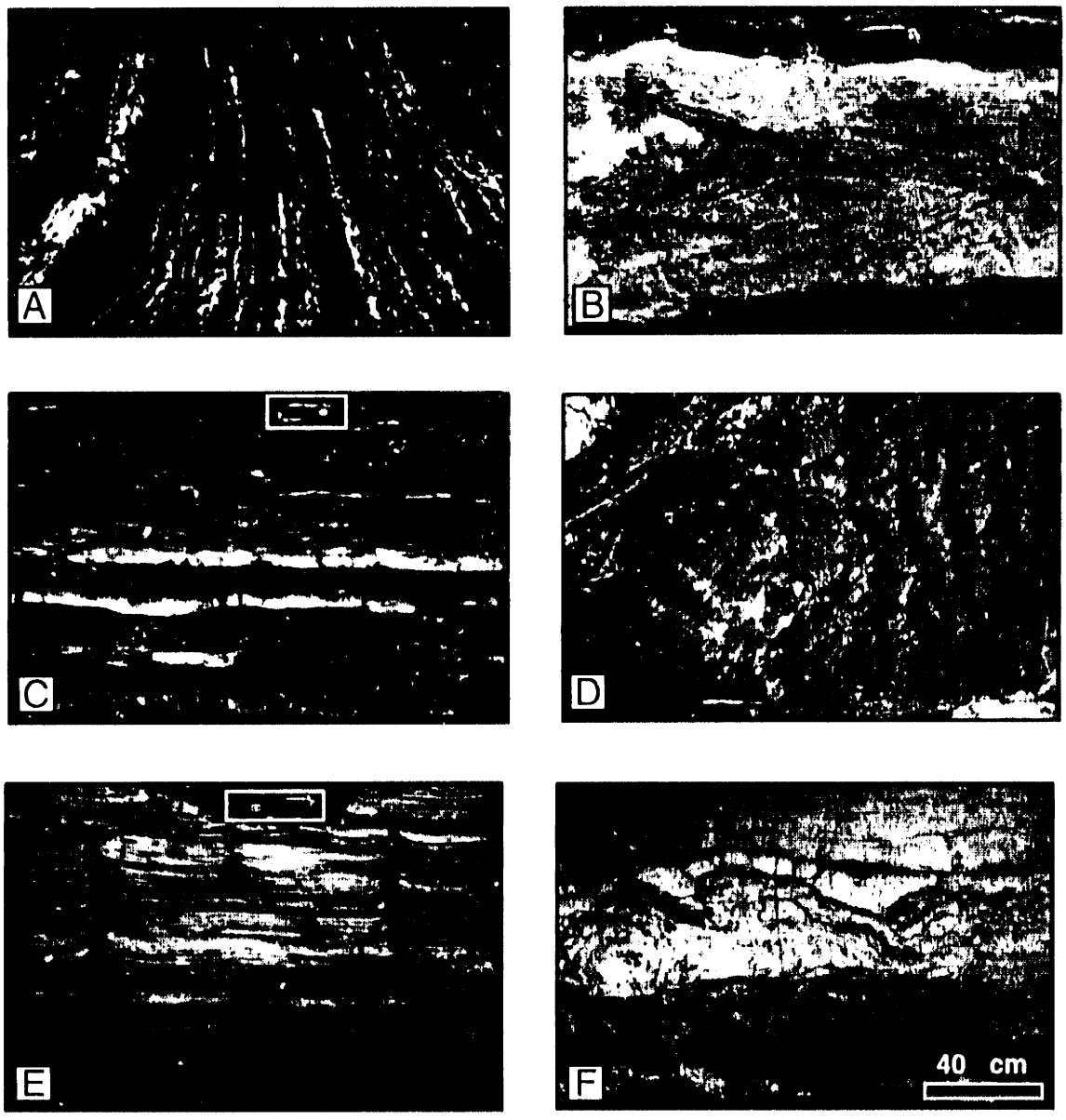

Figure 5.9

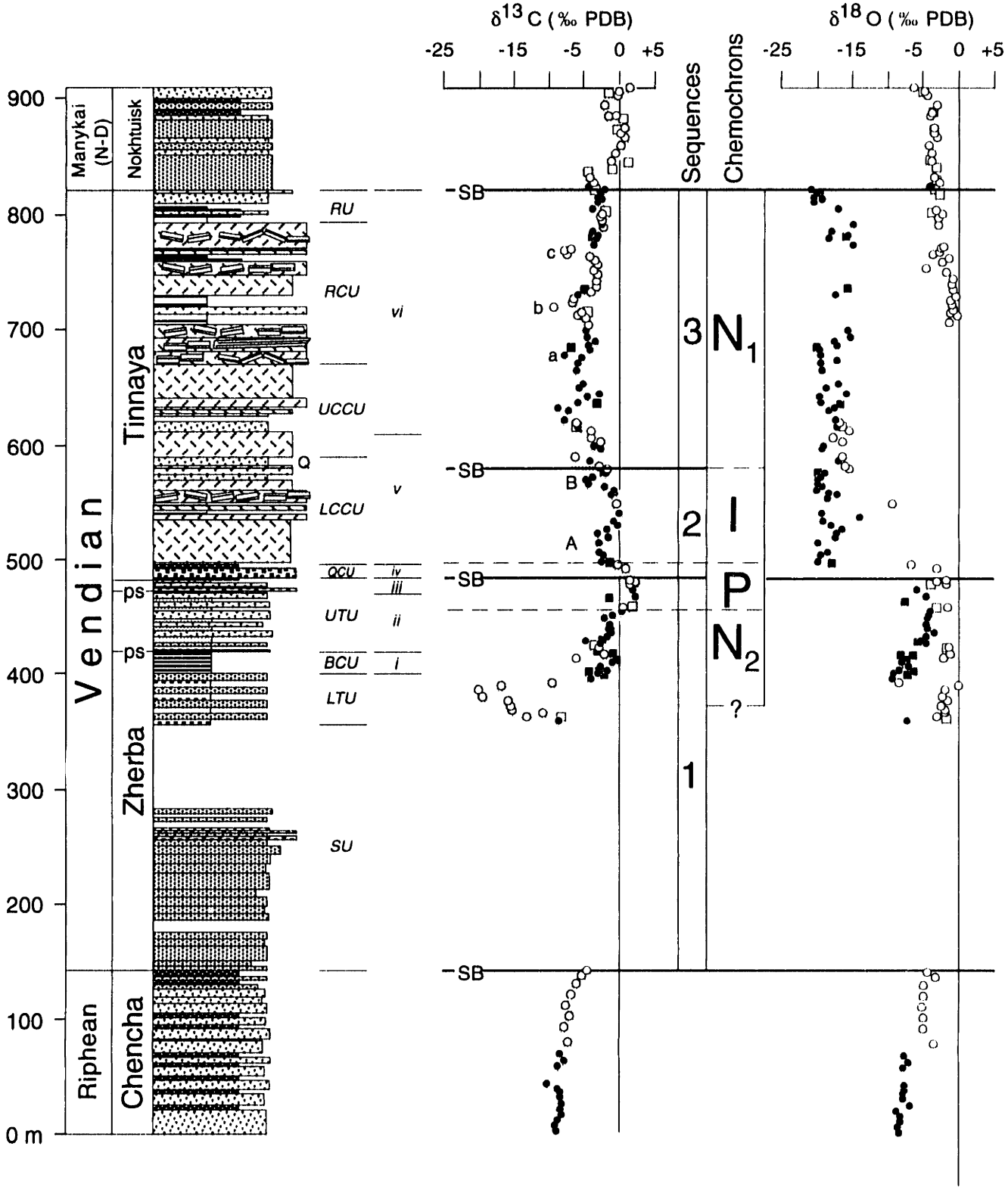
δ13 C (‰ PDB)
-25 -15 -5 0 +5
δ18 O (‰ PDB)
-25 -15 -5 0 +5
Sequences
Chemochrons
900
800
700
600
500
400
300
200
100
0 m
Manykai (N-D)
Nokhtuisk
Vendian
Tinnaya
Zherba
Riphean
Chencha
RU
RCU
UCCU
Q
LCCU
QCU
ps
UTU
ps
BCU
LTU
SU
vi
v
iv
iii
ii
i
SB
SB
SB
c
b
a
B
A
3
2
1
N1
I
P
N2
?

Figure 5.10

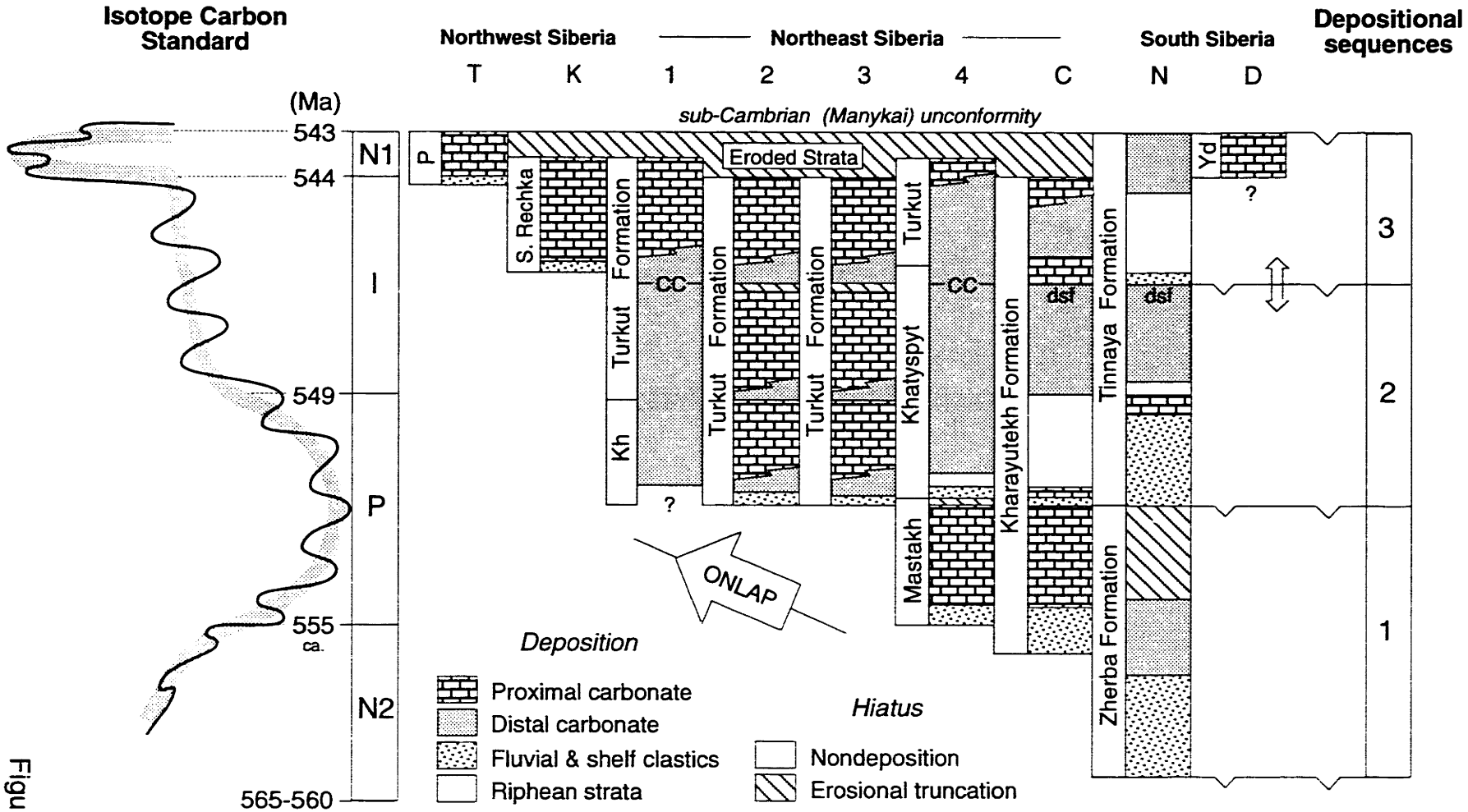
Isotope Carbon Standard
(Ma)
543
544
549
555
ca.
565-560
N1
I
P
N2
Northwest Siberia
Northeast Siberia
South Siberia
T
K
1
2
3
4
C
N
D
Depositional sequences
sub-Cambrian (Manykai) unconformity
Eroded Strata
P
S. Rechka
Turkut Formation
Kh
Turkut
Khatyspyt
Mastakh
CC
?
ONLAP
Kharayutekh Formation
dsf
Tinnaya Formation
Yd
Zherba Formation
3
2
1
Deposition
Proximal carbonate
Distal carbonate
Fluvial & shelf clastics
Riphean strata
Hiatus
Nondeposition
Erosional truncation

Figure 5.11

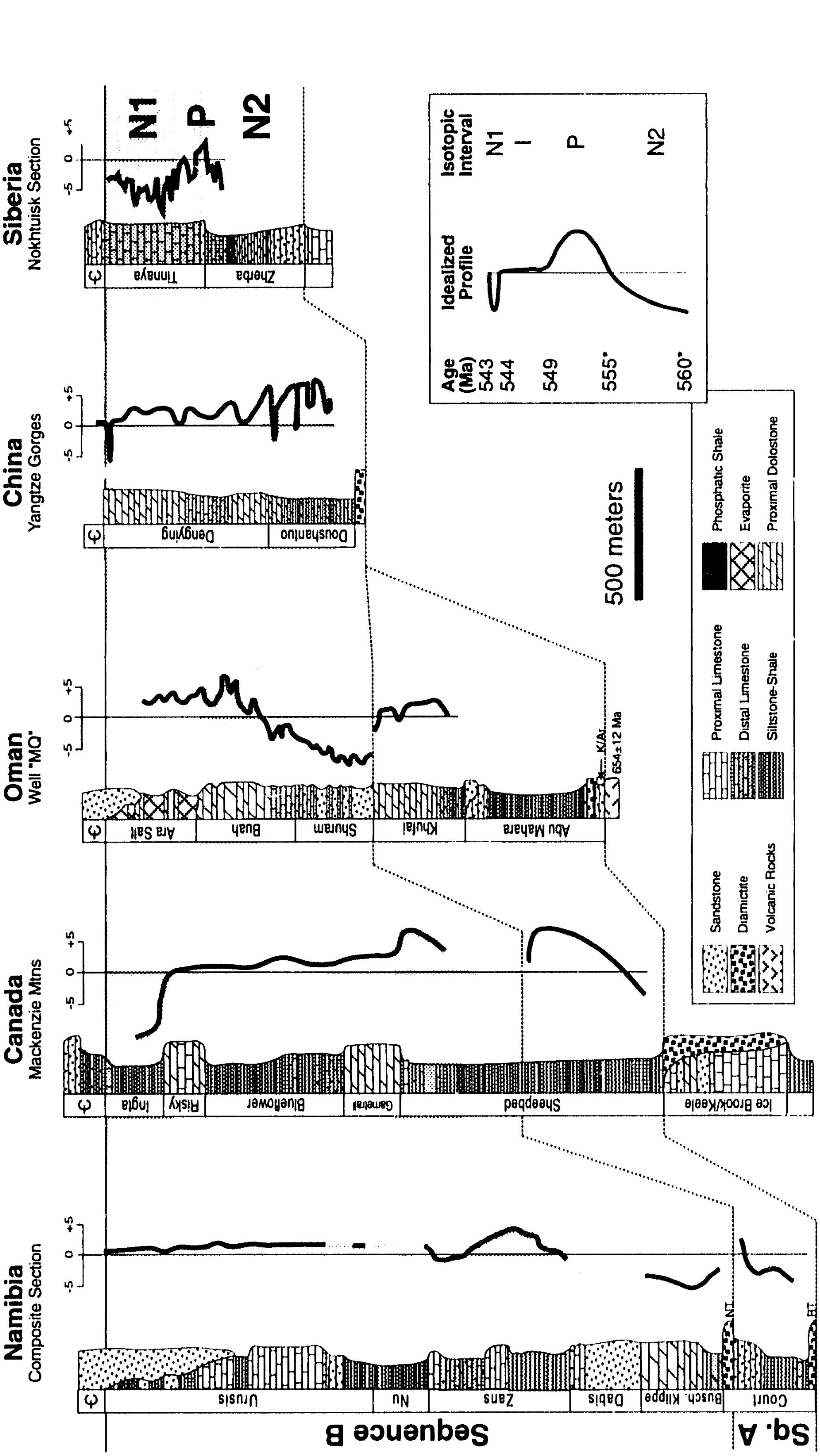
Namibia
Composite Section
Canada
Mackenzie Mtns
Oman
Well "MQ"
China
Yangtze Gorges
Siberia
Nokhtuisk Section
Sequence B
Sq. A
N1
P
N2
Age (Ma)
Idealized Profile
Isotopic Interval
500 meters
Sandstone
Diamictite
Volcanic Rocks
Proximal Limestone
Distal Limestone
Siltstone-Shale
Phosphatic Shale
Evaporite
Proximal Dolostone

Figure 5.12

Chapter 6

Architecture of a Vendian-to-Cambrian-Age Giant Oil Field (Olenek Uplift) in Northern Siberia

ABSTRACT

The Olenek uplift of northeast Siberia represents an exhumed giant oil field with nearly 2 billion m^3 of in-place reserves in reservoirs that straddle a major paleokarst along the Vendian-Cambrian boundary. This occurrence, together with additional surface accumulations of bitumen across northern Siberia from the Lena River to the Anabar shield define the Lena-Anabar petroleum province. The paleokarst separates Vendian-age platform carbonates and Early Cambrian-age siliciclastic shelf deposits and reflects regional rift-related uplift across the northern margin of the Siberian craton in response to separation of Siberia and Laurentia in the Early Cambrian. Reservoir development was strongly influenced by local variations in karst erosion and depositional facies. The major petroleum reservoirs are represented by karsted and fractured Vendian shallow platform carbonates. Bitumen associated with these reservoirs is sourced from the Vendian Khatyspyt Formation - a succession of bituminous distal ramp limestones that occur downdip of the reservoirs.

The Lena-Anabar province, illustrated by the Olenek field, represents one of several petroleum provinces of this age: the Lena-Tunguska province of southern Siberia; the Sichuan basin of China; and, most notably, the "Infracambrian" basins of the Arabian shield in the Middle East, Pakistan and northern India. Collectively, these basins record wide-spread accumulation of organic-rich sediments and are considered to represent a distinct petroleum system analogous to the petroleum systems of the Phanerozoic record.

INTRODUCTION

Hydrocarbons occur throughout the Proterozoic record (Murray 1965; Becker and Patton 1968; Trofimuk, et al. 1968; Meyeroff 1980; Edgell 1991; Hieshima and Pratt 1991; Jackson and Raiswell 1991; Korsch, et al. 1991; Surkov, et al. 1991) but the most significant discoveries have been made in terminal Neoproterozoic basins (ca.

600 to 543 Ma). The most notable of these basins is represented by the "Infracambrian" Huqf Group of Oman and its correlative strata across the Middle East, Pakistan and northern India. These Middle East basins contain rich petroleum source rocks that have generated significant quantities of oil and gas (Al-Marjeby and Nash 1986; Grantham, et al. 1987; 1990; Hughes Clarke 1988; Husseini 1988; Edgell 1991; Peters, et al. 1995). Other significant terminal Neoproterozoic petroliferous basins are represented by the Lena-Tunguska province in southern Siberia (Fig. 6.1; Trofimuk, et al. 1968; Meyeroff 1980a; 1980b; Kontorovich, et al. 1990) and the Sichuan basin of China (Korsch, et al. 1991).

The Olenek uplift in northeast Siberia represents a giant oil field with an estimated 10^{11} m^3 of in-place bitumen (Figs. 6.1 and 6.2; North 1990; Kashirtsev, et al. 1993) in Vendian, Cambrian, and Permian reservoirs. The major source rocks for this bitumen includes the Vendian-age Khatyspyt Formation and correlative strata of northeast Siberia (Kashirtsev 1994). Bitumen derived from Vendian-age source rocks and emplaced in Vendian and Cambrian reservoirs occurs throughout northern Siberia, including the Kharaulakh Mountains near the mouth of the Lena River and on the east flank of the Anabar shield in northwest Siberia (Fig. 6.1; Kashirtsev 1994; Pelechaty, pers. observ.). This region of northern Siberia, herein referred to as the Lena-Anabar province, represents a largely unexplored petroliferous basin with surface evidence for extensive generation and entrapment of hydrocarbons derived from Vendian limestones.

This paper investigates another example of a terminal Neoproterozoic petroleum province with a case study of the Vendian-Cambrian petroleum geology of the Olenek field. The distribution of petroleum reservoirs and source rocks of this region are examined in a regional stratigraphic and tectonic framework established by other studies (Knoll, et al. 1995; Pelechaty 1996; Pelechaty, et al. 1996a; 1996b). This study emphasizes the influence of regional tectonism and local facies on the development of this petroleum province. The chronostratigraphy for this region is based on integrated

carbon isotope chemostratigraphy, sequence stratigraphy and biostratigraphy. It provides a framework for high-resolution correlation of the Vendian carbonates, and is herein highlighted for its utility in regional basin analysis and petroleum geology (e.g. evaluating lateral continuity and quality of subsurface reservoirs across a basin).

REGIONAL GEOLOGY

The following section provides a brief overview of the regional stratigraphic and tectonic framework for the Vendian-Cambrian petroleum geology of the Olenek uplift and adjacent areas.

Stratigraphy

In northern Siberia, Vendian-age rocks are represented by less than 500 m of carbonates and rare siliciclastic deposits. Vendian strata include the Khorbosuonka Group in the Olenek uplift area and the Kharayutekh Formation in the Kharaulakh Mountains (Fig. 6.2). Vendian strata of northern Siberia rest with angular unconformity on older Proterozoic rocks and are in turn overlain by Cambrian deposits along a major paleokarst (Fig. 6.3). In northeast Siberia, the Vendian carbonates thicken and depositional facies deepen towards the east along a regional platform-to-basin transition (Figs. 6.3 and 6.4). Early Cambrian (Nemakit-Daldyn stage) rocks overlying the karst consist of mixed siliciclastic shelf sediments with minor marine carbonates and volcanic rocks, which form a depositional sequence up to 100 m thick. The Nemakit-Daldyn shelf sequence is unconformably overlain by nearly 800 m of Early (Tommotian and younger) and Middle Cambrian open marine limestones, which are in turn overlain by Permian sedimentary deposits.

Tectonic Evolution

The Vendian and Cambrian deposits of northern Siberia record two major tectonic events (Fig. 6.3): Vendian-age passive margin development along the eastern edge of the Siberian craton and Early Cambrian continental extension along the northern edge of the craton (Pelechaty 1996; Pelechaty, et al. 1996b). The Vendian-age passive margin is considered to post-date an episode of Neoproterozoic-age rifting at about 720 Ma (Zonenshain, et al. 1990; Condie and Rosen 1994; Pelechaty 1996) along the eastern margin of the craton from the Kharaulakh Mountains to the east flank of the Aldan shield in the south (Fig. 6.1). A relative highstand in sea level at the close of Vendian time culminated in marine flooding and onlap of a thin succession of platform carbonates across the northern craton (Khomentovsky 1986).

The post-Vendian record, including the sub-Cambrian paleokarst and overlying Cambrian deposits record an episode of continental extension along the northern margin of the Siberian craton (Fig. 6.3). On the basis of regional carbon isotope chemostratigraphy of the Vendian carbonates, rift-related uplift and erosion of the Vendian carbonates was restricted to the northern edge of the craton and is attributed to the development of a broad rift-shoulder from 543 Ma and 530 Ma, prior to the onset of post-rift thermal subsidence (Pelechaty, et al. 1996b). This uplift influenced the regional extent of karstification and subsequent development of Vendian reservoirs throughout northern Siberia. Continental extension is marked by the influx of Early Cambrian (Nemakit-Daldyn) clastics from the north over the paleokarst landscape and synchronous bimodal volcanism in the Olenek uplift and Kharaulakh Mountains areas. The northward truncation of the Nemakit-Daldyn shelf sequence illustrates that uplift continued until ca. 530 Ma. Tommotian and younger age limestones record southward onlap of the craton onto the exposed Nemakit-Daldyn shelf sequence and a return to quiescent depositional conditions, which is considered to mark the onset of post-rift

differential subsidence in northern Siberia (Pelechaty, et al. 1996b). The evidence of continental extension in northern Siberia is attributed to the separation of Siberia and Laurentia during final breakup of Rodinia (Pelechaty 1996).

The major petroleum reservoirs in northern Siberia are developed along the sub-Cambrian and the sub-Tommotian unconformities (Fig. 6.3). The regional distribution of these reservoirs reflect the tectonic history of the northern Siberian basin: the regional distribution of Vendian-age karsted reservoirs across the north coincides with the aerial extent of the Early Cambrian rift shoulder. In the following sections, we focus on the Vendian-Cambrian petroleum geology of the Olenek field. Reservoir quality is shown to be influenced by variation in the depth of erosion along the sub-Cambrian paleokarst and depositional facies that occur above and below the karst.

PETROLEUM GEOLOGY OF THE OLENEK FIELD

Integrated Chronostratigraphy

The Olenek uplift is approximately 8,000 km^2 in area. Vendian and Early Cambrian strata crop out and dip gently (< 5° dip) along the periphery of the uplift, which is cored by older Proterozoic (Riphean) sedimentary rocks and Archean crystalline basement (Fig. 6.2). Permian strata unconformably overlie these deposits cutting down section across the uplift to the east where they rest directly on Archean basement rocks. The uplift has been episodically exposed since Riphean time but final uplift, erosion and breaching of the Olenek field was probably Cretaceous in age, coincident with development of the Verkoyansk fold belt. Vendian strata crop out along several rivers that incise the Olenek uplift, including the Olenek River on its west flank, the Khorbosuonka River to the north, and the Kytyngeder and Oolakhan Ooektekh rivers on the south flank of the uplift. Vendian and Cambrian strata also crop out in the

Kharaulakh Mountains to the east on the steeply dipping limbs of large-scale anticlines of the Verkoyansk fold belt (Fig. 6.2).

Correlation of the Vendian carbonates is based on integrated sequence stratigraphy and carbon isotope chemostratigraphy of several stratigraphic sections (Knoll, et al. 1995; Pelechaty, et al. 1996a; 1996b), which are positioned throughout the basin nearly parallel to the platform-to-basin transition (Fig. 6.4). The Khorbosuonka Group reveals carbon isotope anomalies that compare well with the calibrated global standard for latest Neoproterozoic time (see Inset of Fig. 6.4; Knoll and Walter 1992; Bowring, et al. 1993; Grotzinger, et al. 1995). The carbonates reveal three major carbon isotope events that span the latest 10 m.y. of Vendian time (i.e. section 4 of Fig. 6.4): a lower positive excursion (P interval), an interval of moderately positive values (I interval) and a prominent negative excursion at the Vendian-Cambrian boundary (N1 interval). Recognition of these isotopic shifts throughout the basin forms the basis for intrabasinal chemostratigraphy (Pelechaty, et al. 1996a). Three chemochrons are traced between the stratigraphic sections: chemochron 1 corresponds to the maxima of the P interval; chemochron 2 marks the top of the P interval; and chemochron 3 marks the base of the N1 interval.

The carbonates also are partitioned into three major depositional sequences dominated by platform carbonates with minor transgressive clastics at the bases of sequences 1 and 2 (Fig. 6.4). The carbonates formed east-facing ramps with shallow water facies in the Olenek area and their distal components located to the east. The loci of shallow water deposition shifted eastward only during lowstands in relative sea level as shown by the lowstand wedge at the base of sequence 3 in the Kharaulakh Mountains. Together, the sequence boundaries and chemochrons divide the Vendian System of northeast Siberia into 1 to 3 m.y. time slices (see Inset of Fig. 6.4).

The chemochrons aid in constraining the geometry of inter-sequence strata (Fig. 6.4). For instance, chemochron 1 at the base of sequence 1 illustrates onlap of strata to

the west during initial flooding of the craton. Chemochron 2 indicates downlap of distal ramp facies to the east onto transgressive clastics at the base of sequence 2. The truncation of chemochron 3 along the sub-Cambrian paleokarst surface topping sequence 3 indicates variation in the depth of erosion, which is shown below to aid in evaluating reservoir quality and continuity across the basin. The variation in stratigraphic separation of chemochrons 2 and 3 illustrates enhanced basin subsidence along the platform-to-basin transition.

Carbonate Platform Architecture

The architecture of the Khorbosuonka ramps appears to have greatly influenced the quality and distribution of potential petroleum reservoir and source rocks in the basin. The Khorbosuonka Group carbonates form extensive ramp platforms analogous to the carbonate ramps of the Phanerozoic (Read 1985) and Proterozoic (Grotzinger 1989) records.

The Khorbosuonka carbonates form low-relief homoclinal ramps composed of four major depositional facies (Fig. 6.5). They include, in an off-ramp direction, tidal flat, lagoon, shoal and distal ramp facies. The salient characteristics of these facies are taken from detailed descriptions given elsewhere (Knoll, et al. 1995; Pelechaty, et al. 1996b). Shallow ramp deposits (i.e. tidal flat, lagoon and shoal) commonly are dolomitic whereas distal ramp carbonates are represented as limestones. Tidal flat dolostones consist of thinly bedded, desiccation-cracked biolaminites and mudstones, and rippled oolitic and intraclastic sands (i.e. packstones and grainstones). The lagoon facies is dominated by low-relief domal stromatolites and lesser accumulations of carbonate mud, sand and gravel that drape stromatolitic topography. Further basinward, the shoal facies is represented by medium to thick bedded packstones, grainstones and rudstones. These clastic deposits are variably laminated, current rippled and trough cross-

stratified illustrating the high energy depositional nature of this facies. These deposits, as well as the grainy carbonates of the tidal flat and lagoon facies, are composed mainly of intraclastic and oncolitic grains; they form the main Vendian reservoirs of the Olenek field and across the Lena-Anabar province. Black bituminous limestones basinward of the shoals represent accumulation of sediments below storm wave base on the distal part of the ramp. These organic-rich deposits are considered to be one of the main source rock intervals in Siberia (Chersky 1986; Bolshakov 1987; Kashirtsev, et al. 1993; Kashirtsev 1994).

Reservoir Development

Distribution

The major reservoir horizons within the basin are associated with sequence boundaries (Fig. 6.4). Vendian reservoirs are developed at the top of sequence 2 in the southern Olenek uplift, at the top of sequence 3 beneath the sub-Cambrian paleokarst across the Olenek field (Fig. 6.6a), the Kharaulakh Mountains (Figs. 6.4 and 6.7), and on the east flank of the Anabar shield (Fig. 6.1; Kashirtsev 1994). The Cambrian reservoirs occur in conglomerates, sandstones and rare carbonates at the base and, locally at the top of the Nemakit-Daldyn shelf sequence. The main reservoir interval in northeast Siberia straddles the sub-Cambrian paleokarst and is described below.

Three main reservoir types are recognized: karst, fracture and siliciclastic (Figs. 6.7 and 6.8). Their distribution across the Olenek uplift and Kharaulakh Mountains is controlled by facies and their stratigraphic position relative to the sub-Cambrian paleokarst. The best developed reservoirs are represented by Vendian-age karsted shoal carbonates and clastic carbonates associated with adjacent lagoon and tidal flat facies (Figs. 6.6b to 6.6d). Locally, karst dissolution accentuates stromatolitic lamination (Fig. 6.6e). Fracture porosity is commonly associated with dolomudstones of

the tidal flat and lagoon facies (Fig. 6.6f). Solid bitumen lines fractures as well as some bedding planes and stromatolitic laminae similar to that described in the Ara Formation of the upper Huqf Group in Oman (Hughes Clarke 1988). In northeast Siberia, the fractures are oriented vertically and are 10's of cm's in length. Extensive fracture networks occur over many 10's of meters beneath the sub-Cambrian paleokarst. The importance of this fracture system in terms of its effectively porosity is difficult to determine; however, such fracture systems represent significant reservoirs in the Weiguan gas field in China (Korsch, et al. 1991) and in the Berezov and Prepatom troughs of southern Siberia (Kashirtsev, pers. comm. 1996). Additional reservoirs are represented by the Early Cambrian conglomerates and sandstones that drape and infill the sub-Cambrian paleokarst surface. The conglomerates and sandstones are black in outcrop because bitumen occludes up to 5 to 20% porosity associated with this facies.

Figures 6.5 and 6.6 summarize the distribution of bitumen along the sub-Cambrian paleokarst. The karst reservoirs correspond to occurrences of bitumen found in grainstones and rudstones of the shoal facies and thin beds of grainy carbonates developed in the lagoon and tidal flat facies (i.e. Fig. 6.6d); the fractured dolostones correspond to bitumen developed in the lagoon facies (i.e. Fig. 6.6f); and the siliciclastic reservoirs occur at the base of the Cambrian sequence and in caves that cut the Vendian carbonates. The tidal flat carbonates at the top of section 2 are dominated by grainstones with karstic porosity. On the basis of field studies, bitumen occurs over relatively thick stratigraphic intervals above and below the karst at every section throughout the Olenek uplift and Kharaulakh Mountains. Bitumen occurs in porous carbonates up to 40 m below the paleokarst and in conglomerates and sandstones for up to 5 m above the karst. In general, bitumen is associated primarily with Vendian-age fractured dolostones across the Olenek field but the most significant Vendian reservoirs are represented by the karsted shoal facies gravels (i.e. rudstones) in the Kharaulakh Mountains (Fig. 6.6d).

Nature of Karst Reservoirs

Karst-related dissolution of the Vendian platform carbonates is facies specific being most prevalent in the clastic carbonates (i.e. rudstones and grainstones) belonging to the tidal flat, lagoon, and primarily shoal facies. Within these carbonates, the karst-related porosity is fabric-selective (Fig. 6.9). Microscopically, these deposits are composed of sand- and gravel-size intraclasts and oncoliths. The intraclasts are rip-up clasts of dolomudstones whereas oncoliths are accretionary particles represented as simple coated intraclasts and grapestones (Fig. 6.9a). The rims of these grains consist of finely laminated micritic carbonate similar to oncolitic sediments found in other basins (Peryt 1983). The matrix for this sediment consists of micritic sediment/cement and finely crystalline spar. The most pronounced aspect of the karst porosity is the selective dissolution of the intraclasts. The oncolitic coatings, however, remain intact and reveal no evidence of meteoric corrosion (Figs. 6.6d and 6.9b).

Several lines of evidence suggest that the fabric-selective porosity in these rocks is related to the original mineralogy of the sediment. The mudstones, especially those composed of limestone, and intraclasts contain high concentrations of total strontium (200 to 2500 ppm) whereas the oncolitic rims and other stromatolitic deposits composed of limestone are depleted in total strontium (<200 ppm; Pelechaty, et al. 1996a). The variable strontium composition and preferential dissolution of the intraclastic grains suggest that the shoal facies sediments were originally bimineralic (Davis 1977; James and Choquette 1984; Aissaoui 1985; Tucker 1986); the intraclasts were most likely aragonite and the stromatolitic carbonates where probably originally composed of calcite.

Subsequent diagenesis of these sediments led to slight reduction of the original karstic porosity (Figs. 6.9c and 6.9d). Several stages of cementation and partial occlusion of karst porosity are represented, including early-stage precipitation of vadose pendant cements and phreatic, isopachous cements, and late-stage deposition of

coarse baroque dolospar (Fig. 6.6d). Additional diagenetic alteration is marked by local compaction of grains (Fig. 6.9c), and formation of stylolites and fractures. The remaining porosity was later occluded by black bitumen (Figs. 6.6d and 6.9d). The rims of the baroque dolomite crystals tend to be etched where they occur adjacent to pore-filling bitumen, indicating that liquid oil probably migrated into these reservoirs following burial diagenesis of the carbonates.

Predicting Lateral Continuity of Karst Reservoirs

The most spectacular karstic porosity is developed within the shoal facies gravel deposits (i.e. oncolitic rudstones) at the top of section 5 in the Kharaulakh Mountains (Figs. 6.6d and 6.7). Here, rudstones in the upper 20 m of the Kharayutekh Formation exhibit an average of 10% porosity but includes nearly 5 m of section, represented by scatter 1 to 2 m thick beds through the upper part of the formation with 30 to 50% bitumen-occluded porosity. Similar carbonate gravels in the Olenek uplift occur at sections 1 and 4 on the northern flank of the Olenek uplift (Figs. 6.2, 6.6d and 6.7) but these gravel deposits are completely cemented and do not reveal evidence of meteoric diagenesis and associated porosity development. Karsted grainy carbonates in the Olenek area occur as thin beds intercalated with other carbonates of the tidal flat and lagoon facies. Throughout the Olenek uplift, the thicker intervals of shoal gravels and sands are overlain by lagoon facies carbonates, which consist of tight stromatolitic and muddy dolostones. The occurrence of lagoon carbonates between the karst and the tight shoal carbonates across the field suggests that they likely were an aquitard preventing downward percolation of corrosive rain water during karst formation.

Regional chemostratigraphy provides insight into the lateral continuity of the various Vendian reservoir types across the basin and enables prediction of the subsurface reservoir quality between the Olenek field and Kharaulakh Mountains. Regional mapping of chemochron 3 shows that the karst cuts deeper into Vendian

stratigraphy from sections 1 to 5 (Fig. 6.7), suggesting that the lagoon dolostones become truncated from the Olenek uplift to the Kharaulakh Mountains. This observation further implies that subsurface shoal gravels east of the Olenek outcrop belt may occur in closer proximity to the sub-Cambrian karst and exhibit significant karst-related porosity similar to the porous shoal carbonates of the Kharaulakh Mountains, which are situated directly under the sub-Cambrian karst.

Estimated In-place Vendian-Cambrian Reserves

The Olenek uplift represents a *giant* oil field with estimated in-place reserves of 100 billion m^3 of bitumen in Vendian, Early Cambrian and Permian reservoirs (North 1990; Kashirtsev 1994). The in-place reserves for only the Vendian-Cambrian reservoirs are determined using reservoir parameters (e.g. reservoir area, thickness, porosity) based on field observations from this study. The minimum aerial extent of the field is taken as the present-day distribution of Vendian outcrops across the Olenek uplift. Because of limited subsurface geologic data for this study, the calculation does not take into account the subsurface resources contained updip of the spill point for the Olenek anticline. On the basis of a minimum reservoir thickness of 10 m, reservoir porosity of 10%, and water saturation of 25%, the Vendian-Cambrian reservoirs are estimated to contain minimum in-place reserves of 2 billion m^3 of bitumen, indicating that the Vendian-Cambrian level of the Olenek field alone constitutes a giant-size field (North 1990).

Vendian Source Rocks

The Khorbosuonka Group ramps are associated with superb petroleum source rocks, which occur downdip of the fractured and karsted shallow ramp carbonates (Fig. 6.4). The Khatyspyt Formation is represented by distal ramp facies at section 4 and parts of the Kharayutekh Formation at section 5, and together, represent nearly 180 m

of organic-rich limestones that accumulated across the northeast Siberian basin. These limestones have been extensively studied for their petroleum source rock potential (Chersky 1986; Bolshakov 1987; Fowler and Douglas 1987; Kashirtsev, et al. 1993; Kashirtsev 1994) and are considered to represent one of several major source rock intervals for the enormous bitumen reserves of the Olenek field and adjacent regions (Kashirtsev 1994). Apart from the Vendian source rocks, bitumen found at higher stratigraphic levels in the Olenek field are considered to have been sourced from several Cambrian-age source rocks, including oil shales of the Middle Cambrian Kynomka Formation (Kashirtsev 1994). On the basis of comparative organic geochemistry, the Vendian-age black limestones are considered to be the source of bitumen in the Vendian and Early Cambrian reservoirs (Kashirtsev, et al. 1993; Kashirtsev 1994). Thermal alteration studies of Permian coals on the north flank of the Olenek uplift also indicate that the Vendian limestones were not deeply buried and thus represent mature source rocks that experienced minimal thermal alteration conducive for hydrocarbon generation (Kontorovich, et al. 1995). These limestones emit a strong fetid odor when struck with a hammer reflecting high abundance of sedimentary organic matter within these rocks. The Khatyspyt and Kharayutekh limestones contain an average of 2% total organic carbon (TOC) and locally contain up to 11% TOC (Klubov 1983; Kashirtsev, et al. 1993; Knoll, et al. 1995). Isotopically, the organic matter ranges between -29 and -34.5‰ $\delta^{13}C$ with an average composition of -30‰ (Kashirtsev 1994; Knoll, et al. 1995) similar to other terminal Neoproterozoic source rocks and oils in the Middle East and China (Korsch, et al. 1991; Peters, et al. 1995).

DISCUSSION

The Olenek oil field symbolizes the vast hydrocarbon potential for latest Neoproterozoic sedimentary basins. The Siberian platform alone contains three major

petroleum provinces (see Fig. 6.1) and has long been recognized as a significant region for Neoproterozoic hydrocarbons since the discovery of oil and gas in the Lena-Tunguska province of southwest Siberia (Trofimuk, et al. 1968; Meyeroff 1980a; 1980b; Kontorovich, et al. 1990). Potential in-place reserves for the Lena-Tunguska province have been estimated to include 60 billion m^3 of oil and 6 trillion m^3 of gas within Riphean and Vendian molasse deposits (Kontorovich, et al. 1990). The Berezov and Predpatom troughs on the Lena River in southern Siberia represent a third petroleum province and is characterized by Neoproterozoic petroleum trapped within paraautochthonous Vendian and Cambrian strata along the leading edge of the Predpatom fold belt.

Outside of Siberia, the "Infracambrian" Huqf Group of the Sultanate of Oman represents the most notable and economically significant Neoproterozoic petroleum province. It contains rich oil-prone source rocks that have generated enormous reserves now trapped in Precambrian and Phanerozoic structures throughout Oman (Al-Marjeby and Nash 1986; Grantham, et al. 1987; Hughes Clarke 1988; Grantham, et al. 1990). Source rocks of this age also occur throughout the Middle East, Pakistan and northern India within numerous fault-bounded basins that developed at this time (Husseini 1988; Edgell 1991; Peters, et al. 1995). The Sichuan basin in China represents yet another Neoproterozoic petroleum province. Over 60 gas fields and 10 oil fields have been discovered in this basin, including the Weiyuan Gas field, which has produced over 13.6 billion m^3 of gas since 1987 (Korsch, et al. 1991).

Major source rocks of terminal Neoproterozoic age include the Khatyspyt Formation and correlative limestones of the Siberian craton (Kashirtsev, et al. 1993; Kashirtsev 1994; Kontorovitch, et al. 1995); the Shuram, Buah and Ara formations of Oman and their counterparts throughout the Middle East (Grantham, et al. 1987; Peters, et al. 1995); and the Dengying Formation of the Sichuan basin (Korsch, et al. 1991).

Many factors were probably conducive for the wide-spread accumulation of petroleum source rocks during terminal Neoproterozoic time. (1) The terminal Neoproterozoic period is marked by dramatic changes in climate associated with multiple episodes of growth and retreat of polar ice caps (Saylor 1996; Kaufman, et al. in review; Saylor, et al. in review), which greatly affected ocean over-turn and the development of anoxic ocean basins (Grotzinger and Knoll 1995; Knoll, et al. 1996). (2) The major petroleum provinces of this age are associated with cratons that were located at low latitudes close to the paleoequator (Khramov, et al. 1981; Husseini 1989; Kirschvink, et al. 1991; McKerrow, et al. 1992; Li, et al. 1995; Pelechaty 1996), and thus were sites for wide-spread accumulation of tropical marine carbonates and evaporites associated with warm, moist climates conducive for sustaining high rates of organic productivity. Furthermore, the margins of these low-latitude cratons may have been sites of upwelling induced to wind-shear. (3) The breakup of Rodinia during the Neoproterozoic (Bond, et al. 1984; Hoffman 1991; Moores 1991; Dalziel 1992), coupled with highstands in sea level led to accumulation of thick organic-rich sediments over broad cratonal regions, such as the Vendian bituminous limestones of eastern Siberia. (4) While many Neoproterozoic basins contain organic-rich sediments (i.e. Nama basin of Namibia; Saylor 1996), the presence of Neoproterozoic hydrocarbon reserves in basins of Siberia, the Middle East and China reflects their unique post-depositional thermal history. Significantly, all three areas share an incomplete Phanerozoic stratigraphic record, which prevented these Neoproterozoic successions from being deeply buried and thermally altered (Visser 1991; Korsch, et al. 1991).

The growing number of terminal Neoproterozoic petroleum basins world wide underscores the importance of this period in Earth's history for preservation of wide-spread organic-rich sediments. The Phanerozoic record of petroleum source rocks is characterized by only six major stratigraphic intervals that account for the majority (90%) of the world's discovered oil and gas (Klemme and Ulmishek 1991). The

terminal Neoproterozoic period is recognized to contain several significant source rocks of the same age, and collectively, support the notion that this period may be regarded as the seventh petroleum system.

REFERENCES

Aissaoui, D.M., 1985, Botryoidal aragonite and its diagenesis: Sedimentology, v. 32, p. 345-362.

Al-Marjeby, A. and Nash, D., 1986, A summary of the geology and oil habitat of the Eastern Flank Petroleum Province of south Oman: Marine and Petroleum Geology, v. 3, p. 306-314.

Becker, L.E. and Patton, J.B., 1968, World occurrence of petroleum in pre-Silurian rocks: American Association of Petroleum Geologists Bulletin, v. 52, p. 224-245.

Bond, G.C., Nickeson, P.A. and Kominz, M.A., 1984, Breakup of a supercontinent between 625 Ma and 555 Ma: new evidence and implications for continental histories: Earth and Planetary Science Letters, v. 70, p. 325-345.

Bowring, S.A., Grotzinger, J.P., Isachsen, C.E., Knoll, A.H., Pelechaty, S.M. and Kolosov, P., 1993, Calibrating Rates of Early Cambrian Evolution: Science, v. 261, p. 1293-1298.

Condie, K.C. and Rosen, O.M., 1994, Laurentia-Siberia connection revisited: Geology, v. 22, p. 168-170.

Dalziel, I.W.D., 1992, On the organization of American Plates in the Neoproterozoic and the breakup of Laurentia: Geological Society of America Today, v. 2, p. 237, 240-241.

Davis, G.R., 1977, Former magnesium calcite and aragonite submarine cements in Upper Paleozoic reefs of the Canadian Arctic: a summary: Geology, v. 5, p. 11-15.

Edgell, H.S., 1991, Proterozoic salt basins of the Persian Gulf area and their role in hydrocarbon generation: Precambrian Research, v. 54, p. 1-14.

Fowler, M.G. and Douglas, A.G., 1987, Saturated hydrocarbon biomarkers in oils of late Precambrian age from eastern Siberia: Organic Geochemistry, v. 11, p. 201-213.

Grantham, P.J., Ligmback, G.W.M. and Posthuma, J., 1990, Geochemistry of crude oils in Oman, *in* J. Brooks, ed., Classic Petroleum Provinces: Geological Society Special Publication, 50, p. 317-328.

Grantham, P.J., Lijmback, G.W.M., Posthuma, J., Hughes Clark, M.W. and Willink, R.J., 1987, Origin of crude oils in Oman: Journal of Petroleum Geology, v. 11, p. 61-80.

Grotzinger, J.P., 1989, Facies and evolution of Precambrian carbonate depositional systems: Emergence of the modern platform archetype, *in* ed., Controls on Carbonate Platform and Basin Development: SEPM Special Publ., 44, p. 79-106.

Grotzinger, J.P., Bowring, S.A., Saylor, B.Z. and Kaufman, A.J., 1995, Biostratigraphic and geochronological constraints on early animal evolution: Science, v. 270, p. 598-604.

Grotzinger, J.P. and Knoll, A.H., 1995, Anomalous carbonate precipitates: Is the Precambrian the Key to the Permian: Palios, v. 10, p. 578-596.

Hieshima, G.B. and Pratt, L.M., 1991, Sulfur/carbon ratios and extractable organic matter of the Middle Proterozoic Nonesuch Formation, North American midcontinent rift: Precambrian Research, v. 54, p. 65-79.

Hoffman, P.H., 1991, Did the breakout of Laurentia turn Gondwanaland inside out?: Science, v. 252, p. 1409-1413.

Hughes Clarke, M.W., 1988, Stratigraphy and rock unit nomenclature in the oil-producing area of interior Oman: Journal of Petroleum Geology, v. 11, p. 5-60.

Husseini, M.I., 1988, The Arabian Infracambrian extensional system: Tectonophysics, v. 148, p. 93-103.

Husseini, M.I., 1989, Tectonic and depositional model of late Precambrian-Cambrian Arabian and adjoining plates: American Association of Petroleum Geologists Bulletin, v. 73, p. 1117-1131.

Jackson, M.J. and Raiswell, R., 1991, Sedimentology and carbon-sulfur geochemistry of the Velkerri Formation, a mid-Proterozoic potential oil source in northern Australia: Precambrian Research, v. 54, p. 81-108.

James, N.P. and Choquette, P.W., 1984, Diagenesis 9. Limestones - the meteoric diagenetic environment: Geoscience Canada, v. 11, p. 161-194.

Kashirtsev, V.A., 1994, Natural bitumen and bituminous deposits of the northeastern Siberian platform, Novosibersk, Russian Academy of Sciences, 35 p.

Kashirtsev, V.A., Philp, R.P., Allen, J., Galvec-Senebalde, A., Zyeba, E.N., Chalaya, O.H. and Andreev, E.N., 1993, Biodegradation of bitumen within bituminous rocks of the Olenek uplift: Geology and Geophysics, v. 34, p. 44-54 (in Russian).

Kaufman, A.J., Knoll, A.H. and Narbonne, G.M., in review, Isotopes, ice ages and terminal Proterozoic Earth history: Nature, v. p.

Khomentovsky, V.V., 1986, The Vendian System of Siberia and a standard stratigraphic scale: Geological Magazine, v. 123, p. 333-348.

Khramov, A.N., Petrova, G.N. and Pechersky, D.M., 1981, Paleomagnetism of the Soviet Union, M. W. McElhinny and D. A. Valencio]: AGU Geodynamics Series, 2, 177-194 p.

Kirschvink, J.L., Magaritz, M., Ripperdan, R.L., Zhuravlev, A.Y. and Rozanov, A.Y., 1991, The Precambrian-Cambrian boundary: Magnetostratigraphy and carbon isotopes resolve correlation problems between Siberia, Morocco, and south China: GSA Today, v. 1, p. 69-91.

Klemme, H.D. and Ulmishek, G.F., 1991, Effective petroleum source rocks of the world: Stratigraphic distribution and controlling depositional factors: American Association of Petroleum Geologists Bulletin, v. 75, p. 1809-1851.

Klubov, B.A., 1983, Natural bitumen of the north, Moscow, Nauka, 205 p.

Knoll, A.H., Bambach, R.K., Canfield, D.E. and Grotzinger, J.P., 1996, Comparative Earth history and Late Permian Mass Extinction: Science, v. 273, p. 452-457.

Knoll, A.H., Grotzinger, J.P., Kaufman, A.J. and Kolosov, P., 1995, Integrated approaches to terminal Proterozoic stratigraphy: An example from the Olenek Uplift, northeastern Siberia: Precambrian Research, v. 73, p. 251-270.

Knoll, A.H. and Walter, M.R., 1992, Latest Proterozoic stratigraphy and Earth History: Nature, v. 356, p. 673-678.

Kontorovich, A.E., Kashirtsev, V.A. and Philp, R.P., 1995, Biohopanes in Precambrian deposits of the northeast Siberian platform: Doklady Akademia Nauk, v. 345, p. 106-110.

Kontorovich, A.E., Mandel'Baum, M.M., Surkov, V.S., Trofimuk, A.A. and Zolotov, A.N., 1990, Lena-Tunguska upper Proterozoic-Palaeozoic petroleum superprovince, *in* J. Brooks, ed., Classic Petroleum Provinces: Geological Society Special Publication, 50, p. 473-489.

Korsch, R.J., Huazhao, M., Zhaocai, S. and Gorter, J.D., 1991, The Sichuan basin, southeast China: a Late Proterozoic (Sinian) petroleum province: Precambrian Research, v. 54, p. 45-63.

Li, Z.-X., Zhang, L. and Powell, C.M., 1995, South China in Rodinia: Part of the missing link between Australia-East Antarctica and Laurentia?: Geology, v. 23, p. 407-410.

McKerrow, W.S., Scotese, C.R. and Brasier, M.D., 1992, Early Cambrian continental reconstructions: Journal of the Geological Society of London, v. 149, p. 599-606.

Meyeroff, A.A., 1980a, Geology and petroleum fields in Proterozoic and Lower Cambrian strata, Lena-Tunguska petroleum province, Eastern Siberia, USSR, *in* M. T. Halbouty, ed., Giant oil and gas fields of the decade 1968-1978: Tulsa, OK, AAPG Memoir 30, p. 225-252.

Meyeroff, A.A., 1980b, Petroleum Basins of the Soviet Union: Geological Magazine, v. 117, p. 101-210.

Moores, E.M., 1991, Southwest U.S.-East Antarctic (SWEAT) connection: A hypothesis: Geology, v. 19, p. 425-428.

Murray, G.E., 1965, Indigenous Precambrian petroleum: American Association of Petroleum Geologists Bulletin, v. 49, p. 3-21.

North, F.K., 1990, Petroleum Geology, Boston, Unwin Hyman, 631 p.

Pelechaty, S.M., 1996, Stratigraphic constraints for the Siberia-Laurentia connection and early Cambrian rifting: Geology, v. p. 719-722.

Pelechaty, S.M., Kaufman, A.J. and Grotzinger, J.P., 1996a, Evaluation of $\delta^{13}C$ isotope stratigraphy for intrabasinal correlation: Vendian strata of the Olenek uplift and Kharaulakh Mountains, Siberian platform, Russia: GSA Bulletin, v. 108, p. 992-1003.

Pelechaty, S.M., Grotzinger, J.P., Kashirtsev, V.A. and Zhernovsky, V.P., 1996b, Chemostratigraphic and sequence stratigraphic constraints on Vendian-Cambrian basin dynamics, Northeast Siberian craton: Journal of Geology, v. 104, p. 543-564.

Peryt, T.M., 1983, Classification of coated grains, *in* T. M. Peryt, ed., Coated Grains: New York, Springer-Verlag, p. 3-6.

Peters, K.E., Clark, M.E., Gupta, U.D., McCaffrey, M.A. and Lee, C.Y., 1995, Recognition of an Infracambrian source rock based on biomarkers in the Baghewala-1 oil, India: American Association of Petroleum Geologists Bulletin, v. 79, p. 1481-1494.

Read, J.F., 1985, Carbonate platform facies models: AAPG Bulletin, v. 69, p. 1-21.

Saylor, B.Z., 1996, Sequence stratigraphic and chemostratigraphic constraints on the evolution of the terminal Proterozoic to Cambrian Nama basin, Namibia [unpubl. Ph.D. thesis]: Massachusetts Institute of Technology, 215 p.

Saylor, B.Z., Kaufman, A.J., Grotzinger, J.P. and Urban, F., in review, The partitioning of terminal Neoproterozoic time: Constraints from Namibia: Journal of Sedimentary Research, v. p.

Surkov, V.S., Grishin, M.P., Larichev, A.I., Lotyshev, V.I., Melnikov, N.V., Kontorovich, A.E., Trofimuk, A.A. and Zolotov, A.N., 1991, The Riphean sedimentary basins of the Eastern Siberia Province and their petroleum potential: Precambrian Research, v. 54, p. 37-44.

Trofimuk, A.A., Vail'yev, V.G., Karasev, I.P., Kosorotov, S.P., Mandel'baum, M.M., Mustafinov, A.N. and Samsonov, V.V., 1968, Main problems of prospecting the Markovo oil field in eastern Siberia: Petroleum Geology, v. p. 13-18.

Tucker, M.E., 1986, Formerly aragonitic limestones associated with tillites in the Late Proterozoic of Death Valley, California: Journal of Sedimentary Petrology, v. 56, p. 818-830.

Visser, W., 1991, Burial and thermal history of Proterozoic source rocks in Oman: Precambrian Research, v. 54, p. 15-36.

Zonenshain, L.P., Kuzmin, M.I. and Natapov, L.M., 1990, Geology of the USSR: A plate-tectonic synthesis, B. M. Page]: Washington, D.C., American Geophysical Union, 21, 17-26 p.

FIGURE CAPTIONS

Figure 6.1
Regional map of eastern Siberia showing the present-day tectonic boundary of the Siberian platform. The shaded areas represent major Neoproterozoic age petroleum provinces. The box in the northeast corner of the platform is illustrated in Fig. 6.2, and includes the Olenek uplift and Kharaulakh Mountains. Major rivers are shown.

Figure 6.2
Geology of the Olenek uplift and Kharaulakh Mountains of the northeast Siberian platform. The ellipse outlines the probable aerial extent of bitumen deposits in upper Vendian and Early Cambrian strata. Cross-section of the Olenek field is a schematic.

Figure 6.3
Summary of tectonic history associated with Vendian and Early Cambrian strata of northeast Siberia based on results of Pelechaty et al. (1996b) and Pelechaty (1996). Tecontic history: (i) the Khorbosuonka Group represents development of a passive margin along the eastern edge of the Siberian craton; (ii) Early Cambrian rifting on the northern edge of craton associated with regional uplift and karstification of Vendian carbonates, influx of Cambrian-age clastics and igneous (Ig) activity; (iii) post-rift differential subsidence. Arrows denote horizons along which bitumen is concentrated in porous strata. Symbols: R, Riphean; V, Vendian; ND, Nemakit-Daldyn; T, Tommotian.

Figure 6.4
Cartoon cross-section of the Vendian strata of northeast Siberia along the regional platform-to-basin transition based on integrated sequence stratigraphy and carbon isotope chemostratigraphy (see Fig. 6.2 for location of sections). Details of facies and isotope profiles are shown for sections 1 and 4. Inset illustrates an idealized terminal Proterozoic carbon isotope profile (Knoll and Walter 1992) with isotopic intervals and chemochrons (Pelechaty, et al. 1996a). Ages of chemochrons and sequence boundaries based on U-Pb ages (denoted by "*"; Bowring, et al. 1993; Grotzinger, et al. 1995) and estimated sediment accumulation rates (Pelechaty, et al. 1996a). C = Cambrian; R = Riphean.

Figure 6.5
Idealized ramp geometry and associated depositional facies for the Khorbosuonka Group and its correlative deposits across northeast Siberia.

Figure 6.6
Field photographs. (A) Bitumen-saturated sandstone of Early Cambrian age filling a karst cavern in the upper part of the Vendian-age Khorbosuonka Group along the Olenek River on the west flank of the Olenek uplift. Cave is approximately 1 m wide. (B) Oncolitic rudstone (gravel) of the shoal facies. This deposit occurs beneath lagoon facies carbonates at section 1 (see Fig. 6.4) and is tight with no evidence of karst-related dissolution and porosity development. (C) Example of karstic porosity in shoal facies grainstones at section 5 in the Kharaulakh Mountains (see Figs. 6.4 and 6.7). (D) Karsted shoal facies rudstone at the top of section 5 (see Figs. 6.4 and 6.7). Note the individual grains with showing dark oncolitic rims; these particles are filled with baroque dolomite cement (arrow on light-colored material) and solid bitumen (arrow on dark-colored material). (E) Karst-accentuated stromatolitic lamination in lagoon facies dolostone. (F) Bitumen lining a fracture developed in a lagoon facies dolostone.

Figure 6.7
Stratigraphic cross-section of the upper Khorbosuonka Group carbonates and basal Cambrian-age siliciclastic deposits. Section is hung on the sub-Cambrian karst. The sections show distribution of bitumen in fractured dolostones of the lagoon facies, in karsted shoal facies carbonates, and in intergranular porosity associated with Early Cambrian-age siliciclastic reservoirs. Note that chemochron 3 and the shoal gravels are truncated beneath the sub-Cambrian paleokarst towards the Kharaulakh Mountains (section 5). See Fig. 6.2 for location of sections.

Figure 6.8
Cartoon illustrating the distribution of bitumen and reservoir type across the sub-Cambrian karst surface. Inclined dashed lines indicate the zone over which bitumen occurs with the various reservoir types.

Figure 6.9
Interpreted diagenetic origin of karst-related porosity and subsequent porosity-occlusion in shoal facies grainstones and rudstones.

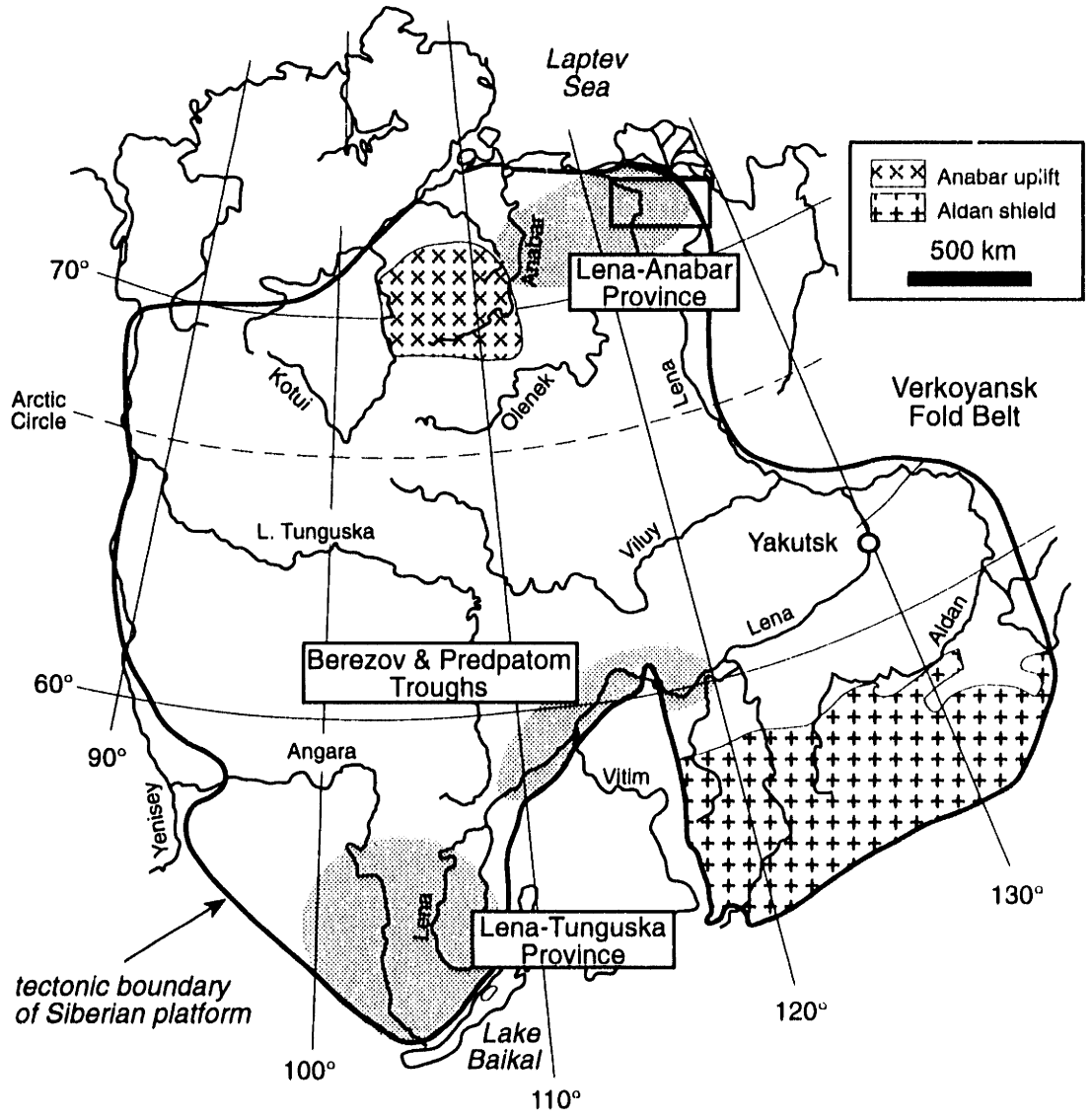
Laptev Sea
Anabar uplift
Aldan shield
500 km
Lena-Anabar Province
Anabar
70°
Kotui
Olenek
Lena
Arctic Circle
Verkoyansk Fold Belt
L. Tunguska
Viluy
Yakutsk
Lena
Aldan
Berezov & Predpatom Troughs
60°
90°
Angara
Vitim
Yenisey
Lena
Lena-Tunguska Province
130°
tectonic boundary of Siberian platform
120°
Lake Baikal
100°
110°

Figure 6.1

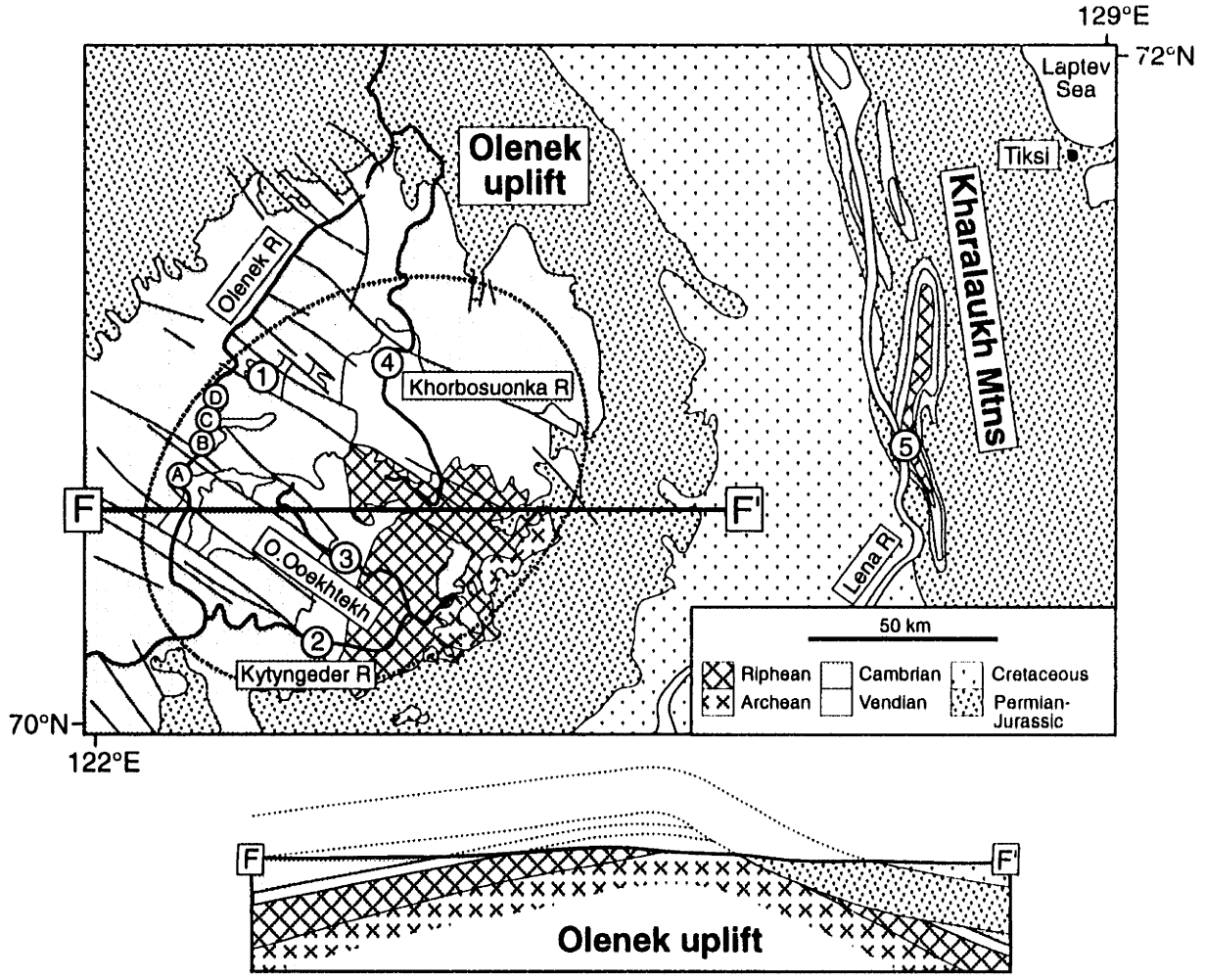
129°E
72°N
Laptev Sea
Tiksi
Olenek uplift
Olenek R.
Khorbosuonka R.
Kharalaukh Mtns
Lena R.
O.Ooekhtekh
Kytyngeder R.
70°N
122°E
50 km
Riphean
Archean
Cambrian
Vendian
Cretaceous
Permian-Jurassic
F
F'
Olenek uplift

Figure 6.2

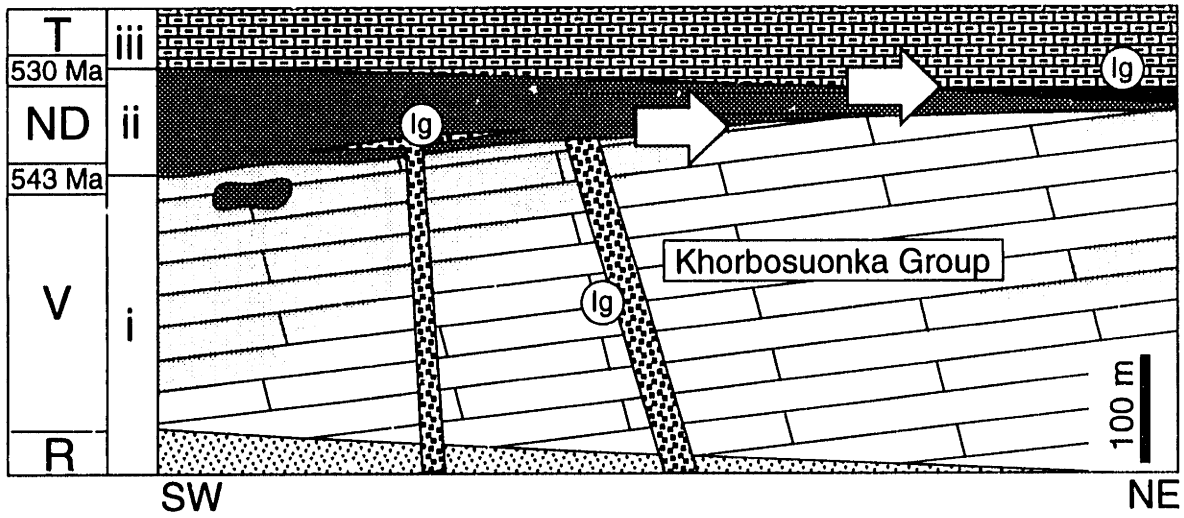
T
530 Ma
ND
543 Ma
V
R
iii
ii
i
lg
lg
lg
Khorbosuonka Group
100 m
SW
NE

Figure 6.3

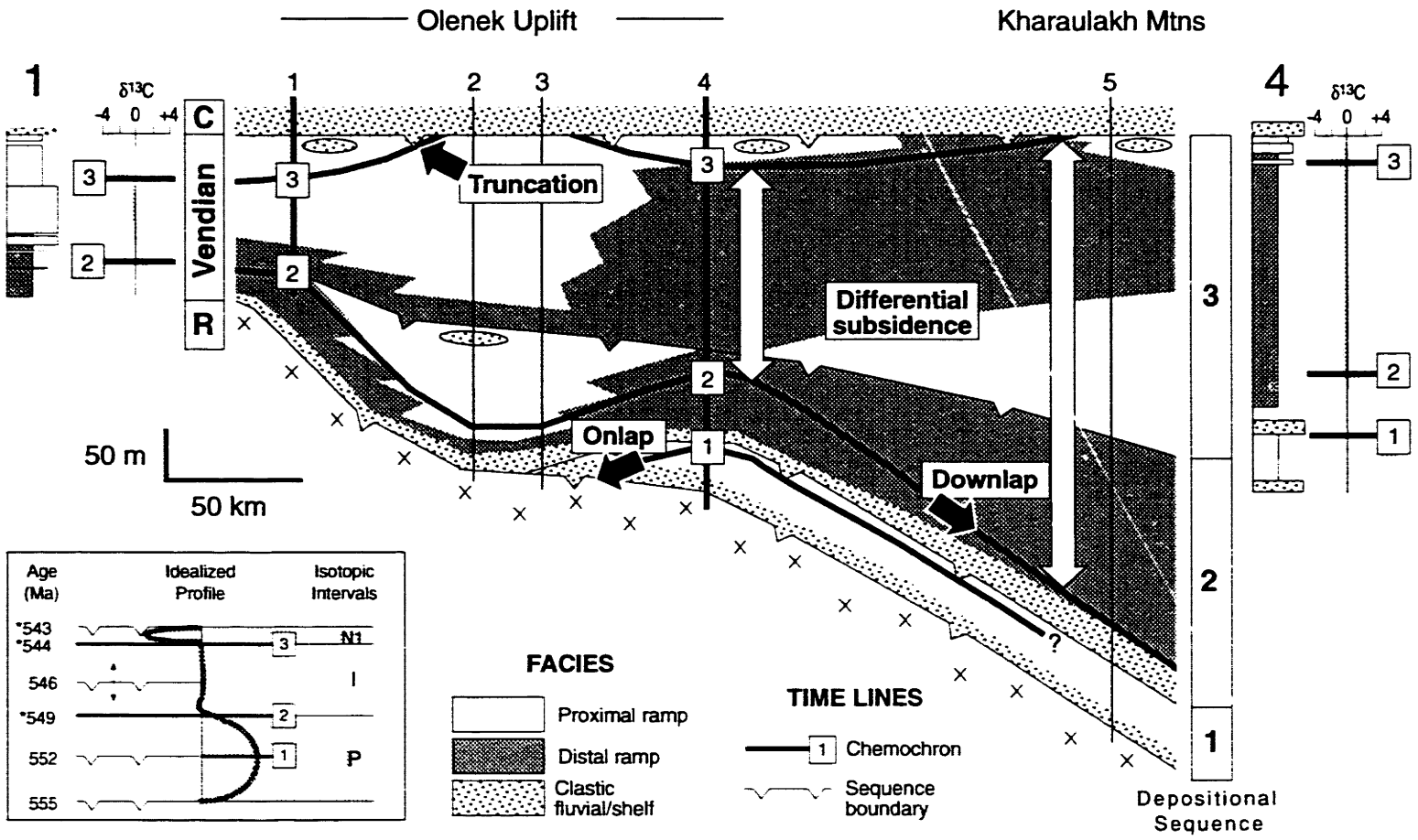
Olenek Uplift
Kharaulakh Mtns
1
δ13C
-4 0 +4
C
Vendian
R
3
2
1 2 3 4 5
Truncation
Differential subsidence
Onlap
Downlap
50 m
50 km
4
δ13C
-4 0 +4
3
2
1
3
2
1
?
Depositional Sequence
Age (Ma)
Idealized Profile
Isotopic Intervals
*543
*544
546
*549
552
555
N1
I
P
FACIES
Proximal ramp
Distal ramp
Clastic fluvial/shelf
TIME LINES
Chemochron
Sequence boundary

Figure 6.4

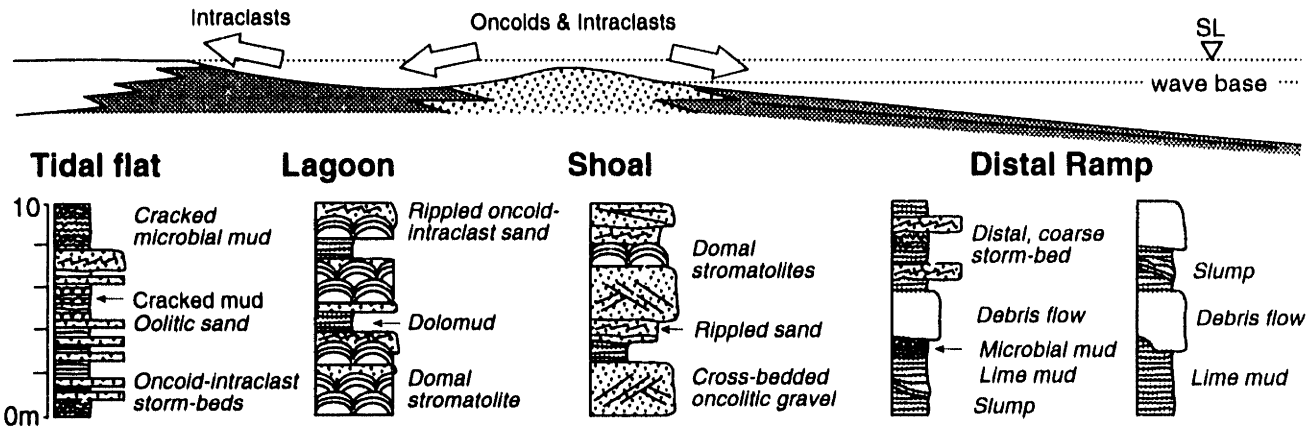
Intraclasts
Oncolds & Intraclasts
SL
wave base
Tidal flat
Lagoon
Shoal
Distal Ramp
10
0m
Cracked microbial mud
Cracked mud
Oolitic sand
Oncoid-intraclast storm-beds
Rippled oncoid-intraclast sand
Dolomud
Domal stromatolite
Domal stromatolites
Rippled sand
Cross-bedded oncolitic gravel
Distal, coarse storm-bed
Debris flow
Microbial mud
Lime mud
Slump
Slump
Debris flow
Lime mud

Figure 6.5

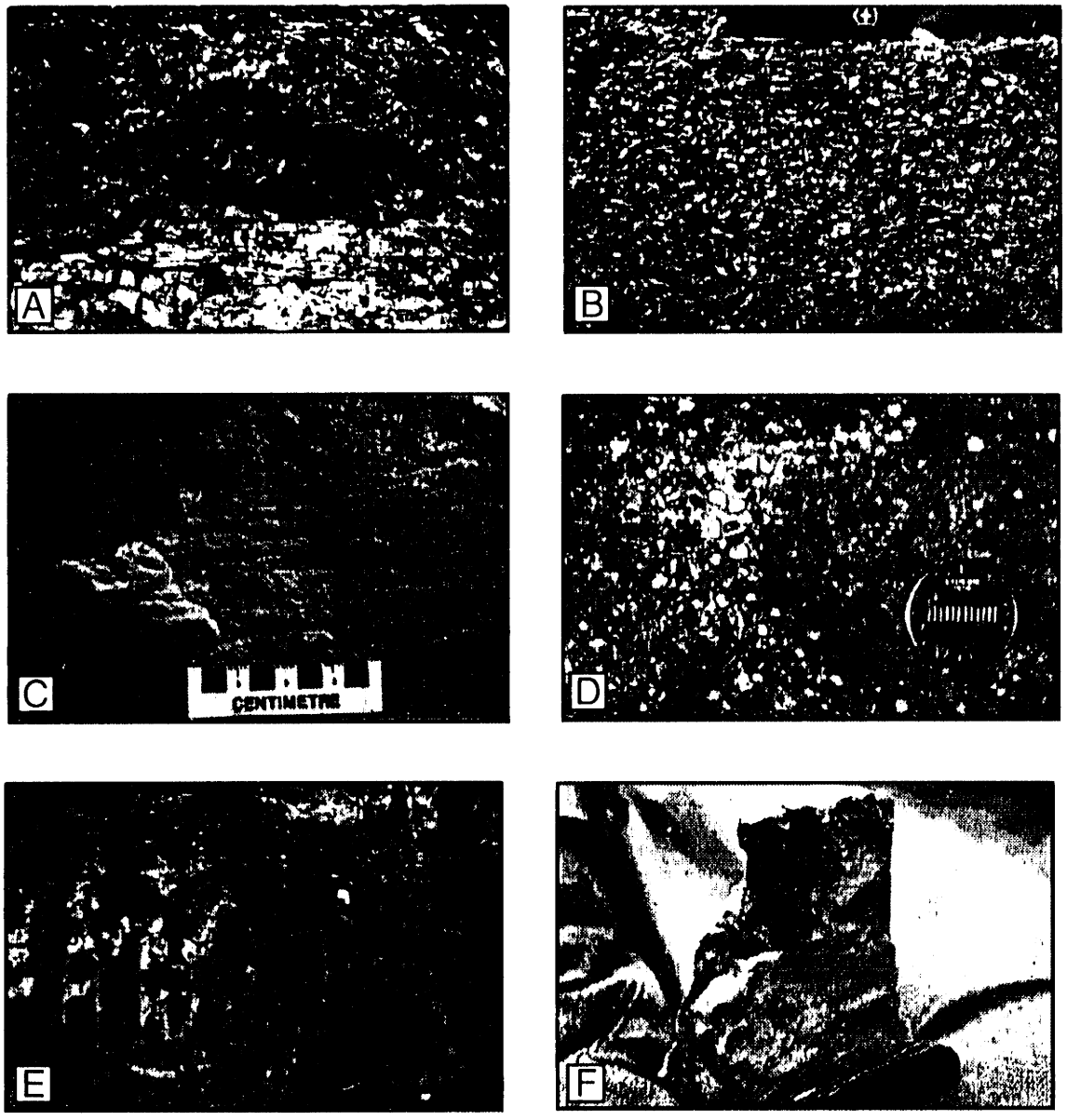

Figure 6.6

130 km
Karst
Chemochron 3
Karst
S3
S2
Khorbosuonka Group
C
2
A
B
C
D
1
4
5
Facies
Marine shale
Marine & fluvial sandstone
Tidal flat
Lagoonal
Shoal
Gravel
Sand
Distal ramp
Bituminous Limestone
Bitumen
Carbonates
0
50
Vertical Scale (meters)
Location Map
Olenek uplift
Kharaulakh Mountains
Vendian Outcrop
Lena River
Olenek R.
20 km
A
B
C
D
1
2
4
5

Figure 6.7

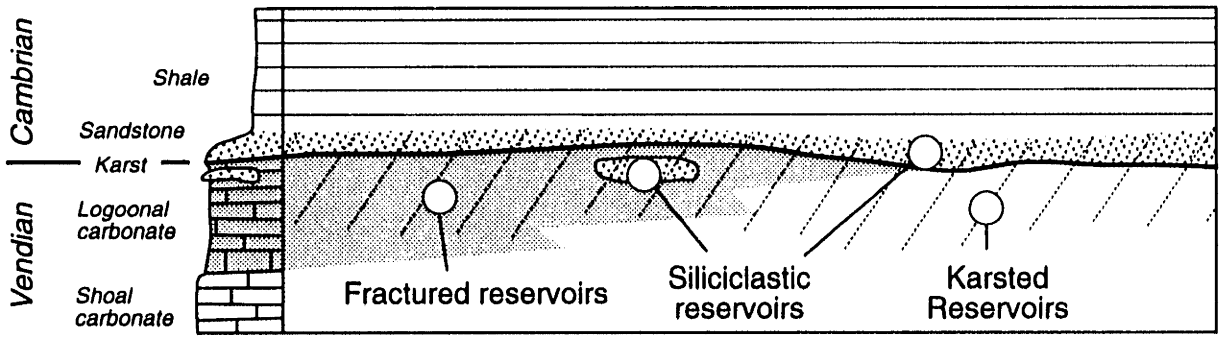
Cambrian
Shale
Sandstone
Karst
Vendian
Logoonal carbonate
Shoal carbonate
Fractured reservoirs
Siliciclastic reservoirs
Karsted Reservoirs

Figure 6.8

Deposition & cementation
Karst-related corrosion
Early-stage porosity occlusion
Late-stage porosity occlusion
A
B
C
D
Grapestone
Oncolitic rim of former calcite
Intraclast of former aragonite
Detritial or cement matrix
Corrosion of matrix
Partial corrosion
Intra-grapestone corrosion of intraclasts & matrix
Complete corrosion of intraclast nuclei
Compaction
Isopachous marine cement
Vadose pendant cement
Dolo-etching by bitumen
Solid bitumen
Incomplete baroque dolocement

Figure 6.9